UNIVERSITY OF LONDON THESIS

Degree PhD Year 2006 Name of Author VUJOVIC
Sonja

Transcriptional profiling of mesenchymal stem cells, undergoing chondrogenesis, and mesenchymal tumours

Sonja Vujovic

A thesis submitted to the University of London for the degree of Doctor of Philosophy

November 2006

Wolfson Institute for Biomedical Research
The Cruciform Building
University College London
Gower Street
London WC1E 6BT

ProQuest LLC
789 East Eisenhower Parkway
P.O. Box 1346
Ann Arbor, MI 48106-1346

ABSTRACT

Mesenchymal stem cells (MSC) represent an adult stem cell population isolated from the bone marrow with the ability to differentiate down various mesenchymal lineages including cartilage. The development of cartilage is a complex multiphase process regulated by the interplay of factors such as cell density and oxygen availability as well as many signalling pathways including TGFβ, MAPK, FGF and Wnt. Using microarrays, the temporal transcriptional changes occurring in the *in vitro* MSC chondrogenesis model were analysed. The results obtained support the validity of the MSC model system for the study of chondrogenesis, as genes known to play a role in the process such as collagens 2, 9 and 11, aggrecan and the transcription factor Sox9, are expressed in the chronological pattern expected. Genes were also identified that had been previously noted to be expressed in limb development but whose role in chondrogenesis remains unknown, as well as a group of novel factors not previously associated with chondrogenesis. Hes1 and Hey1, the targets of Notch signalling were both found to be upregulated early, and their role in chondrogenesis was investigated by inhibiting Notch signalling. Abolishing the expression of Hes1 and Hey1 had a deleterious effect on the accumulation of the chondrogenic matrix, indicating that these transcription factors are implicated in chondrogenesis.

Microarray analysis was also used to compare the expression profiles of a broad range of mesenchymal tumours, resulting in the identification of factors specific to each. The brachyury gene was found to be specifically expressed on chordomas, a tumour derived from notochordal remnants often misdiagnosed for a chondrosarcoma. Immunohistochemistry was performed using a polyclonal antibody to this molecule and was found to distinguish chordomas from over 300 other lesions, including a wide variety of chondroid neoplasms. Brachyury is therefore a specific marker for chordomas, and can be exploited for diagnostic purposes.

ACKNOWLEDGEMENTS

I would like to thank everyone who offered help and encouragement throughout my PhD project and the writing of this thesis.

I am very grateful to each member of Prof Chris Boshoff's group for their friendship and advice and for providing a wonderful working environment. In particular, I would like to thank Claire Westwood for being a friend and an accomplice and for putting up with me for 4 years.

Special thanks go to my supervisors Dr Mark Clements and Prof Adrienne Flanagan. Dr Mark Clements has been a source of practical counsel and support throughout. Prof Adrienne Flanagan has provided invaluable guidance and inspiration. I am indebted to them both for their time and patience.

I would like to thank Chris Skene for his endless support and care, in particular through the last few months of my thesis.

Most of all, I would like to thank my family for their faith in me.

PUBLICATIONS

(Resulting in part from the work presented in this thesis)

- *Brachyury, a crucial regulator of notochordal development, is a novel biomarker for chordomas.*
  S Vujovic, S Henderson, N Presneau, E Odell, T Jacques, R Tirabosco, C Boshoff, A M Flanagan. June 2006. The Journal of Pathology 209(2):157-65.

- *Diagnosing an extra-axial chordoma of the proximal tibia with the help of brachyury, a molecule required for notochordal differentiation.*
  Paul O'Donnell, R Tirabosco, S Vujovic, W Bartlett, T W R Briggs, S Henderson, C Boshoff, A M Flanagan. 2006. Skeletal Radiology. (Epub ahead of print)

- *A molecular map of mesenchymal tumours.*
  S Henderson, D Guiliano, N Presneau, S McLean, R Frow, S Vujovic, J Anderson, N Sebire, J Whelan, N Athanasou, A M Flanagan, C Boshoff. Aug 2005. Genome Biology.

- *Chondroblastomas but not chondromyxoid fibromas express cytokeratins: an unusual presentation of a chondroblastoma in the metaphyseal cortex of the tibia.*
  Kostas Bousdras, Paul O'Donnell, Sonja Vujovic, Stephen Henderson, Chris Boshoff and A.M. Flanagan. Histopathology. 2006. (In press).

TABLE OF CONTENTS

LIST OF FIGURES

LIST OF TABLES

LIST OF ABBREVIATIONS

0H	0 hour time point of the time course experiment of MSC differentiating into chondrocytes
12H	12 hour time point of the time course experiment of MSC differentiating into chondrocytes
14D	14 day time point of the time course experiment of MSC differentiating into chondrocytes
24M	MSC isolated from bone marrow derived from a 24 year old male
2D	2 day time point of the time course experiment of MSC differentiating into chondrocytes
31M	MSC isolated from bone marrow derived from a 31 year old male
38M	MSC isolated from bone marrow derived from a 38 year old male
3H	3 hour time point of the time course experiment of MSC differentiating into chondrocytes
46F	MSC isolated from bone marrow derived from a 46 year old female
55F	MSC isolated from bone marrow derived from a 55 year old female
6H	6 hour time point of the time course experiment of MSC differentiating into chondrocytes
AER	Apical ectodermal ridge
BCIP	5-bromo-4-chloro-3-indolyl phosphate
BDNF	Brain derived neurotrophic factor
bFGF	Basic fibroblast growth factor
bHLH	Basic helix-loop-helix
BMP	Bone morphogenetic protein
CAM	Cell adhesion molecule
Cbfa1	Core binding factor alpha 1
CD	Cluster of differentiation
CDH2	N-cadherin
cDNA	'Complementary' deoxyribonucleic acid
CHB	Chondroblastoma
CHL2	Chordin-like protein 2
CHS	Chondrosarcoma
CK	Cytokeratin
CMA	Chordoma
CMF	Chondromyxoid fibroma
CMP	Cartilage matrix protein
Col	Collagen
COMP	Cartilage oligomeric matrix protein
cRNA	'Complementary' ribonucleic acid

Ctrl	Control
DAPT	N-[N-(3,5-Difluorophenacetyl-L-alanyl)]-S-phenylglycine *t*-butyl ester
DDIT3	DNA damage-inducible transcript 3
DEPC	Diethylpyrocarbonate
DEX	Dexamethasone
DIG	Digoxigenin
DMSO	Dimethyl sulfoxide
DNA	Deoxyribonucleic acid
dpc	Days post coitum
DPT	Dermatopontin
EB	Embryoid body
EBP	Emopamil binding protein
ECM	Extracellular matrix
EGF	Epidermal growth factor
EMA	Epithelial membrane antigen
ES	Embryonic stem
ETRA	Endothelin Receptor A
FACS	Fluorescence activated cell sorting
FCFC	Fibroblast colony forming cells
FGF	Fibroblast growth factor
GAPDH	Glyceraldehyde-3-phosphate dehydrogenase
GDF	Growth and differentiation factors
GEM	Gene expression microarray
GLI3	GLI-Kruppel family member 3
H&E	Haematoxylin and eosin
HES	Hairy and enhancer of split
HEY	Hairy/enhancer of split related with YRPW motif
HIF1	hypoxia-inducible factor 1
HSC	Hematopoietic stem cells
IBMX	Isobutyl methyl xanthine
IBSP	Bone sialoprotein
ID	Inhibitor of differentiation
IGF	Insulin-like growth factor
IHC	Immunohistochemistry
Ihh	Indian hedgehog
ISH	*In situ* hybridization
KLF4	Kruppel-like factor 4
LB	Luria-Bertani
MAPC	Multipotent adult progenitor cells
MAPK	Mitogen activated protein kinase
MAS	Microarray suite
MATN	Matrillin
MDS	Multi-dimensional scaling
MGP	Matrix gla protein
MIAMI	Marrow-isolated adult multilineage inducible

MMP	Matrix metalloproteinases
MSC	Mesenchymal stem cells
N24M	MSC isolated from bone marrow derived from a second 24 year old male
NBT	Nitro blue tetrazolium
N-CAM	Neural cell adhesion molecule
NDRG1	N-Myc downstream regulated gene
NHAC	Normal human articular chondrocytes
NICD	Notch intracellular domain
p	passage
PBS	Phosphate buffered saline
PDGF	Platelet derived growth factor
PDGFRA	Platelet-derived growth factor receptor alpha
PKA	Protein kinase A
PLA	Processed lipoaspirate
PLZF	Promyelocytic leukaemia zinc finger
PTHR	Parathyroid hormone receptor
PTHrP	Parathyroid hormone related peptide
RA	Retinoic acid
RMA	Robust multi-array average
RNA	Ribonucleic acid
RS1	Rapidly self-renewing cells
RT-PCR	Reverse transcription polymerase chain reaction
Shh	Sonic hedgehog
Sox	SRY-box
SPP	Osteopontin
TAE	Tris-acetate-EDTA
TBX2	T-box 2
TGFß	Transforming growth factor β family
TXNIP	Thioredoxin interacting protein
Wnt	Wingless type MMTV integration site family member

1. INTRODUCTION

1.1 MESENCHYMAL STEM CELLS

Mesenchymal stem cells (MSC) are an adult progenitor cell population, isolated from the bone marrow, that have the ability to differentiate towards various mesenchymal lineages. They provide a useful tool for modelling differentiation *in vitro* and may also have clinical applications in treating conditions ranging from bone fracture to myocardial ischemia. Here, a review is given of the history of research on MSC, followed by a description of their phenotype and conditions required for maintaining and differentiating them *in vitro*. A discussion of the MSC differentiation potential as well as the reported sources of MSC follows.

1.1.1 History

The first experiments suggesting that a cell capable of osteogenesis resides in adult bone marrow were performed by Urist and Mclean in 1952 (1). They were interested in studying the osteogenic potency of cells from different tissues and performed autologous transplants of bone marrow, periosteum, callous bone as well as blood clots into the eyes of rats. They discovered that all these tissues, with the exception of blood clots, had osteogenic potential. In addition, the bone marrow transplants also formed cartilage and bone marrow stroma, in fact forming an ossicle - a primary marrow cavity surrounded by bone and cartilage. Further bone marrow transplants were performed by Tavassoli and Crosby using large pieces of undisrupted tibia bone marrow, which they would scoop out with a spatula and implant into other tissues such as spleen, liver or muscle. Again, the development of osteoid at the site of transplantation was noted, and within a few weeks the development of bone marrow stroma surrounded by a layer of

bone was observed, just as occurred in the Urist and McLean experiments (2).

The cells responsible for this osteogenic response were isolated from guinea pig bone marrow and cultured *in vitro* by Friedenstein in 1974, who named them fibroblast colony forming cells (FCFC). FCFC are extremely adherent cells, and this is the property that allowed Friedenstein to isolate them (3). He found that over 90% of FCFC would adhere to glass within 90 minutes in the absence of serum. The cells were few in number, spindle shaped and dormant for 2 to 4 days after isolation, after which they multiplied rapidly. FCFC had the ability to differentiate into osteocytes when placed in diffusion chambers and transplanted into other sites, such as the kidney *in vivo,* but would not undergo spontaneous osteogenesis while in monolayer culture. Castro-Malaspina *et al* and Piersma *et al* went on to characterize these cells further and found them to express bone marrow matrix proteins such as type 1 and 3 collagen and fibronectin (4;5).

Different terms are currently used to describe the FCFC population, the most common ones being MSC and bone marrow-derived stem cells.

1.1.2 MSC phenotype

The bone marrow houses a myriad of cells including blood and stromal cells as well as both hematopoietic and non-hematopoietic stem cells. Specifically: endothelial cells, adipocytes, macrophages, reticular cells, fibroblasts, osteoprogentors, various stem cell populations and their progeny all reside within the bone marrow stroma (6). MSC are isolated from the mononuclear layer of the bone marrow, which is considered the non-hematopoietic compartment (7). Morphologically MSC resemble fibroblasts and are spindle-shaped when isolated. When kept in culture for prolonged periods however, the cells enlarge and lose their spindle shape.

Determining the cell surface marker profile of MSC has been a common research goal, and a summary of the expression of many cluster of

differentiation (CD) molecules on MSC is presented in Table 1.1. Unlike the haematopoietic stem cells (HSC) isolated from bone marrow, MSC do not express haematopoietic cell surface markers such CD34, CD45 or CD14 (although the expression of CD14 has been detected by some groups (8;9)) or epithelial markers CD1a, CD31 and CD56 (10). MSC also do not express the epithelial antigen ESA but do express cytokeratins (10). MSC are positive for SH2, SH3 and SH4 mesenchymal markers and α-smooth muscle actin and also express a large variety of proteins that facilitate cell to cell and cell to matrix interactions such as α and β integrins (α1/2/3/5/6 and β1/3/4) and cell adhesion molecules (ICAM-1 and 2, VCAM-1) on their surface (10-13). The MSC extracellular matrix (ECM) is rich in collagens 1, 3, 4, 5 and 6, fibronectin and laminin, with which the integrins can interact (14). As yet no unique marker has been found that is expressed by MSC and no other cell type that would aid in their isolation and identification.

Stro-1 binds to about 10% of the bone marrow mononuclear cells and is often used as a method for identifying MSC. Stro-1 is not MSC specific as it also identifies erythroid precursors but does not bind to other hematopoietic precursor cells (15). Using Stro-1, in combination with negative selection for glycophorin A expressing cells, isolates a population of cells that adheres to tissue culture plastic and has the potential to differentiate down all MSC lineages (15).

Cluster of differentiation n°	Other names[a]	Remarks	Expressed by MSC
CD1a	R4; HTA-1	Thymocyte antigen	NO
CD14	LPS-R	Considered a hematopoietic marker identifying macrophages	Mixed reports (see text)
CD31	GPIIa'; endocam; PECAM-1	Endothelial cell and fibroblast marker	NO
CD56	Leu-19; NKH1; NCAM	Expressed on neurons, glia and skeletal muscle	NO
CD29	Platelet GPIIa; VLA-beta chain; integrin β1	One of the integrins expressed by the MSC	YES
CD34	gp105-120; HPCA	Hematopoietic and endothelial marker	NO
CD44	ECMRIII; H-CAM; HUTCH-1; Hermes; Lu, In-related; Pgp-1; gp85	Hyaluronic acid receptor, interacts with osteopontin and collagens	YES
CD45	B220; CD45R; CD45RA; CD45RB; CD45RC; CD45RO; EC3.1.3.4; LCA; T200; Ly5	Expressed by all hematopoietic cells except erythrocytes	NO
CD49a	Integrinα1	Attachment to ECM	YES
CD49b	Integrinα2	Attachment to ECM	YES
CD49c	Integrinα3	Attachment to ECM	YES
CD49e	Integrinα5	Attachment to ECM	YES
CD49f	Integrinα6	Attachment to ECM	YES
CD54	ICAM-1	Adhesion molecule	YES
CD61	Integrinβ3	Attachment to ECM	YES
CD71	T9; transferrin receptor	Mediates iron uptake	YES
CD77	Pk blood group antigen; BLA; CTH; Gb3	Mainly expressed on B-lymphocytes	YES
CD90	Thy-1; Theta antigen	Mainly expressed by T-cells	YES
CD102	ICAM-2	Adhesion molecule	YES
CD104	Integrinβ4	Attachment to ECM	YES
CD106	INCAM-110; VCAM-1	Mediates monocyte to lymphocyte adhesion	YES
CD117	c-kit; SCRF	Receptor for stem cell factor regulating differentiation, in particular hematopoietic	NO
CD120a	TNFRI; p55	Tumour necrosis factor receptor	YES
CD124a	IL-4R	Interleukin receptor	YES

(Legend on following page)

[a] Source of alternative nomenclature: http://www.sciencegateway.org/resources/prow/index.html

Table 1.1: Summary of the expression of various cluster of differentiation (CD) molecules on MSC (6;10-13)

MSC are known to express high levels of vimentin, a mesenchymal marker, identifying cells of mesodermal origin, and have also been found to express various neural genes, suggesting that they may have the potential to differentiate into neural lineages (16;17). Wagner *et al* also demonstrated that altering the media in which MSC are grown has a very significant impact on their expression profile, adding another variable alongside the isolation procedure and yet another factor to be taken into account when comparing the results obtained by various groups (16).

1.1.3 MSC culture conditions

Establishing MSC in culture is slow, as they are thought to be in a quiescent state when isolated. The rate of proliferation of MSC is related to their density and when cells are seeded too sparsely the doubling time becomes very slow and apoptosis frequent. It is therefore difficult to culture MSC as single cell clones (although work has been published on cells grown in this manner as described below) and there is some suggestion that they may be programmed to die when single, as cell death naturally occurs during development of mesenchymal tissues in processes such as endochondral ossification and digit formation (18). There are also differences in MSC growth requirements between different species (19).

Conget and Minguell report that MSC can be passaged up to 25 times without displaying dramatic morphological or immunophenotypical changes, after which they gradually lose the expression of specific surface antigens and begin to display apoptotic characteristics (20). The average doubling time was 33 hours and a large proportion (20%) of the cells were found to be in the G0 phase of the cell cycle which could be seen as an indicator of their self-renewal potential. Conget and Minguell also demonstrate the vast, but

not unlimited, expansive potential of MSC, where each cell grown *in vitro* has the capability to give rise to ~5.5 x 10^8 cells (20).

The growth rates of MSC vary *in vitro* depending on the donor, but differences can also be noted with samples taken from the same donor at different times (21;22). Cryopreserving and thawing MSC appears to have no effect on their growth and differentiation (21;22). The donor variation noted by Phinney *et al* could not be correlated with donor age or gender, while Mareschi *et al* found that MSC from younger donors proliferated more rapidly (21;23). However, all the donors used by Phinney *et al* were over 19 years of age, whereas Mareschi *et al* investigated the proliferative potential from paediatric (2 - 13 year old) and adult donors and found that they underwent twice as many population doublings as the MSC isolated from the adults in the same time period (21;23).

Telomerase overexpression can extend MSC lifespan apparently indefinitely (over 260 population doublings) without impairing, and potentially even enhancing osteogenic differentiation (24;25). Okamoto *et al* overexpressed telomerase and E6/E7 papillomavirus genes and claimed that the MSC continue to differentiate towards osteocytes, adipocytes and chondrocytes (26).

The addition of basic fibroblast growth factor (bFGF) significantly accelerates the doubling time of MSC, without limiting the differentiation potential into chondrogenic, adipogenic or osteogenic lineages and so allows rapid expansion of MSC, thus making them a more convenient cell type for manipulation (27).

1.1.4 Differentiation potential

Two types of assays are used to determine MSC differentiation potential: the first are *in vitro* assays where growth factors are added to cells in culture in order to induce differentiation toward a specific lineage and the second are *in vivo* studies where MSC are injected into a particular site

(usually in a murine model) and then analysed microscopically for morphology and immunohistochemically for expression of specific molecules.

MSC can differentiate to cells of mesenchymal origin including chondrocytes, osteocytes, and adipocytes *in vitro* (11;28). In addition, they can produce marrow stroma and serve as feeder layers for haematopoietic stem cell expansion (11;29). As marrow is surrounded by bone, and marrow is often replaced with fat with age – the osteogenic, chondrogenic and adipogenic potential of these cells is not surprising.

MSC have also been shown to differentiate *in vitro* into muscle as demonstrated by the presence of cells with contractile myotubes (30). Further evidence of myogenesis was provided by bone marrow cells from *lacZ* expressing transgenic mice contributing to muscle fibres when injected into wildtype recipients (30;31). Upon fractionation of the bone marrow cells, Ferrari *et al* concluded that the adherent population (therefore the MSC) has myogenic potential, but that these cells would contribute only minimally to actual muscle regeneration normally (31).

According to some research, when MSC are injected into the adult murine heart they appear to differentiate into cardiomyocytes, as shown by the expression all the cardiomyocyte genes (32). However, a more recent investigation showed no evidence of differentiation of MSC into cardiomyocytes and no restoration of myocardial function when human MSC were injected into ischemic rat hearts (33).

There have also been reports of MSC differentiation into non-mesodermal lineages including neural cells and hepatocytes. When MSC were injected into murine brains, they differentiated into neurons and astrocytes (34). *In vitro,* MSC were found to express neural markers (Section 1.1.2 and ref (17)) and could be induced to exhibit a neural morphology when cultured in the presence of retinoic acid and brain-derived neurotrophic factor (BDNF) (35). However, this study did not address whether the cells generated were functional neurons. Zhao *et al* transduced the BDNF gene

into human MSC and detected not only the expression of neural markers but also an electric current using the patch clamp technique, hence the cells they produced also functionally resembled neurons (36).

Sato *et al* inoculated various cell populations from bone marrow into damaged rat livers and found that only MSC differentiated into hepatocytes and expressed alpha-fetoprotein, albumin and cytokeratins (37). *In vitro* MSC differentiation into hepatocytes has been achieved by 3-dimensional pellet cultures and supplementation of growth medium with bFGF, hepatocyte growth factor and oncostatin M (38).

The reported *in vivo* differentiation experiments seeking to show that a single cell has the ability to differentiate toward different mesenchymal lineages are somewhat contentious. This is because it is difficult to prove that cell fusion does not occur between the injected cell and an endogenous (host) cell, leading them to express markers of both cell types (39). In this respect, *in vitro* studies investigating the differentiation from a presumed MSC are less problematic as fusion to another cell population is not possible. However, in contrast to *in vivo* experiments, the *in vitro* differentiation conditions are artificial, and it is not clear whether the selected cells would behave as they would *in vivo*. Another contentious issue is how differentiation into another cell type is defined, as it could be argued that solely the expression of genes associated with a certain lineage is not sufficient evidence to confirm differentiation. It is therefore essential to define what functionally determines a certain cell type such as the formation of lipid droplets in an adipocyte or the firing of action potentials by a neuron, and apply standardized tests for these.

1.1.5 Sources of MSC-like cells

For the purposes of this thesis, MSC are defined as cells isolated from the bone marrow. However cells resembling the MSC, in terms of their phenotype and differentiation potential have been isolated from a variety of

tissues. Adipose-derived stem cells, termed processed lipoaspirate cells (PLA) have been shown to differentiate towards osteogenic, chondrogenic and adipogenic lineages *in vitro* (40;41). Cells derived from trabecular bone and the periosteum also differentiate towards these three lineages (42;43). It may seem more likely that it is these, local, stem cell populations that are recruited in tissue repair rather than the pluripotent bone marrow populations, but their relative contributions are unknown and the relationship between MSC and committed progenitors remains unclear. The isolation of MSC-like cells, shown to differentiate towards adipogenic, osteogenic and myogenic lineages, has also been reported from tendon, synovial membrane, lungs and, recently, the appendix (44-48).

Meirelles *et al* attempted a large scale isolation of MSC-like cells from a wide variety of tissues including: spleen, muscle, aorta, vena cava, kidney, lung, liver, brain and thymus (49). The morphology of the cells isolated from all tissues resembled MSC, but the cells were more flattened and less spindle-shaped (Section 1.1). Fluorescence activated cell sorting (FACS) analysis of the immunophenotype of these cells showed all populations to express similar surface antigens and be CD29 and CD44 positive, with variable expression of CD90 and CD49e, normally found on MSC (Section 1.1.2) (49). All the cell lines showed some ability to differentiate into adipocytes and osteocytes and could undergo over 50 population doublings (49).

Another point of debate has been whether MSC are present in circulating blood. Meirelles *et al* were unable to establish MSC cultures from peripheral blood, as were Wexler *et al*, who also attempted to perform the isolation on cord blood unsuccessfully (49;50). However, others have isolated an MSC population from peripheral blood and mobilized peripheral blood, and shown it to display MSC characteristics, such as Stro-1 expression, as well as the MSC differentiation potential (51). An additional complexity arises from the finding that MSC-like cells can be cultured from blood vessels. Hence, any damage caused to this structure during the

collection of a blood sample could result in the release of MSC-like cells that would then be assumed to be derived from the peripheral blood itself rather than the vessel wall (49). Finally, MSC may be released into peripheral blood from the bone marrow as a response to injury, even if they are not normally present in the circulation (52).

1.1.6 The uniformity of mesenchymal stem cells

In 1999, Pittenger *et al* addressed the question whether MSC were truly a multipotent cell population or simply a mixture of committed progenitor cells. This was done by growing clonal populations from single cells, and then testing their *in vitro* differentiation potential (11). Of the 6 clones tested, all underwent osteogenesis, of these 5 also differentiated into adipocytes of which 3 were also capable of differentiation into chondrocytes. The finding that not all 6 colonies differentiated into all the lineages could either be accounted for by a loss of multipotentiality due to a high passage number (necessary to obtain a sufficient number of cells) or it could indicate that MSC are indeed a mixed population of truly multipotent cells and committed progenitors.

Muraglia *et al* performed a similar assay with somewhat different results to Pittenger *et al* (53). They analysed 185 clones for differentiation into all 3 lineages and conclude that all differentiated into osteocytes, while the majority differentiated into chondrocytes and only a third could undergo adipogenic differentiation. They did not find any clones capable of undergoing adipogenesis and osteogenesis only. This discrepancy with the Pittenger *et al* data may be due to different conditions used by the two groups to induce differentiation as well as different methods for testing whether cells had undergone differentiation. Muraglia *et al* did not perform staining for calcification to assess for osteogenesis or for proteoglycans to test for chondrogenesis as Pittenger *et al* did, instead they performed

immunohistochemistry for proteins expressed in cartilage and bone (Collagen 2 and Osteocalcin respectively).

Beside the experiments on clonal populations detailed above, many researchers have identified subpopulations of cells within the MSC population, indicating that MSC are a heterogeneous population of cells.

Colter *et al* identified a morphologically distinct subpopulation of MSC that they referred to as: "small, round, rapidly self-renewing cells" (RS1) (54). Through continuous passaging of the MSC, the RS1 subpopulation seems to be lost but the RS1-enriched populations show higher levels of differentiation: the osteoblasts show higher levels of mineralization, a higher proportion of cells differentiate into adipocytes and the chondrocytes produce more matrix (54).

Pochampally *et al* used serum deprivation to select for a subpopulation of MSC that displayed longer telomeres and expressed low levels of genes normally attributed to embryonic stem cells, such as Oct-4 and telomerase (55). Whether these cells also have an increased differentiation capacity remains to be elucidated.

D'Ippolito *et al* isolated a population of bone marrow cells they refer to as marrow-isolated multilineage inducible (MIAMI) cells. These were selected without gradient centrifugation in an attempt to replicate the *in vivo* niche of the stem cells. MIAMI cells were found to express Oct-4 and telomerase as well as Rex-1, another embryonic stem cell gene. Their differentiation potential is reported to span all three germ layers, although differentiation was only evaluated in terms of marker expression and morphology but not function (Section 1.1.4) (56).

Multipotent adult progenitor cells (MAPC) are a population of cells, similar to the MSC, that are also purified from the bone marrow. They are enriched by negative selection with immuno-magnetic beads, which bind all CD45 and Glycophorin A positive cells (57). MAPC are also cultured in different conditions to the MSC: they are grown in low serum concentration, with epidermal growth factor (EGF) and platelet derived growth factor

(PDGF) added, and are plated on fibronectin-coated plates. *In vitro* human MAPC can be induced to differentiate not only down the osteogenic, adipogenic and chondrogenic lineages but also into skeletal muscle, hepatocytes, neuroectoderm and endothelium (57-59). MAPCs can also be expanded for longer in culture than MSC (more than 80 population doublings). Murine MAPC were found to express low levels of embryonic stem cell markers Oct-4 and Rex1. Single cell cultures of these cells could be induced to differentiate *in vitro* into tissue types from all three germ layers, and when a single MAPC was injected into the early blastocyst it was capable of contributing to all somatic cell lines (58). While the potential existence of a pluripotent adult stem cell is an exciting possibility, so far this data has not been reproduced by any researchers other than those associated with the group responsible for the above publications (Verfaille and co-workers). Therefore the experiments presented above are somewhat contentious and the MAPC are considered by some to be a culture artefact rather than an *in vivo* population.

As all the above-mentioned populations are isolated differently and cultured under different conditions, it is difficult to compare the results of studies analysing them and determine whether the RS1 cells, the MIAMI cells and the MAPC represent the same subpopulation of MSC. It also remains unknown whether these populations represent an earlier precursor of what is commonly defined as an MSC or an entirely unrelated population of cells.

1.2 CHONDROGENESIS

During embryonic development, the generation of cartilage from mesoderm is an essential process in the creation of the future skeleton. Insight into chondrogenesis has so far been obtained through the creation of knockout mice, analysis of genetic mutations affecting the human skeleton, and *in vitro* cultures of chondroblasts and other progenitor cells that have chondrogenic potential, including periosteal cells and MSC.

1.2.1 Skeletogenesis

Skeletogenesis in human embryos begins in the third and fourth weeks of development and in mouse embryos around day 10 post coitum (60). The process of limb formation starts with an outgrowth referred to as the limb bud, at the centre of which mesenchymal cells condense into cartilaginous anlagen. The close cell to cell contact in these condensations, along with signalling molecules such as the transforming growth factor β family (TGFß) and the bone morphogenetic protein (BMP) family induce the formation of chondroblasts, which further differentiate into chondrocytes and start producing the extracellular matrix (ECM) characteristic of cartilage. Cartilage has a very low cell to matrix ratio, and the few cells embedded in the matrix appear spherical in shape (61). Induced by further signalling molecules, such as indian hedgehog (Ihh) and transcription factors, including core binding factor alpha 1 (Cbfa1), the chondrocytes undergo hypertrophy and enlarge five to tenfold. Hypertrophy leads to some chondrocytes lysing, which alters the pH of the matrix, and allows calcification to proceed. The osteoblasts, located in the periosteum, contribute to the mineralisation of the cartilage matrix and consequently the hypertrophic cells die, while the osteoblasts mature into osteocytes, thereby replacing cartilage by bone (62). This process of cartilage formation and subsequent hypertrophy and replacement by bone is referred to as endochondral ossification, and the

majority of the bones develop in this way (61). The exception are the flat bones of the skull, some of the facial bones and most of the clavicle, which form through intramembranous ossification (63).

1.2.2 Formation of mesenchymal condensations

The formation of pre-cartilaginous condensations is a crucial step in skeletal development. Mesenchymal cells express hyaluronan and collagen type I in their extracellular matrix, preventing close cell to cell contact. As condensation starts hyaluronidase activity increases, facilitating closer contact between cells (61). This change in cell density is accompanied by a change in expression levels of extracellular matrix molecules as well as enhanced cell to cell contact, leading to activation of signalling cascades, associated with initiation of differentiation (61;64).

Prior to condensation it is important that the cells of the limb bud have proliferated sufficiently to form the future limb. The signals required for limb bud growth originate in the apical ectodermal ridge (AER), a layer of cells present at the tip of the outgrowth. The main signalling molecules produced by the AER are the fibroblast growth factor (FGF) family proteins, as shown by experiments in which beads soaked in recombinant FGF rescued the phenotype of chick limbs where the AER has been removed (65). In FGF4 and FGF8 double knockout mice, hindlimb development is completely abolished and only small cartilaginous elements are observed, showing these molecules to be essential for skeletal development and proliferation of the progenitor cell population prior to the formation of the condensations (66).

Various other molecules are involved in the specification of the timing and location of the cartilage formation. A recently identified pair of factors involved in the formation of the proximal elements of the hind limb are the GLI-Kruppel family member 3 (GLI3) and promyelocytic leukaemia zinc finger (Plzf). The absence of these molecules in knockout mice results in

normal limb bud size but a complete absence of the femur, tibia and fibula (67).

The key molecule involved in the adhesion of cells in the mesenchymal condensations is N-cadherin, but N-CAM, fibronectin and their respective interacting molecules are also upregulated. The expression of N-cadherin first appears in the core of the condensation and only later at the periphery, when the expression in the core is lost (61). N-cadherin is a cell membrane spanning protein that can interact with N-cadherins on neighbouring cells via its extracellular domain. N-cadherin is dependent on Ca^{2+}, and adding exogenous Ca^{2+} *in vitro* to cells about to undergo condensation enhances chondrogenesis (68). The presence of N-cadherin is essential for condensations to form but it must be downregulated for chondrogenesis to proceed. Therefore, its production is tightly regulated (69). Retinoic acid, TGFß and Wnt signalling are all involved in modulation of N-cadherin levels.

Retinoic acid (RA) is a strong inhibitor of early chondrogenic differentiation and activated signalling through the RA receptors is capable of overriding the chondrogenic effect of the BMPs. The shutdown of RA signalling, on the other hand, is an equally potent inducer of chondrogenesis and can bring about differentiation even in the presence of BMP inhibitors such as Noggin (70). One of the ways by which RA signalling acts to inhibit chondrogenesis is by sustaining the expression of N-cadherin and so preventing cells from undergoing further differentiation after they have formed the condensations (69).

TGFß family molecules regulate chondrogenesis by inducing mitogen activated protein kinase (MAPK) signalling, which in turn also modulates N-cadherin levels. When MAPK signalling is inhibited, N-cadherin levels remain high and chondrogenesis cannot proceed, suggesting that MAPKs play a role in downregulating N-cadherin (71). In addition, TGFßs also affect wingless type MMTV integration site family member (Wnt) signaling by

upregulating Wnt7a, which transiently prolongs N-cadherin stabilization, and so suppresses further chondrogenic differentiation (72).

1.2.3 Production of the cartilage ECM

Once mesenchymal cells have condensed they begin to differentiate into chondrocytes and produce the extracellular matrix. Mature cartilage comprises only 5-10% of cells and up to 95% of cartilage matrix, and it is the ECM that gives cartilage its functional properties. The primary function of a chondrocyte is the synthesis and the maintenance of the matrix (73). Matrix maintenance involves a balance of matrix degradation and synthesis, and a disruption of this balance leads to degenerative joint disease, osteoarthritis. The cartilage matrix comprises a network of collagens and proteoglycans, the former providing tensile strength while the latter's affinity for water allows for cartilage swelling and compression, and thus its load-bearing ability. The major collagen synthesized by cartilage is collagen 2 (75-90% of collagen synthesis), and it forms collagen heterofibrils together with collagens 9 and 11 (74). These ~20nm wide fibrils are thought to consist of a collagen 11 core surrounded by a thicker layer of collagen 2 to which collagen 9 molecules can bind (75). The most abundant proteoglycan in cartilage is aggrecan: others include versican, a protein expressed early in chondrogenesis, but downregulated upon aggrecan deposition, perlican and link (76). In addition, the ECM contains proteins that are neither collagens nor proteoglycans. One of these proteins, the cartilage oligomeric matrix protein (COMP), binds collagens, and mutations in the gene encoding COMP cause chondrodysplasia in humans, characterised by short stature and osteoarthritis (77). Matrix proteins do not only serve as structural proteins but can also be involved in signalling. COMP for example, when overexpressed in chondrogenic cultures *in vitro*, brings about reduced levels of proliferation while inducing differentiation (78).

The crucial transcription factor in chondrogenesis is SRY-box (Sox) 9, as it orchestrates the production of the cartilage collagens as well as aggrecan (Figure 1.1). Haploinsufficency in Sox9 results in a lethal condition called campomelic dysplasia, which involves severe skeletal malformations (79). Bi *et al* generated Sox9-/- embryonic stem (ES) cells and analyzed their behaviour in mouse chimeras (80). None of these cells ever contributed to cartilage, but instead clustered around cartilage nodules and retained a spindle shaped appearance. Sox9 -/- ES cells do not express ECM genes and when teratomas are derived from these cells, no cartilage forms (81). Sox9 has DNA binding and transcriptional activity, attaching to an enhancer element to activate the transcription from its targets (80).

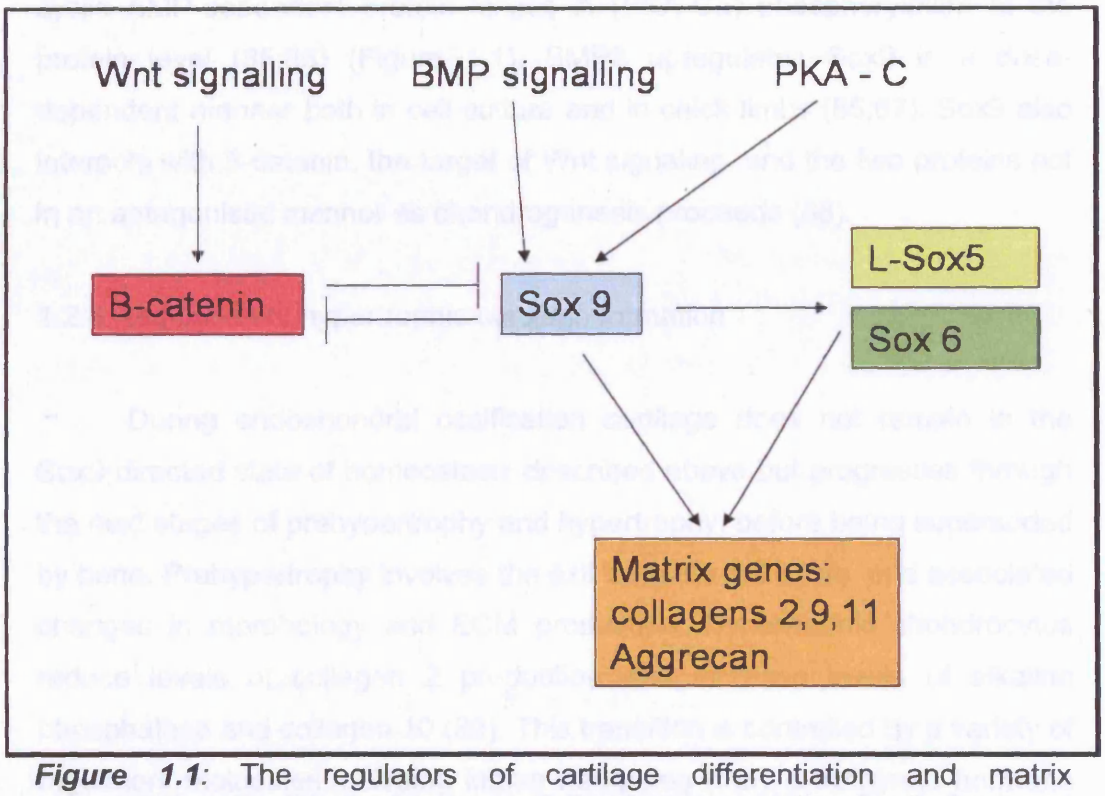

Figure 1.1: The regulators of cartilage differentiation and matrix accumulation. Sox9 is the key transcription factor regulating Sox5, Sox6 and matrix gene transcription. BMP, Wnt and PKA-c signalling regulate Sox9 levels and activity.

Lefebvre *et al* found that Sox9 is coexpressed in cartilage with two more Sox genes Sox5 and Sox6, and that these form homo- and hetero-

dimers and cooperatively activate transcription of ECM genes with Sox9 (82). Sox5 and Sox6 are essential for cartilage formation. Double Sox5 and Sox6 knockout mice are embryonic lethal and single knockout mice of either Sox5 or Sox6 develop to birth but die soon after with respiratory distress (83). These mice do not show overt skeletal abnormalities and are the same weight and size as wildtype newborns (83). Therefore, Sox5 and Sox6 must be at least partially redundant. Sox9 can activate transcription of ECM genes alone, but to a much lower level than in the presence of L-Sox5 and Sox6 (83). Later experiments showed that Sox9 is in fact necessary for the expression of Sox5 and Sox6 (84).

Sox9 is regulated by BMP signalling at the transcriptional level and cyclic AMP-dependent protein kinase A (PKA-Cα) phosphorylation at the protein level (85;86) (Figure 1.1). BMP2 upregulates Sox9 in a dose-dependent manner both in cell culture and in chick limbs (85;87). Sox9 also interacts with β-catenin, the target of Wnt signaling, and the two proteins act in an antagonistic manner as chondrogenesis proceeds (88).

1.2.4 Regulation of hypertrophic cartilage formation

During endochondral ossification cartilage does not remain in the Sox9 directed state of homeostasis described above but progresses through the next stages of prehypertrophy and hypertrophy, before being superseded by bone. Prehypertrophy involves the exit from the cell cycle, and associated changes in morphology and ECM production. Hypertrophic chondrocytes reduce levels of collagen 2 production and increase levels of alkaline phosphatase and collagen 10 (89). This transition is controlled by a variety of regulatory molecules including indian hedgehog (Ihh), parathyroid hormone related peptide (PTHrP), Cbfa1 and the previously mentioned proteins involved in BMP, FGF, Wnt and MAPK signalling (Figure 1.2).

Most experiments exploring the role of PTHrP and Ihh in chondrogenesis were performed by Vortkamp *et al.* They found that both of

these signals suppress hypertrophy and that Ihh upregulates PTHrP, but that signaling from the activated PTHrP receptor represses Ihh production, thereby creating a negative feedback loop (Figure 1.2). The PTHrP receptor (PTHrPR) is expressed on proliferating chondrocytes and its activation prevents hypertrophy (90). PTHrP acts by signaling to PKA-Cα, which then phosphorylates Sox9, enhancing its DNA binding activity, and inhibiting transition to hypertrophy (81). PTHrP is secreted by cells of the perichondrium and hypertrophic cells (79).

BMP and FGF signaling act in an antagonistic manner, with, BMP signaling upregulating Ihh and thus delaying hypertrophy and FGF signaling accelerating chondrocyte terminal differentiation and promoting hypertrophy (91). FGF2 treatment of embryos or overexpression of a constitutively active FGF receptor (such as FGFR3) leads to a shortening of limbs and to disorders characterized by short stature such as achondroplasia (79). FGF signaling reduces the domain of BMP and Ihh expression, but restoring Ihh expression does not rescue the phenotype (92).

Wnt5a and Wnt5b overexpression leads to delayed and reduced ossification and a delay in the expression of Ihh and Col10, hence both of these have a role in preventing premature hypertrophy. However, simply overexpressing Ihh does not fully rescue the phenotype of Wnt5a knockouts, so the role of Wnt5a must be more complex than just the upregulation of Ihh (93).

The intracellular pathway of PTHrP signaling is partially mediated by inhibition of p38 MAPK activity. Inhibition of p38 leads to a decrease in collagen 10 production and an increase in the expression of some prehypertrophic markers such as cartilage matrix protein (CMP). However, PTHrP also acts in a p38 independent manner, for example causing an increase in the expression of link protein, an effect not seen just by inhibiting p38 signalling (94).

Cbfa1 is the main transcription factor expressed by the hypertrophic chondrocytes. Its expression is regulated negatively by PTHrP and positively

by retinoid signaling (95). Mice deficient in Cbfa1 also lack hypertrophic chondrocytes and show no expression of collagen 10, or the later marker of calcification osteopontin (95).

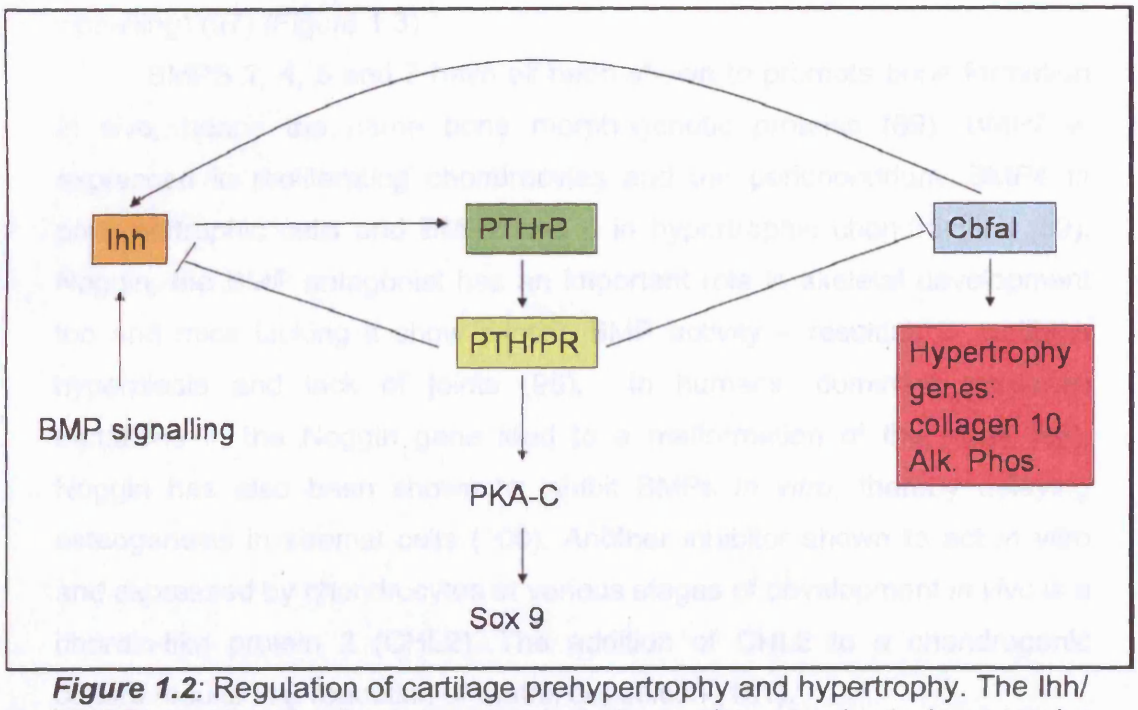

***Figure 1.2**:* Regulation of cartilage prehypertrophy and hypertrophy. The Ihh/ PTHrP negative feedback loop controls the prehypertrophy to hypertrophy transition and the expression of the hypertrophy transcription factor Cbfa1.

1.2.5 TGFß family member involvement in chondrogenesis

The TGFß superfamily consists of TGFß proteins, BMP proteins, activins, and growth and differentiation factors (GDF). TGFß family proteins bind to serine/threonine kinase receptors type I and type II, and the interaction between the 2 receptors is required for signal transduction. The binding of the ligand to the receptor can be interfered with by a range of proteins including Noggin, Chordin, DAN, Sclerostin and Folistatin (96). As the ligand binds, the type I receptor is phosphorylated by the type II receptor and the type I receptor phosphorylates a Smad protein – Smad 1, 5 or 8 in the case of BMP proteins or in the case of TGFß proteins Smad 2 and 3 (96). This phosphorylated Smad is now able to form a complex with Smad 4

and translocate into the nucleus, where it activates transcription of target genes, provided the dimerization is not interfered with by the inhibitory Smads -Smad6 (BMP signalling specific) and Smad 7 (BMP and TGFß signalling) (97) (Figure 1.3).

BMPS 2, 4, 5 and 7 have all been shown to promote bone formation *in vivo,* hence the name bone morphogenetic proteins (89). BMP7 is expressed in proliferating chondrocytes and the perichondrium, BMP4 in prehypertrophic cells and BMP2 and 6 in hypertrophic chondrocytes (89). Noggin, the BMP antagonist has an important role in skeletal development too and mice lacking it show excess BMP activity – resulting in cartilage hyperplasia and lack of joints (98). In humans, dominant missense mutations in the Noggin gene lead to a malformation of the joints (99). Noggin has also been shown to inhibit BMPs *in vitro*, thereby delaying osteogenesis in stromal cells (100). Another inhibitor shown to act *in vitro* and expressed by chondrocytes at various stages of development *in vivo* is a chordin-like protein 2 (CHL2). The addition of CHL2 to a chondrogenic culture results in a reduction of matrix deposition (101).

BMPs enhance chondrogenesis although the precise effect exerted differs from one family member to another. BMP4, for example, accelerates the formation of the mesenchymal condensations, induces chondrogenesis and promotes chondrogenic maturation (102). BMP6, on the other hand, plays a more important part in the later stages of chondrogenic differentiation, inducing hypertrophy (103).

Members of the GDF subfamily have also been reported to play a part in chondrogenesis. GDF5, in particular, induces chondrogenesis and mutations in GDF5 cause alterations in the skeleton, especially in the limbs (102;104).

The overexpression of constitutively active BMP receptors in culture is a sufficiently potent chondrogenic inducer to override the inhibition caused by retinoic acid (Section 1.2.3) (97). The overexpression of the downstream proteins Smad1 or Smad5, however, only has a weak chondrogenic effect,

whereas the overexpression of the inhibitory Smad6 leads to a reduction of levels in BMP7-induced chondrogenesis (97).

BMP signalling is essential for cartilage formation and hence normal skeletal development, but it is also important in the maintenance of cartilage after birth when the absence of a BMP receptor in mouse joints leads to a gradual loss of the cartilage and the development of a condition resembling human osteoarthritis in the affected mice (105).

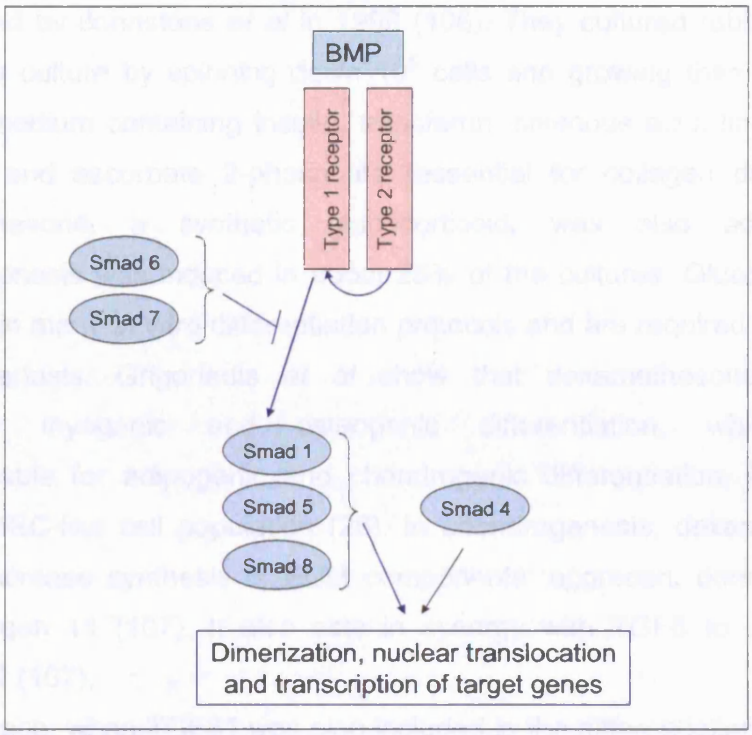

Figure 1.3: BMP signalling cascade. The blue lines represent phosphorylation that begins with the type 2 receptor phosphorylating the type 1 receptor and continues with the phosphorylation of Smad 1, 5 or 8 by the type 1 receptor. This second phosphorylation step can be inhibited by Smad 6 or 7.

1.2.6 *In vitro* chondrogenesis

From *in vivo* studies of chondrogenesis, it is apparent that two main criteria must be met in order to generate chondrocytes in culture. The first is the dependency of chondrogenesis on cell to cell contact and therefore the density at which the cells are cultured and the second is the provision of the appropriate signalling molecules.

In vitro conditions for the culture of chondrocytes from MSC were established by Johnstone *et al* in 1998 (106). They cultured rabbit MSC in aggregate culture by spinning down 10^5 cells and growing them in a high glucose medium containing insulin, transferrin, selenous acid, linoleic acid, pyruvate and ascorbate 2-phosphate (essential for collagen deposition). Dexamethasone, a synthetic glucocorticoid, was also added and chondrogenesis was induced in about 25% of the cultures. Glucocorticoids are used in many *in vitro* differentiation protocols and are required for *in vitro* chondrogenesis. Grigoriadis *et al* show that dexamethasone addition increases myogenic and osteogenic differentiation, while being indispensable for adipogenic and chondrogenic differentiation, in a bone derived MSC-like cell population (28). In chondrogenesis, dexamethasone acts to increase synthesis of ECM components: aggrecan, dermatopontin and collagen 11 (107). It also acts in synergy with TGFß to upregulate collagen 2 (107).

Hence, when TGFβ1 was also included in the differentiation media all the cultures showed a chondrogenic morphology and increased production of cartilage ECM molecules such as collagen 2 and 10 while decreasing the expression of the MSC ECM protein, collagen 1. Mackay *et al* adapted the Johnstone protocol to human MSC and used TGFβ3 to add to cultures instead of TGFβ1, with very similar results (108).

Other members of the TGFß family have also been tested for their ability to induce chondrogenesis *in vitro*. TGFβ2, when transfected in human MSC, also stimulates the expression of collagen 2 and aggrecan, and

retroviral overexpression of BMP2 in murine MSC has the same effect (109;110). Palmer *et al* expressed TGFβ1, BMP2 and IGF1 in MSC with the use of an adenoviral vector and found that TGFβ1 and BMP2 but not IGF1 induced chondrogenesis (111).

Majumdar *et al* employed a different strategy to the one described above for providing the necessary cell to cell interactions for chondrogenesis. They placed the MSC in a 3-D matrix of alginate beads and then cultured them in the presence of BMP2 and BMP9 (112). They observed that both of these molecules enhanced the expression of Sox9 and matrix genes, with BMP9 causing greater upregulation than BMP2. Therefore, both TGFßs and BMPs are able to induce the expression of genes required for chondrogenesis independently but the highest levels of induction are seen when the two are combined. Sekiya *et al* used both TGFβ3 and BMP6 to greatly upregulate cartilage matrix synthesis in differentiating MSC (113).

Another condition that has so far been shown to affect chondrogensis *in vitro* is oxygen tension. Cartilage is a non-vascularised tissue and the oxygen tension is thought to be as low as 1% in the deepest layers, so the atmospheric levels of 21% oxygen, most commonly used in tissue culture are quite different to *in vivo* conditions (114). Domm *et al* showed that lower oxygen tension of 5% is stimulatory to chondrogenesis and induced higher levels of collagen production in bovine articular chondrocytes (115). The key factor involved in the hypoxic response in cells is hypoxia-inducible factor 1 (HIF1), and, if the α subunit of this factor is lacking in hypoxic chondrocytes, results in cell death: hence it appears to be an essential factor for chondrogenesis (116). Furthermore, HIF1α also has an effect on levels of ECM synthesis, and when chondrocytes lacking this protein are placed in hypoxic conditions levels of collagen 2 and aggrecan decrease significantly, whereas they are maintained (and collagen 2 levels are even increased) in wildtype cells (117). To date no experiments have been published detailing the human MSC response to lower oxygen tension in chondrogenesis.

The cell populations used for studying chondrogenic differentiation *in vitro* are very diverse and range from the pluripotent embryonic stem (ES) cell to the fully committed chondroblasts isolated from mature cartilage. ES cells can differentiate into cartilage when grown as embryonic bodies (EB) as seen by the expression of mRNAs such as aggrecan and Sox9 (118). However, only a minority of these cells undergo chondrogenesis. Dexamethasone addition does not enhance the efficiency of chondrogenesis from ES cells whereas culture in micromass or pelleted cultures after EB dissociation does (118). The addition of the full chondrogenic cocktail consisting of BMP2, TGFβ1, insulin and ascorbic acid induces a chondrogenic phenotype, including the upregulation of all the expected chondrogenic genes, albeit at levels significantly lower than those seen in cultures of MSC (119). From a therapeutic viewpoint, the advantage of using ES cells over the more committed mesenchymal or prechondrocyte cells is that they are available in a potentially infinite supply. However, as autologous transplantation cannot be performed, there may be problems with immunological rejection, unless the ES cells are genetically altered so as not to express such proteins on their cell surface (120). It is also clear that the conditions for efficient chondrogenic differentiation of ES cells are still not optimised.

A recently described means of generating chondrocytes from ES cells is via an MSC intermediate. Barberi *et al* used human ES cell lines and co-cultured them with OP9 cells inducing the ES cells to undergo mesenchymal differentiation, prior to exposing them to MSC differentiation protocols, such as that needed for chondrogenesis (121).

If ES cell lines lie at one end of the spectrum, unipotent chondroblasts, isolated from cartilage lie at the other. The advantage of using MSC or chondroblasts over ES cells is that there is a potential for autologous transplantation. This means that cells can be isolated from a patient, expanded *in vitro,* and then reintroduced back into the patient, in the area where they are required for treatment. This procedure has already

shown promising results for the repair of articular cartilage in knee joints (122). When chondrocytes are grown *in vitro* they lose their chondrogenic morphology and the expression of ECM genes. These de-differentiated chondrocytes can be expanded in monolayer cultures and then re-implanted into sites of injury where they potentially differentiate back into fully functional chondrocytes (122). However, whether well formed cartilage forms to repair the defect in the treated patients remains uncertain as these cells have a limited proliferative potential. This is particularly problematic in older patients where treatment for degenerative diseases is more likely to be required .

1.2.7 Summary

Through the help of *in vivo* studies and *in vitro* model systems, the regulation of chondrogenesis is quite well understood, especially with respect to the chondrogenic matrix and the regulation of its production. Less well elucidated are the earlier stages of chondrogenesis, when the commitment of mesenchymal progenitor cells to the chondrogenic lineage is determined. To investigate these early chondrogenic events, the MSC chondrogenesis *in vitro* model system can be used in conjunction with microarray analysis, thereby providing an overview of a large part of the transcriptome and identifying the genes involved in this process.

1.3 GENE EXPRESSION MICROARRAYS

Gene expression microarrays (GEM) are a relatively new tool, enabling the global analysis of expression levels of genes within a population of cells grown *in vitro* or from a tissue sample. This technique makes it possible to compare the levels of expression of many genes between two or more populations within the scope of a few experiments. The procedure involves first harvesting the RNA from the cells of interest, then labelling it, and finally hybridizing it to an array of probes representative of genes of interest. The probes can be cDNA derived 100-2000bp PCR products attached to a glass or nylon matrix to produce the array, or synthesized ~30mer oligonucleotides printed on 'gene chips' such as those manufactured by Affymetrix (123).

Experiments can be performed using one or two-colour microarrays. Two-colour microarray analysis allows the direct comparison of the expression levels between the control state and the state of interest as the samples are labelled with different fluorescent tags (for example cyanine 3 and cyanine 5) and then allowed to hybridize competitively to the same array. Alternatively, the one colour procedure used for most studies employing oligonucleotide chips requires hybridization of a single sample per chip and comparison of the signal intensities between chips (124). There are many possible experimental applications for microarray technology, including the investigation of disease and developmental processes and the effects of various treatments, for example the exposure to a drug, on a population of cells (123).

The biggest problem associated with GEM experiments is also their biggest advantage – the amount of data generated. Some of the more recent chips, such as the Affymetrix HGU133+2 chip, contain probes corresponding to all the genes in the human genome, culminating in the analysis of more than 47,000 transcripts (http://www.affymetrix.com). In order to interpret this data and make it comparable between different experiments, a great deal of

statistical manipulation is necessary and the methods used by investigators are variable (Section 4.1). Furthermore, the results obtained for the same experiment by different groups can vary, an issue not helped by the restriction on the number of replicates done for each experiment due to the high costs of the procedure (125).

1.3.1 Microarrays in chondrogenesis

The comparison of normal and disease states of a tissue is probably the most common use for microarrays, and has become very popular in cancer biology. In the context of chondrogenesis, experiments have been performed comparing normal and osteoarthritic cartilage to investigate which genes are differentially expressed between the two and are therefore likely to be implicated in cartilage degeneration seen in osteoarthritis (126). Matrix metalloproteinases (MMPs) are known to be involved in the process of cartilage matrix turnover. Aigner *et al* found MMP3 to be expressed in normal cartilage and early osteoarthritis and therefore speculated its involvement in the regular turnover of the ECM (126). In more advanced osteoarthritic cartilage, MMP2 and MMP13 were found to be expressed, which may indicate that they have a role in cartilage degeneration (126). Expression of MMPs was also investigated in the cartilaginous neoplasms chondrosarcomas, due to their ability to invade bone (127). Increased expression of MMP13 and 14 was found, with some samples also showing elevated levels of MMP1, 7 and 9. These results indicate that MMPs may be useful as indicators of more aggressive lesions (127). A more recent GEM study, performed by Rozeman *et al* compared chondrosarcomas of different grades and found differences in their metabolism (128). Higher grade tumours upregulated genes involved in glycolysis whilst downregulating the expression of ECM-associated genes (128). Therefore, microarrays can provide information about disease states which can lead to the identification of genes for use in providing diagnoses.

Microarray analysis is also well suited as a method for elucidating the effects of signalling molecules on a population of cells. Dailey *et al* investigated the effect of FGF signalling on the proliferation of a rat chondrosarcoma cell line by exposing the cells to FGF1 and then harvesting the RNA after 3, 6, 9 and 12 hours of exposure (129). GEM analysis allowed them to look at a wide range of molecules involved in the cell cycle and investigate the stages at which FGF signalling is activated. Gaur *et al* used microarrays with probes specific to genes involved in the Wnt signalling pathway to look at differences between wildtype osteoblasts and those where a negative regulator of Wnt signalling had been knocked out and found that the expression of many Wnt-dependent genes was disrupted (130).

The *in vitro* differentiation systems for cartilage mentioned in the previous section can be used in conjunction with microarray experiments to provide information about cartilage development. Tallheden *et al* used dedifferentiated human articular chondrocytes which they re-differentiated *in vitro*. They collected RNA at different time points for analysis on cartilage chips with over 300 probe sets, specific to genes known to be involved in cartilage development and homeostasis (131). The results provide some insight into the temporal sequence of the expression of genes previously implicated in chondrogenesis.

James *et al* recently published a detailed microarray analysis of various time points using mouse micromass chondrogenesis cultures, and identified some general trends, such as changes involved in signal transduction and transcriptional regulation. However, their classifications were generally too broad to be truly enlightening (132). They finished by focusing on a specific factor called rgs2 shown to be involved in the hypertrophy phase of chondrogenesis. Rgs2 was expressed in the growth plate and its overexpression was associated with increased expression of ECM molecules (132).

Microarray analysis has also previously been performed on human MSC undergoing chondrogenesis by Sekiya *et al* (113). Even though they did not use cartilage-specific chips but instead a general Affymetrix chip for expression analysis of a range of human transcripts, they restricted their analysis to genes with a previously described role in chondrogenesis and used their results to support the validity of the MSC differentiation as a model for the study of the development of cartilage *in vitro*. Consequently, they concentrated on later time points in MSC chondrogenesis where the expression of ECM genes becomes apparent (113) .

In a recent study, mouse MSC were used by Robins *et al* to investigate the effect of hypoxia on the expression profile of chondrogenesis (133). Hypoxia induced higher levels of expression of many ECM genes as well as Sox9. Robins *et al* also took the overall description of their microarray data a step further than the James *et al* paper, described above, and found that the greatest expressional differences in response to hypoxia were seen in metabolic genes, along with the expected increase in angiogenic genes (133).

Therefore, GEM experiments have previously been performed on cells undergoing chondrogenesis, but the two time course experiments looking at differentiation stages have not provided a global transcriptional overview of the process nor have they identified novel factors involved in the early stages of chondrogenesis.

The true power of microarray technology lies in the ability to investigate the expression levels of thousands of genes at once and obtain a global picture of the processes occurring. In chondrogenesis, the use of GEM technology in monitoring the transcriptional changes occurring during the early phases could provide insight into the regulatory processes guiding mesenchymal condensation and the commitment of MSC to the chondrogenic lineage.

1.4 CONNECTIVE TISSUE TUMOURS AND CHORDOMAS

1.4.1 A microarray study of connective tissue tumours

A wide spectrum of tumours arise in connective tissue, including bone and soft tissue, that are referred to as sarcomas when malignant. All these tumours presumably originate from mesenchymal precursor cells, and yet show a surprising range of morphologies, which frequently overlap, and the lineage of differentiation is not known in a significant number. Bone and cartilage sarcomas, for example, can both show regions of chondroid and osteoid differentiation as well as dedifferentiated areas with spindle shaped cells and myxoid regions (134). Small needle core biopsies are often all the material available for a diagnosis and correctly identifying the neoplasm can be difficult.

Certain sarcomas, such as pPNET/Ewing's sarcoma, can be identified on the basis of a tumour specific translocation. However others lack such a hallmark and show a complex karyotype, tending to have abnormalities in the commonly affected pathways in cancer – such as the retinoblastoma or p53 pathway (135).

A GEM analysis study was recently published comparing the expression profiles of a broad range of 96 well-defined connective tissue neoplasms (134). These tumours were classified on the basis of their morphology and immunohistochemistry, as well as with the use of molecular genetics, where possible. The aim of this study was to asses the relationship between different tumour types and identify unique molecular fingerprints that could aid in the diagnosis of particular neoplasms. The results showed that differentiated tumours clustered in groups reflecting common tissue types: neurofibromas and schwannomas (both showing nerve sheath differentiation), alveolar and embryonal rhabdomyosarcomas (showing myogenic differentiation), and well-differentiated liposarcomas and lipomas (showing adipocytic differentiation) (Figure1.4.1) (134). Similarities were also

found between the expression profiles of chondrosarcomas and chordomas. The diversity of gene expression was greatest in osteosarcomas, leiomyosarcomas and pleomorphic sarcomas. Many of the genes identified as the molecular fingerprints of a particular tumour type were related to the metabolism or function of its tissue of origin: adipocytic tumours were distinguished by the expression of perilipin and lipoprotein lipase, genes involved in lipid metabolism (136;137). Similarly, the rhabdomyosarcomas expressed cholinergic receptor alpha 1, the muscle acetylcholine receptor and the neurofibromas and the schwannomas expressed Sox10, a gene involved in glial development (138;139). A particularly interesting finding was that, brachyury, a transcription factor known to be involved in notochordal development, was uniquely expressed in chordomas.

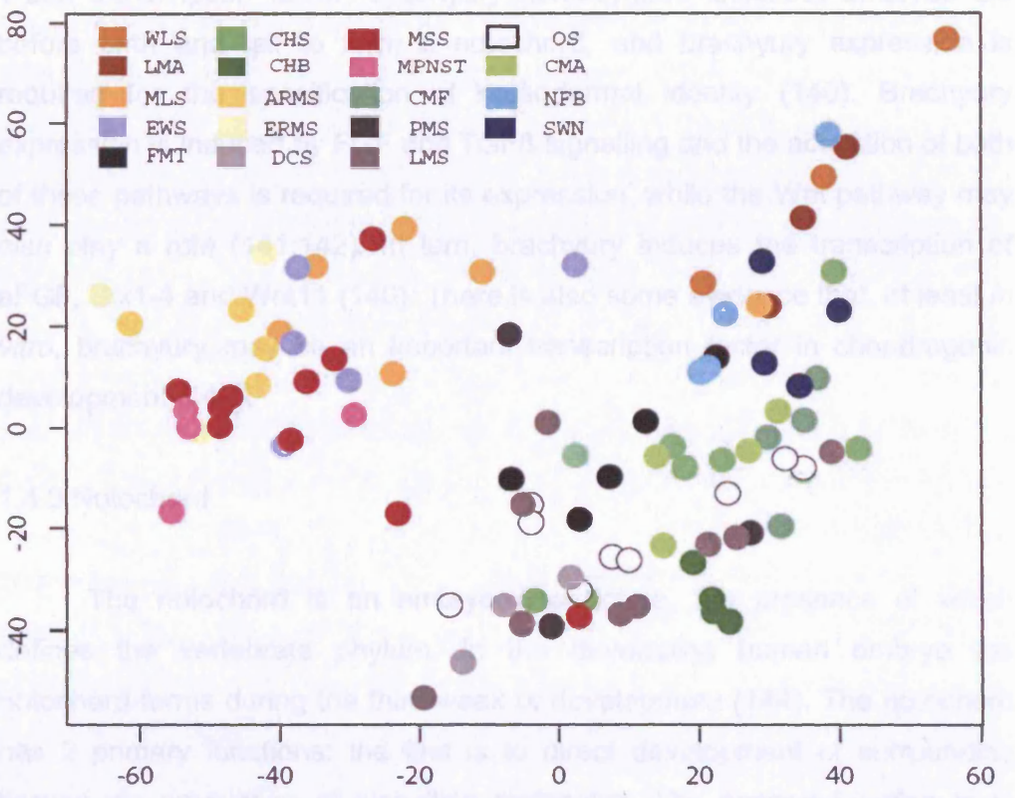

(Figure legend on following page)

Figure 1.4: Multi-dimensional scaling of all 96 mesenchymal tumor samples representing how the GEM profiles of the various tumours relate to each other in a 2-dimensional space. WLS, well-differentiated liposarcoma; LMA, lipoma; MLS, myxoid liposarcoma; EWS, Ewing's sarcoma; FMT, desmoid fibromatosis; CHS, chondrosarcoma; CHB, chondroblastoma; ARMS, alveolar rhabdomyosarcoma; ERMS, embryonal rhabdomyosarcoma; DCS, dedifferentiated chondrosarcoma; MSS, monophasic synovial sarcoma; MPNST, malignant peripheral nerve sheath tumors; CMF, chondromyxoid fibroma; PMS, pleomorphic sarcoma; LMS, leiomyosarcoma; OS, osteosarcoma; CMA, chordoma; NFB, neurofibroma; SWN, schwannoma. (Figure adapted from (134))

1.4.2 Brachyury

One of the key genes regulating notochord formation is brachyury, a T-box transcription factor. Brachyury homozygous knockout embryos die before birth and fail to form a notochord, and brachyury expression is required for the specification of mesodermal identity (140). Brachyury expression is induced by FGF and TGFß signalling and the activation of both of these pathways is required for its expression, while the Wnt pathway may also play a role (141;142). In turn, brachyury induces the transcription of eFGF, Bix1-4 and Wnt11 (140). There is also some evidence that, at least *in vitro*, brachyury may be an important transcription factor in chondrogenic development (143).

1.4.3 Notochord

The notochord is an embryonic structure, the presence of which defines the vertebrate phylum. In the developing human embryo the notochord forms during the third week of development (144). The notochord has 2 primary functions: the first is to direct development of surrounding tissues via production of signalling molecules. The second function is to provide the necessary structural support for the developing embryo, by acting as a turgid rod of cells (145). The notochord secretes a variety of

cytokines, the principal one being Sonic hedgehog (Shh), which is involved in fate specification of various tissues (146). The primary signalling role of the notochord is in specifying the ventral fates in the central nervous system. As the notochord is located beneath the neural tube a gradient of Shh signalling is formed through the developing nervous system, thereby initiating different transcriptional responses in the neural tube cells depending on their proximity to the notochord. In addition, the notochord controls aspects of left right asymmetry, induces the differentiation of pancreatic cells and controls the arterial versus venous identity of blood vessels (147).

In higher vertebrates, the notochord is a temporary tissue, eventually becoming segmented and being superseded by the vertebrae. In lower vertebrates it can persist throughout life and fulfil a structural role. As a tissue, the notochord most closely resembles cartilage and expresses many chondrogenic genes such as collagen 2 and 9, aggrecan, chondromodulin and Sox9 (147). The primary difference between the cells of the notochord and those of cartilage is that while the notochord produces many of the cartilaginous ECM molecules it retains them in large vacuoles rather than excreting them into the extracellular matrix (147). Therefore, in the notochord cells, it is these collagen and proteoglycan filled vacuoles that allow it to exert pressure and perform its structural roles. In humans, as in most vertebrates, the notochord eventually becomes segmented and replaced by bone (vertebral bodies) and by the nucleus pulposus in the intervertebral disc (148). However, the actual contribution of notochordal cells to the nucleus pulposus is unclear. The nucleus pulposus is itself composed of two types of cells – one producing an extracellular matrix, small and chondroid in appearance and the other, much less abundant cell type, more notochordal in appearance with a vacuolated cytoplasm (149). It is this second cell type that is presumed to be notochord derived.

The persistence of small (from a few mm to 2cm) notochordal remnants has been documented at the skull base at an incidence of 0.5-2%

in autopsies (144). More recent evidence supporting the existence of notochordal remnants within the vertebral column has been presented by Yamaguchi *et al*, and indicates that these lesions may be far more common than previously thought (150;151). They examined vertebral columns microscopically, and found small lesions in 20% of the cases. These lesions were mostly located at either end of the spine in the clival and sacro-coccygeal vertebrae with a few found in the cervical and lumbar vertebrae.

1.4.4 Chordoma morphology

Chordomas are rare malignant tumours occurring along the spine and thought to arise from notochordal remnants. The distribution of these lesions is very similar to that seen of the benign notochordal remnants discussed above with 52% occurring in the sacro-coccygeal region, 35% at the skull base and the rest in the cervical and lumbar regions (152). Macroscopically, chordomas appear gelatinous and blue-grey in colour (153). Morphologically, the tumour cells appear in lobules and are of various sizes and shapes, with often prominent vacuoles conferring the typical physalipherous appearance. The cells are embedded in a myxoid matrix.

It is a common finding for chordomas to exhibit some degree of chondroid differentiation. In particular, skull-base chordomas can appear chondroid and therefore be misdiagnosed for chondrosarcomas. Chordomas can also resemble epithelial tumours as well as exhibit nuclear pleomorphism. Occasionally, cases of dedifferentiated chordomas occur, where, in addition to a typical chordoma component, a sharply demarcated region of spindle-shaped 'dedifferentiated' cells is also seen (154).

1.4.5 Chordoma immunophenotype

As chordomas often resemble other tumours such as chondrosarcomas, malignant melanomas, carcinomas, and in particular, renal cell carcinomas, there has been an effort to identify markers that can be used for immunohistochemical classification of the tumour. Cytokeratins (CK) are expressed by chordomas and can be used to distinguish between these and chondroid lesions. O'Hara *et al* reported that chordomas express CK 8 and 19 along with HBME-1 marker (155). However, cytokeratins are epithelial markers and are therefore also expressed by renal cell carcinomas. HBME-1, on the other hand, was not expressed by the renal cell carcinomas but was found to be invariably expressed by chondrosarcomas as well as by most extraskeletal myxoid chondrosarcomas (155). Similarly, S100 and vimentin were expressed by all the chondrosarcomas tested as well as by a majority of the chordomas (155;156). CD10 is another marker useful for distinguishing between renal cell carcinomas and chordomas as it is expressed by the majority of renal cell carcinomas but not by chordomas (157).

In addition to the cytokeratins, chordomas express other epithelial markers such as epithelial membrane antigen (EMA), and in most cases E-cadherin, along with variable expression of catenins α, β and γ all of which interact with E-cadherin (158). Most chordomas also express the neural cell adhesion molecule (N-CAM) (158) .

A combination of these markers can be used to distinguish chordomas from most other tumours but none of them are chordoma specific. While a positive result for cytokeratin expression will indicate that a lesion is not a chondroid tumour, the differential diagnosis of a renal cell carcinoma must still be taken into account. Conversely, if the expression of S100 excludes the diagnosis of a carcinoma, cytokeratin expression still needs to be performed to exclude the possibility of a chondroid lesion. As S100 is not expressed in all chordomas, the diagnosis can not simply be

based upon the combination of S100 and cytokeratin expression, although in many cases, this together with morphological analysis and clinical imaging has been enough to diagnose chordomas confidently.

An additional difficulty arises with small needle core biopsy samples as some reports have shown that cytokeratin expression is not always uniform throughout the sample, particularly in the chondroid component (156;159). These samples may also not be large enough to make a confident morphological diagnosis as they often contain a mixture of cell types.

1.4.6 Extra-axial chordomas

A small number of chordomas arising outside the vertebral column have been reported, some of these within bones (chordoma peripheric um) and others in soft tissue (parachordomas) (160). However, the nomenclature has been a source of some confusion, and the above classification is not always adhered to. Nielsen *et al* state that, while both parachordomas and chordoma peripheric um occur extra-axially, parachordomas are histologically and immunohistochemically distinct from chordomas whereas chordoma peripheric um are not (160). Whether parachordomas and chordomas do actually have distinct immunophenotypes has been a source of controversy not helped by the difficulties in recognising the extra-axial lesions in the first place and the very small numbers of samples available for analysis due to the rare occurrence of these lesions (161;162).

1.5 AIMS

The first aim of this project was to isolate MSC and establish a robust model for their chondrogenic differentiation. Following this, the temporal progression of chondrogenic development was to be investigated using GEM technology, with an initial focus on providing a global description of the process. This could aid in identifying novel factors involved in the early phases of chondrogenesis. This was to be followed by a more detailed analysis of the role of the factors identified in cartilage development and in MSC differentiation in general.

The second part of this project followed on from previous GEM studies of connective tissue tumours and aimed to examine further the relationship between chordomas and chondroid neoplasms, particularly in relation to brachyury, a molecule crucial to notochordal development.

2. METHODS

2.1 OPTIMISATION AND ESTABLISHMENT OF THE MSC CHONDROGENESIS MODEL SYSTEM

2.1.1 MSC isolation

Mesenchymal stem cells were isolated from human bone marrow aspirates obtained after informed consent according to local ethical guidelines (Bone marrow samples provided by Dr Kwee Yong, Department of Haematology, Royal Free and University College Medical School, 98 Chenies Mews, London WC1E 6HX, UK). Donors were healthy individuals aged between 24-55 years old. 10ml of bone marrow was strained through a 40μm cell strainer and an equal volume of phosphate buffered saline (PBS, Invitrogen, Paisley, UK) added. 20ml of Ficoll (Ficoll-Paque PLUS, GE, Little Chalfront, UK) was dispensed into a 50ml falcon tube and the bone marrow/PBS mixture was layered carefully on top. After centrifugation at 1800rpm for 30minutes the interface (containing the MSC) on top of the Ficoll layer was removed with a sterile disposable pipette. The cells were washed in PBS, centrifuged into a pellet and then resuspended in Mesencult media (StemCell Technologies, Vancouver, Canada) containing 10% supplement (StemCell Technologies, Vancouver, Canada) and 1ng/ml bFGF (R&D systems, Minneapolis, MN, USA) and plated on two 10cm dishes. 10ml of media was used per 10cm diameter dish.

2.1.2 MSC culture

The MSC adhered to the culture dish and the non-adherent cells were washed off in a media change 2 days after isolation. After this, the media was changed every 3 days until the cells began to form colonies on the plate after which they were passaged. Generally, the cells were split 1 in 4 every 3

days, and were not allowed to become confluent during expansion. The procedure for splitting cells involved washing them with 5ml phosphate buffered saline (PBS, Invitrogen, Paisley, UK), adding 1.5ml of 0.25% trypsin (Invitrogen, Paisley, UK) and allowing them to dissociate from the tissue culture plate by incubating them at 37°C for 2-3 min. The cells were then washed off the plate with growth medium and transferred to a 15ml falcon to be centrifuged in order to remove any residual trypsin. Cell counts were not performed with every expansion, but when they were, this split approximately equated to 3 x 10^5 cells being seeded per 10cm dish. After expansion, the MSC were frozen down using 1 ml of supplement with 10% v/v dimethyl sulfoxide and stored in liquid nitrogen.

2.1.3 Growth curves

The growth curve assays were performed using an amended version of the 3T3 protocol (163). The experiments were performed in 6-well plates, 35mm in diameter. Initially 6 x 10^5 cells were seeded and allowed to grow for 3 days, when they were detached from the well using 300µl of 0.25% trypsin, resuspended with 1ml of media and counted using a haemocytometer. After the counts, 6 x 10^5 cells were seeded again. The cell counts were performed in triplicate per culture condition or cell sample by seeding 3 wells per sample. In order to calculate the population doubling time the cell counts obtained after 3 days in culture were divided by the initial number of cells seeded (6 x 10^5) and these values were Log2 transformed.

2.1.4 Osteogenic differentiation

MSC were grown to confluence at which point the osteogenic medium, comprising Mesencult and 100nM dexamethasone, 10µM β-glycerol phosphate and 50µg/ml ascorbate-2-phosphate was added. The

medium was changed every 3 days and differentiation was allowed to proceed for 14 to 21 days (All reagents obtained from: Sigma, Poole, UK).

A kit was used to detect the presence of alkaline phosphatase (all reagents obtained from: Sigma, Poole, UK). This involved exposing the cells to a 2% citrate/60% acetate solution for 30 seconds, and then rinsing twice with dH_2O. The stain (1 dye capsule dissolved in 49ml dH_2O with 2ml Naphthol AS-MX) was applied for 30 seconds, after which the cells were rinsed with dH_2O for 2 min. Mayer's Haematoxylin solution was applied for 10 minutes, when it was removed by 2 washes with dH_2O.

Calcium deposition during osteogenic differentiation was assessed with Alizarin Red staining. Cells were fixed with ice-cold 100% methanol for 15 minutes, and then washed 3 times with dH_2O and stained for 10 minutes with 1.5% w/v Alizarin red (pH 4.2 with ammonium hydroxide). Excess stain was removed with further dH_2O washes and cells were left to air-dry before being visualized (all reagents obtained from: Sigma, Poole, UK).

2.1.5 Adipogenic differentiation

MSC were grown to confluence at which point the adipogenic medium comprising Mesencult with 1μM dexamethasone (Sigma, Pool, UK), 500μM IBMX (Sigma, Pool, UK), 2μM indomethacin (Sigma, Pool, UK), 10μg/ml insulin (Roche, Indianapolis, IN, USA) was added. The medium was changed every 3 days and differentiation was allowed to proceed for 7 to 14 days.

Adipocytes were identified using the oil red O lipid stain (all reagents obtained from: Sigma, Poole, UK). This entailed removing the medium from the plates, rinsing the cells with PBS, and fixing the cells by applying 8ml of 4% formaldehyde, 75mM sodium phosphate buffer, 3% methanol for 30 minutes. The fixative was then removed and the plate washed 3 times with PBS, before applying 8ml of oil red dye (600μg/ml oil red dissolved in

isopropanol; diluted 60:40 in water and filtered) and incubating in the dark for 1 to 4 hours. Plates were rinsed with 50% ethanol and covered with PBS.

2.1.6 Chondrogenic culture

Chondrocyte differentiation media was comprised of high glucose DMEM (Invitrogen, Paisley, UK) with 1% penicillin/streptomycin (Invitrogen, Paisley, UK), 10^{-7}M Dexamethasone (Sigma, Poole, UK), 50µg/ml ascorbate-2-phosphate (Sigma, Poole, UK), 40µg/ml l-proline (Sigma, Poole, UK), 100µg/ml sodium pyruvate (Sigma, Poole, UK) , 50 mg/ml ITS + Premix (6.25µg/ml insulin, 6.25µg/ml transferrin, 6.25ng/ml selenious acid, 1.25mg/ml BSA, 5.25mg/ml linoleic acid) (BD Biosciences, Franklin Lakes, NJ, USA), 500ng/ml BMP6 (R&D systems, Minneapolis, MN, USA), 10ng/ml TGFβ3 (R&D systems, Minneapolis, MN, USA). 2.5 x 10^5 MSC were suspended in 500µl of chondrocyte differentiation media, placed in a 15ml falcon tube and centrifuged at 600g for 5 minutes so the cells formed a loose pellet at the bottom. These pellets were incubated in the falcon tubes at 37°C, 5% CO_2 for 4 days before the first media change after which the differentiation media was changed every 3 days and differentiation was allowed to proceed for 14 to 21 days.

Experiments that were performed under hypoxic (3% [O_2]) conditions were carried out within a humidified anaerobic chamber (Coy Laboratory Products, Grass Lake, MI, USA). The chamber was digitally set at the required O_2 concentration and was maintained at 37°C by a thermostatic controller.

2.1.7 Wax embedding of pellets and sectioning

Pellet measurements were taken using a graticule eye-piece. For histology, chondrocyte pellets were fixed in 4% paraformaldehyde (Sigma,

Poole, UK), 2X PBS (Invitrogen, Paisley, UK) overnight at 4°C. Pellets were then placed in 'Cellsafe' biopsy capsules (Raymond Lamb, Eastbourne, UK) and put through the following dehydration steps: 30% ethanol, 10 minutes; 80% ethanol, 10 minutes; 95% ethanol, 10 minutes; 100% ethanol, 30 minutes; xylene, 20 minutes. Pellets were then embedded in paraffin (Raymond Lamb, Eastbourne, UK) and left overnight to set at 4°C. Wax sections were cut 5µm thick and floated in a water bath at 40°C before being applied to polysine coated slides, and allowed to dry on a hotplate overnight.

Slides were de-waxed in xylene for 10 minutes, rehydrated in 100% ethanol 5 minutes, 90% ethanol 5 minutes, 70% ethanol 5 minutes and washed in distilled water. The toluidine blue stain (0.1%w/v toluidine blue dissolved in 0.1M sodium phosphate buffer – 188ml of 0.1M NaH_2PO_4 and 12ml 0.1M Na_2HPO_4) (Sigma, Poole, UK) was applied for 45 seconds and washed with distilled water. The slides were then dehydrated by consecutive ethanol washes (70%, 90%, 100%), and dipped in xylene for 5 minutes. Slides were air dried and mounted with DPX (BDH, Poole, UK).

2.1.8 Culture of normal human articular chondrocytes (NHAC)

NHAC cells were obtained from Cambrex (Cambrex, Nottingham, UK) and cultured according to the manufacturer's instructions. The cells were first expanded using the Chondrocyte Growth Medium Bullet kit (Basal medium with R3-IGF-1, bFGF, insulin, transferrin, fetal bovine serum 5%, gentamicin/ amphotericin) (Cambrex, Nottingham, UK) and then differentiated using the protocols detailed under 2.1.4, 2.1.5 and 2.1.6.

2.1.9 RNA isolation

RNA was isolated from cells using the RNAeasy kit (Qiagen, Crawley, UK). 600µl of RLT buffer were applied directly to a 10cm dish or 350µl per well of a 6-well plate. The cells were then disrupted by centrifuging them

through a QIAshredder column (Qiagen) and the RNA isolated using the RNAeasy mini kit (Qiagen, Crawley. UK) according to the manufacturer's instructions.

2.1.10 RNA isolation from pellets

For RNA isolation, pellets grown in chondrogenic differentiation media for longer then 5 days were first incubated with 3mg/ml collagenase IV (Invitrogen, Paisley, UK), 1mg/ml hyaluronidase (Sigma, Poole, UK) and 0.25% trypsin (Invitrogen, Paisley, UK) for 3h at 37°C. The pellets were then dissociated with repeat pipetting before being placed in 350µl RLT buffer (Qiagen, Crawley, UK) and centrifuged through a QIAshredder (Qiagen, Crawley, UK) column to disrupt the cells. RNA was then isolated using the RNAeasy mini kit (Qiagen, Crawley, UK) according to the manufacturer's instructions. MSC or cells grown in chondrogenic culture for less then 5 days were placed in RLT buffer and disrupted by rapid pipetting and passing through a QIAshredder column before RNA isolation with the RNA easy mini kit according to the manufacturer's instructions. The isolated RNA was stored at -80°C.

2.1.11 RNA isolation from MSC differentiated into adipocytes

RNA from MSC exposed to adipogenic media for more then 7 days was isolated using the RNAeasy lipid mini kit (Qiagen, Crawley, UK). 1ml of Qiazol reagent (Qiagen, Crawley, UK) was applied to the cells in a 10cm dish and left on the cells for 2 to 3 minutes. The cells were scraped off using a cell-scraper and spun through a QIAshredder (Qiagen, Crawley, UK) column before proceeding with the RNA isolation according to the manufacturer's instructions.

2.1.12 RT-PCR

Reverse transcription PCRs were performed using the Superscript II enzyme kit (Invitrogen, Paisley, UK) according to manufacturer's instructions and with 100ng starting RNA. Briefly, 1µl OligodT_{18} (500µg/µl) and 1µl dNTP mix (Promega, Madison, WI, USA) was added to 100ng total RNA, and the volume made up to 12µl with RNAse free water (Invitrogen, Paisley, UK). This mixture was incubated for 5 minutes at 65°C and briefly chilled on ice before the addition of 4µl of 5X First Strand Buffer (Invitrogen, Paisley, UK) and 2µl 0.1M DTT (Invitrogen, Paisley, UK). This mixture was then incubated at 42°C for 2 minutes, before the addition of 1µl of the Superscript II reverse transcriptase (Invitrogen, Paisley, UK) The subsequent PCRs were performed in 25µl reaction volumes with 2.5µl of 10X reaction buffer with 50mM $MgCl_2$, 0.5µl of 10mM dNTP, 0.5µl of 10uM of each primer, 0.2µl of 5U/µl Taq polymerase, 1µl cDNA (from the reverse transcription reaction). For GAPDH, Sox5, osteocalcin, Col1a1, aP2 and PTHrPR primers, 1.25µl DMSO was added to a reaction mix containing 2.5µl of 10X reaction buffer with 50mM $MgCl_2$, 1µl of 10mM dNTP, 2.5µl of 10µM of each primer, 0.3µl of 5U/ul Taq polymerase and 1µl cDNA. The cycling times were, 94°C for 2 minutes; and then 30 cycles of 94°C for 30 seconds, 55°C for 1 minute, 72°C for 45 seconds; 72°C for 10 minutes. The reactions were then run on a 2% agarose gel, in 1X TAE buffer (National Diagnostics, Hessle Hull, UK). The following primers were used:

OSTEOCALCIN (forward)	TGAGAGCCCTCACACTCCTC
OSTEOCALCIN (reverse)	CTGGAGAGGAGCAGAACTGG
COL1A1 (forward)	CACTGGTGCTAAGGGAGAGC
COL1A1 (reverse)	CTCCAGCCTCTCCATCTTTG
COL2A1 (forward)	TTCAGCTATGGAGATGACAATC
COL2A1 (reverse)	AGAGTCCTAGAGTGACTGAG
COL10A1 (forward)	CACCAGGCATTCCAGGATTCC
COL10A1 (reverse)	AGGTTTGTTGGTCTGATAGCTC
COMP (forward)	TGGGCCCGCAGATGCTTC

COMP (reverse)	AGGTTTGTTGGTCTGATAGCTC
LINK (forward)	CCTATGATGAAGCGGTGC
LINK (reverse)	TTGTGCTTGTGGAACCTG
SOX5 (forward)	AGCCAGAGTTAGCACAATAGG
SOX5 (reverse)	CATGATTGCCTTGTATTC
SOX6 (forward)	ACTGTGGCTGAAGCACGAGTC
SOX6 (reverse)	TCCGCCATCTGTCTTCATACC
SOX9 (forward)	GAACGCACATCAAGACGGAG
SOX9 (reverse)	TCTCGTTGATTTCGCTGCTC
PTHrP (forward)	CTCGGAGCGTGTGAACATTCC
PTHrP (reverse)	CTTCCGGAAAGTTGATTCCAC
PTHrP-R (forward)	AGGAACAGATCTTCCTGCTGCA
PTHrP-R (reverse)	TGCATGTGGATGTAGTTGCGCGT
BMP-2 (forward)	CAGAGACCCACCCCCAGCA
BMP-2 (reverse)	CTGTTTGTGTTTGGCTTGAC
BMP-6 (forward)	CTCGGGGTTCATAAGGTGAA
BMP-6(reverse)	ACAGCATAACATGGGGCTTC
AGGRECAN (forward)	GAAGGAGGTAGTGCTGCTGG
AGGRECAN (reverse)	ACGTCCTCACACCAGGAAAC
GAPDH (forward)	GATCATCAGCAATGCCTCCT
GAPDH (reverse)	TGTGGTCATGAGTCCTTCCA

2.2 MICROARRAY ANALYSIS OF CHONDROGENESIS

2.2.1 Preparation of RNA for microarrays

RNA isolated from the differentiations was quantified using a nanodrop machine and quality tested using RNA 6000 Nano chips on Agilent 2100 Bioanalyser according to the manufacturer's instructions (Agilent Technologies, Cheshire, UK). RNA quality-control threshold was 28s/18s<2. 2μg of total RNA from each sample was then processed using the One-Cycle cDNA Synthesis Kit (Affymetrix, Santa Clara, CA, USA) according to manufacturer's instructions. Briefly, 2μg RNA was reverse-transcribed into cDNA and then the second strand was synthesized. The resulting double stranded cDNA was *in vitro* transcribed to obtain biotinylated cRNA, quantified using the nanodrop and 20μg were fragmented for hybridization. The cRNA was hybridized to HG-U133A Human Chips (Affymetrix, Santa Clara, CA, USA), according to the manufacturer's recommendations. Hybridization of the synthesised probes and scanning of the images were performed by the scientific services team (Scientific Services, Wolfson Institute for Biomedical research, The Cruciform Building, Gower Street, University College London, London, WC1E 6BT) who also produced the CEL data files for further analysis.

2.2.2 Analysis of microarray data

Most of the initial data analysis was performed by Dr Stephen Henderson (Wolfson Institute for Biomedical research, The Cruciform Building, Gower Street, University College London, London, WC1E 6BT) using the R statistical software and programming language with the packages 'affy' and 'limma'. Robust multi-array average (RMA) was used to background correct, to normalize the data and then to calculate expression values for each probe set (164). The levels of differential expression between arrays were then

calculated using moderated standard deviation and the P-value adjusted for multiple testing using the false discovery rate model (165). Cluster and Treeview (http://rana.lbl.gov/EisenSoftware.htm) were then used to organize genes, showing a significant amount of change, by behavioural patterns with hierarchical clustering. The steps of analysis listed above were performed by Dr Stephen Henderson and are described in more detail in the microarray results chapter 4.

The lists obtained from the statistical analysis above were used for further analysis with other tools such as the WebGestalt ontology tool, GeneCard and Pubmed (Section 4.1.2).

2.3 NOTCH SIGNALLING IN CHONDROGENESIS

2.3.1 DMSO treatment of MSC

DMSO concentration was optimized for the chondrogenic *in vitro* model system (Sigma, Poole, UK). MSC were exposed to various concentrations of DMSO (1µl/ml, 2µl/ml and 5µl/ml) 16 hours prior to induction of differentiation and alongside the differentiation inducers throughout the differentiation (as detailed under 2.6). Differentiation was allowed to proceed for 21 days and the pellets were measured with a graticule eye-piece at days 7, 14 and 21 before being fixed and stained as detailed in Section 2.1.7.

2.3.2 DAPT treatment of MSC

DAPT (Merck Biosciences, Darmstadt, Germany) was dissolved in DMSO (Sigma, Pool, UK) to make 20mM and 10mM stocks which were then added to the MSC cultures at 1:1000 dilution producing a final concentration of 10µM DAPT and 20µM DAPT. In all cases where DAPT treatment was used in conjunction with differentiation medium, DAPT or DMSO was applied 16 hours prior to induction of differentiation and alongside the differentiation inducers throughout the differentiation. MSC were allowed to reach confluence before DAPT or DAPT and 100nM dexamethasone treatment.

2.3.3 DAPT treatment in chondrogenesis

Chondrogenesis was performed as detailed under 2.1.6. Six pellets were grown per condition, and the experiment was performed in duplicate. In the case of DAPT treatment, the MSC were exposed to 1µl/ml DMSO, 10µM DAPT or 20µM DAPT for 16 hours prior to growing in pellet cultures and throughout the differentiation process (Section 2.1.6). Differentiation was

allowed to proceed for 21 days and the pellets were measured with a graticule eye-piece at days 7, 14 and 21 before being fixed and stained as detailed under 2.1.7.

2.3.4 RNA isolation and RT-PCR

The RNA isolation was performed as detailed under 2.1.11, 2.1.12 and 2.1.13. Reverse transcription PCRs were performed using the Superscript II enzyme kit (Invitrogen, paisley, UK) according to the manufacturer's instructions and with 100ng starting RNA. The subsequent PCRs were performed using DyNAzyme kits (Finnzymes, Espoo, Finland) in 25µl reaction volumes using 2.5µl of 10X reaction buffer containing 50mM $MgCl_2$, 1µl of 10mM dNTP (Promega, Madison, WI, USA), 2.5µl of 10µM of each primer (Thermo), 0.25µl of 5U/µl Taq polymerase, 1.25µl DMSO and 1µl cDNA. The cycling times were, 94°C for 2 minutes; and then 28 cycles of 94°C for 30 seconds, 55°C for 1 minute, 72°C for 45 seconds; 72°C for 10 minutes. The reactions were then run on a 1.5% agarose gel, in 1X TAE buffer (National Diagnostics, Hessle Hull, UK). The following primers were used:

HES1 (forward)	CTACCCCAGCCAGTGTCAAC
HES1 (reverse)	CATTGATCTGGGTCATGCAG
HEY1 (forward)	AACTGTTGGTGGCCTGAATC
HEY1 (reverse)	CCAGTTCAGTGGAGGTCGTT
Col2a1 (forward)	TTCAGCTATGGAGATGACAATC
Col2a1 (reverse)	AGAGTCCTAGAGTGACTGAG
GAPDH (forward)	GATCATCAGCAATGCCTCCT
GAPDH (reverse)	TGTGGTCATGAGTCCTTCCA

2.3.5 DAPT treatment in osteogenesis and adipogenesis

Adipogenesis was carried out as detailed under 2.4. The media was changed every 3 days. In the case of DAPT treatment the hMSC were exposed to either 1µl/ml DMSO, 10µM DAPT or 20µM DAPT 16 hours prior to exposing to differentiation media and thereafter. Adipogenesis was allowed to proceed for 14 days before the cells were stained with oil red O (as detailed in Section 2.1.4).

Osteogenesis was carried out as detailed under 2.1.5. The media was changed every 3 days. In the case of DAPT treatment, the hMSC were exposed to either 1µl/ml DMSO, 10µM DAPT or 20µM DAPT 16 hours prior to exposing to differentiation media and thereafter. Osteogenesis was allowed to proceed for 21 days before the cells were stained with alizarin red or for alkaline phosphatase activity as described in section 2.1.5. When osteogenic and adipogenic staining were combined the cells were first stained for alkaline phosphatase activity before staining for oil red O (as detailed in Section 2.1.4 and 21.5 respectively).

2.3.6 *In situ* hybridizations

2.3.6.1 Fixing of mouse embryos for *in situ* hybridizations

Pregnant female wildtype mice were culled at day 11.5 (E11.5), 13.5 (E13.5) and 15.5 (E15.5) gestation. The bodies of E11.5, E13.5 and the limbs of E15.5 were fixed overnight in 4% paraformaldehyde at 4°C (Sigma, Poole, UK), and then placed in 20% w/v sucrose (Sigma, Poole, UK) in diethylpyrocarbonate (DEPC) (Sigma, Poole, UK) treated PBS (Invitrogen, Paisley, UK) overnight at 4°C. The embryo bodies and limbs were then embedded in OTC compound (Raymond Lamb, Eastbourne, UK), snap frozen on dry ice and kept at -80°C. Sections 10µm thick were cut on a cryostat and placed on Superfrost slides (VWR, Leuven, Belgium).

2.3.6.2 Cloning the collagen 2 template for probes

RNA was isolated from an E13.5 mouse embryo using the TRIzol LS reagent (Invitrogen, Paisley, UK) according to the manufacturer's instructions. 750µl of TRIzol LS reagent was added to the embryo tissue and the tissue was homogenized using a power homogenizer. The samples were incubated for 5 minutes at room temperature and 200µl of chloroform was added. Tubes were then shaken for 15 seconds, left to stand for 5 minutes at room temperature and centrifuged at 12,000g for 15 minutes at 4°C. Following centrifugation, the aqueous phase was transferred to a new tube and the RNA precipitated using 500µl isopropanol and incubating at room temperature for 10 minutes. The mixture was then centrifuged at 12,000g for 10 minutes at 4°C and the supernatant discarded. The pellet was washed with 1ml of 75% ethanol, vortexed and centrifuged at 7,500g for 5 minutes at 4°C. The supernatant was then discarded, the RNA pellet air-dried for 5-10 minutes and re-dissolved in 100µl DEPC-treated water.

The RNA was reverse transcribed as detailed in section 2.1.12

In order to amplify the mouse collagen 2a1 gene, a PCR was set up using the E13.5 cDNA and DyNAzyme kits (Finnzymes, Espoo, Finland) in a 50µl reaction. 2.5µl DMSO was added to a reaction mix containing 5µl of 10X reaction buffer with 50mM $MgCl_2$, 2µl of 10mM dNTP, 5µl of 10µM of each primer, 0.6µl of 5U/ul Taq polymerase and 1µl cDNA. The cycling times were, 94°C for 2 minutes; and then 30 cycles of 94°C for 30 seconds, 55°C for 1 minute, 72°C for 45 seconds; 72°C for 10 minutes. The reaction was run on an 0.8% gel, in 1X TAE buffer (National Diagnostics, Hessle Hull, UK). The following primers were used:

mCOL2A1 (forward) CTGGAGCCAAAGGATCCGCT
mCOL2A1 (reverse) CGGAATTCTTCTCCTTGATCACCCTTGG

After PCR amplifying the sequence and running it on a 1% agarose gel in TAE buffer (National Diagnostics, Hessle Hull, UK), the DNA fragment was cut out and purified using a QIAquick gel extraction kit (Qiagen, Crawley, UK). As the primers used to amplify collagen 2 were designed to include the *BamHI* and *EcoRI* sequence, a restriction digest was set up using these two enzymes (Promega, Madison, WI, USA) and the reaction incubated at 37°C for 1 hour. The same digest was performed on the pSPT18 (Roche, Indiannapolis, IN, USA). Both of these reactions were run on a 1% agarose gel and purified using the QIAquick gel extraction kit (Qiagen, Crawley, UK). A ligation was set up using 1µl of the purified linearised plasmid DNA and 3µl of the purified collagen 2 sequence with T4 DNA ligase (Promega, Madison, WI, USA) and incubated at 16°C overnight. The ligated plasmid was transformed into TOP10 chemically competent cells (Invitrogen, Paisley, UK). Colonies were checked for presence of plasmid and insert and a positive clone inoculated into 500ml Luria-Bertani (LB) broth (Sigma, Poole, UK). The plasmid was then purified using The QiaPrep Maxi kit (Qiagen, Crawley, UK).

2.3.6.3 Cloning the Sox9 template for probes

A pCMV-mmSox9 plasmid was obtained from Prof Michael Wegner (Lehrstuhl für Biochemie und Pathobiochemie, Universität Erlangen-Nürnberg, Fahrstraße 17, 91054 Erlangen, Germany). The Sox9 fragment was isolated using the *BamHI* and *XbaI* enzymes (Promega, Madison, WI, USA) and incubating at 37°C for 1 hour. The same digest was performed on the pSPT18 (Roche, Indiannapolis, IN, USA). Both of these reactions were run on a 1% agarose gel and purified using the QIAquick gel extraction kit (Qiagen, Crawley, UK). A ligation was set up using 2µl of the purified linearised plasmid DNA and 3µl of the purified Sox9 sequence, with T4 DNA ligase (Promega, Madison, WI, USA) and incubated at 16°C overnight. The ligated plasmid was transformed into TOP10 chemically competent cells

(Invitrogen, Paisley, UK). Colonies were checked for presence of plasmid and insert and a positive one inoculated into 500ml Luria-Bertani (LB) broth. The plasmid was then purified using The QiaPrep Maxi kit (Qiagen).

2.3.6.4 Cloning the HES1 and HEY1 template for probes

IMAGE clones were purchased of HES1 and HEY1 sequences (IMAGE numbers: 6478994 and 374164, NCBI accession numbers: BQ938563 and AI414254 respectively). The HES1 sequence was cloned within the pCMV-SPORT6 vector that already contained a T7 promoter in the appropriate orientation with respect to the insert. The HEY1 sequence was within pT7T3D but not in the correct orientation for the T7 promoter to be used and therefore needed to be inserted into a different vector. The HEY1 sequence was isolated using a *NotI* and *EcoRI* digest (enzymes from Promega, Madison, WI, USA) and a pCR2.1-TOPO vector (Invitrogen, Paisley, UK) was linearised using the same enzymes. A ligation was set up using 2µl of the purified linearised pCR2.1-TOPO DNA and 3µl of the purified HEY1 sequence with T4 DNA ligase (Promega, Madison, WI, USA) and incubated at 16°C overnight. The ligated plasmid was transformed into TOP10 chemically competent cells (Invitrogen, Paisley, UK). Colonies were checked for presence of plasmid and insert and a positive clone inoculated into 500ml LB broth (Sigma, Poole, UK). The pCMV-SPORT6-HES1 was also inoculated into 500ml LB broth (Sigma, Poole, UK). The plasmids were then purified using the QiaPrep Maxi kit (Qiagen, Crawley, UK).

2.3.6.5 *In vitro* transcription of probes

10µg of each plasmid DNA (pSPT18-mCol2, pSPT18-mSox9, pCMV-SPORT6-HES1, pSPT18-HEY1) was linearised using 5µl of an enzyme that cuts at the beginning of the insert sequence and incubated at 37°C for 2 hours. The enzyme was inactivated by adding 5µl of 10% sodium dodecyl

sulphate (Sigma, Poole, UK) and 1µl of 20mg/ml Proteinase K (Roche, Indiannapolis, IN, USA) to the restriction digest and incubating at 55°C for 15 min. The linearised plasmids were then purified using the QIAquick gel extraction kit (Qiagen, Crawley, UK).

For the *in vitro* transcription reaction the DIG RNA Labelling Kit (Roche, Indiannapolis, IN, USA) was used according to the manufacturer's instructions. Briefly, RNAse-free water was added to 1µg of purified template DNA to a final volume of 13µl and then 2µl of 10 x NTP labeling mixture, 2µl transcription buffer, 1µl RNase inhibitor and 2µl RNA polymerase T7 was added. This mixture was incubated at 37°C for 2 hours, then 80µl of RNase-free water was added and 5µl ran on a 1% gel for quantification. The probe was kept at -80°C until used.

Ready made PDGFRA probe were a kind gift from Dr Nikoletta Tekki-Kessaris (Wolfson Institute for Biomedical research, The Cruciform Building, Gower Street, University College London, London, WC1E 6BT).

2.3.6.6 In situ hybridization

Probes were diluted in *in situ* hybridisation buffer 1:1000 and denatured by incubating at 70°C for 10 min. 200µl of diluted probe was added to each slide and the slides were covered with 22mm x 50mm coverslips (previously incubated overnight at 220°C). The probes were hybridised to the cut sections overnight at 65°C in a sealed Perspex box lined with Whatman paper soaked in *in situ* wash buffer. The following day, the slides were transferred into coplin jars and washed in *in situ* wash buffer at 65°C for 15 minutes to allow the coverslips to fall off. This was followed by 2 more washes in *in situ* wash buffer at 65°C for 30 minutes each. The slides were then incubated in MABT at room temperature twice for 30 minutes. Slides were then transferred to a humidifying chamber, 400µl of blocking buffer was applied to each slide and incubated for 1 hour at room temperature. The anti-DIG-AP, Fab fragments (Roche, Indiannapolis, IN,

USA) antibody was diluted in blocking buffer 1:1500, 400µl was applied to each slide and incubated overnight at 4°C. The next day, the sections were washed in room temperature MABT 4 times for 20 min and then rinsed in staining buffer without nitro blue tetrazolium (NBT) and 5-bromo-4-chloro-3-indolyl phosphate, p-toluidine salt (BCIP). Slides were then transferred to staining buffer and incubated at 37°C for 3 hours for those stained with the col2 probe and overnight for the sox9, HES1 and HEY1 probes. Finally, the slides were rinsed in dH_2O, dehydrated (with consecutive 5 minutes ethanol washes in 50%, 80% and 95% ethanol, and immersed in xylene for 5 minutes) and mounted with DPX (BDH, Poole, UK).

2.3.6.7 Composition of reagents for *in situ* hybridization

In situ hybridization buffer

For 10 ml: 1ml of 10X salts (2M NaCl, 50mM EDTA, 100mM Tris-HCl pH 7.5, 50mM $NaH_2PO_4.2H_2O$, 50mM Na_2HPO_4), 5ml deionised formamide, 2ml of 50% w/v dextran sulphate, 1ml of 10mg/ml baker's yeast rRNA, 100µl of 100X Denhardt's Solution (2% w/v BSA, 2% w/v Ficoll, 2% w/v PVP in DEPC-treated water) and 900µl DEPC-treated distilled water. This mixture was aliquoted and stored at -20°C until used (all reagents from Sigma, Poole, UK).

MABT – maleic acid buffer

100mM maleic acid, 150mM NaCl – pH to 7.5 with NaOH. Finally, 0.1% v/v Tween 20 was added and the mixture was stored at room temperature (all reagents from Sigma, Poole, UK).

Blocking buffer

Boehringer blocking reagent (Roche, Indiannapolis, IN, USA) was made up in MABT as a 10% stock. This was heated to 65°C and autoclaved. The

solution applied to the slides was further diluted to 2% boehringer blocking reagent and 10% sheep serum (Sigma, Poole, UK).

Staining buffer without NBT and BCIP

For 200ml: 4ml 5M NaCl, 10ml 1M $MgCl_2$, 20ml 1M Tris pH9.5, 200µl Tween 20 (all reagents from Sigma, Poole, UK).

Staining buffer

To 20ml staining buffer without NBT and BCIP, 1ml 1M $MgCl_2$, 87µl NBT, 67µl BCIP and 20ml poly-vinyl alcohol (10% w/v) was added (all reagents from Sigma, Poole, UK).

2.4 IDENTIFICATION OF BRACHYURY AS A CHORDOMA MARKER

The work presented in this chapter is based upon previously published work by the group (134).

2.4.1 Microarray analysis

Microarray analysis for this study was performed as detailed under 2.2.2 using the R statistical environment in Bioconductor. The 'affy' package was used to perform the normalization steps using the RMA algorithm (chapter 4 offers a more detailed description). The 'limma' package was used to select statistically significant differences in expression between tumour groups. The heatmaps were produced using Cluster and Treeview software. This analysis was performed by Dr Stephen Henderson (Wolfson Institute for Biomedical research, The Cruciform Building, Gower Street, University College London, London, WC1E 6BT).

2.4.2 RT-PCR analysis

RNA was extracted using the TRIzol reagent (Invitrogen, Paisley, UK) followed by purification with RNeasy columns (Qiagen, Crawley, UK) according to the manufacturer's instructions. Tumour RNA was converted to cDNA using the Superscript II RT-PCR kit (Invitrogen, Paisley, UK) according to the manufacturer's instructions using 200ng of total RNA and OligodT primers (Thermo, Ulm, Germany). PCR was performed using 1µl of the cDNA reaction and 30 cycles of 94°C for 30 seconds, 55° for 1 minute, 72° for 1 minute using PCR DyNAzyme kit (Finnzymes, Espoo, Finland). The products were resolved by electrophoresis on a 1.5% agarose gel in 1X TAE buffer (National Diagnostics, Hessle Hull, UK)

Brachyury (forward) GCCAGACTGGAGAGTTGAGG

Brachyury (reverse)	CAGGTGGTCCACTCGGTACT
GAPDH (forward)	GATCATCAGCAATGCCTCCT
GAPDH (reverse)	TGTGGTCATGAGTCCTTCCA

2.4.3 Tissue retrieval

Cases of chordomas, other tumors and normal tissue were retrieved from the archives of the Royal National Orthopaedic Hospital NHS Trust, University College NHS Trust, the Institute of Neurology, UCL and Guy's and St.Thomas' Hospitals, and this study was approved by the ethics committees of these hospitals. The selection was restricted to paraffin-embedded tissue, resected within the last 6 years.

2.4.4 Immunohistochemistry

3μm thick sections were cut from paraffin-embedded samples, dewaxed in xylene, rehydrated and then pressure-cooked for 2 minutes in antigen-unmasking solution (Vector Laboratories, Peterborough, UK). The iVIEW™ DAB Detection Kit and NexES immunohistochemistry system (Ventana Medical Systems, Inc. Tucson, AR, USA) was used according to the manufacturer's instructions. Briefly, the endogenous peroxidase activity was inhibited and the sections incubated with the primary brachyury antibody (Santa Cruz, Santa Cruz, CA, USA) for 30minutes, followed by a biotinylated Ig secondary antibody (Ventana Medical Systems, Tucson, AR, USA) and a streptavidin – horseradish peroxidase conjugate (Ventana Medical Systems, Tucson, AR, USA). Finally, a copper DAB enhancer (Ventana Medical Systems, Tucson, AR, USA) was applied. Sections were counterstained with Harris' Haematoxylin (HD supplies, Aylesbury, UK), dehydrated and mounted with a glass coverslip. The other antibodies used were S100 (Dako, Glostrup, Denmark), AE1/AE3 (Dako, Glostrup, Denmark) and MNF116 (Dako, Glostrup, Denmark). The S100 antibody was used at a dilution of 1 in 1600 and the slides were pretreated with protease for 6 minutes. AE1/AE3

antibody was diluted 1 in 50 and the slides were pretreated with protease for 12 minutes. MNF116 was used at a dilution of 1 in 100 and the slides were pretreated with protease for 14 minutes.

Most S100 and cytokeratin immunohistochemistry was performed following tumour resection for diagnostic purposes and therefore was not repeated for the purposes of this project.

3. MESENCHYMAL STEM CELL ISOLATION, CULTURE AND DIFFERENTIATION

3.1 INTRODUCTION

Mesenchymal stem cells (MSC) are isolated from adult bone marrow and have the capacity to differentiate into various connective tissue lineages (Section 1.1). The proliferative potential of these cells is very high and can be further enhanced by culturing them in media containing bFGF (Section 1.1.3).

The interest in optimising protocols for MSC growth and differentiation primarily stems from the potential application of these cells for therapeutic purposes. MSC have a higher replicative potential than the more committed local progenitor cell populations and therefore a higher potential for repair of damaged tissues. MSC have been used or proposed as treatment for a variety of conditions, ranging from osteogenesis imperfecta and intervertebral disc degeneration to myocardial ischemia (166-168). The use of MSC to repair damaged cartilage has also been a therapeutic aim, due to the prevalence of cartilage injuries and diseases such as osteoarthritis (169).

Besides the therapeutic potential presented by MSC, they are also a valuable tool for modelling developmental processes such as chondrogenesis, as they represent an earlier developmental stage than the committed chondrocytes used in other model systems. Chondrogenesis is a complex process involving a multitude of signalling and transcription factors leading to the formation of an extracellular matrix that is crucial for cartilage strength and durability (Section 1.2). Insight into the process of cartilage development has been obtained through the studies of mutations in humans and mice and through various model systems.

The composition and function of the cartilage extracellular matrix as well as the signalling processes involved in cartilage growth, maturation and hypertrophy are well elucidated. However, much less is known about the

transcriptional events involved in the commitment of mesenchymal cells to the chondrogenic lineage and guiding the formation of mesenchymal condensations.

3.1.1 Aims

The first aim of this project was to optimise the conditions for the isolation and expansion of MSC and to determine the variability in MSC proliferation and differentiation between bone marrow donors. Next, the procedure for differentiating MSC was optimised, with a particular focus on establishing the *in vitro* chondrogenic differentiation system. An additional area of interest was the comparison between chondrogenesis of the multipotent MSC and the unipotent normal human articular chondrocyte cells (NHAC). The final aim for this section was to monitor chondrogenesis at the molecular level using RT-PCR analysis of chondrogenic markers, in order to determine the temporal time frame of events as MSC undergo chondrogenesis.

3.2 MSC ISOLATION AND ESTABLISHMENT OF CULTURES

Ficoll gradient centrifugation of filtered bone marrow resulted in the separation of erythrocytes and granulocytes in the pellet and mononuclear cells, including the MSC, in the interphase (Methods: Section 2.1.1). When the bone marrow mononuclear cells from the interphase were seeded on a culture dish, the MSC adhered to the plates while the non-adherent cells were subsequently lost during media changes (Methods: Section 2.1.1). The population of adherent cells was confirmed to uniformly express SH2, SH4 and Stro-1 by FACS analysis, as in previous publications (Section 1.1.2) (experiments performed by Stephen Elliman and Claire Westwood, personal communication, manuscript submitted).

Two to three days after isolation, small groups, consisting of 2 or 3 MSC, were visible on the plate (Figure 3.1) (Methods: Section 2.1.2). The cells continued to proliferate, forming colonies, and were ready to be passaged after 7 days in culture. The MSC had a spindle-shaped, elongated morphology and grew in small clusters. During expansion, MSC were not allowed to become confluent and were passaged when the cells covered 70-75% of the culture dish. If the cells were allowed to reach confluency, they formed a swirling pattern on the plate (Figure 3.2).

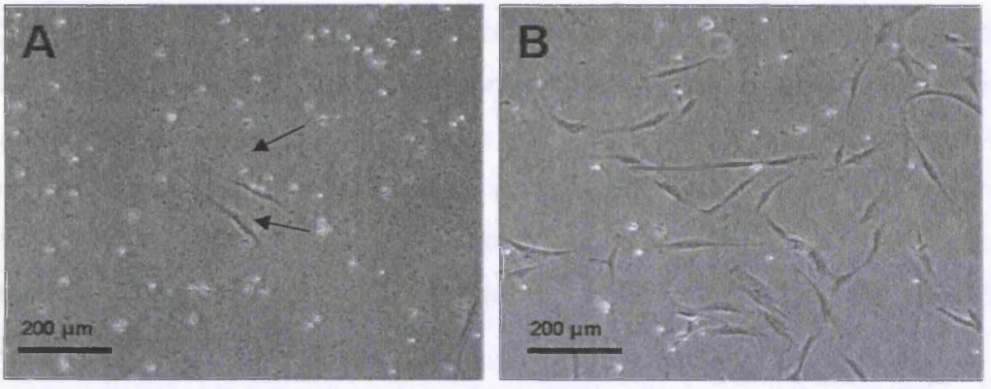

Figure 3.1: Emerging MSC, 3 days after isolation (A, arrow) and 5 days after isolation (B) with Ficoll gradient centrifugation.

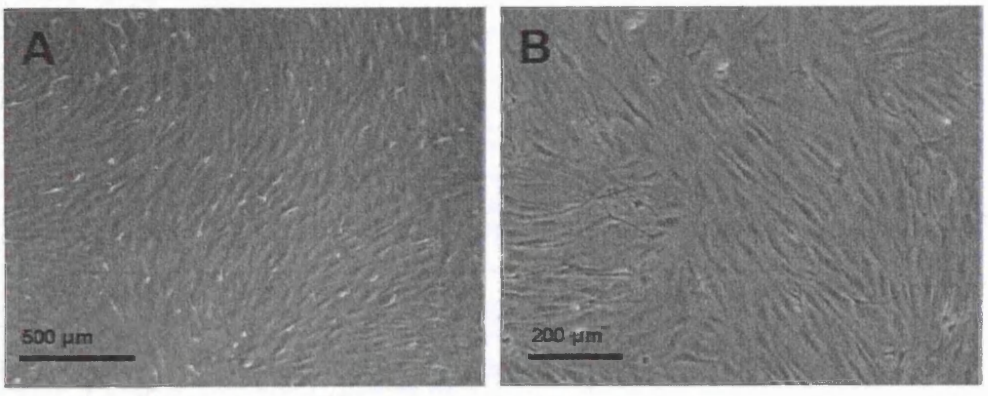

Figure 3.2: MSC that have reached confluence, 9 days after isolation, forming a swirling pattern on the plate.

MSC were routinely grown in a basal media supplemented with 10% serum and 1ng/ml bFGF. The addition of bFGF has been reported to enhance the proliferative capacity of MSC by increasing the doubling rate and allowing the MSC population to be expanded for more population doublings (27) (Section 1.1.3).

In order to test the effect of bFGF, growth curve assays, similar to the 3T3 assay were set up (Methods: Section 2.1.3) (Figure 3.3 - assay performed by Claire Westwood). During the assay, the MSC cultured in the presence of bFGF were passaged every 3 days while the cells grown in the absence of bFGF could only be passaged every 6 days due to their slow rate of proliferation. The growth curve assay was carried out for 30 days and both populations were still proliferating when it was terminated, by which time the cells cultured with bFGF had undergone ~14 population doublings and those cultured without bFGF had undergone ~5. These results correlated well with the published results of Tsutsumi *et al* (27). MSC ability to undergo differentiation was unimpaired by addition of bFGF (Claire Westwood, personal communication, (27)) therefore, bFGF was added to all MSC cultures unless stated otherwise.

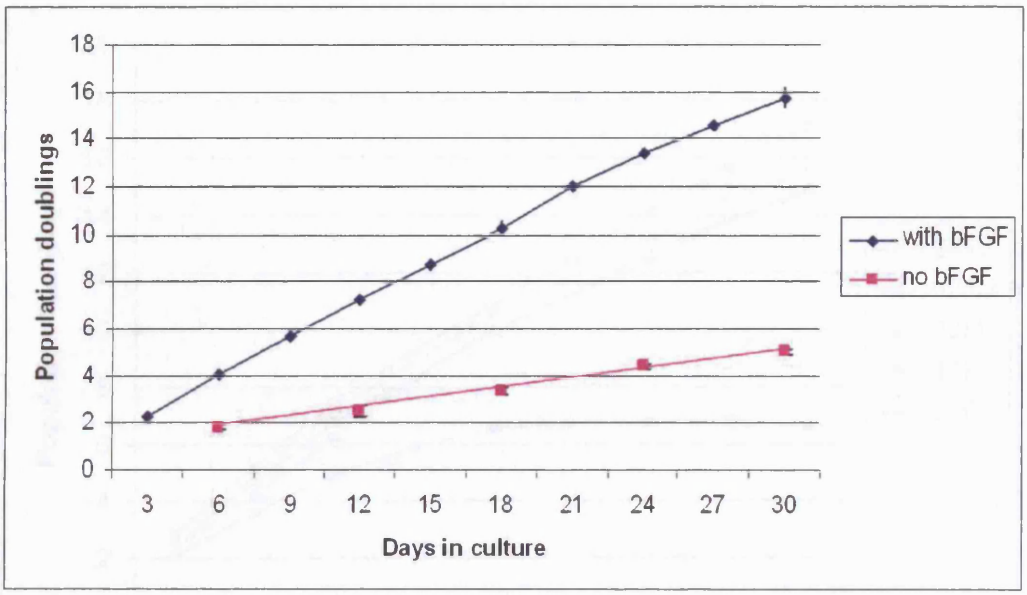

Figure 3.3: The effect of bFGF addition on MSC proliferation as assessed by the 3T3 assay. MSC were grown in triplicate with 1ng/ml bFGF added. Cell numbers were counted every 3 days for cells grown with bFGF and every 6 days for the cells grown without bFGF.

As MSC from different donors are reported to vary in their proliferative potential, growth curve assays were performed on MSC isolated from donors of both genders and a variety of ages (Figure 3.4) (Methods: Section: 2.1.3)(21;23). The donors included: two 24 year old males (labelled 24M and n24M), a 38 year old male (38M), a 46 year old female (46F) and a 55 year old female (55F). Considerable variability was noted between MSC growth rates from different donors. In particular, the MSC isolated from the eldest donor, 55F, showed very slow rates of growth and the cells growth arrested after the 6^{th} passage. The other populations continued to proliferate throughout the 9 passages until the assay was terminated on day 27. While some differences were noted in the growth rates of the other donors' MSC these did not seem to correlate with donor age. Using a paired t-test, the doubling rates of the 38M and the n24M MSC were shown to be significantly different ($p<0.05$), with the older donor MSC multiplying more rapidly. The reasons for this variability are unclear.

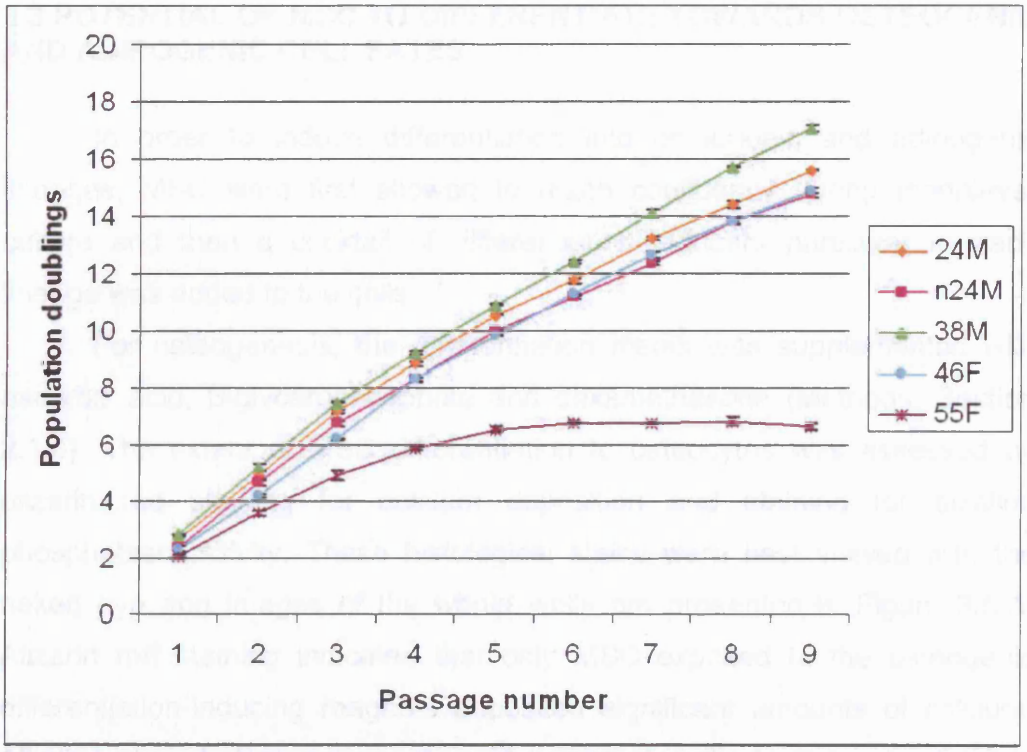

Figure 3.4: Proliferation of MSC isolated from different donors as assessed by the 3T3 assay. Different donors' MSC were grown in triplicate and cell numbers counted every 3 days.

3.3 POTENTIAL OF MSC TO DIFFERENTIATE TOWARDS OSTEOGENIC AND ADIPOGENIC CELL FATES

In order to induce differentiation into osteogenic and adipogenic lineages, MSC were first allowed to reach confluency during monolayer culture and then a cocktail of differentiation inducers particular to each lineage was added to the cells.

For osteogenesis, the differentiation media was supplemented with ascorbic acid, β-glycerophosphate and dexamethasone (Methods: Section 2.1.4). The extent of MSC differentiation to osteocytes was assessed by alizarin red staining for calcium deposition and staining for alkaline phosphatase activity. These histological stains were best viewed with the naked eye and images of the whole wells are presented in Figure 3.5.A. Alizarin red staining indicated that only MSC exposed to the osteogenic differentiation-inducing reagents deposited significant amounts of calcium. Alkaline phosphatase activity showed a characteristic deep purple staining, which was seen in the differentiated cells, while the cells kept in the regular MSC media remained unstained. When observed under the microscope, morphological changes were also obvious in the cells that have undergone osteogenesis (Figure 3.5.B). While the undifferentiated MSC were spindle-shaped and formed swirling patterns on the culture dish, the osteoblasts appeared more rounded (Figure 3.5.B inset).

Adipogenesis was induced by the addition of isobutyl methyl xanthine (IBMX), indomethacin, insulin and dexamethasone (used at a higher concentration than for osteogenesis) (Methods: Section 2.1.5). Adipogenesis was assessed using oil red O that stains lipids red (Figure 3.5.B). By day 2 of adipogenic differentiation, the MSC changed morphology from a spindled to a more rounded appearance and began to acquire the characteristic lipid droplets in the cytoplasm that were stained with oil red O (data not shown). The cells continued to accumulate lipid throughout culture with the size and the number of the droplets increasing, culminating in an overall increase in the size of the individual adipocytes (Figure 3.5.B inset).

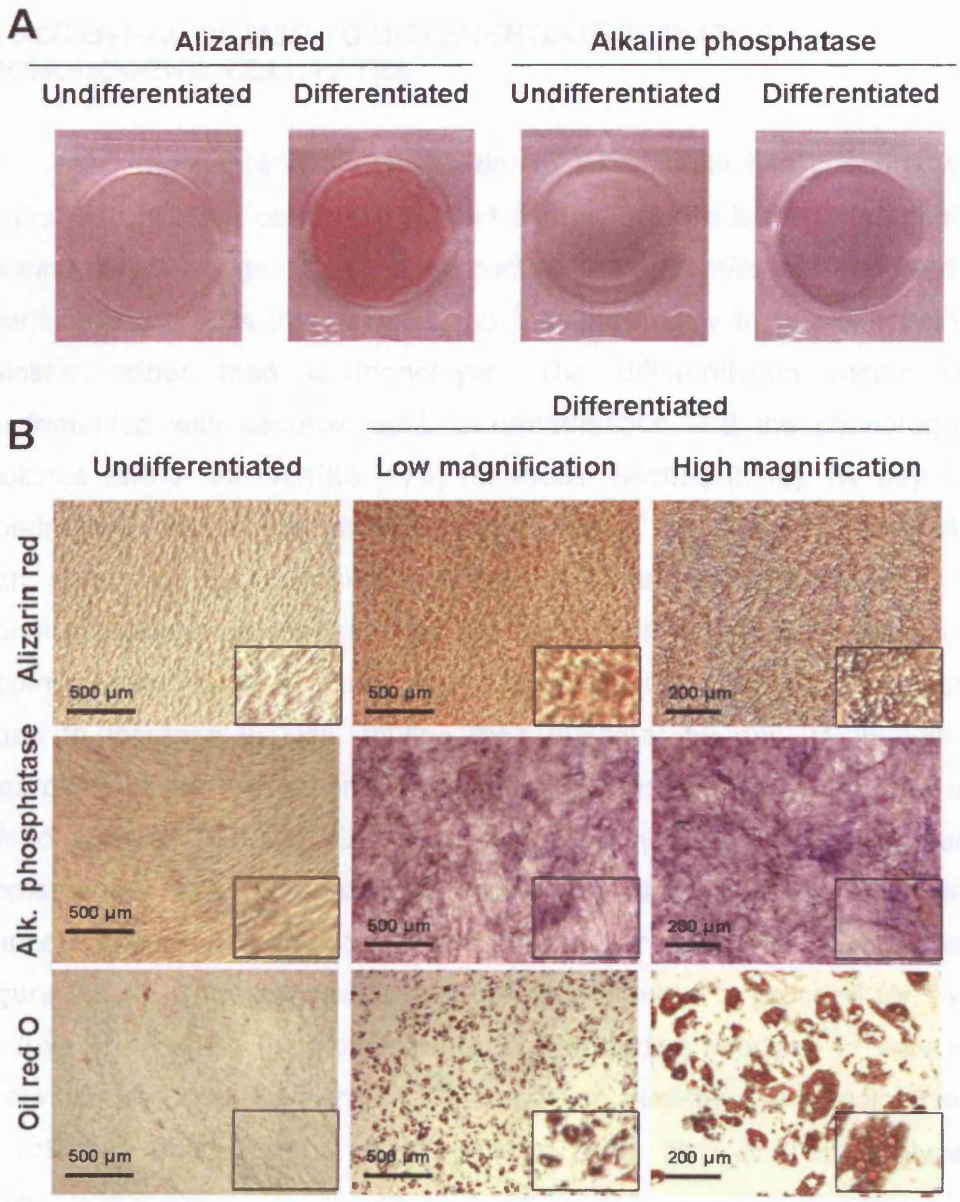

Figure 3.5: Osteogenic and adipogenic differentiation of MSC. A) Scanned images of 12-well plates with MSC undergoing osteogenesis. B) Photomicrographs of undifferentiated MSC and those that have undergone osteogenesis and adipogenesis, with higher magnifications inset.

3.4 POTENTIAL OF MSC TO DIFFERENTIATE TOWARDS CHONDROGENIC CELL FATES

MSC require two factors in order to differentiate into chondrocytes: the first is very close cell to cell contact and the second is the differentiation inducing chemical signals. The close contact between cells was achieved by centrifuging the cells into a pellet, so that they grew in a 3-dimensional structure rather than a monolayer. The differentiation media was supplemented with ascorbic acid, dexamethasone and the chondrogenic cytokines BMP6 and TGFβ3 (170) (Methods: Section 2.1.6). By day 1 of chondrogenic culture the pelleted cells formed a flat disc and adhered to each other but not the sides of the tube they were cultured in. As chondrogenesis proceeded, the discs became more spherical in shape until becoming fully rounded. From day 6 onwards the chondrocyte spheres began to increase in size, tripling their diameter by day 21 in culture. Regardless of the media composition, the MSC adhered to each other and formed spheres, but the size increase was only seen in those cultures supplemented with differentiation media. The chondrogenic pellets also changed appearance and became slightly clear and hard to the touch (Figure 3.6.A). Chondrogenesis was normally allowed to proceed for 14 to 21 days after which the pellets were dehydrated, embedded in wax and sectioned (Methods: Section 2.1.7). The 10μm sections were stained with the toluidine blue dye that stains nucleic acids blue and proteoglycans purple.

At the microscopic level the changes taking place during chondrogenesis could be observed more closely. The previously mentioned increase in pellet size was found to be due to the production and accumulation of the chondrogenic matrix that was visualized by purple toluidine blue staining (Figure 3.6.B). By day 8 of the chondrogenic culture, some matrix accumulation was apparent and this coincided with the observed size increase of the pellets at this time. Matrix production

continued and much greater proteoglycan deposition could be observed by day 12. There were areas within the pellet that showed increased matrix accumulation as chondrogenesis appeared to begin at multiple sites. In addition, by day 12, changes in the cell morphology could be observed: as a typical chondrogenic 'rounding' of previously spindle shaped cells and a development of lacunae around the main body of the cells was observed. In many cultures there was also a layer of flattened cells around the edge of the pellet which remained spindle shaped, and it has been speculated that these cells may be an *in vitro* version of the perichondrium (18). Palmer *et al* found these cells to express collagen 1 at higher levels than the remainder of the pellet (111). Finally, by day 15 the sections resembled true cartilage with a high ratio of matrix to cells, and a large number of rounded cells present, some beginning to enlarge and appear hypertrophic.

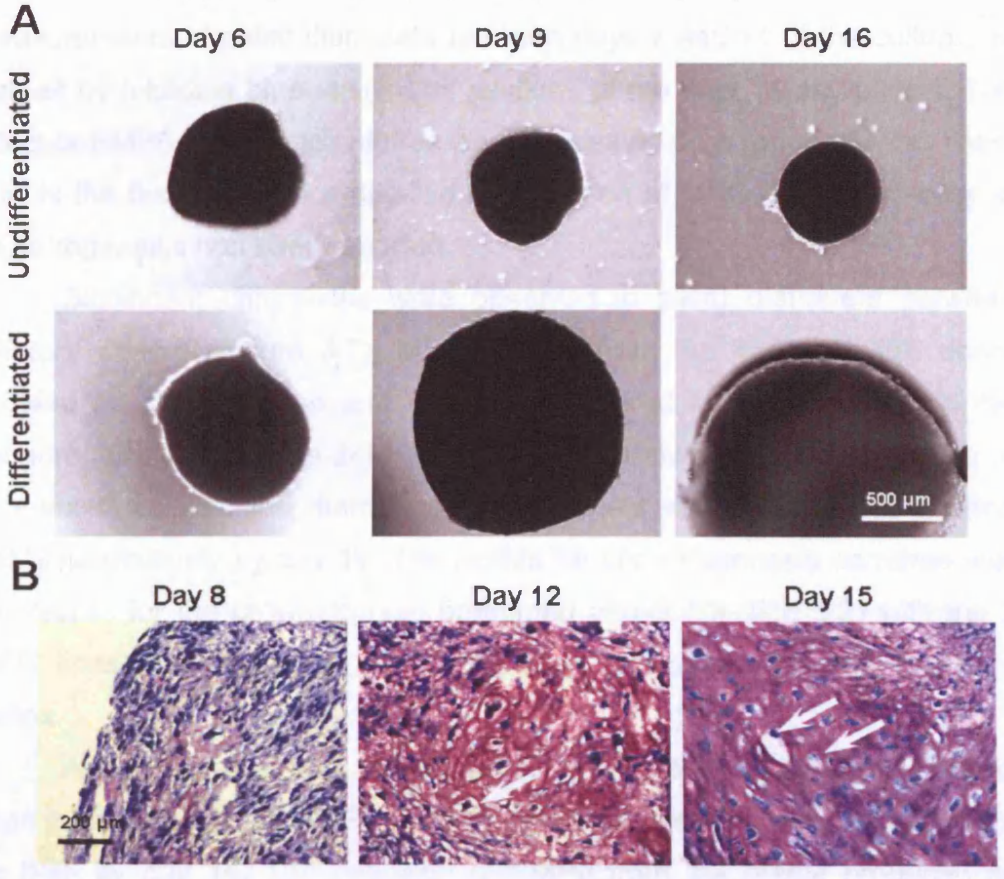

(Figure legend on following page)

Figure 3.6: Chondrogenic differentiation of MSC. A) Photomicrographs of pelleted MSC in media without any cytokines added (undifferentiated) and with cytokines (differentiated). B) Toluidine blue-stained sections of differentiating pellets. Cells within lacunae are marked with an arrow.

3.4.1 Donor variation of chondrogenic potential

Of all the MSC *in vitro* differentiation model systems, MSC differentiation into cartilage is the most sensitive to passage number with the chondrogenic potential, as measured by matrix accumulation, already diminishing after passage 6 (27). As MSC rates of proliferation were found to vary between different donors' MSC (Section 3.2), the variability between their chondrogenic potentials was also tested. The MSC derived from different donors were all induced to differentiate at the 5^{th} passage (p5). The extent of chondrogenesis was assessed by graticule eye-piece measurements of pellet diameters between days 7 and 14 of the culture, as well as by toluidine blue staining of sections of the final 14 day pellets. The effect of BMP6 addition to cultures was also tested on a range of MSC lines. This is the first time that a detailed examination of MSC donor variability in chondrogenesis has been reported.

Significant differences were observed in pellet diameters between different donors (Figure 3.7). MSC derived from the 46F and 55F donor showed no size increase and may have required longer exposure to the chondrogenic media. The 24M and 38M MSC showed the highest levels of differentiation, with the diameters of the pellets increasing by ~35% and ~55% respectively by day 14. The results for chondrogenesis correlate with the results for the growth curves presented above (Section 3.2) with the 2 MSC lines that proliferate the fastest also producing the most cartilage matrix.

A size increase was still observed for the 24M and the 38M pellets even in the absence of BMP6 but this was much less dramatic, being ~15% for both by day 14. The omission of BMP6 from the media produced no

effect on the cells that did not respond to the chondrogenic stimulus such as the 46F and 55F. Therefore, BMP6 addition significantly enhanced chondrogenesis, but only in those MSC that respond positively to the chondrogenic stimulus in the first place.

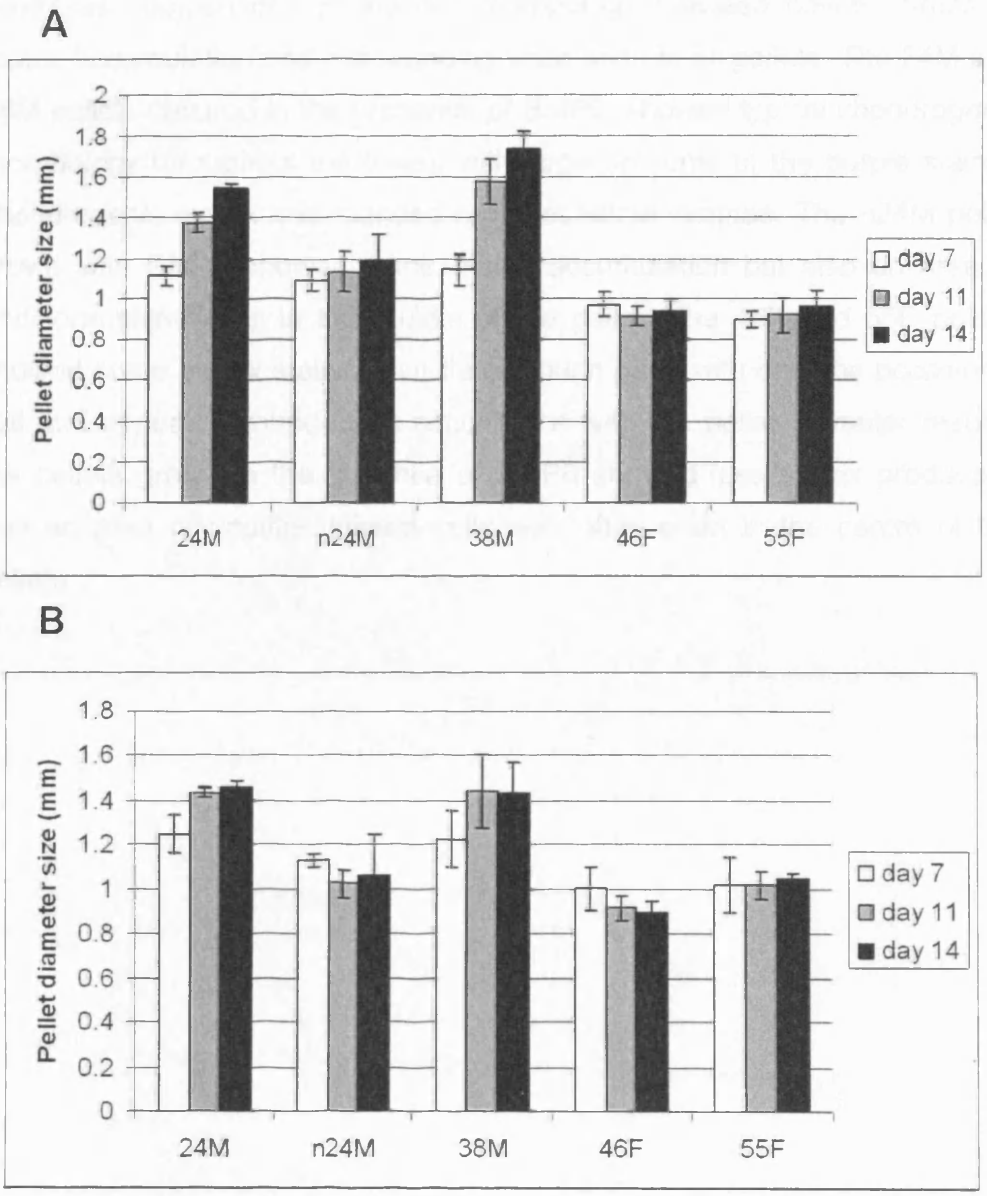

Figure 3.7: Pellet size increase during chondrogenesis. Chondrogenesis was performed on 5 different MSC lines and the pellet diameters measured. A) Pellets grown under regular chondrogenic conditions. B) Pellets grown in the absence of BMP6.

Histological examination of the day 14 pellets further illustrates the differences in chondrogenic potential (Figure 3.8). The size of the pellets in this figure was not necessarily representative of the actual diameter size as it was very difficult to section the spheres at their equator, so the images are useful as comparisons of the cell morphology between pellets. Areas of matrix accumulation and cell rounding were seen in all pellets. The 24M and 38M pellets cultured in the presence of BMP6, showed typical chondrogenic morphology throughout the pellet, with large amounts of the purple stained chondrogenic matrix and rounded cells set within lacunae. The n24M pellet grown with BMP6 showed some matrix accumulation but also an area of undifferentiated cells in the middle of the pellet. The 46F and 55F pellets showed some matrix staining but this is much paler with only the occasional cell that appeared rounded. In accordance with the pellet diameter results, the pellets grown in the absence of BMP6 showed less matrix production and an area of undifferentiated cells was often seen in the centre of the pellets.

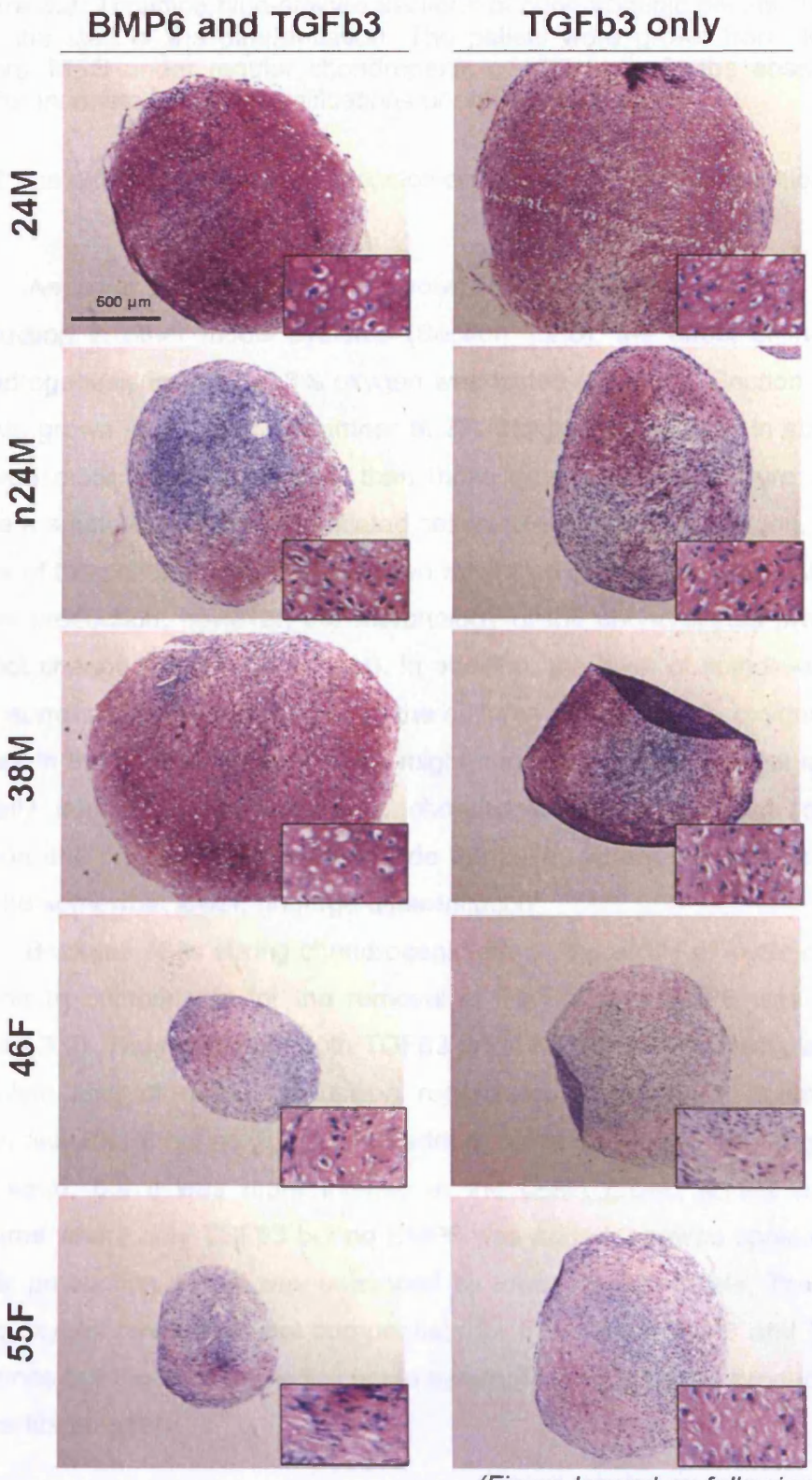

(Figure legend on following page)

Figure 3.8: Toluidine blue-stained sections of chondrogenic pellets, 14 days after the start of the differentiation. The pellets were grown from different donors' MSC under regular chondrogenic conditions or in the absence of BMP6. Inset are higher magnifications of cartilaginous areas.

3.4.2 The effect of lower oxygen tension on chondrogenic differentiation

As lower oxygen levels are known to induce higher levels of matrix production in other model systems (Section 1.2.6), the effect of inducing chondrogenesis in MSC at 3% oxygen was tested (Methods: Section 2.1.6). Pellets grown in a hypoxic chamber at 3% oxygen were larger in size and showed more matrix deposition than those grown at 21% (Figure 3.9.A). While a small area of undifferentiated cells was seen at 21% oxygen, all the areas of the pellet grown at 3% oxygen appeared differentiated and showed matrix production, however, the morphology of the chondrocytes produced did not change (Figure 3.9.A inset). In addition, the layer of spindle-shaped cells surrounding the pellet, seen in the cultures grown at 21% oxygen, was absent in the hypoxic cultures. This might suggest that the external layer is actually inhibited from undergoing chondrogenesis by the high oxygen tension and only the cells further inside the pellet, where the oxygen levels may be somewhat lower, undergo differentiation.

Because of its strong chondrogenic effect, the ability of lower oxygen tension to compensate for the removal of TGFβ3 and BMP6 was tested (Figure 3.9). The removal of both TGFβ3 and BMP6 from the media led to a complete lack of matrix deposition regardless of oxygen concentration. When only BMP6 but no TGFβ3 was added, some staining for proteoglycans was seen, but it was more intense in the pellet grown at 3% oxygen. Cultures where only TGFβ3 but no BMP6 was added, showed considerable matrix production, which was enhanced by lower oxygen levels. Therefore, lower oxygen tension did not compensate for the lack of BMP6 and TGFβ3 cytokines but the two seemed to act in synergy to enhance the production of the cartilage matrix.

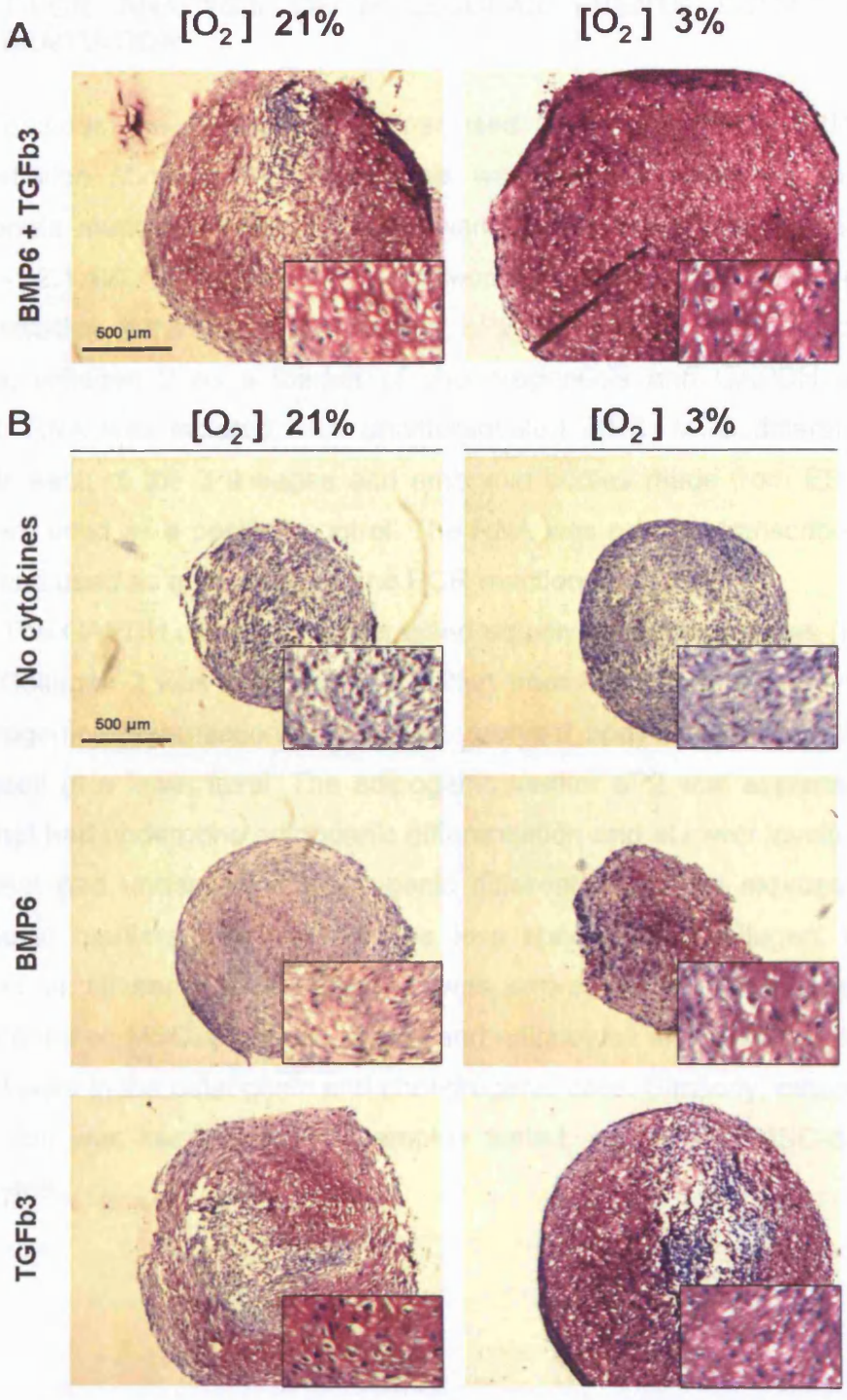

Figure 3.9: Toluidine blue-stained sections of cartilage pellets. A) The effect of varying [O_2] on chondrogenic differentiation. B) The effect of varying [O_2] and removal of cytokines on chondrogenic differentiation.

3.5 RT-PCR ANALYSIS OF MOLECULAR EVENTS DURING MSC DIFFERENTIATION

Besides the histological stains used to determine the extent of differentiation above, RT-PCR analysis was also performed to check if appropriate markers for each lineage were expressed (Methods: Sections 2.1.9 - 2.1.12). Collagen 1 and osteocalcin were chosen as genes representative of the osteogenic lineage, aP2 as a marker of the adipogenic lineage, collagen 2 as a marker of chondrogenesis and GAPDH as the control. RNA was isolated from undifferentiated MSC, MSC differentiated towards each of the 3 lineages and embryoid bodies made from ES cells, that were used as a positive control. The RNA was reverse transcribed into cDNA and used as a template for the PCR reactions.

The GAPDH control was expressed equally in all the samples (Figure 3.10). Collagen 2 was detected in the RNA from MSC that had undergone chondrogenic differentiation and in the embryoid body RNA, where it was expressed at a lower level. The adipogenic marker aP2 was expressed by MSC that had undergone adipogenic differentiation and at lower levels in the MSC that had undergone chondrogenic differentiation. The expression of osteogenic markers was found to be less specific and collagen 1 was detected in all samples. Collagen 1 was expressed at lower levels by undifferentiated MSC, embryoid bodies and adipocytes and at comparatively higher levels in the osteogenic and chondrogenic cells. Similarly, osteocalcin expression was seen in all the samples tested, except the MSC-derived adipocytes.

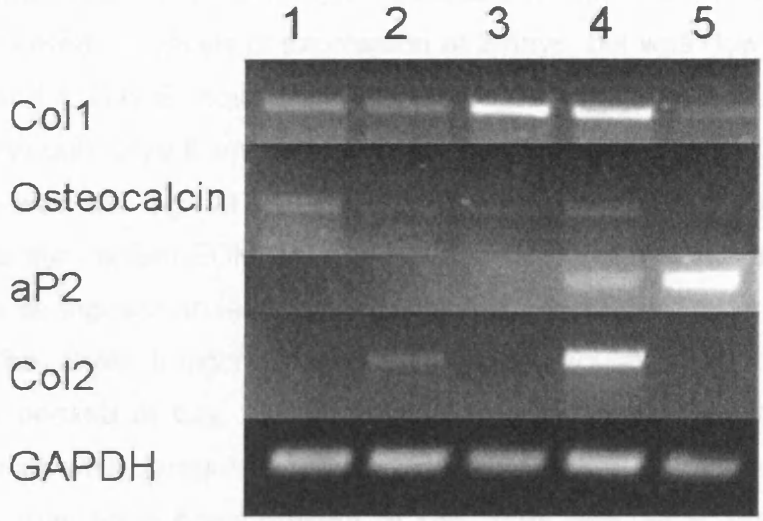

Figure 3.10: Gel electrophoresis showing RT-PCR analysis of the expression of osteogenic, chondrogenic and adipogenic lineage markers in undifferentiated MSC (1), embryoid body (2), osteogenic MSC (3), chondrogenic MSC (4) and adipogenic MSC (5) cDNA.

To examine the molecular progression of MSC chondrogenesis, a selection of chondrogenic genes was tested for expression using RT-PCR analysis (Methods: Section 2.1.9 – 2.1.12). RNA was isolated from differentiating MSC every day for the first week of differentiation and then at the 2 and 3 week time points. The genes tested for expression included the matrix proteins: collagens 2 and 10, aggrecan and link, the transcription factors: Sox 5, 6 and 9 and the BMPs (Figure 3.11).

The expression of many regulatory molecules involved in chondrogenesis, when assessed using RT-PCR analysis, remained constant throughout the differentiation. BMP2 and 6, as well as Sox9 were already expressed by the undifferentiated MSC, and their expression continued throughout the differentiation. This was in contrast to the matrix molecules, which were upregulated as chondrogenesis proceeded. All the ECM molecules tested showed the highest levels of expression at the 14 day time point. The 14 day time point was the only time when the expression of aggrecan was detected. Collagen 10 and link transcript showed low levels of expression up to 7 days, upregulated at 14 days and then somewhat

downregulated again by the 21 day time point. Collagen 2, the main cartilage collagen, showed low levels of expression at 2 days, but was downregulated at days 3 and 4. Day 5 showed another increase in collagen 2 levels, which persisted through days 6 and 7 and reached a peak at day 14. Collagen 2 expression was still high at day 21 when the time course was terminated. COMP was the earliest ECM gene to be detected, and was upregulated at day 1, with its expression levels increasing throughout the time course until day 14. The Sox6 transcription factor was upregulated at day 5, the expression peaked at day 14, but was no longer detected in the day 21 sample. Sox5 was upregulated earlier, at day 2, although a low level of expression may have been present at day 1 as well, after which it was expressed throughout the time course. PTHrP was present in the undifferentiated MSC and throughout the time course but its receptor was expressed at low levels at day 2 and higher levels after day 7, reaching a peak at 14 days.

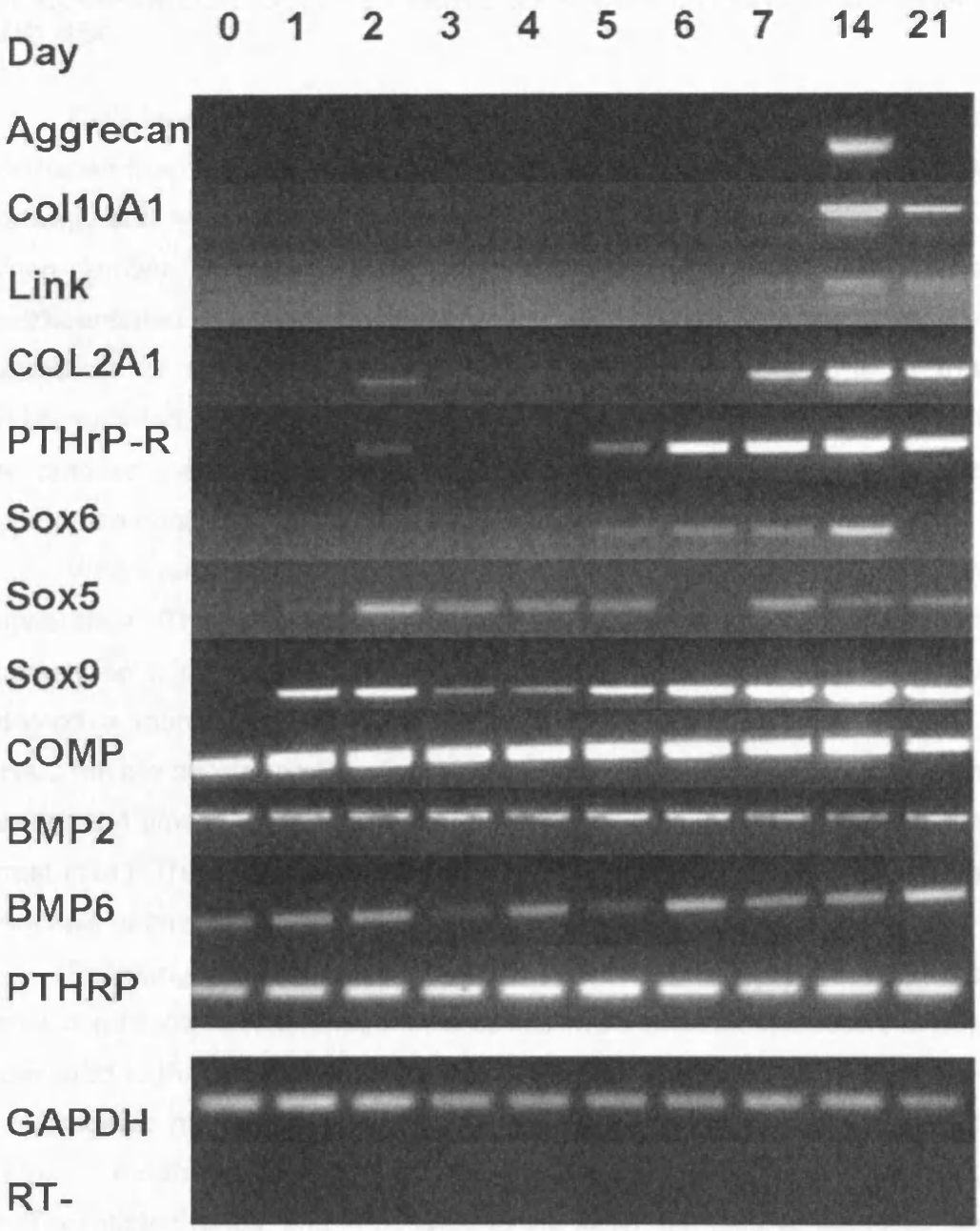

Figure 3.11: Gel electrophoresis showing RT-PCR analysis of the expression of genes reported to be involved in cartilage development throughout the chondrogenic differentiation of MSC.

3.6 COMPARISON OF THE CHONDROGENIC POTENITIAL OF NHAC AND MSC

Cells labelled as 'normal human articular chondrocytes' (NHAC) were purchased from Cambrex. These cells had been isolated from human knee cartilage and were differentiated chondrocytes when placed into culture. When grown in the absence of chondrogenic stimuli, the cells dedifferentiated and lost their chondrogenic phenotype, such as the expression of matrix molecules, within 2 or 3 passages. It is in this undifferentiated state that the cells were received. These cells were sold on the premise that they could be expanded and redifferentiated under the appropriate conditions (171).

When cultured in a monolayer the NHAC were similar to MSC in appearance. The NHAC were spindle-shaped when they were seeded sparsely on a plate, but as the cell cultures approached confluency, they adopted a more polygonal shape (Figure 3.12)(Methods: Section 2.1.8). NHAC have a shorter proliferative lifespan than the MSC and could only be passaged 4 times, equating to about 15 population doublings, before growth arrest (171). The culture procedure is very similar to the MSC and the cells were split before reaching confluence, which is usually every 4 days.

Following expansion in culture, the p5 NHAC were placed under the same conditions for chondrogenesis as the MSC (Methods: Section 2.1.6). Compared to the MSC pellets, the NHAC pellets were larger after 14 days in chondrogenic media (Figure 3.13). The differentiated NHAC also showed matrix production throughout the pellet without displaying any undifferentiated areas, and in contrast to the MSC, the cells at the outer rim were chondrogenic in morphology. Unlike the MSC chondrocytes, the differentiated NHAC did not appear hypertrophic or produce the lacunae seen in the differentiating MSC.

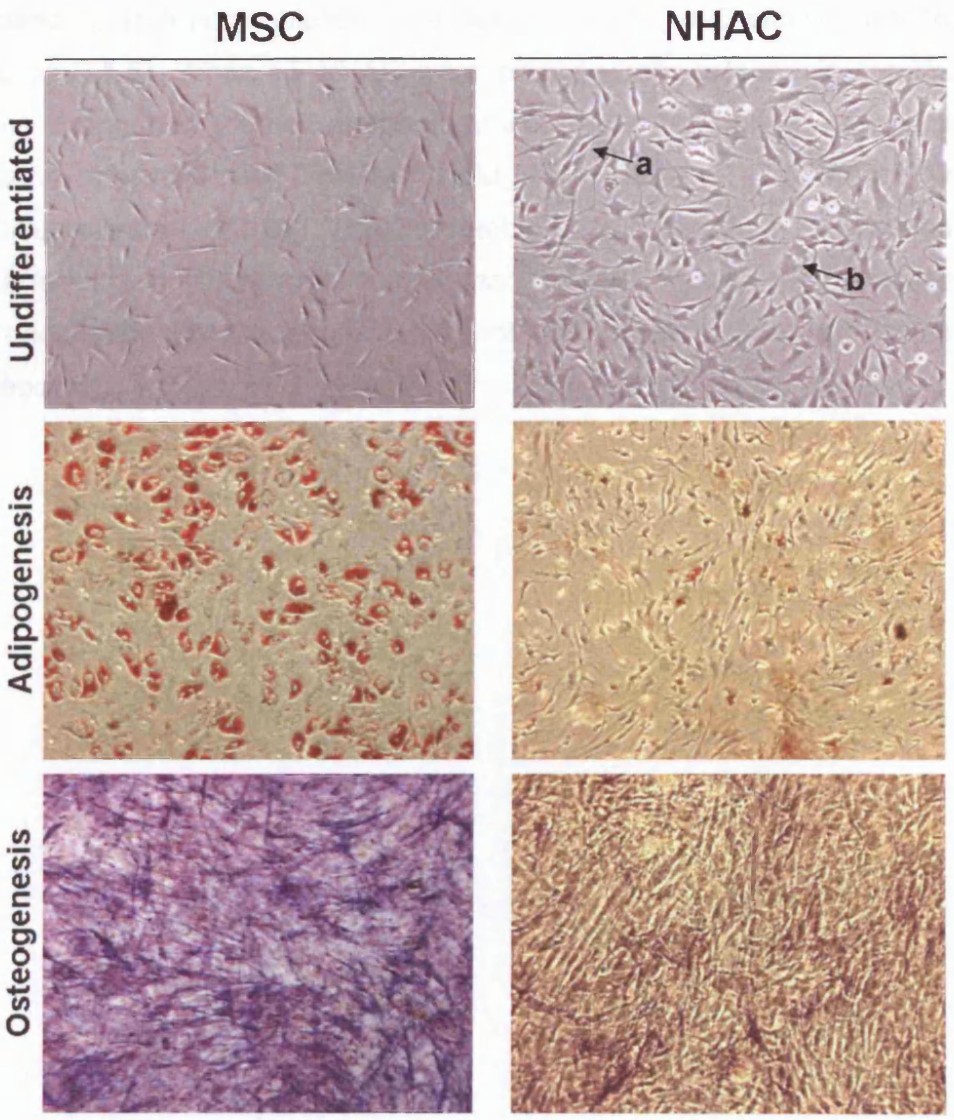

Figure 3.12: Photomicrographs showing MSC and NHAC morphology when undifferentiated and after adipogenic and osteogenic differentiation. Undifferentiated NHAC cultures consist of a spindle-shaped (a) and a polygonal (b) subpopulation. Adipogenic differentiation was assessed by Oil red O staining and osteogenic differentiation by staining for alkaline phosphatase activity.

The ability of NHAC to differentiate in culture to other mesenchymal lineages was also tested (Figure 3.12). When grown under adipogenic conditions, p5 NHAC did not change their morphology as MSC did and

showed no lipid accumulation as assessed by oil red O staining (Methods: Section 2.1.5). When p5 NHAC were placed under osteogenic conditions, some changes in the cell morphology were seen but only low amounts of alkaline phosphatase activity could be detected. Therefore, while undifferentiated MSC and NHAC resemble each other, the NHAC appear to be a more committed progenitor cell than the MSC, that is, they are capable of undergoing chondrogenesis but not differentiating into adipocytes or osteocytes.

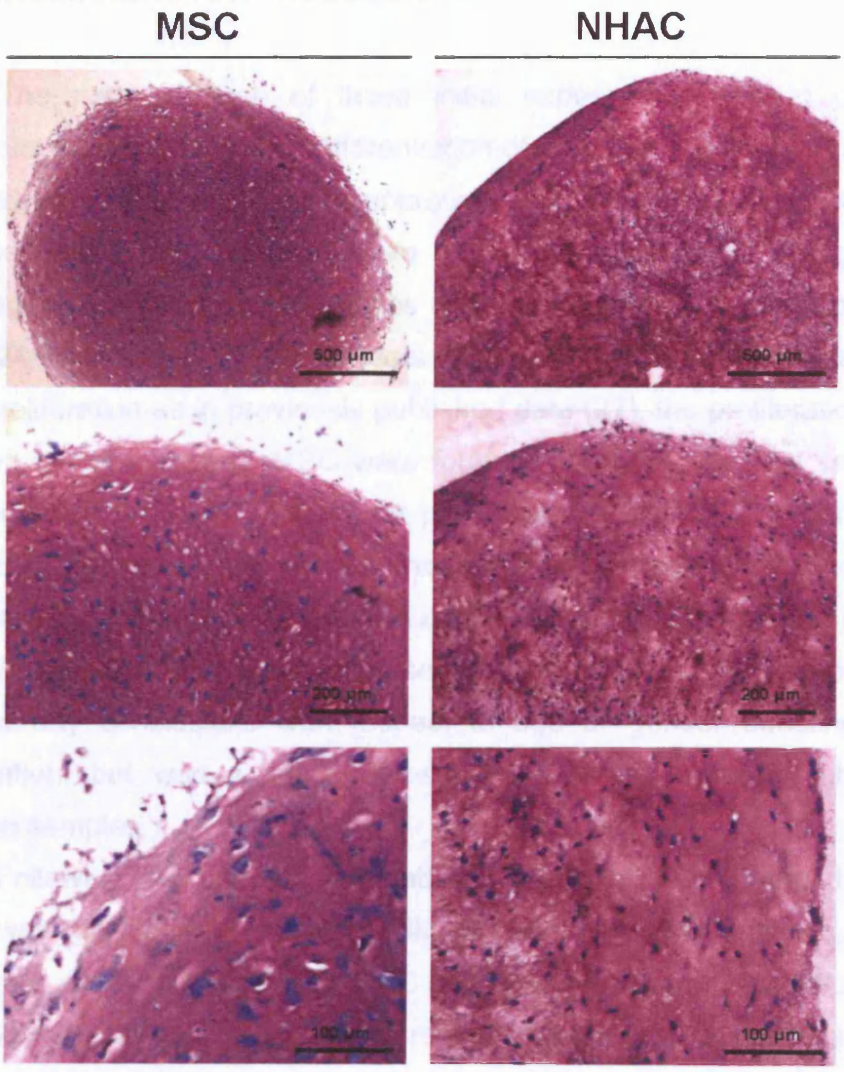

Figure 3.13: Toluidine blue-stained sections of day 21 MSC and NHAC chondrogenic pellets at various magnifications. Both the MSC and the NHAC were at p5 at the start of the differentiation.

3.7 CONCLUSIONS AND DISCUSSION

The main purpose of these initial experiments was to optimise conditions for the growth and differentiation of MSC, as well as to establish a chondrogenic model system in preparation for a microarray study (Chapter 4). The MSC were isolated from donor bone marrows by gradient centrifugation. Bone marrow samples were available from a range of donor ages (24-55 years) and both genders. While the addition of bFGF affected MSC proliferation as in previously published data (27), the proliferation rates between different donors' MSC were found to vary greatly. This variability has been documented in previously published studies (21;23). Donor age has been suggested as one of the potential variables affecting MSC proliferation – although not all studies agree on this (21;23). The sample size used in the growth curve assays presented here (section 3.2) was too small to draw any conclusions with respect to age or gender affecting MSC proliferation, but was a good representation of the variability observed between samples.

Following the successful establishment of MSC cultures, the next focus was on optimising the conditions for MSC differentiation. Using previously published methods, MSC were differentiated into adipocytes, osteocytes and chondrocytes, but were found to undergo chondrogenesis at various rates of efficacy. MSC from all donors could produce some chondrogenic matrix and showed changes in cell morphology but the amount of matrix accumulated was very variable as quantified by the size increase of the pellets. The same cell lines that showed the highest rates of proliferation also showed the highest levels of chondrogenic matrix accumulation. This correlation is interesting as it indicates that there may be a link between the ability of cells to proliferate and the extent of differentiation they can undergo.

In agreement with previously published data, the addition of BMP6 to chondrogenic cultures was found to enhance matrix accumulation (170) but

only in those MSC lines that were able to produce high amounts of matrix even in the absence of this factor. The MSC that showed limited ability to differentiate into chondrocytes also showed no response to the addition of BMP6. These cells may have had a better response to stimulation with higher concentrations of these cytokines, or may need a different chondrogenic cocktail. A recent study suggest that a combination of TGFβ2 and IGF-I promotes chondrogenesis in MSC derived from older adults (>50 years old) but does not attempt to compare how cells from younger donors respond to the same stimuli (172). Most combinations of TGFß and BMP molecules stimulate chondrogenesis (106;108-110;170), but it has recently been suggested by Sekiya *et al* that the most potent is a mix of TGFβ3 and BMP2 (173). It would be of interest to know if TGFβ3 and BMP2 would be effective in stimulating chondrogenesis of the less responsive MSC lines. In an attempt to imitate the *in vivo* chondrogenic conditions, the most effective way to induce chondrogensis may be to expose the cultures to different growth factors at the start of the differentiation, to induce the formation of the condensations, and later, to enhance matrix accumulation.

Another factor which was found to enhance chondrogenesis was the culture of the pellets under lower oxygen tension. Growing the pellets at 3% oxygen rather than the atmospheric 21% normally used in tissue culture produced larger pellets with greater extracellular matrix accumulation. This inductive effect of lowering oxygen concentration on chondrogenesis has been documented previously on other cell lines, such as bovine articular chondrocytes but not MSC (115). As cartilage is a non-vascularised tissue, the hypoxic growth conditions are in fact more representative of the true environment that the *in vivo* chondroblasts would be exposed to. Due to the potent chondrogenic effect of the lower oxygen conditions, the ability of hypoxia to substitute for TGFβ3 and BMP6 addition was tested. However it was shown that lowering the oxygen tension could not compensate for the removal of these cytokines from the differentiation media. This finding shows

that the addition of cytokines and a hypoxic environment are not redundant, but instead the optimal chondrogenic differentiation conditions require both.

To monitor the progress of MSC chondrogenesis and help in the selection of time points appropriate for microarray analysis, RT-PCRs were performed that examined the levels of various genes known to be involved in chondrogenesis. The RT-PCRs validated the MSC chondrogenesis model system, showing that all the cartilage markers expected were expressed. By day 14 of the differentiation all extracellular matrix markers expressed by mature cartilage are present. MSC-derived chondrocytes expressed a mixture of mature cartilage markers (such as collagen 2 and aggrecan) as well as markers of hypertrophic cartilage (such as collagen 10), corresponding to the slightly hypertrophic morphology seen. Chondrogenic markers could be detected as early as day 2 of the differentiation even though morphological changes, such as the accumulation of the matrix were not obvious till later.

In order to investigate chondrogenesis *in vitro,* models using already committed chondrocytic cells are more commonly used than ones using multipotent progenitors such as MSC. However, a comparison between the two model systems has not previously been described. The NHAC could be induced to undergo chondrogenesis with the same stimuli as the MSC, but the resulting pellets produced more matrix and fewer hypertrophic cells. Unlike the MSC, the NHAC did not differentiate into osteocytes or adipocytes, indicating that they are committed to the chondrogenic fate. Despite their morphological similarity to the MSC, the NHAC must have differences at the molecular level restricting their ability to differentiate into adipogenic and osteogenic lineages and enhancing their chondrogenic ability. One way of pinpointing these changes at the transcriptional level is to perform microarray profile comparisons between the two cell populations. Therefore, microarrays can be used to address questions about differences between undifferentiated MSC and NHAC as well as between the chondrocytes that they produce when differentiated.

While the later events in chondrogenic development are well documented, the molecules involved in the early stages of commitment to the chondrogenic lineage remain unclear. In an attempt to elucidate these early processes, microarray analysis was performed, investigating the transcriptional progression of MSC chondrogenesis and this is presented in the following chapter.

4. MICROARRAY ANALYSIS OF MESENCHYMAL STEM CELLS UNDERGOING CHONDROGENESIS

4.1 INTRODUCTION

The exposure of a progenitor cell to the signals inductive of differentiation, triggers a response involving transcription factors and signalling molecules that activate the expression of their downstream targets and lead to the cell assuming a differentiated phenotype.

In vivo chondrogenesis is known to be a dynamic process, commencing with mesenchymal cells that form cartilaginous condensations and then begin to produce the chondrogenic ECM and other molecules associated with cartilage (Section 1.2). MSC can differentiate *in vitro* to form chondrocytes, amongst other lineages such as adipocytes and osteocytes (Chapter 3). While the regulatory processes involved in the formation and maintenance of the cartilage matrix and the consequent hypertrophy of the chondrogenic cells have been investigated in detail, less is known of the early processes involved in the commitment of the mesenchymal cells to cartilage, and in particular the transcription factors involved in such a process.

The MSC *in vitro* chondrogenesis model system is well suited for the investigation into the early chondrogenic events as it involves the differentiation of a multipotent progenitor into a cell that morphologically and functionally resembles mature chondrocytes. The resulting cartilage from MSC differentiation is very similar to that obtained by differentiating committed chondrocytes isolated from adult cartilage (Section 3.5).

4.1.1 Previous GEM studies into chondrogenesis

Gene expression microarray (GEM) analysis is a method appropriate for examining the global expression profiles of cells and tissues and

comparing normal and disease states as well as the response of cells to different culture conditions, such as exposure to growth factors (Section 1.3).

A number of GEM studies have already been performed on MSC chondrogenic differentiation (Section 1.3.2). The first GEM study, performed by Sekiya *et al* validated the use of MSC as a chondrogenic model system, by showing that MSC that had undergone chondrogenesis expressed all chondrogenic markers including high levels of matrix collagens and proteoglycans (113).

A more recent study by James *et al* attempted to provide a global overview of chondrogenesis of mouse MSC (132). They isolated RNA at different time points during the differentiation but began at day 3, thereby not capturing any earlier events. The genes that changed expression levels during chondrogenesis were also classified using broad gene ontology categories, revealing that many upregulated genes had roles in signal transduction, while a high proportion of the downregulated genes had roles related to molecular transport or transcription.

Another recent study on the chondrogenic differentiation of a mouse stromal cell line investigated the effect of hypoxic growth conditions on the expression profile (133). Hypoxic growth conditions increased the level of HIF1α in the nucleus and activated the Sox9 promoter but also induced the expression of metabolic and signal transducing genes.

Therefore neither of these recent studies described the global transcriptional profile in detail. Furthermore, both of these studies were performed on mouse cell lines rather than human MSC.

4.1.2 Affymetrix HGU133A chips and data analysis

For the analysis presented here, commercially available oligonucleotide gene chips were employed. The Affymetrix HGU133A chips used contained 22,000 probe sets representing 14,500 genes. Probe sets comprised 11 pairs of sequence probes and each probe was 25

oligonucleotides in length. The probes were selected so that they are sequence specific to their target gene and tended to be located more towards the 3' end as this was likely to be better transcribed and represented in the biotinylated cDNA. Each probe pair consisted of a perfect match and a mismatch sequence. The mismatch sequence differed from the perfect match by one base located in the middle of the 25-mer sequence. The results from the hybridizations were obtained in the form of a signal intensity for each probe.

When a GEM experiment is conducted, a large amount of data is generated and statistical analysis needs to be performed to extract meaningful information from this data. In order to make datasets comparable between different chips, a process of normalization is required and different algorithms are available for this. The first step is to combine the information from the 11 probe pair sets into an expression value for that transcript. The algorithm provided with the Affymetrix software and entitled microarray suite (MAS), calculates the robust average (Tukey biweight) of the differences between the perfect match and the mismatch probe. The usefulness of the mismatch probe has been disputed because, in almost one third of the probe sets, the mismatch signal is actually higher than the one obtained for the perfect match (164). Another algorithm often used is the robust multi-array average (RMA). RMA does not include the mismatch probe into its calculation but instead takes the robust average of the log transformed difference between the perfect match and the background (164). There are other, slightly different algorithms also available for data analysis, such as dChip but a recent study confirmed that of all the normalization methods, RMA gave the most reproducible results when compared with quantitative PCR (174;175).

To analyse lists of differentially expressed genes obtained from GEM profiling, a variety of tools are available. The data-mining programme WebGestalt can be used for data retrieval of a large number of genes at once (176). WebGestalt retrieves information including: gene ontology (177),

tissue expression pattern, chromosome distribution, metabolic pathways, signaling pathways and protein domain information. There is also a statistics module available that can perform statistical tests, comparing the list of genes of interest to a control gene list (such as the whole of the human genome, or the genes present on a particular gene chip) and suggesting biological areas that are important in the gene set of interest which may warrant further investigation.

The WebGestalt tool also has a feature that searches for the over-represented KEGG pathways for the group of genes of interest. KEGG is a manually annotated database integrating knowledge on molecular interaction networks, responsible for various cellular processes. KEGG provides a list of proteins involved in any particular pathway as well as maps describing the interaction between these proteins (www.kegg.com).

In addition to using the WebGestalt tool, manual analysis can be performed using the following databases: GeneCard (www.genecards.org), OMIM (http://www.ncbi.nlm.nih.gov/Omim) and PubMed (www.pubmed.gov). These databases can only be searched for information on single genes rather than whole gene lists. GeneCard provides information on gene expression, orthologies, alternative nomenclature and a brief synopsis of gene function. OMIM describes the human diseases associated with the gene, and the mutations responsible for the disease phenotype.

4.1.3 Aims

Using the insight obtained from the optimisation of the chondrogenic model system and the RT-PCR analysis of the expression of chondrogenic genes (Chapter 3), a GEM experiment was set up and performed. The aim of this GEM experiment was to generate reproducible data representing the changes in the expression profile of MSC undergoing chondrogenesis with a particular emphasis on the early events. This data was then analysed with

the objective of providing a global overview of chondrogenesis and identifying novel factors involved in this process.

4.2 STATISTICAL MANIPULATION OF DATA

4.2.1 Sample preparation, hybridization and visualization of data

RNA isolated from undifferentiated MSC and MSC undergoing chondrogenesis was reverse transcribed into cDNA, put through second strand synthesis and then *in vitro* transcribed into biotinylated cRNA (Methods: Section 2.2). The labelled cRNA was hybridized onto the HGU133A gene chips. Due to the variability in chondrogenic potential noted between the MSC isolated from different donors (Section 3.4.1), this experiment was performed in triplicate using cells isolated from the 24M donor only. The MSC derived from this donor were shown to differentiate well into chondrocytes (Section 3.4.1)

Microarray results were, in the first instance, obtained in the form of a scanned image (Figure 4.1.A). It was important to perform quality control on this image and check that it was free of irregularities, such as shadows or scratches. As the biotinylated cRNA bound to the probes in the chip, each probe appeared as a spot on this image, and the brightness of the spot varied according to how much cRNA has bound. The intensities of the hybridized spots on the gene chips were then converted into numerical values representing the signal intensity for each probe.

Prior to normalization, the signal intensities were checked, to ensure that background signal intensities were comparable between the different chips. This was done by producing a boxplot of log transformed signal intensities (Figure 4.1.B). The log transformation is necessary to convert the otherwise skewed distribution into a normal one that is easier to handle with statistical tools. The box plot indicates the median and the 25% boundaries on either side; hence 50% of the data are included in the box while the remainder are represented by the dashed lines. Minor variation between the microarrays is inevitable and was corrected by normalization, but for others

(such as sample 17 in Figure 4.1.B) the background intensity was too high and such samples could not be used in the analysis.

Following the quality control, normalization was performed. The RMA algorithm was used that normalizes each probe intensity using rank normalization (164)(Section 4.1.2). This process levels all the median signal intensities as well as achieving the same spread for all arrays, thereby making them comparable.

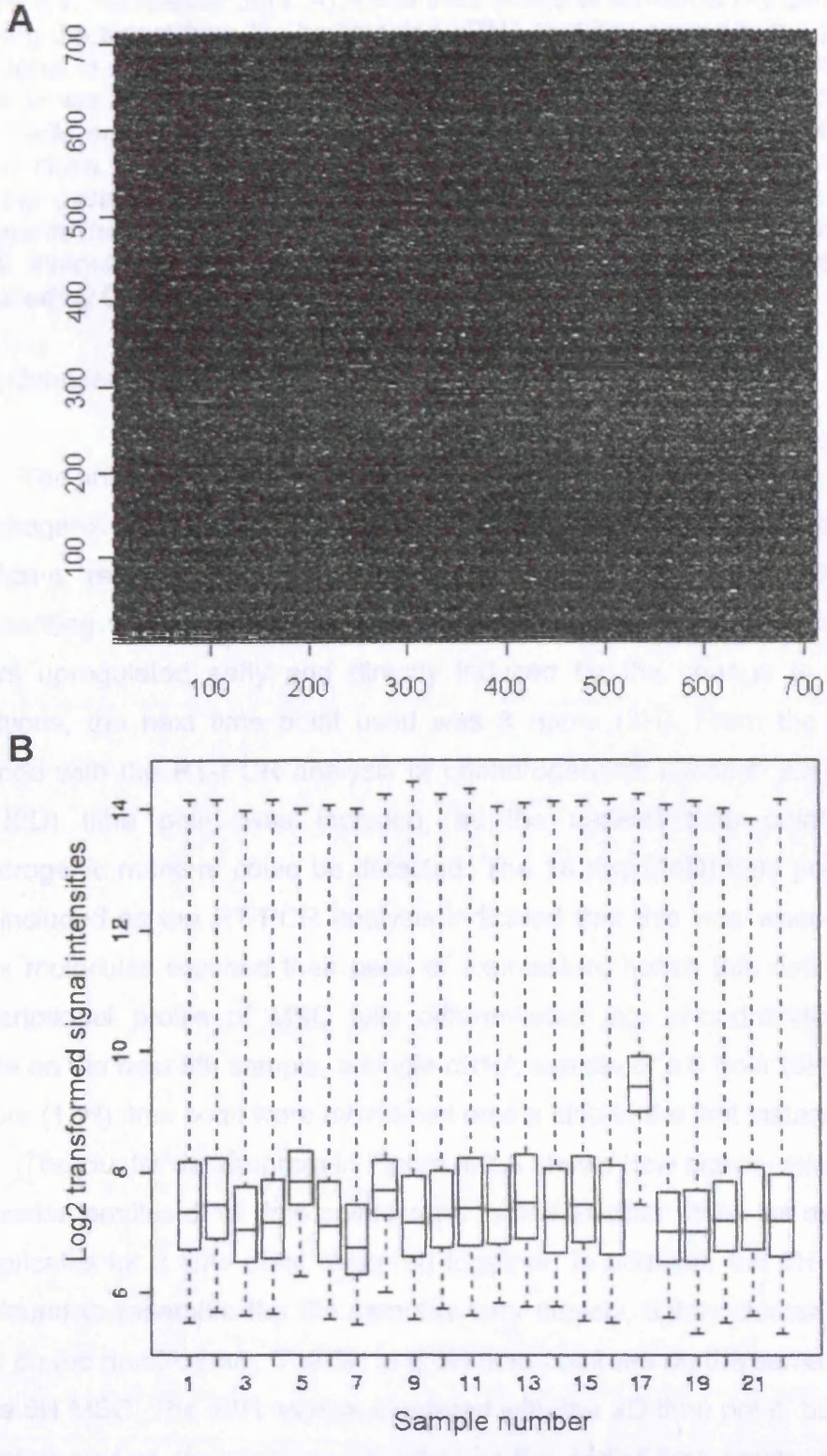

(Legend on following page)

Figure 4.1: Microarray data. A) A scanned image of a microarray gene chip, showing the signal from the biotinylated cRNA that has bound to the probes. The signal is visible as areas of white on the chip. A brighter signal indicates higher levels of expression of the mRNA specific to this probe. B) Box plots of all GEM analyses performed showing the distribution of signal intensities on the chips. The boxes represent the median 50% of expression values, with the dashed lines representing the rest. The central line in the boxes represents the median expression value. Sample 17 had an abnormally high signal intensity and was therefore excluded from analysis (Figure 4.1.B produced by Dr Stephen Henderson).

4.2.2 Overview of data

The initial aim was to perform microarrays of 5 time points during chondrogenic differentiation of MSC, each in triplicate, to obtain statistically significant results. The first time point included was 0 hours (0H), representing undifferentiated MSC. In order to investigate the transcription factors upregulated early and directly induced by the change in culture conditions, the next time point used was 3 hours (3H). From the results obtained with the RT-PCR analysis of chondrogenesis (Section 3.5), the 2 day (2D) time point was included, as the earliest time point when chondrogenic markers could be detected. The 14 day (14D) time point was also included as the RT-PCR analysis indicated that this was when all the matrix molecules reached their peak of expression; hence this defined the transcriptional profile of MSC fully differentiated into chondrocytes. To decide on the best 5th sample, a single cRNA sample of a 6 hour (6H) and a 12 hour (12H) time point were hybridized onto a chip in the first instance.

The cluster dendrogram in Figure 4.2.A shows how closely related the expression profiles of all time points were to one another other. As expected all replicates for a time point clustered together. In addition, the 6H sample was found to resemble the 3H samples very closely, tightly clustering with these on the dendrogram. The 3H and 6H time point are on the same branch as the 0H MSC. The 12H sample clustered with the 2D time point, but these did not cluster as closely to one another as the earlier time points, as seen

by the height of the respective nodes. Therefore, the 12H time point was more representative of an intermediate between 3H and 2D than the 6H time point and was repeated in triplicate. The fully differentiated chondrocytes of the 14D time point are on a separate branch to the other samples, indicating that their expression profile is most divergent to the earlier timepoints. The single 6H sample is present both in the dendrogram and the heatmaps (Figure 4.2) but was not used for any of the later statistical analysis.

Figure 4.2: Microarray data analysis. A) Cluster dendrogram showing the relationship between the expression profiles of different samples and time points. The height of the nodes is representative of the degree of difference between the two connected samples. B) Heatmap showing all 1,394 significantly changing probe sets as ordered by hierarchical clustering (Figure produced by Dr Stephen Henderson).

Multi-dimensional scaling (MDS) is another way to demonstrate graphically the overall similarities and differences seen between different arrays. MDS summarizes the data obtained, and rearranges it in a given

number of dimensions. For microarray data this involves combining the values for the 22,000 probe sets present on a chip into 2 or 3 values that can be mapped onto a plot. The MDS plot in Figure 4.3 shows the same distribution of phases of chondrogenesis as seen with the dendrogram. Again, the replicates from the same time point cluster together. The 0H (MSC) and 3H samples cluster closely together with the 12H and 2D sample forming a separate group. The final time point (14D) forms a distinct group that is most divergent from any of the others and therefore further away on the MDS plot.

Overall, 3 phases of chondrogenic differentiation were seen. The earliest phase was represented by the 3H samples as these formed a distinct, but closely related, group to the 0H samples. The next phase included the 12H and 2D samples. At these time points the expression levels of many genes were different from the 0H/3H group but were also distinct from the final 14D profile, which was in itself a distinct phase.

Figure 4.3: Multi-dimensional scaling plot showing the relationship between the different time points of MSC undergoing chondrogenesis (figure produced by Dr Matthew Trotter).

4.2.3 Identifying differentially expressed genes

The relevance of the different time points lay in the particular transcripts that change from one time point to the next. A moderated standard deviation test was performed on the normalized data to obtain lists of most significantly changing genes from 0H to 3H, 3H to 12H, 12H to 2D and 2D to 14D. The p-value obtained was adjusted for multiple testing using the false discovery rate thus producing the q value (178). It was particularly important to take the false discovery rate into account due to the large amounts of data obtained from microarray analysis and the multiple hypotheses being tested, as opposed to testing the expression levels for

each gene separately (178). In such cases the p-values were likely to be inaccurate and produce many false positives, hence the tests used needed to be adjusted.

An initial significance cut-off was placed at $q<0.01$. This cut-off generated a list of 375 probe sets with expression values that change significantly between 0H and 3H. However, using this cut-off, probe lists generated for the later time points were too long for further analysis to be performed on them. Therefore, only the top 500 most significantly differentially expressed genes were chosen for analysis of the changes between the later timepoints. Between the 3H and 12H time point, the top 500 most significantly changing genes had a q value < 0.0003. The top 500 genes were also chosen for the 12H to 2D step and 2D to 14D step giving $q<0.0005$ and $q < 0.0000015$, respectively. As some of these probe sets changed significantly in more then one of the steps, when combined, the q-value test generated a list of 1,394 probe sets, equalling 1,109 genes as some genes were represented by more than one probe set. The full list of the 1,394 probe sets is provided in a digital format on a CD-ROM in supplementary data (Section 9).

To get an overall visual impression of the expressional changes occurring to these probe sets during the time course, a heatmap was produced (Figure 4.2.B). Hierarchical clustering was used to group these probe sets according to their behaviour (*i.e.* their expression values) across all the chips examined. Hierarchical clustering orders the expression patterns by similarity. The process works by first picking out the two probe sets showing the greatest similarity in terms of gene expression and then grouping them together to make a node, which consequently operates as one unit. This search for most similar nodes continues, until all the genes are connected into one node and the nodes are numbered in the order in which they are created. The results from the clustering are visualized in the form of a heat map. The mean expression value for each gene is calculated, and the deviation from this mean is what is displayed on the heat map rather than

the actual expression values. If the expression value is higher than the mean the field is represented by red on the heat map. If it is equal to the mean the field is black and if it is lower than the mean, the field is green. The more an expression value deviates from the mean the stronger the colour that is displayed.

4.3 VALIDATION OF GEM DATA

The microarray data was validated in a variety of ways. Firstly, the data was shown to be reproducible between the samples for the same time point. The Pearson correlation coefficient is a measure of the similarity between replicates; this takes into account how well the values obtained for each probe set correlate with one another. A Pearson correlation value of 1 would signify that the two datasets are identical whereas a value of -1 would mean that the datasets are exact opposites of each other. In this dataset the correlation values were as follows: 0.99 for the 0H time points, 0.99 for the 3H time points, 0.99 for the 12H time points and 0.98 for the 14D time points. For comparison, previously published microarray data have obtained Pearson correlation coefficients as low as 0.73 for replicates, showing that the data presented here is robust (179).

The dendrogram and the MDS plot (Figure 4.1.A and 4.2) also validated the microarray data as all the timepoint replicates were more similar to each other than to the profile at any other time point. In addition, the time points cluster in a temporal order.

To see if the expression profiles obtained through the microarray data could be replicated by another technique, RT-PCR analysis was used. Nine genes exhibiting different patterns of expression were chosen – including genes upregulated early (HES1), upregulated late (Col2) and downregulated (ADAMTS1). The gene expression patterns seen using RT-PCR analysis are similar to those obtained with microarray analysis. Furthermore, even some subtle changes seen in the heatmaps are reproduced with the RT-PCR technique (Figure 4.4).

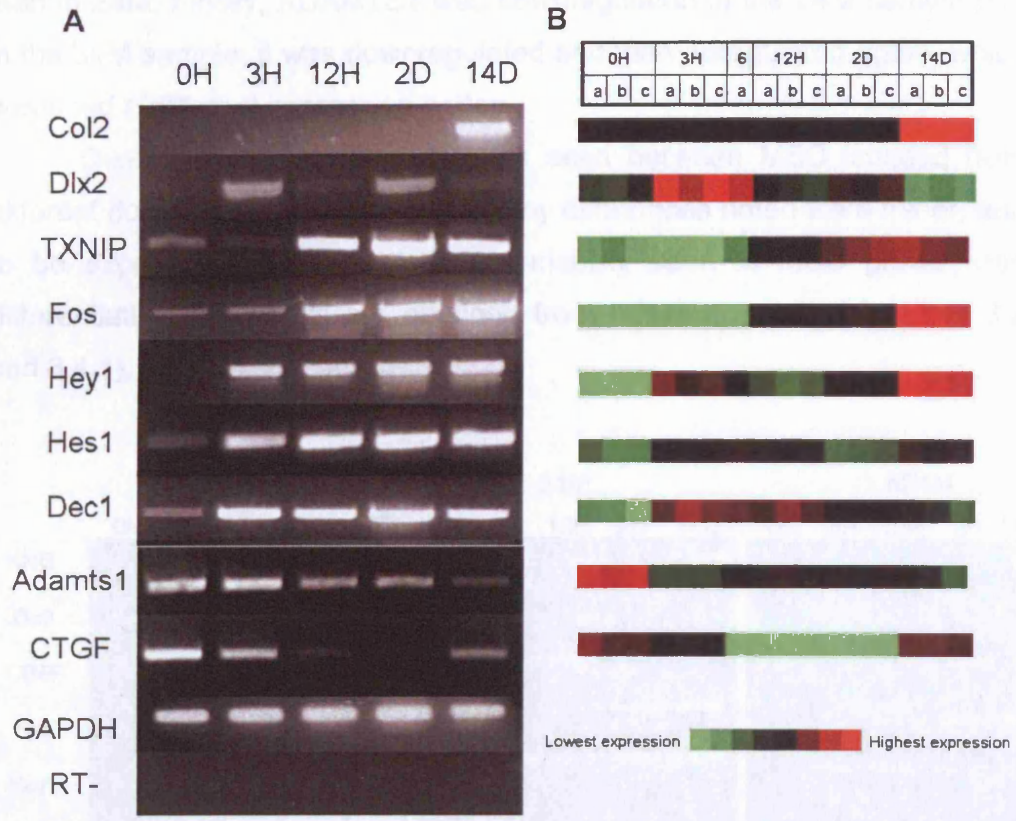

Figure 4.4: A) Gel electrophoresis showing RT-PCR analysis of a selection of genes with significantly altered levels of expression during MSC chondrogenic differentiation. B) Heatmap showing the GEM expression patterns for the genes in A, selected from the overall heatmap in figure 4.2.B.

As the microarray analysis replicates were performed on MSC isolated from only one donor, the next step in the validation was to check whether the same expression patterns could be seen in MSC samples derived from other donors. These results were confirmed using RNA isolated from MSC undergoing chondrogenesis of 2 further bone marrow donors (a 31 year old male - 31M, and a second 24 year old male sample - n24M) (Figure 4.5). The expression of 6 genes (col2, fos, HES1, HEY1, dec1, CTGF) was the same between different MSC lines. Dlx2 was upregulated at 3H in all samples but the second upregulation at 2D noted in the 24M, could only be seen at very low levels in the 31M and not at all in the n24M. TXNIP was upregulated in all samples but much less dramatically in n24M and 31M

than in 24M. Finally, ADAMTS1 was downregulated in the 24M sample but, in the 31M sample, it was downregulated and then upregulated again, which produced a different expression pattern.

Overall, the expression patterns seen between MSC isolated from different donors were very similar and any differences noted were minor, and to be expected due to the known variability seen in MSC growth and differentiation when cells are obtained from different donors (Sections 3.2 and 3.4.1).

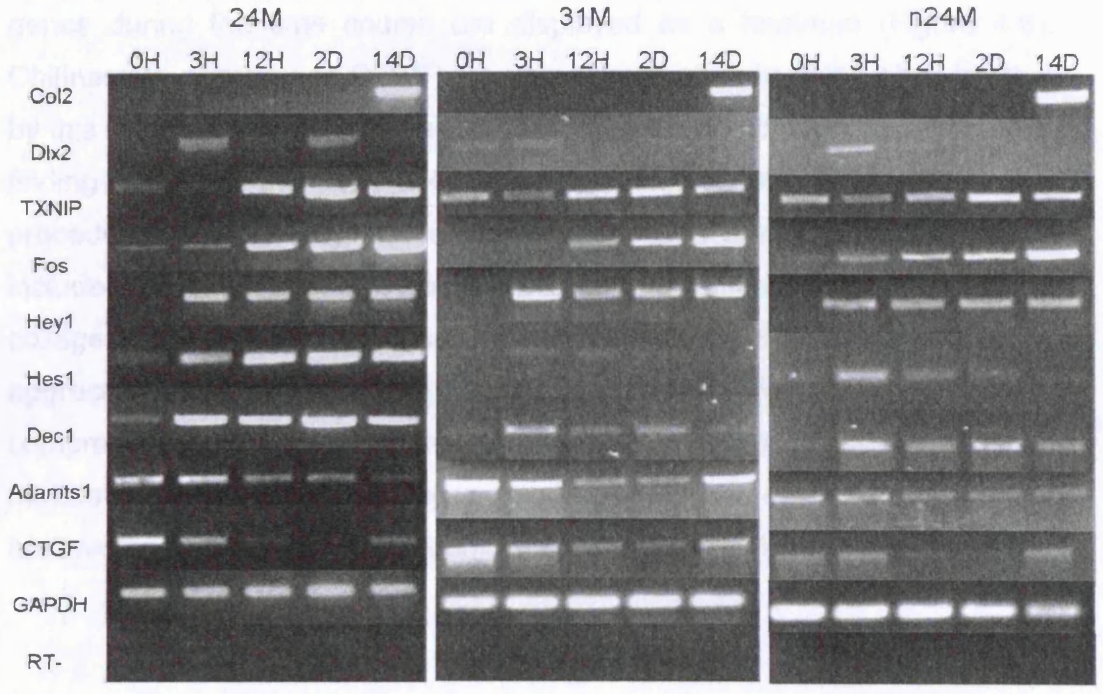

Figure 4.5: Gel electrophoresis showing RT-PCR analysis comparing the transcript levels of a selection of genes expressed by MSC undergoing chondrogenic differentiation. The MSC were isolated from 3 different donors: 24M (that the GEM experiments were performed on), 31M and n24M.

4.4 SIMILARITY OF GEM DATA TO *IN VIVO* CARTILAGE DEVELOPMENT

Microarray data was reproducible between replicates and robust when validated by a different technique to measure changes in gene expression. Therefore the next issue addressed was whether the MSC *in vitro* chondrogenesis model system is a good representation of cartilage development.

The most striking confirmation that MSC form cartilage *in vitro* is in the expression of ECM genes. The change in expression levels of ECM genes during the time course are displayed as a heatmap (Figure 4.6). Chitinase 3, decorin and COMP are upregulated already at 2D, showing that by this time point, the MSC could already be considered chondroblastic. This finding confirms the RT-PCR results obtained during the optimisation procedure (Section 3.6). Matrix genes expressed during the time course included the main cartilage collagens 2, 9 and 11 that form the cartilage collagen fibres, giving it its tensile strength, as well as proteoglycans such as aggrecan and cartilage linking protein, responsible for allowing cartilage compression. Some of the upregulated matrix proteins are associated with mature cartilage (such as collagen 2, collagen 11 and aggrecan) but others are involved in the later hypertrophic stages (collagen10 and osteopontin).

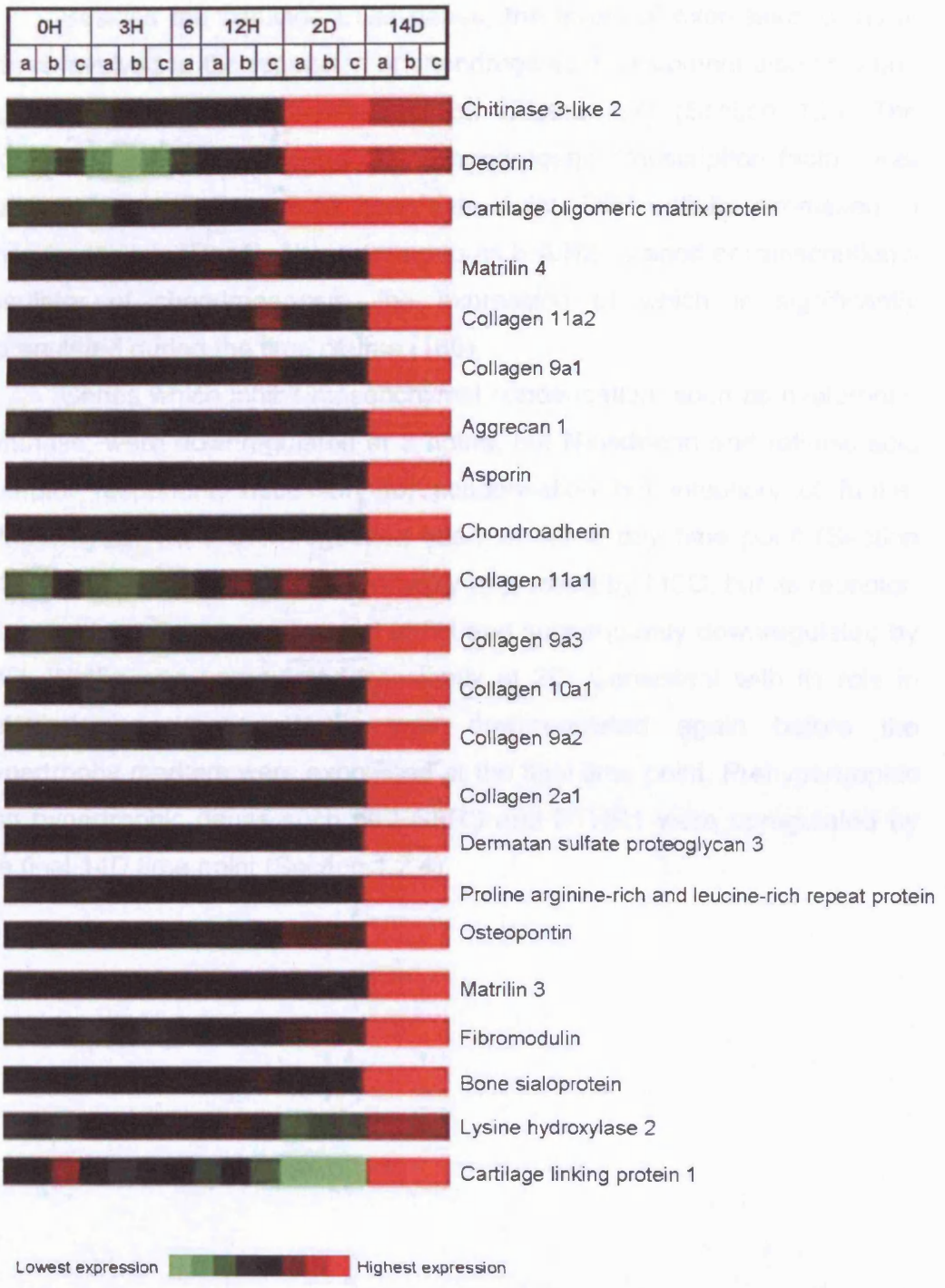

Figure 4.6: Heatmap showing changes in expression levels of ECM genes selected from the overall heatmap in figure 4.2.B.

Besides the cartilage ECM genes, the levels of expression of other genes involved in the regulation of chondrogenic development also changed significantly during MSC differentiation (Figure 4.7) (Section 1.2). The expression level of Sox9, the main chondrogenic transcription factor, was strongly elevated by the 12 hour time point. Differentially expressed in chondrogenesis (Dec1), also referred to as bHLH2, is another transcriptional regulator of chondrogenesis, the expression of which is significantly upregulated during the time course (180).

Genes which inhibit mesenchymal condensation, such as hyaluronan synthase, were downregulated at 3 hours, but N-cadherin and retinoic acid receptor responder, necessary for condensation but inhibitory of further differentiation were downregulated later, at the 2 day time point (Section 1.2.2). Fibronectin was already strongly expressed by MSC, but its receptor, integrin alpha 5 was upregulated at 3H and subsequently downregulated by 14D. Wnt5a was upregulated transiently at 2D. Consistent with its role in delaying hypertrophy, Wnt5a was downregulated again before the hypertrophy markers were expressed at the final time point. Prehypertrophic and hypertrophic genes such as FGFR3 and PTHR1 were upregulated by the final 14D time point (Section 1.2.4).

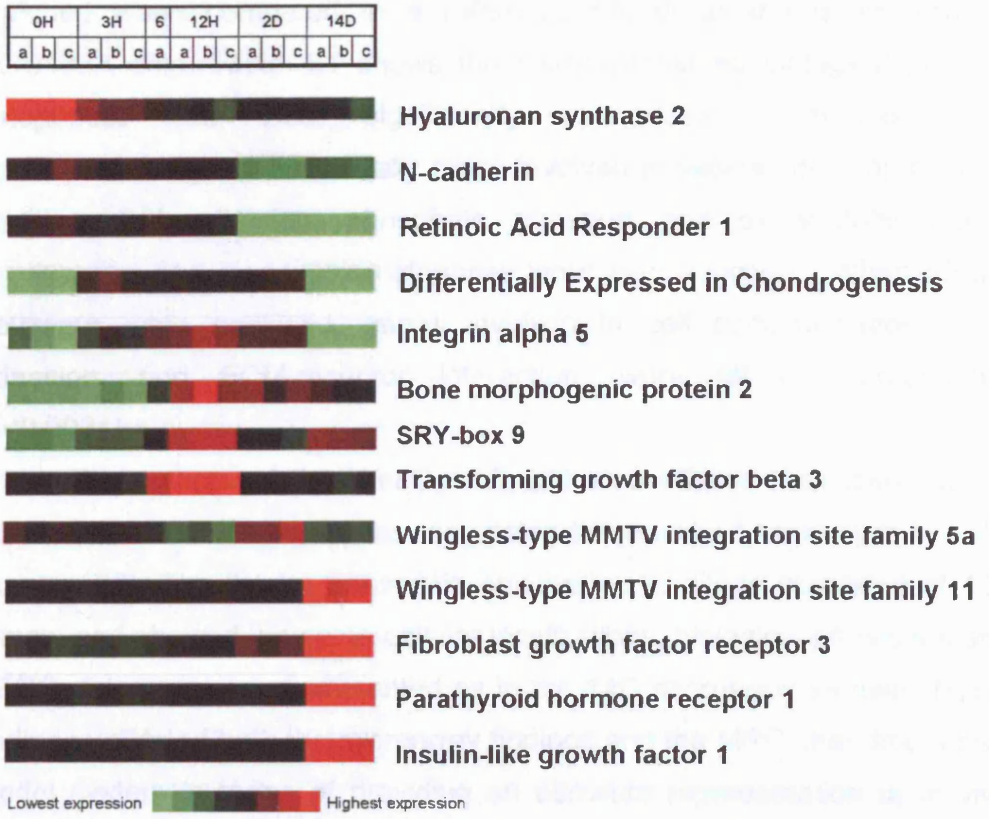

Figure 4.7: Heatmap showing changes in expression levels of genes with known roles in chondrogenic development selected from the overall heatmap in figure 4.2.B.

To study further the similarity of the gene expression profile between the final time point (14D) and normal cartilage, the expression profiles obtained at 0H and 14D were compared, and the 100 probe sets, where the expression levels were most significantly altered, identified ($q<0.0001$). Of these probe sets, 76 were expressed 4 fold or more higher in the 14D than in the 0H time point (representing 58 genes, as, in some cases, 2 or more probe sets represented the same gene). The gene list obtained was analyzed by the WebGestalt gene ontology tool (http://bioinfo.vanderbilt.edu/webgestalt/ (176)). As may be expected, genes encoding proteins located in the extracellular region (24 genes, $p<0.0001$) and their subset, the extracellular matrix genes (17 genes, $p<0.0001$) were

enriched when compared to a reference set of all the genes on the HGU133A chip. Table 4.1 shows the over-represented biological process categories. The most significantly upregulated categories were developmental genes, especially those involved in skeletal development. In addition, cell adhesion, phosphate transport and extracellular matrix organization and biogenesis categories were also enriched. When KEGG pathways were analysed, genes involved in cell communication, focal adhesion, and ECM-receptor interaction, were all over-represented ($p<0.0001$).

The authors of the WebGestalt tool also offered their own lists of genes for various tissue types, comprising the enriched transcripts in each tissue (176). The list for transcripts enriched in cartilage consisted of 101 genes, and showed the same cellular localizations, biological processes and KEGG pathways over-represented as in the 14D microarray sample. These findings validated both the microarray findings and the MSC chondrogenesis model system in terms of providing an accurate representation of *in vivo* cartilage development.

0H-14D COMPARISON			
G0 CATEGORY	**N**	**P value**	**GENES**
Cell Adhesion	8	0.00030	DPT OMD COMP COL11A1 COL11A2 AGC1 SPP1 IBSP
Extracellular matrix organization and biogenesis	3	0.00080	MATN3 COL11A1 COL11A2
Phosphate transport	7	<0.0001	C1QTNF3 COL10A1 COL11A1 COL11A2 COL9A2 COL9A3 COL2A1
Development	25	<0.0001	MEF2C MATN3 KLF4 HEY1 SCRG1 PRELP COL11A1 FGFR3 COMP PTHR1 COL10A1 IBSP PTCH SPP1 IGFBP5 COL2A1 COL9A2 COL11A2 PMP22 ANGPTL2 IGF1 FOS PAPSS2 GPL4 PTGS2
- Organ development	16	<0.0001	MEF2C MATN3 HEY1 PRELP COL11A1 FGFR3 COMP PTHR1 COL10A1 IBSP SPP1 COL2A1 COL9A2 COL11A2 IGF1 PAPSS2
- - Skeletal development	14	<0.0001	MATN3 PRELP COL11A1 FGFR3 COMP PTHR1 COL10A1 IBSP SPP1 COL2A1 COL9A2 COL11A2 IGF1 SPP1
- Tissue development	4	0.00973	IBSP SPP1 KLF4 COL11A1
Sensory perception	7	0.00233	RBP4 AOC2 COL11A1 COL11A2 COL2A1 IGF1 PMP22

Table 4.1: The WebGestalt results of significantly over-represented biological processes. The analysis was performed on the gene list comprising the most significantly upregulated genes between the 0H and 14D time points. As many of these genes have multiple names, their recognized gene symbols are used. Indented gene ontology categories are subsets of the category above.

4.5 GENE ONTOLOGY ANALYSIS OF PROBE SETS WITH SIGNIFICANTLY CHANGING EXPRESSION LEVELS BETWEEN TIME POINTS

To provide an overview of the transcriptional changes that occur as MSC undergo chondrogenesis, the genes identified as having significantly altered expression levels above could not be considered individually (Section 4.2.4). Instead, a tool needed to be used that could group these genes according to their characteristics. Gene ontology analysis provided such groupings, according to the biological processes that the protein products are involved in, their cellular localization and molecular function. The advantage of using WebGestalt over other gene ontology programmes is in the statistical features of WebGestalt. WebGestalt is not only able to group the input genes by gene ontology but also provides statistical values for over-representation of genes in a particular category as compared to a reference set.

To perform the WebGestalt gene ontology analysis, the lists obtained for the probe sets with most significantly changing levels of expression between consecutive time points (Section 4.2.4) was further divided into those that were upregulated and those that were downregulated. The full gene lists are provided in the supplementary data (Section 9). The number of probe sets and the number of genes that these represent for each time point is presented in Table 4.2. Gene ontology analysis was performed using the WebGestalt programme and the HGU133A gene list as a reference list for comparison. The HGU133A gene chips, used for the GEM experiments, did not contain all the genes of the human genome, it was therefore important to only include the subset of human genes present on these chips as the reference list.

The analysis presented here focuses on biological processes and cellular localization as molecular function was not found to be informative for the purposes of this study. Significantly over-represented categories were chosen using the hypergeometric test and a cut-off of 2.5% of genes from

the gene list was set in order to exclude categories with only 2 or 3 genes. The cut-off p-value chosen was $p<0.01$.

Category	Number of probe sets	Number of genes
0H-3H Upregulated	246	164
0H-3H Downregulated	129	87
3H-12H Upregulated	229	146
3H-12H Downregulated	271	205
12H-2D Upregulated	292	203
12H-2D Downregulated	208	136
2D-14D Upregulated	215	152
2D-14D Downregulated	285	182
Total	1394	1109

Table 4.2: Numbers of significantly upregulated and downregulated probe sets between time points and the number of genes that these probe sets correspond to.

4.5.1 Gene ontology analysis for biological processes

Changes in gene expression occurring between the 0H and 3H time points

In order to induce MSC to undergo chondrogenesis they were placed in differentiation media and grown in pellet cultures. The cytokines added to the media as well as the close cell to cell contact induced changes at the transcriptional level that eventually led to the MSC differentiating into cartilage.

Between 0H and 3H, 246 probe sets were upregulated and these represent 164 genes (Table 4.2). A surprising number of gene ontology categories were enriched within this group (Table 4.3). However, the most significantly over-represented categories were those related to transcription and development. As this is the first step of MSC towards chondrogenesis, the over-representation of these categories was not surprising. The upregulated transcription factors may well be the key players in initiating chondrogenesis. Among the upregulated transcription factors are genes

already implicated in chondrogenesis such as BHLH2 (also known as DEC1) (180), Runx1 (181), Dlx5 (182) and Gli2 (183). Id1, 3 and 4 are all also upregulated at this time point. Their expression has previously been noted in cartilage but their roles in chondrogenesis have not been elucidated (184). The function of Id proteins is generally to prevent premature differentiation and it is probable that they play such a role in chondrogenesis through inhibiting the action of subsets of transcription factors upregulated at this stage (185).

The main targets of Notch signalling, HES1 and HEY1 were also both upregulated at this early stage. Notch signalling is known to play a part in the cell fate commitment and differentiation in many tissues and has been implicated in chondrogenesis (186). In addition, Notch signalling is reliant on cell to cell interaction that is also a necessary factor for the progression of chondrogenesis (187) (Section 5.1). As this is a pathway chosen for further analysis, it will be discussed in more detail in Chapter 5.

Nineteen of the genes present in the group of transcriptional regulators are also known to have a role in development, so there is overlap between these two categories. Signal transduction is another enriched category and includes members of the MAPK cascade, known to be involved in the early stages of chondrogenesis (188).

The enriched categories among the 87 downregulated genes also included transcription and development (Table 4.4). Many of the downregulated transcription factors are known to be involved in differentiation into other lineages such as neural (e.g. BDNF, HoxA1 and ENC), adipogenic (NR2F2) and myogenic (MEOX2).

0H-3H UPREGULATED			
G0 CATEGORY	**N**	**P value**	**GENES**
Response to stress	26	0.00110	ADORA2B ANGPTL4 BCL6 CD9 CEBPB DUSP1 EGFR ELN F2RL1 F3 GADD45B HRH1 IFNGR1 IL11 IL1R1 INHBA MAP3K4 NFKBIA NR4A2 POLS PTGS2 REV3L SERPINE1 SMAD7 SNN VEGF
- Response to wounding	12	0.00950	ADORA2B BCL6 CD9 CEBPB F2RL1 F3 HRH1 IL11 IL1R1 INHBA PTGS2 SERPINE1
Response to external stimulus	19	0.00560	ADORA2B ANGPTL4 BCL6 CD9 CEBPB F2RL1 F3 HRH1 IFNGR1 IL11 IL1R1 INHBA NFKBIA NR4A2 PTGS2 SERPINE1 STC1 STC2 VEGF
Transcription	48	<0.0001	BCL6 BCOR BHLHB2 BTAF1 BTG1 CEBPB DLX2 DLX5 ELF1 EPAS1 ERF FOSB FOXO3A GABPB2 GLI2 HES1 HEY1 ID1 ID3 ID4 JARID2 JUNB KLF13 KLF4 KLF9 MAFF MEF2A NFATC1 NFIL3 NR4A1 NR4A2 NR4A3 PER1 PER2 RORA RUNX1 RYBP SAP30 SEC14L2 SMAD7 SNAI2 SPEN TBX2 THRAP1 TLE3 TSC22D3 VGLL4 ZNF189
Cell communication	59	0.00722	ADORA2B ANGPTL4 BMPR2 CD9 CRYAB DNMBP DUSP4 EDNRA EGFR EPAS1 F2RL1 GADD45B GEM GLI2 HMOX1 HRH1 IFNGR1 IL11 IL1R1 INHBA ITGA5 JAG1 JAK1 MAP3K2 MAP3K4 MTSS1 MYO10 NEDD9 NFKBIA NMB NR4A1 NR4A2 PBEF1 PER1 PER2 PGF PIK3R3 RAB20 RAB31 RGS2 RGS3 RHOB RORA RRAD SHB SMAD7 SNF1LK SOCS2 SPEN SPRY4 STC1 STC2 STK24 THRAP1 TLE3 TNFAIP3 TRAF3IP2 TRIO VEGF
- Signal transduction	56	0.00011	ADORA2B BMPR2 CRYAB DNMBP DUSP4 EDNRA EGFR EPAS1 F2RL1 GADD45B GEM GLI2 HMOX1 HRH1 IFNGR1 IL1R1 INHBA ITGA5 JAG1 JAK1 MAP3K2 MAP3K4 MTSS1 MYO10 NEDD9 NFKBIA NMB NR4A1 NR4A2 PBEF1 PER1 PER2 PGF PIK3R3 RAB20 RAB31 RGS2 RGS3 RHOB RORA RRAD SHB SMAD7 SNF1LK SOCS2 SPEN SPRY4 STC1 STC2 STK24 THRAP1 TLE3 TNFAIP3 TRAF3IP2 TRIO VEGF
- - Intracelluiar signalling cascade	25	0.00277	ADORA2B DNMBP DUSP4 EDNRA EGFR GADD45B GEM HMOX1 HRH1 JAK1 MAP3K2 MAP3K4 NFKBIA PIK3R3 RAB20 RAB31 RGS3 RHOB RRAD SHB SNF1LK SOCS2 THRAP1 TNFAIP3 TRAF3IP2
- - - Protein kinase cascade	12	0.00403	ADORA2B DUSP4 GADD45B HMOX1 MAP3K2 MAP3K4 NFKBIA RGS3 SNF1LK SOCS2 TNFAIP3 TRAF3IP2
- - - - MAPKKK cascade	6	0.00179	ADORA2B DUSP4 GADD45B MAP3K2 MAP3K4 RGS3
Positive regulation of enzyme activity	6	0.00336	ADORA2B BTG1 GADD45B MAP3K2 MAP3K4 EDNRA
Apoptosis	14	0.00854	ANGPTL4 BAG3 BTG1 FOXO3A GADD45B INHBA MCL1 NFKBIA NOL3 RHOB RYBP SOCS2 TNFAIP3 VEGF
- Negative regulation of apoptosis	7	0.00153	ANGPTL4 BAG3 MCL1 NOL3 SOCS2 TNFAIP3 VEGF
Development	45	<0.0001	ADARB1 ANGPTL4 BMPR2 BTG1 CD9 DLX2 DLX5 EGFR ELN EMP1 EPAS1 FABP5 FOSB GADD45B GLI2 HES1 HEY1 ID1 ID3 IL11 INHBA JAG1 JARID2 KLF MCL1 MEF2 MTSS1 NDRG1 NEDD9 PGF PTDSR PTGS2 RHOB RUNX1 SEMA4C SLC3A2 SNAI1 SNAI2 SNF1LK SOCS2 SPRY4 SYNE1 TBX2 TLE3 VEGF
- Cell differentiation	20	<0.0001	ANGPTL4 BTG1 CD9 EPAS1 GADD45B IL11 INHBA JAG1 KLF4 MCL1 NDRG1 PGF PTDSR PTGS2 RHOB SEMA4C SNF1LK SOCS2 SYNE1 VEGF
- Nervous system development	14	0.00460	ADARB1 CD9 DLX2 DLX5 HES1 HEY1 INHBA JAG1 JARID2 MTSS1 SEMA4C SNAI1 SOCS2 VEGF
- Morphogenesis	18	0.00112	ANGPTL4 BTG1 ELN EMP1 EPAS1 GLI2 HEY1 INHBA JAG1 KLF4 MTSS1 NEDD9 PGF RHOB SLC3A2 SOCS2 TLE3 VEGF
- Organ development	20	0.00018	ANGPTL4 BMPR2 BTG1 DLX2 DLX5 EGFR ELN EPAS1 GLI2 HEY1 IL11 INHBA JAG1 MEF2A MTSS1 PGF RHOB SNAI1 TLE3 VEGF

Table 4.3: The WebGestalt results of significantly over-represented biological processes. The analysis was performed on the gene list comprising the most significantly upregulated genes between the 0H and 3H time points. As many of these genes have multiple names, their recognized gene symbols are used. Indented gene ontology categories are subsets of the category above.

0H-3H DOWNREGULATED			
GO CATEGORY	N	P value	GENES
Protein kinase cascade	7	0.00474	BCL3 CCL2 EDG2 FGF2 PLK2 RGS4 SOCS5
Cell homeostasis	6	0.00052	TXNRD1 CXCL12 EDG2 TFRC BDKRB1 CCL2
Development	26	0.00081	BDNF CCL2 CDC42EP3 CYR61 DKK1 DLC1 DSCR1 ENC1 FGF2 FGF5 FZD2 GATA6 HMGA2 HOXA1 HOXA5 HOXA9 HOXB2 ID2 KRT10 MCAM MEOX2 PITX2 SOCS5 TNFRSF11B TWIST1 UGCG
Transcription	25	0.00101	AHR ARID5B BCL3 CEBPD CITED2 CRSP9 EGR1 GATA6 HMGA2 HOXA1 HOXA5 HOXA9 HOXB2 ID2 IRX5 LMO4 MEOX2 NR2F2 NRIP1 PITX2 RFP SOX4 TRFP TWIST1 ZNF238

Table 4.4: The WebGestalt results of significantly over-represented biological processes. The analysis was performed on the gene list comprising the most significantly downregulated genes between the 0H and 3H time points. As many of these genes have multiple names, their recognized gene symbols are used.

Changes in gene expression occurring between the 3H and 12H time points

Between 3 and 12 hours, 146 genes were upregulated and 205 downregulated within the 500 probe sets that changed expression levels most significantly (Table 4.2). Genes involved in cell proliferation were over-represented in both the upregulated and downregulated category, with negative regulators of proliferation being upregulated and genes involved in mitosis being downregulated (Table 4.5 and 4.6). Some of these genes were already known to be expressed by cartilage – for example MXI1, which regulates cell cycle through its involvement with the Myc proteins. MXI1 is expressed in both mesenchymal condensations and mature chondrocytes (189;190). GAS1 protein inhibits the G0 to G1 transition and has been found to be expressed in limb bud chondrocytes that have begun differentiating (191).

Another enriched category within the genes upregulated between 3 and 12 hours was glycolysis. As chondrocytes are located within an anaerobic environment, it has been reported that they are mostly glycolytic and have few mitochondria. Therefore, chondrocytes upregulate glycolytic genes including the main glycolytic enzyme PGK1 (192).

Among the downregulated categories, genes involved in cell motility were significantly over-represented. Mesenchymal stem cells are mobile

and it has been proposed that they 'home into' sites of injury (193). However as they begin to differentiate into chondrocytes, they become locked into the cartilaginous matrix and therefore this could explain why they lose expression of the genes required for cell motility.

3H-12H UPREGULATED			
GO CATEGORY	N	P value	GENES
G-Protein signalling	4	0.00925	EDNRA AGTR1 HRH1 PPAP2A
Cell proliferation	17	0.00703	BTG1 ZPF36L2 MXI1 MYC MADREL BCL6 GAS1 EDNRA IFI16 CDKN1B PPAP2A TGFB3 PMP22 MTCPI GRN IFITM1 SESN1
- Regulation of cell proliferation	10	0.00443	BTG1 MXI1 BCL6 GAS1 CDKN1B PPAP2A PMP22 GRN IFITM1 SESN1
- - Negative regulation of cell proliferation	8	0.00082	BTG1 MXI1 GAS1 CDKN1B PPAP2A PMP22 IFITM1 SESN1
Glycolysis	4	0.00440	PGK1 ENO2 PGM1 ALDOC
Cell homeostasis	6	0.00710	MYC EDNRA STC1AGTR1 GLRX GPR24
- Di/ tri valent inorganic cation homeostasis	5	0.00775	MYC EDNRA STC1AGTR1 GPR24

Table 4.5: The WebGestalt results of significantly over-represented biological processes. The analysis was performed on the gene list comprising the most significantly upregulated genes between the 3H and 12H time points. As many of these genes have multiple names, their recognized gene symbols are used. Indented gene ontology categories are subsets of the category above.

3H-12H DOWNREGULATED			
GO CATEGORY	N	P value	GENES
Behaviour	12	0.00642	ACTR3 ANXA1 THBS1 ACSL4 TPBG HAS1 JAG1 CTGF ARPCS PPAP2B NRP1 TNFRSF12A
- Cell motility	11	0.00168	ACTR3 ANXA1 THBS1 TPBG HAS1 JAG1 CTGF ARPCS PPAP2B NRP1 TNFRSF12A
Cell cycle	24	0.00074	BCAR3 C10orf7 CCND1 CCT2 DKC1 DUSP4 DUSP6 EML4 EXT1 FGF2 GAS2L1 KPNA2 MACF1 MAPRE1 MCM5 NEDD9 PCNA PNN POLS RAN SNF1LK STAT1 TARDBP TUBG1
- Mitotic cell cycle	10	0.00244	CCND1 EML4 KPNA2 MAPRE1 NEDD9 POLS RAN SNF1LK TARDBP TUBG1
RNA splicing	8	0.00464	TARDBP SFRS2 SFRS1 SFRS5 SFRS6 SFRS7 SFPQ RBM25
Positive regualtion of enzyme activity	6	0.00950	FGF2 CYCS CARD10 MAP2K3 NALP1 STAT1

Table 4.6: The WebGestalt results of significantly over-represented biological processes. The analysis was performed on the gene list comprising the most significantly downregulated genes between the 3H and 12H time points. As many of these genes have multiple names, their recognized gene symbols are used. Indented gene ontology categories are subsets of the category above.

Changes in gene expression occurring between the 12H and 2D time points

Between 12 hours and 2 days, 203 genes were upregulated and 136 downregulated within the 500 probe sets that changed expression levels most significantly (Table 4.2). Similarly to the changes occurring between 3H and 12H, categories involved in cellular proliferation were over-represented, with many genes with roles in cell cycle arrest upregulated and mitotic genes downregulated. In addition, genes implicated in regulation of differentiation towards other lineages, in particular muscle, were downregulated.

There were also changes in cell surface proteins, with a large number of cell communication and cell adhesion molecules downregulated. N-cadherin (CDH2), a marker of mesenchymal condensations, was downregulated. There was also a group of genes the expression of which was downregulated at 2D and then upregulated again at the final 14D time point, such as CTGF and HAPLN1, which are necessary for the late phase of chondrogenic development.

12H-2D UPREGULATED			
GO CATEGORY	N	P value	GENES
Cell cycle arrest	5	0.00447	CUL3 IL8 GADD45A CDKN1C KHDRBSI
Amine metabolism	14	0.00098	GNPDA1 GUSB DIO2 ARG2 KYNU MAOA AOC3 ASNS PSPH UST CTH CHST7 CHI3L2 GLUL

Table 4.7: The WebGestalt results of significantly over-represented biological processes. The analysis was performed on the gene list comprising the most significantly upregulated genes between the 12H and 2D time points. As many of these genes have multiple names, their recognized gene symbols are used.

12H-2D DOWNREGULATED			
GO CATEGORY	N	P value	GENES
Cell communication	49	0.00838	ADAM12 ADAM9 ALCAM ANGPT2 CD59 CDH2 CFL1 CIB1 COL1A2 COL8A1 CRSP2 CSPG2 CTGF CXCL12 DIRAS3 EDNRA ENPP1 EPAS1 EPHB2 GAS6 GEM GPR24 HAPLN1 HRH1 INHBA ITGB5 MTSS1 NGFB NID2 PLAU PPAP2A PRKCA PTN RGS2 SEMA3C SFRP1 SOCS2 SSX2IP STC2 STK6 TGFB3TGM2 THBS2 TNFRSF12A TOP2A TPM1 TYMS UBE2C
- Cell adhesion	16	0.00028	ADAM12 ALCAM CDH2 CIB1 COL8A1 CSPG2 CTGF CXCL12 HAPLN1 ITGB5 MTSS1 NID2 SSX2IP TGM2 THBS2 TNFRSF12A
- Phosphoinositide mediated signalling	7	<0.0001	TOP2A TYMS UBE2C EDNRA HRH1 STK6 PPAP2A
Cell cycle	23	<0.0001	ASPM BIRC5 CCNB1 CCNB2 CDC2 CENPF DIRAS3 HGF INHBA KIF2C MTSS1 MYC PRC1 PRKCA PSMD1 PSMD2 PTN PTTG1 RGS2 STK6 TGFB3 TPX2 UBE2C
- Mitosis	12	<0.0001	ASPM CCNB1 CCNB2 CDC2 CENPF HGF KIF2C PRC1 PTTG1 STK6 TPX2 UBE2C
Organ development	14	0.00635	EPAS1 ACTA2 CALD1 COL1A2 SOX9 ADAM12 TAGLN ANGPT2 TPM1 MEF2C TGFB3 MTSS1 INHBA TNFRSF12A
- Muscle development	7	0.00228	ACTA2 CALD1 ADAM12 TAGLN TPM1 MEF2C MTSS

Table 4.8: The WebGestalt results of significantly over-represented biological processes. The analysis was performed on the gene list comprising the most significantly downregulated genes between the 12H and 2D time points. As many of these genes have multiple names, their recognized gene symbols are used. Indented gene ontology categories are subsets of the category above.

Changes in gene expression occurring between the 2D and 14D time points

Between 2 days and 14 days, 152 genes were upregulated and 182 downregulated within the 500 probe sets that changed expression levels most significantly (Table 4.2). Most of the upregulated categories involved genes characteristic of cartilage (Table 4.9). As expected, the most significantly over-represented category were genes involved in skeletal development, including matrix proteins such as collagens, matrillin 3, osteopontin, FGF and IGF receptors. Another upregulated category included genes involved in cell adhesion which are characteristic of cartilage such as COMP, CTGF and OMD.

Downregulated categories included genes involved in cell communication as well as those involved in the immune response (Table 4.10).

2D-14D UPREGULATED			
GO CATEGORY	N	P value	GENES
Cell adhesion	19	0.00012	ADAM22 AGC1 ALCAM CD36 COL11A1 COL11A2 COL9A1 COMP CTGF DPT DSG2 HAPLN1 IBSP NINJ2 OMD SPON2 SPP1 THBS1 THBS2
Amine metabolism	10	0.00713	AOC2 ASNS CHST3 IARS MARS ODC1 PSAT1 PTS SLC7A1 WARS
Development	41	<0.0001	ACTC ADAM22 ALPL ANGPTL2 CHAD COL10A1 COL11A1 COL11A2 COL1A2 COL2A1 COL9A1 COL9A2 COMP CSPG4 CTGF FGFR2 FGFR3 FOS GPC4 HEY1IBSP IER3 IGF1 KRT14 LECT1 MATN3 MEF2C NINJ2 PAPSS2 PRELP PTCH PTHR1 PTS S100A1 SMPD3 SPON2 SPP1 THBS1 VIL2 WNT11
- Morphogenesis	15	0.00626	CHAD COL9A1 COMP CSPG4 CTGF FGFR2 FGFR3 GPC4 HEY1 IER3 NINJ2 PTCH SPON2 VIL2 WNT11
- Organ development	22	<0.0001	ACTC ALPL COL10A1 COL11A1 COL1A2 COL2A1 COL9A1 COL9A2 COMP CSPG4 FGFR3 HEY1 IBSP IGF1 LECT1 MATN3 MEF2C PAPSS2 PRELP PTHR1 SPP1
- - Skeletal development	17	<0.0001	ALPL COL10A1 COL11A1 COL11A2 COL1A2 COL2A1 COL9A2 COMP FGFR3 IBSP IGF1 LECT1 MATN3 PAPSS2 PRELP PTHR1 SPP1
- Tissue development	9	0.00050	ALPL COL11A1 CSPG4 CTGF IBSP KRT14 LECT1 NINJ2 SPP1
Organic acid metabolism	13	0.00225	ASNS CD36 HADHSC IARS IGF1 LPL MARS PLA2G4A PSAT1 PTS SLC27A2 SLC7A1 WARS
Amino acid and derivative metabolism	8	0.00522	WARS ODC1 IARS ASNS AOC2 PTS SLC7A1 MARS PSAT1
Phosphate transport	9	<0.0001	C1QTNF3 COL10A1 COL11A1 COL11A2 COL1A2 COL2A1 COL9A1 COL9A2 COL9A3

Table 4.9: The WebGestalt results of significantly over-represented biological processes. The analysis was performed on the gene list comprising the most significantly upregulated genes between the 2D and 14D time points. As many of these genes have multiple names, their recognized gene symbols are used. Indented gene ontology categories are subsets of the category above.

2D-14D DOWNREGULATED			
GO CATEGORY	N	P value	GENES
Cell communication	65	0.00909	RAB11A SDCBP PLP2 TIMP3 TXNRD1 ITGA5 MGST3 NQO1 LAMB1 IFITM1 IGBP1 DKK3 ARL4C COPS2 IL8 ADM IL1R1 STMN2 MTSS1 GPRC5A MME MET HMOX1 ITPR1 MAP3K5 IGFBP6 F2R MAOA GEM CD44 STC1 LTBP2 SRPX LAMA2 NMB AGTR1 ITGBL1 CCL20 PCSK1 ING2 MAP4K4 HMGB2 GABARAPL1 GADD45B PGF CXCL12 RIT1 RORA AKAP12 POSTN IGFBP3 GNG12 NRP1 SPRY1 RND3 RAC2 KHDRBS1 GLUL DIRAS3 PBEF1 JAM2 TREM1 RAB20 ANGPTL4 RAB9A
- Small GTPase mediated signal transduction	9	0.00913	RAB11A ARL4C GEM RIT1 RND3 RAC2 DIRAS3 RAB20 RAB9A
Response to stimulus	49	0.00012	ADM AKR1C1 ANGPTL4 APEX1 C1R C1S CCL20 CLEC2B CXCL12 DDIT3 EFEMP1 F2R FTH1 GADD45B GBP2 GEM HLA DPA1 HLA DPB1 HLA DRA HLA DRB1 HLA E HMGB2 IF IFI16 IFITM1 IGBP1 IL1R1 IL8 KIAA1199 LTA4H MAP3K5 MAP4K4 MGP MGST3 NDRG1 NFIL3 NQO1 PLP2 PSMB8 PTX3 SERPING1 SOD2STC1 TAP1 TFPI TFPI2 TIMP3 TREM1
Immune response	28	<0.0001	C1R C1S CCL20 CLEC2B CXCL12 FTH1 GBP2 GEM HLA DPA1 HLA DPB1 HLA DRA HLA DRB1 HLA E IF IFI16 IFITM1 IGBP1 IL1R1 IL8 LTA4H MGST3 NFIL3 PSMB8 PTX3 SERPING1 SOD2TAP1 TREM1

Table 4.10: The WebGestalt results of significantly over-represented biological processes. The analysis was performed on the gene list comprising the most significantly downregulated genes between the 2D and 14D time points. As many of these genes have multiple names, their recognized gene symbols are used. Indented gene ontology categories are subsets of the category above.

4.5.2 Gene ontology analysis for cellular localization

The gene ontology categories for cellular localization were first subdivided into proteins located inside and outside the cell. Within the cell, there were further subcategories including the different organelles and the cytoplasm (Table 3.11).

Transcriptional regulation, signalling and development were the biological process categories, which were over-represented in the genes that changed expression between 0 and 3 hours (Section 4.5.1). When the cellular localization of the protein products of these genes was considered, there was a significantly higher number of proteins expressed in the nucleus than what would be expected by chance. As the function of many of these proteins is transcriptional, the over-representation of those localized in the nucleus is not surprising.

Between the 3H and 12H time points, genes involved in cell motility were downregulated, in terms of cellular localization, this was demonstrated as an over-representation of cytoskeletal genes.

The changes which occurred between 12H and 2D time points were more difficult to interpret, but involved the downregulation of many cell communication genes and consequently extracellular genes were over-represented.

Between the 2D and 14D time points, the most significant changes involved the expression of cartilage matrix molecules and this was also apparent when the cellular localization of the upregulated proteins was examined. In both the upregulated and the downregulated gene sets, extracellular genes were over-represented, and in the upregulated gene set, these generally consisted of extracellular matrix molecules.

TIMEPOINT	0h-3h up	0h-3h down	3h-12h up	3h-12h down	12h-2d up	12h-2d down	2d-14d up	2d-14d down
INTRA-CELLULAR								
Nucleus	76 ($p=1.695*e^{-9}$)	35 ($p=0.00086$)						
Cytoskeleton				25 ($p=0.00042$)		16 ($p=0.00858$)		
Vacuole					7 ($p=0.00468$)			
EXTRA-CELLULAR						25 ($p=0.00248$)	42 ($p<0.0001$)	30 ($p=0.00213$)
Matrix						12 ($p=0.00155$)	27 ($p<0.0001$)	

Table 4.11: WebGestalt results for over-represented gene ontology categories for cellular localization throughout the time course. For each category, the number of genes is shown, as well as the significance value for the over-representation.

4.5.3 KEGG pathways

The WebGestalt programme can also identify over-represented KEGG pathways of molecular interactions. A summary of the pathways significantly over-represented ($p<0.01$) in this microarray study is presented in Table 3.12.

The TGFß pathway was activated by 3 hours and further upregulated by 12 hours. This is likely to be a response to the addition of TGFβ3 to the chondrogenic media. A consequence of the upregulation of the TGFß pathway was the activation of the MAPK pathway by 12 hours.

A range of metabolic pathways and those involved in glycolysis were upregulated by 12 hours. Wnt signalling, which is known to be an active player in chondrogenesis, was upregulated by 2 days.

Finally, by 14 days, the large number of upregulated extracellular molecules led to pathways such as cellular communication, ECM receptor interaction and focal adhesion being over-represented. These are the same

KEGG pathways that are over-represented in the WebGestalt cartilage expression set mentioned previously in Section 4.4.

Timepoint	KEGG pathway	N	P value	Genes
0H-3H up	TGF-beta signalling	7	0.00031	SMAD7 BMPR2 RHOB INHBA ID1 ID3 ID4
	Adherens junction	5	0.00732	SNAI1 SNAI2 EGFR BAIAP2 RHOB
0H-3H down	No significantly overrepresented categories			
3H-12H up	MAPK signalling	9	0.00595	PLA2G4A MEF2C DDIT3 JUN TGFB3 IL1R1 GADD45B MYC FOS
	Glycolysis	5	0.00152	ENO2 PGK1 PGM1 ALDH2 ALDOC
	TGF-beta signalling	5	0.00596	BMP2 DCN TGFB3 MYC ID2
	Valine, leucine and isoleucine degradation	4	0.00399	HMGCL AUH SH3GLB1 ALDH2
	Starch and sucrose metabolism	4	0.00588	PGM1 ENPP2 UGP2 GBE1
	Arganine and proline metabolism	4	0.00547	SAT ARG2 ALDH2 P4HA2
	Butanoate metabolism	4	0.00308	HMGCL AKR1B10 SH3GLB1 ALDH2
3H-12H down	Axon guidance	7	0.00970	SEMA4C MET CXCL12 EFNB2 RRAS2 NFATC1 NRP1
	Proteasone	5	0.00409	PSMD6 PSMD14 PSMC2 PSMD11 PSMA3
12H-2D up	Wnt signalling	9	0.00131	MMP7 DKK1 WNT5A SMAD2 FZD1 ROCK2 CCND1 TBL1X CSNK2A1
	Glycine, serine and threonine metabolism	4	0.00683	AOC3 MAOA CTH PSPH
12H-2D down	Cell adhesion molecules (CAMs)	6	0.00514	CDH2 SDC1 CSPG2 ALCAM JAM3 NFASC
2D-14D up	Cell communication	12	<0.0001	DSG2 KRT14 THBS2 THBS1 COMP COL11A1 COL11A2 COL1A2 COL2A1 CHAD SPP1 IBSP
	Focal adhesion	12	0.00011	CAPN6 THBS2 THBS1 COMP COL11A1 COL11A2 COL1A2 IGF1 COL2A1 CHAD SPP1 IBSP
	ECM receptor interaction	10	<0.0001	CD36 THBS1 THBS2 COL11A1 COL11A2 COL1A2 COL2A1 CHAD SPP1 IBSP
	Arginine and proline metabolism	5	0.00083	ODC1 AOC2 ALDH1A3 P4AH2 CKB
	Tryptophan metabolism	5	0.00446	WARS HADHSC WBSCR22 AOC ALDH1A3
2D-14D down	Haematopoietic cell lineage	6	0.00430	MME CD44 HLA-DRA HLA-DRB1 ITGA5 IL1R1
	Complement and coagulation cascades	6	0.00134	F2R SERPING1 C1S C1R TFPI CFI

Table 4.12: WebGestalt results for significantly over-represented KEGG pathways throughout the time course of MSC undergoing chondrogenesis (N=number of genes).

4.6 MANUAL ANNOTATION OF MICROARRAY DATA

Gene ontology analysis was useful in providing a global overview of the processes occurring in chondrogenesis but for more in-depth analysis of the function of each gene, manual analysis was performed. All the genes found to change expression were annotated using OMIM and Gene Card searches in the first instance, in order to get an impression of their function. Consequently a search for publications was performed for each gene through PubMed, to check if any reference implicating the gene in skeletal development or differentiation could be found and to obtain a better understanding of the gene function. Some novel patterns emerged through this manual analysis, such as an over-representation of genes regulated by hypoxia. In addition, a group of genes was identified that would make potentially interesting targets for further examination of their role in chondrogenesis.

4.6.1 Hypoxic genes in chondrogenesis

Many of the genes that significantly changed expression as MSC were undergoing chondrogenesis are regulated by low oxygen levels (Figure 4.8). From the *in vitro* studies, it was clear that oxygen tension affected chondrogenesis because lower oxygen levels induced matrix accumulation and differentiation (Section 3.4.2).

Included in the hypoxia-responsive genes are VEGF, DEC1, PGF, ANGPTL4, HOX1, STC1, TIMP3, ITGA5, ADORA2B, JUNB, SHB and F3 (Figure 4.8). This group of genes were all upregulated at 3H and mostly downregulated either by 2D or 14D. The genes include some that are known to play a part in chondrogenesis such as DEC1 and STC1 – both present in the earliest stages of mesenchymal condensations (180) (194) and ITGA5, the fibronectin receptor, but also genes not previously implicated in chondrogenesis such as ADORA2B.

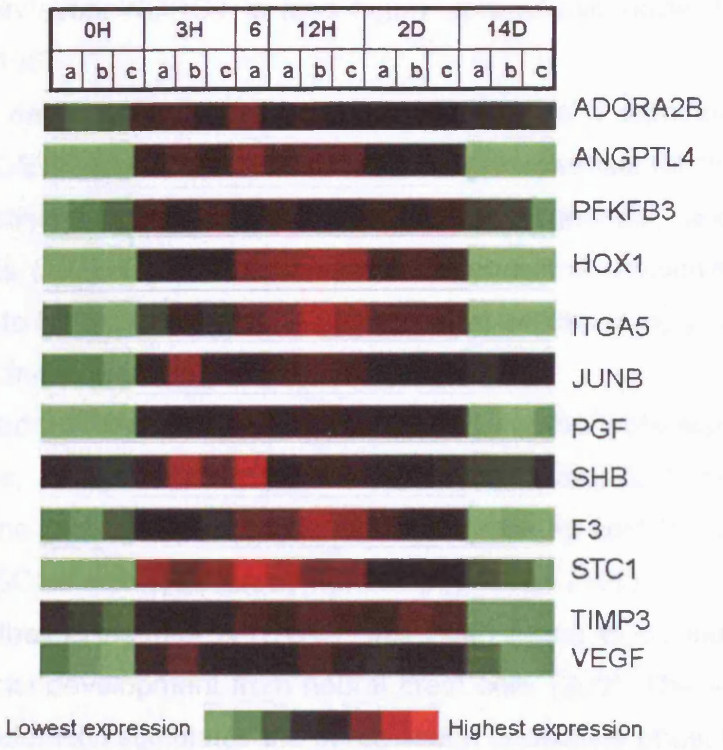

Figure 4.8: A selection of hypoxia responsive genes, the expression levels of which changed significantly as MSC underwent chondrogenesis, selected from the overall heatmap in figure 4.2.B

4.6.2 Interesting candidate genes for future investigation

Genes identified in this study, that have not been implicated in chondrogenesis but may be of interest for further study are summarized in Table 4.13. These genes have been selected as remarkable for a variety of reasons (Table 4.13).

The N-myc downstream regulated gene 1 (NDRG1) is involved in cell cycle arrest and differentiation of epithelial cells (195). Mutations in NDRG1 have been associated with Charcot-Marie-Tooth disease (OMIM: 601455), the symptoms of which include hand and foot deformities as well as muscle weakness and atrophy, making it a possible candidate for involvement in

MSC differentiation. NDRG1 is also highly upregulated under low oxygen conditions (196).

DNA damage-inducible transcript 3 (DDIT3) is a dominant negative inhibitor of C/EBP transcription factors, which are essential for the induction of adipogenesis; hence, DDIT3 blocks adipogenesis and induces osteogenesis (197). DDIT3's role in chondrogenesis is unknown but it has been found to be expressed in the growth plate, which strongly suggests its involvement in the process (198).

Thioredoxin interacting protein (TXNIP) is another potential inhibitor of adipogenesis, as a nonsense mutation in TXNIP leads to hyperlipidemia. Therefore, the protein could play a role in decreasing lipid levels and may influence MSC differentiation away from adipogenesis (199).

Endothelin Receptor A (ETRA) has been found to be indispensable for craniofacial development from neural crest cells (200). The activation of ETRA by Endothelin stimulates the upregulation of alkaline phosphatase and collagen 1 production in bone cells, and proteoglycan synthesis in monolayer rat articular chondrocytes and therefore could be a positive regulator of chondrogenic differentiation (201;202).

On the other hand, emopamil binding protein (EBP) probably has a role as a negative regulator of chondrogenesis and therefore needs to be downregulated for chondrogenesis to proceed. Point mutations in EBP lead to a dominant disorder, chondrodysplasia punctata 2, which includes short stature and other skeletal abnormalities among its symptoms (OMIM: 302960).

All 4 ID proteins showed significant changes in their expression levels during the time course and, as they are normally associated with regulation of differentiation, are also likely candidates for involvement in MSC differentiation. The ID proteins have previously been found to be expressed in the cartilage primordia of mice (184).

Kruppel-like factor 4 (KLF4) and T-box 2(TBX2) expression has also been found in mouse limbs (203;204). TBX2 acts alongside BMP and Sonic

hedgehog (SHH) signalling to specify digit identity (205). The DUSP4 gene is involved in MAPK signaling, providing feedback control of MAPK mediated signaling events (206).

The most promising candidates identified for future investigations were the hairy and enhancer of split1 (HES1) and hairy/enhancer of split related with YRPW motif (HEY1) genes. These genes are targets of Notch signalling, a pathway involved in differentiation and cell fate decisions in many lineages, but to date mainly investigated in neural differentiation. Nevertheless, Notch receptors and ligands have been shown to be expressed by developing cartilage (207). Therefore, further experiments were performed to determine the role of Notch signalling in chondrogenesis, and these are presented in Chapter 5.

Name	Timing	Interesting features
NDRG1	Up at 3H	Hypoxia regulated and involved in cell cycle regulation and differentiation. Mutations in this gene lead to hand and foot deformities
DDIT3	Up at 12H down at 14D	Role in lineage commitment. Inhibitor of adipogenesis, inducer of osteogensis
TXNIP	Up at 12H	Inhibitor of adipogenesis
Endothelin RA	Up at 12H down at 2D	Role in craniofacial development
EBP	Down at 12H	Point mutations lead to a dominant disorder, including short stature and other skeletal abnormalities
ID proteins	Up at 3H and 12H	Preventing premature differentiation of cells by inhibiting HLH transcription factors
DUSP4	Up at 3H down at 12H	Involved in MAPK signalling
TBX2	Up at 3H down at 12H	Involved in mesoderm differentiation
KLF4	Up at 3H	Detected in mesenchymal cells in limb bud
HES1 and HEY1	Up at 3h	Notch signalling targets.

Table 4.13: List of genes identified as differentially expressed as MSC undergo chondrogenesis that may be of interest for further investigation into their roles in cartilage development.

4.7 NHAC MICROARRAYS

Beside the multipotent MSC, committed NHAC were also exposed to the chondrogenic stimuli *in vitro* (Section 3.6). Both NHAC and MSC responded to the chondrogenic *in vitro* conditions by adopting a chondrogenic morphology and producing large amounts of ECM. However, NHAC produced more matrix than MSC and did not show any hypertrophic cells that were seen after MSC underwent chondrogenic differentiation. It was therefore of interest to compare the expression profiles of the differentiated MSC (14D) and the differentiated NHAC (14D) to see the differences in the cartilage produced by these 2 cell types. As NHAC can not differentiate into adipocytes or osteocytes while the MSC can, there must also be molecular differences in the expression profiles of the two cell lines prior to differentiation (0H).

In this section, cRNA from 0H and 14D time points of NHAC undergoing chondrogenesis was hybridized to the HGU133A gene chips. As with the MSC experiments, these 2 time points were performed in triplicate. The results obtained for these microarray experiments were then compared to the microarray results obtained for MSC undergoing cartilage differentiation presented in the previous sections (Sections 4.5 and 4.6)

As with the MSC time course experiment, a cluster dendrogram (Section 4.2.3) was produced showing how the NHAC time points relate to the MSC time points (Figure 4.9). Overall, NHAC microarray results most resembled their equivalent MSC time point. 0H NHAC were on the same branch as the 0H and 3H MSC and 14D NHAC most closely resembled 14D MSC.

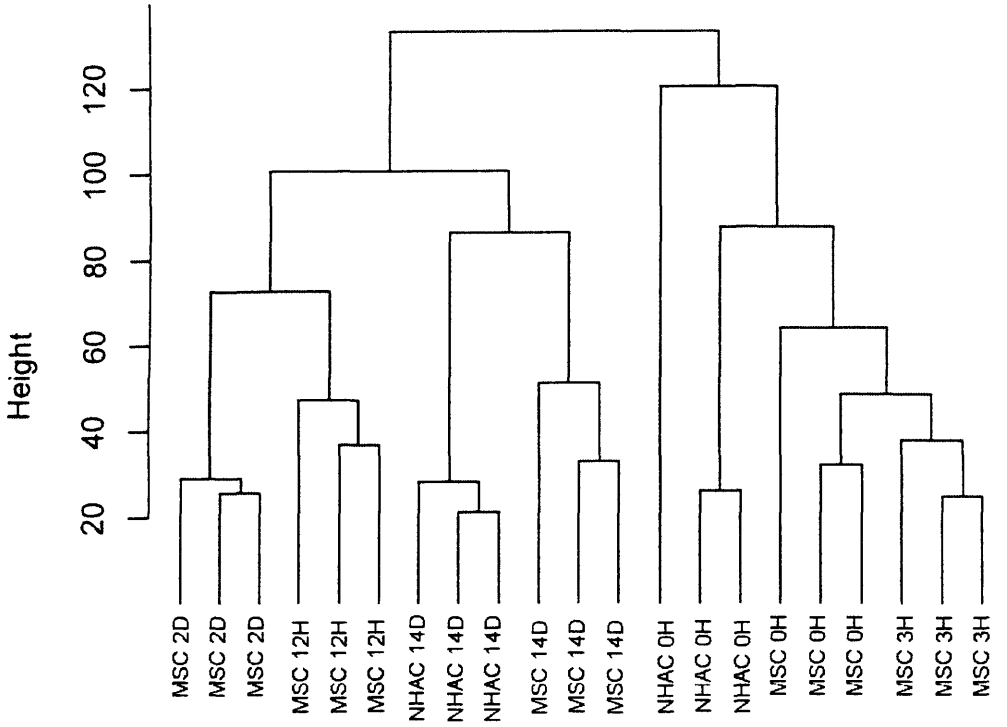

Figure 4.9: Cluster dendrogram showing the relationship between MSC and NHAC samples and time points. The height of the nodes is representative of the degree of difference between the two connected samples.

Lists were compiled of the top 100 probe sets which showed most significantly different ($q<0.01$) levels of expression between 0H MSC and 0H NHAC and the same comparison was done for the 14D MSC and 14D NHAC. This analysis resulted in 54 genes that were expressed at higher levels in 0H MSC than in 0H NHAC, and 32 genes expressed at higher levels in 0H NHAC than in 0H MSC. For the 14D time points, 28 genes were expressed at higher levels in 14D MSC than in 14D NHAC, and 57 genes were expressed at higher levels in 14D NHAC than in 14D MSC. The resulting gene lists were analysed with WebGestalt, using the biological processes classification in the gene ontology module (Tables 4.14-4.17).

Comparison of the two 14D time points showed that even though the transcription profiles of the 14D MSC and the 14D NHAC resembled each other, there were important differences between the two. Most of the

differences involved developmental genes and in particular genes encoding extracellular matrix proteins. When analysed with WebGestalt, of the 28 genes expressed at higher levels by the differentiated MSC than the differentiated NHAC, 12 were assigned a developmental role ($p<0.0001$) in the biological process class and 10 were located in the extracellular region ($p=0.00089$) (Table 4.16). Most of these genes are known markers of hypertrophic chondrocytes such as collagen 10 (COL10A1), osteopontin (SPP), bone sialoprotein (IBSP), parathyroid hormone receptor (PTHR1) and matrillin 3 (MATN3). Of the 57 genes expressed at higher levels in the NHAC than in the MSC, 24 were extracellular ($p<0.0001$), and again mostly involved matrix proteins such as collagen 21 (COL21A1), dermatopontin (DPT) and matrix Gla protein (MGP) (Table 4.17). Therefore, even though MSC and NHAC were exposed to the same chondrogenic media, the matrix of the differentiated MSC comprised both mature and hypertrophic cartilage matrix molecules while the NHAC did not express genes involved in hypertrophy.

The biological significance of the different genes between the 0H MSC and 0H NHAC was more difficult to interpret. Undifferentiated MSC expressed many extracellular genes not present on the NHAC (extracellular region $p=0.001$). These included cell adhesion proteins and members of the MHC class 1 and 2 family. MSC also expressed genes involved in organ development, among these 2 genes associated with osteoblast differentiation: CDH11 and POSTN ($p=0.00441$). NHAC expressed genes involved with the mitotic cell cycle (<0.0001) and DNA metabolism ($p=0.00669$) at higher levels than the MSC.

MSC 0H – NHAC 0H			
GO CATEGORY	N	P value	GENES
Cell adhesion	9	0.00036	AMIGO2 CDH11 COL5A1 CXCL12 LAMB1 POSTN SRPX TGM2 THBS2
Organ development	7	0.00441	ANGT1, CD11, GATA6, GJA1, POSTN, SERPINF1, TGM2, THBS2
Response to biotic stimulus	10	0.0023	HLA-DMA, HLA-DPA1, HLA-DRA, HLA-DRB1, HLA-DRB5, CXCL12, CXCL6, IF, PTGES, TRIM22
- MHC class 2	5	<0.0001	HLA-DMA, HLA-DPA1, HLA-DRA, HLA-DRB1, HLA-DRB5

NHAC 0H – MSC 0H			
GO CATEGORY	N	P value	GENES
Cell cycle	7	0.00042	BIRC5, CDC20, CDC45C, GTSE1, MKI67, PLK1, PTTG1
DNA metabolism	5	0.00669	PTTG1 TYMS RRM2 CDC45L IL7R

MSC 14D – NHAC14D			
GO CATEGORY	N	P value	GENES
Development	12	<0.0001	COL10A1, CSRP1, DACT1, GPC4, HEY1, IBSP, IGF1, IGFBP5, MATN3, PTHR1, SERPINF1, SPP1
Cell proliferation	6	0.00089	CDKN1C, CSRP2, GPC4, IGF1, SERPINF1

NHAC 14D – MSC14D			
GO CATEGORY	N	P value	GENES
Cell Adhesion	8	0.00411	CD44, COL22A1, DPT, KAL1, MFAP4, PTPNS1, THBS3, TLN2
Skeletal develooment	5	0.00031	ETS2, FRZB, GDF10, MGP, TNFRSF11B

Table 4.14- 4.17: The WebGestalt results of significantly over-represented biological processes. The analysis was performed on the gene list comprising those with most significantly different expression between the MSC and NHAC. As many of these genes have multiple names, their recognized gene symbols are used. Indented gene ontology categories are subsets of the category above.

4.8 CONCLUSIONS AND DISCUSSION

The MSC *in vitro* chondrogenesis model system is a faithful representation of the *in vivo* process, progressing in a temporal order which mimics cartilage development and concludes with cells that expressed cartilage markers and which were both morphologically and functionally chondrogenic.

The power of microarray analysis lies in its ability to offer a global overview of chondrogenic development. Gene ontology analysis was used to this end and a summary of the results obtained is presented in Figure 4.10.

Three phases of chondrogenesis could be identified – early, middle and late. The early phase, represented by the 3H time point, involved the upregulation of many transcription factors, signalling pathways and developmental genes in response to the chondrogenic media. The first phase also involved the downregulation of a variety of transcription factors associated with development towards lineages other than cartilage. It is interesting that undifferentiated MSC expressed such a large number of developmental transcription factors. This finding suggests that MSC are in a poised state, expressing low levels of transcription factors that play a part in a variety of differentiation processes. Once MSC are induced to differentiate toward a particular lineage, the transcription factors for that lineage are upregulated while those involved in the differentiation toward other lineages are downregulated. While some of the genes upregulated by 3H are known to have a chondrogenic role, there was also a large number of genes not previously associated with chondrogenesis. This group of genes may have important roles in early chondrogenic differentiation in particular, or may have a more general role in MSC differentiation.

The intermediate phase of chondrogenesis was represented by the 12H and 2D time points. MSC no longer divided in the chondrogenic cultures and consistent with this was the downregulation of genes involved in cell cycle progression. Metabolic pathways were consequently upregulated in

preparation for matrix production in the final phase. As chondrocytes have few mitochondria and largely rely on glycolysis for their energy requirements, glycolysis genes were also upregulated including the main glycolytic enzyme PGK1 (192). During this phase the cells also lost many of the MSC cell surface markers and there was a downregulation of genes involved in cell motility as the previously motile MSC become fixed in their role as chondrocytes. It is possible that the transcription factors upregulated in the early phase were responsible for these later changes seen in the expression profile.

The late phase of chondrogenesis, represented by the 14D time point, involved transcriptional changes geared towards extracellular matrix production and skeletal development. A range of extracellular matrix proteins were upregulated including the collagens and proteoglycans that comprise the extracellular matrix (e.g. collagen 2, 9, 11, aggrecan and cartilage linking protein). Markers of both mature and hypertrophic cartilage were expressed by the 14D cells, making the developmental stage of these cells somewhat ambiguous.

Many of the transcripts that significantly changed expression levels during chondrogenesis were found to be induced by low oxygen levels. However, the pellets on which the microarrays were performed were grown in the atmospheric (21%) oxygen conditions and it therefore seems surprising that a large number of genes are upregulated that are responsive to hypoxic conditions. It is possible that by growing the cells in pellet culture, a state of hypoxia is induced in the cells close to their centres, and that this accounts for the large number of hypoxia responsive genes seen in this node. However, HIF1α, the main regulator of hypoxia, has been shown to have an effect on chondrocyte growth both in culture and *in vivo*, regardless of the oxygen levels. Even in normoxic conditions, chondrocytes lacking HIF1α show reduced ATP levels (117). Therefore, it is likely that even if the cells are not in a hypoxic environment the genes regulated by HIF1α are still essential for chondrogenesis

In addition to the MSC time course, microarray analysis was performed on the NHAC cell line before and after undergoing chondrogenesis. NHAC are different to MSC in that they are unipotent and only differentiate to cartilage whereas the MSC are multipotent. The most prominent differences between the 0H NHAC and 0H MSC expression levels were seen in the genes encoding extracellular proteins. While MSC expressed a range of adhesion and cell communication molecules these were not expressed by NHAC. When put through the same chondrogenic *in vitro* differentiation assay as MSC, NHAC produced more extracellular matrix and the cells did not appear hypertrophic as the MSC did (Section 3.7). This finding was confirmed at the transcriptional level, where 14D NHAC did not express markers of hypertrophy such as collagen 10, that were expressed by 14D MSC. This different transcriptional response of the two cell types to the same stimulus is interesting and suggests a fundamental biological difference between them.

Besides providing a global overview of the chondrogenic process in MSC and NHAC, the microarray analysis has also identified numerous transcripts that changed expression levels during the time course but have not previously been associated with chondrogenic development or the role of which in chondrogenesis has not been elucidated. Two such transcripts were the HES1 and HEY1 targets of Notch signalling, and their role in MSC differentiation is investigated in the following chapter.

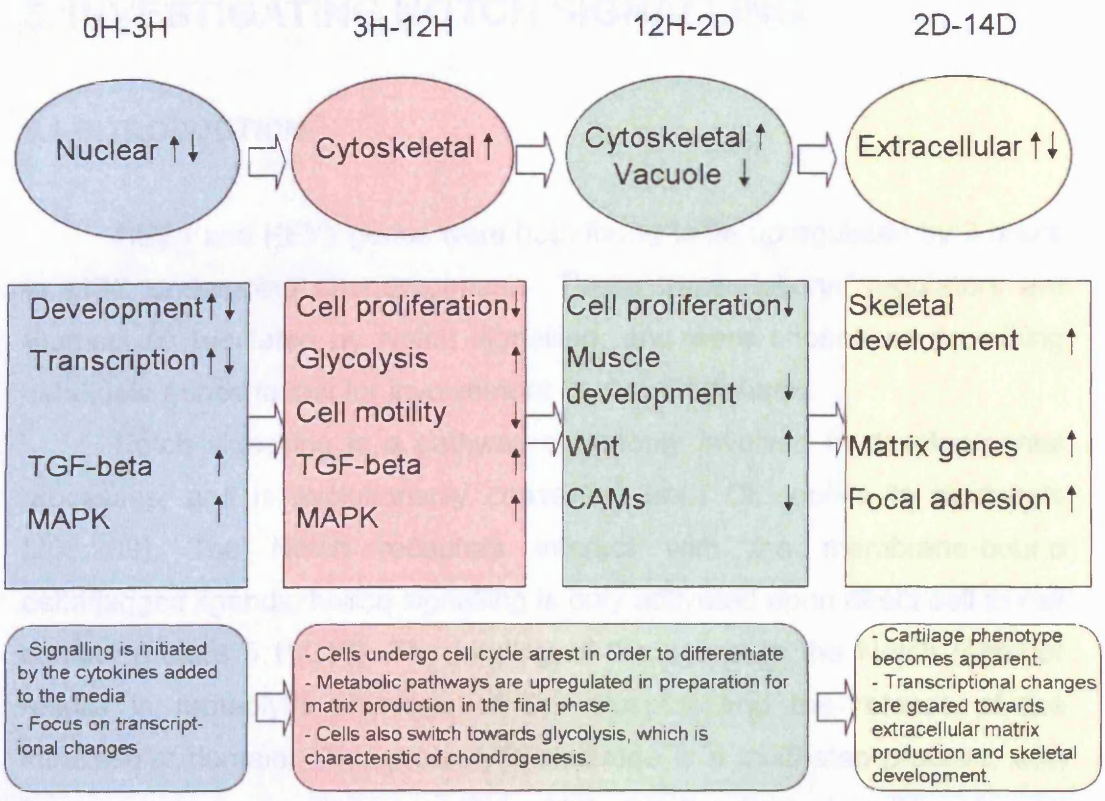

Figure 4.10: A summary of the GEM results providing an overview of the transcriptional events occurring as MSC undergo chondrogenesis, combining the gene ontology analysis for biological processes and cellular localization, as well as phenotypic observations made during the time course experiment.

5. INVESTIGATING NOTCH SIGNALLING

5.1 INTRODUCTION

HES1 and HEY1 genes were both found to be upregulated by 3 hours in MSC undergoing chondrogenesis. These transcriptional regulators are themselves regulated by Notch signalling, and were chosen as promising candidate genes to test for involvement in chondrogenesis.

Notch signalling is a pathway commonly involved in developmental processes, and is evolutionarily conserved from *Drosophila* to mammals (208;209). The Notch receptors interact with the membrane-bound delta/jagged ligands, hence signalling is only activated upon direct cell to cell contact (Figure 5.1)(210). The binding of the ligand to the Notch receptor results in proteolytic cleavage of the receptor and the release of the intracellular domain. This proteolytic cleavage is a multi-step process, with the γ-secretase enzyme, presenilin, catalysing the final step. The cleaved notch intracellular domain (NICD) translocates into the nucleus and activates the transcription of HES and HEY gene family. HES and HEY proteins are basic helix-loop-helix (bHLH) transcriptional regulators that act as both homo- and hetero-dimers in repressing the transcription of target genes. This inhibition can occur either directly by the HES and HEY dimer binding to specific repressor binding sites, or indirectly by binding to bHLH transcription factors, such as MyoD, and preventing them from forming functional heterodimers with other bHLH family proteins (211).

The role of Notch signalling in the developmental processes of a variety of organisms has been studied by the use of γ-secretase inhibitors including L-685,458 and N-[N-(3,5-Difluorophenacetyl-L-alanyl)]-S-phenylglycine *t*-butyl ester (DAPT) (212;213). Exposure of *Drosophila* to DAPT blocks the release of NICD and produces the same phenotype as that resulting from mutations in the components of the Notch signalling pathway

(214). DAPT is also an accepted inhibitor of Notch signalling in *in vitro* studies (215-217).

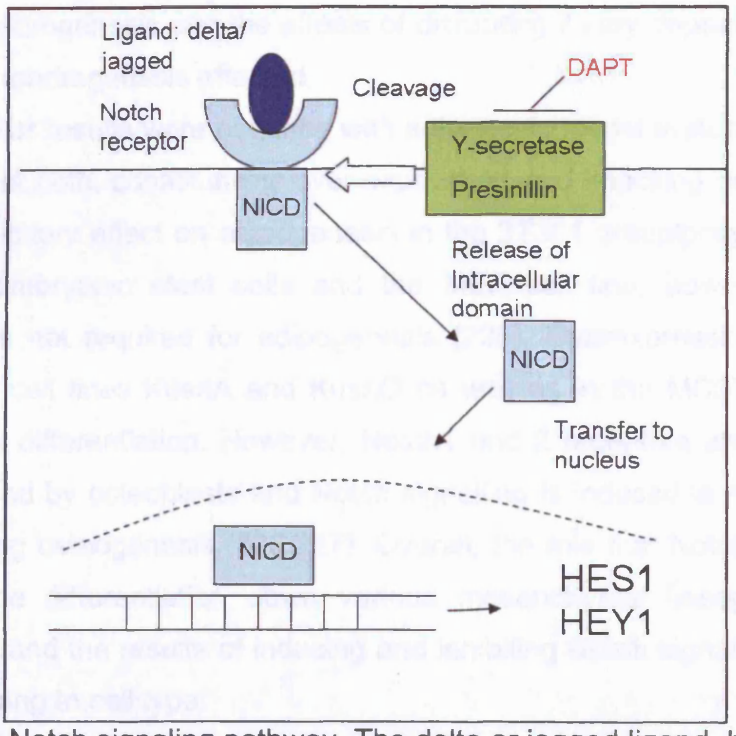

Figure 5.1: Notch signaling pathway. The delta or jagged ligand binds to the Notch receptor causing it to be cleaved by the presenilin γ-secretase enzyme. The intracellular domain of the receptor then translocates into the nucleus and activates expression of target genes, such as HES1 and HEY1. DAPT inhibits Notch receptor cleavage by interacting with the γ-secretase.

The role of Notch signalling in MSC growth and differentiation is largely unknown. Notch signalling has been implicated in cardiomyocyte and neuronal differentiation of rat MSC (218;219). In C2C12 mouse mesenchymal cells, Notch target genes are known to be upregulated in response to BMP2-induced osteogenesis and BMP4-induced inhibition of myogenesis (220;221).

During chondrogenesis *in vivo*, both the Notch receptors and the ligands are expressed, and mutations in these genes lead to defects including those affecting cartilage (186;222). When chondroblasts from joints are isolated, inhibiting Notch signalling inhibits matrix deposition, but in ATDC5 prechondrocyte cultures, the overexpression of NICD leads to a

suppression of chondrogenic differentiation as well as proliferation (186;223). Therefore, Notch signalling appears to play a crucial and complex part in chondrogenesis and the effects of disrupting it vary depending on the phase of chondrogenesis affected.

Similar results were obtained with adipogenic model systems. Ross *et al* found that both, constitutively over-expressing and knocking down HES1, had an inhibitory effect on adipogenesis in the 3T3L1 preadipocyte cell line (224). In embryonic stem cells and the MEF cell line, however, Notch signalling is not required for adipogenesis (225). Overexpressing NICD in osteogenic cell lines KusaA and KusaO as well as in the MC3T3 cell line suppresses differentiation. However, Notch1 and 2 receptors are known to be expressed by osteoblasts and Notch signalling is induced in response to BMPs during osteogenesis (226;227). Overall, the role that Notch signalling plays in the differentiation down various mesenchymal lineages is still ambiguous and the results of inducing and inhibiting Notch signalling *in vitro* vary according to cell type.

5.1.2 Aims

This section investigates the involvement of Notch signalling in chondrogenesis. First, the DAPT Notch signalling inhibitor was used with the aim of analysing the effects of abolishing Notch signalling during MSC proliferation and differentiation. In the second section of this chapter, *in situ* hybridization was employed, with the aim of detecting the region of HES1 and HEY1 expression in mouse cartilage development *in vivo.*

5.2 DAPT NOTCH SIGNALLING INHIBITION

5.2.1 Optimizing the conditions for DAPT treatment

Due to the variability in the MSC response to chondrogenic media (Section 3.4), the MSC cell lines chosen for this experiment were the 24M and the 38M, both of which underwent chondrogenesis efficiently. DAPT is poorly soluble in water and requires dissolution in dimethyl sulfoxide (DMSO), which is known to affect differentiation and cellular processes (228). There have also been some findings suggesting that both chondrogenesis and adipogenesis could be affected by DMSO treatment (229;230) . Therefore, the effect of the DMSO vehicle alone was tested prior to treatment with the DAPT inhibitor (Methods: Section 2.3.1).

The extent of chondrogenesis was assessed by measuring the size of the pellets at day 7, day 14 and day 21 of the chondrogenic culture (Figure 5.2). The average percentage size increase for pellets, representing the extent of matrix accumulation, under each condition between days 7 and 21 is presented in Figure 5.3. No size difference was observed when cells were treated with 1µl/ml DMSO. However, at 2µl/ml, DMSO had a significant effect on pellet growth. This effect was enhanced by increasing the DMSO concentration to 5µl/ml.

When the pellets were sectioned and stained with toluidine blue, changes in cell morphology were also apparent (Figure 5.4). There was a decrease in the amount of purple matrix accumulated in the pellets that were exposed to DMSO and the cells were less rounded in appearance. Because of these findings, all the following experiments were performed with 1µl/ml DMSO as the control. DAPT was solubilised in DMSO to make 10mM and 20mM stocks. These stocks were added to cultures at 1µl/ml making the final DAPT concentration 10µM and 20µM and DMSO concentration 1µl/ml (hereafter this treatment is referred to as 10µM DAPT and 20µM DAPT).

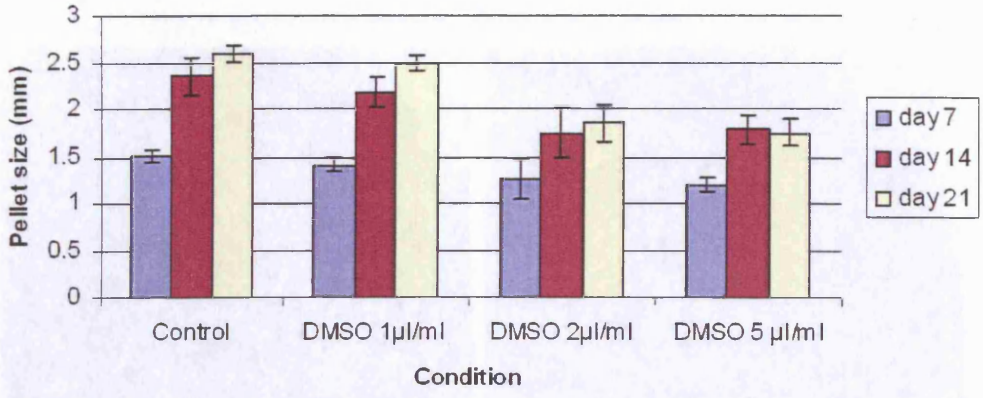

Figure 5.2: The effect of DMSO treatment on MSC undergoing chondrogenesis as measured by pellet diameter size. Pellet diameters were measured every week.

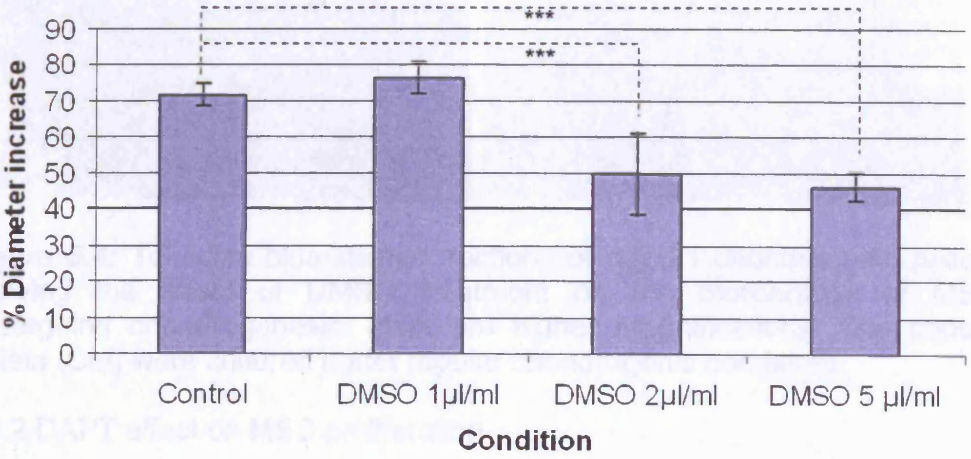

Figure 5.3: The effect of DMSO treatment on the percentage increase in pellet diameters between day 7 and day 21 of differentiation (presented in Figure 5.2). Student's t-test Control vs DMSO-treated pellets *** $p < 0.001$.

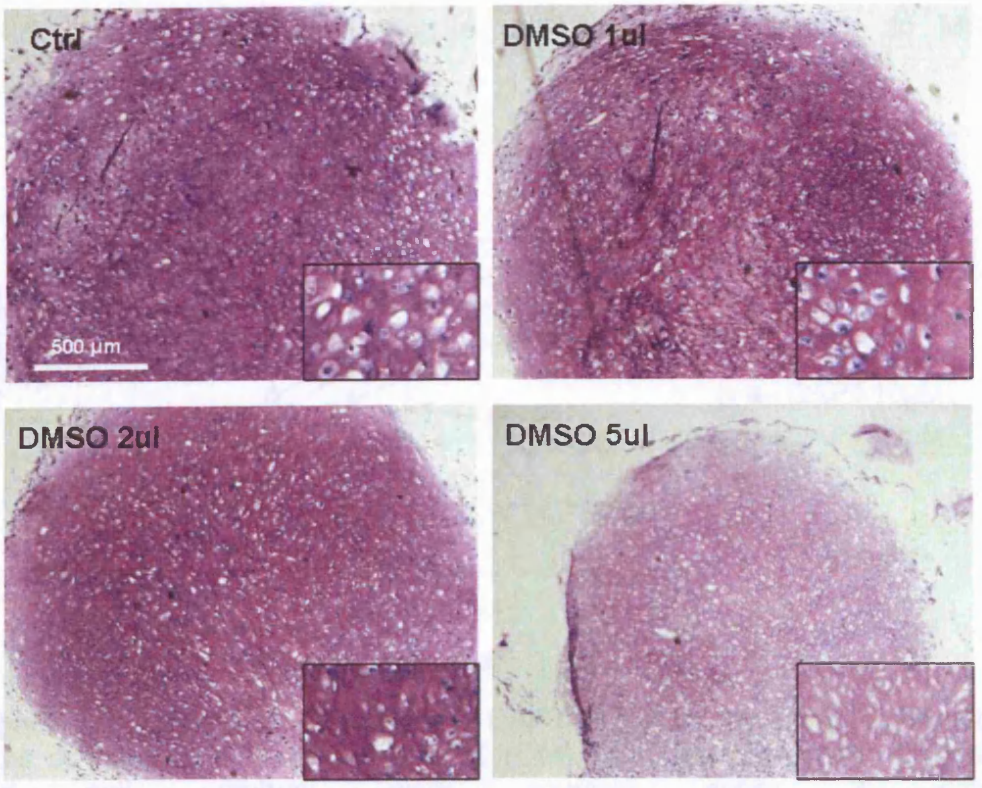

Figure 5.4: Toluidine blue-stained sections of day 21 chondrogenic pellets showing the effect of DMSO treatment on the morphology of MSC undergoing chondrogenesis. Inset are higher magnifications. The control pellets (Ctrl) were cultured under regular chondrogenic conditions.

5.2.2 DAPT effect on MSC proliferation

To investigate if DAPT affected proliferation of MSC, growth curve assays, similar to the 3T3 assay, were performed using the 38M MSC (Figure 5.5) (Methods: Section 2.1.3). MSC were grown in regular MSC media (ctrl) or media supplemented with 1µl/ml DMSO, 10µM DAPT and 20µM DAPT (Methods: Section 2.3.2). The addition of 1µl/ml of the DMSO vehicle alone to growing MSC did not affect their doubling rate. However, the addition of 10µM DAPT slowed MSC growth and finally inhibited cell division after 6 passages. Increasing the concentration of DAPT to 20µM inhibited cell division within 4 passages and resulted in growth arrest. Therefore,

although DAPT did not immediately inhibit MSC growth, long-term exposure led to growth arrest implicating a role for Notch signalling in MSC proliferation.

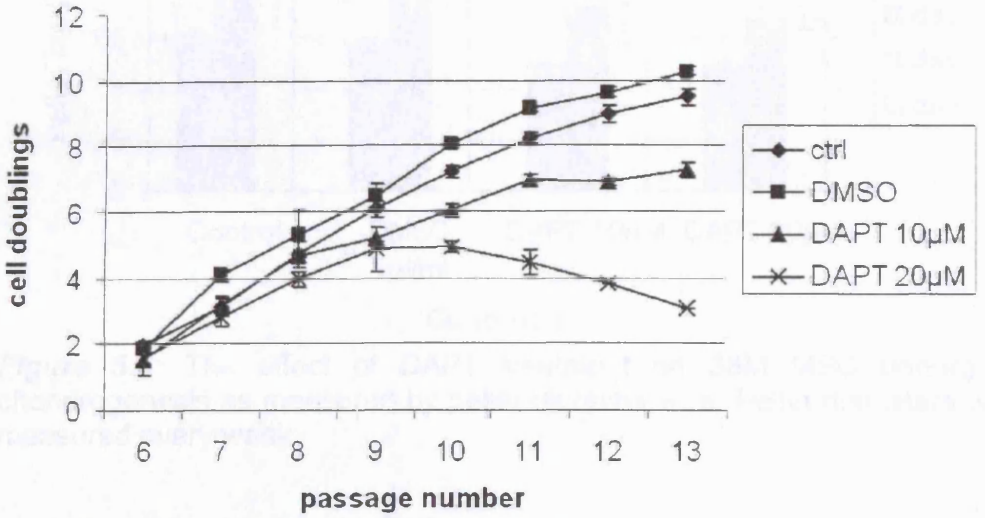

Figure 5.5: The effect of DMSO and DAPT treatment on MSC proliferation rates as compared to untreated MSC (Ctrl). MSC were grown in triplicate and cell numbers were counted every 3 days.

5.2.3 DAPT effect on chondrogenesis

The effect of the DAPT γ-secretase inhibitor on chondrogenesis was assessed by pellet measurements and histological staining, in the same way as the effect of DMSO in Section 5.2.1 (Methods: Section 2.3.3). Six pellets were cultured per condition and the experiment was performed on 2 different bone marrow samples, 38M and 24M. The MSC derived from the 38M bone marrow sample showed a profound response to DAPT treatment as seen by the pellet size measurements at days 7, 14 and 21 and the percentage size increase between day 7 and day 21 (Figure 5.6 and 5.7). The addition of 1μl/ml DMSO had no effect on pellet size but the addition 10μM or 20μM DAPT decreased the final pellet size by ~40% as compared to the control. No difference was observed between the two concentrations of the DAPT inhibitor.

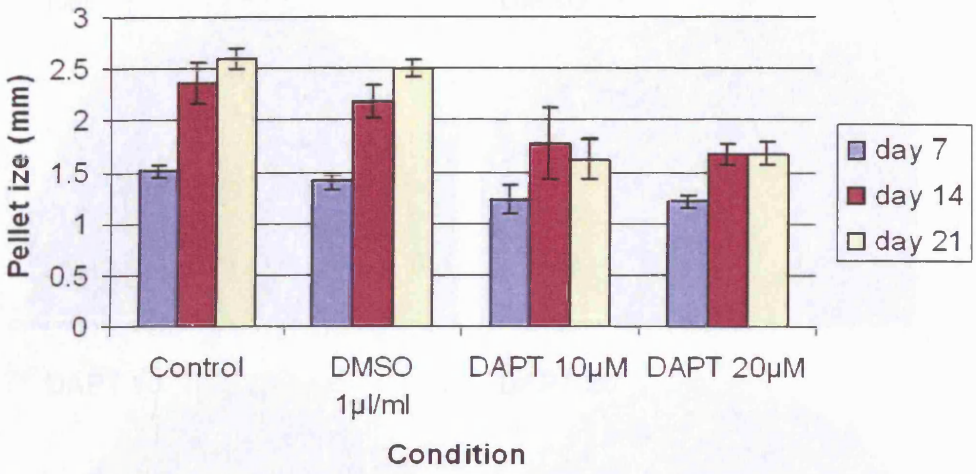

Figure 5.6: The effect of DAPT treatment on 38M MSC undergoing chondrogenesis as measured by pellet diameter size. Pellet diameters were measured every week.

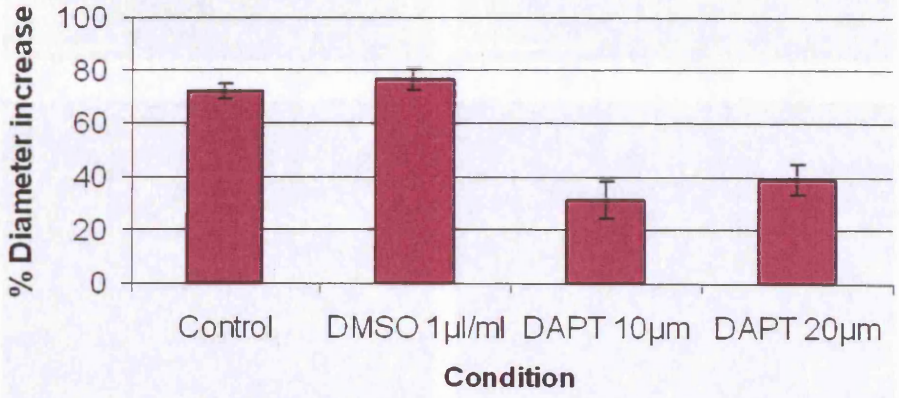

Figure 5.7: The effect of DAPT treatment on the percentage increase in pellet diameters between day 7 and day 21 of chondrogenic culture of 38M MSC (presented in Figure 5.6). Student's t-test DMSO vs DAPT *** $p < 0.001$.

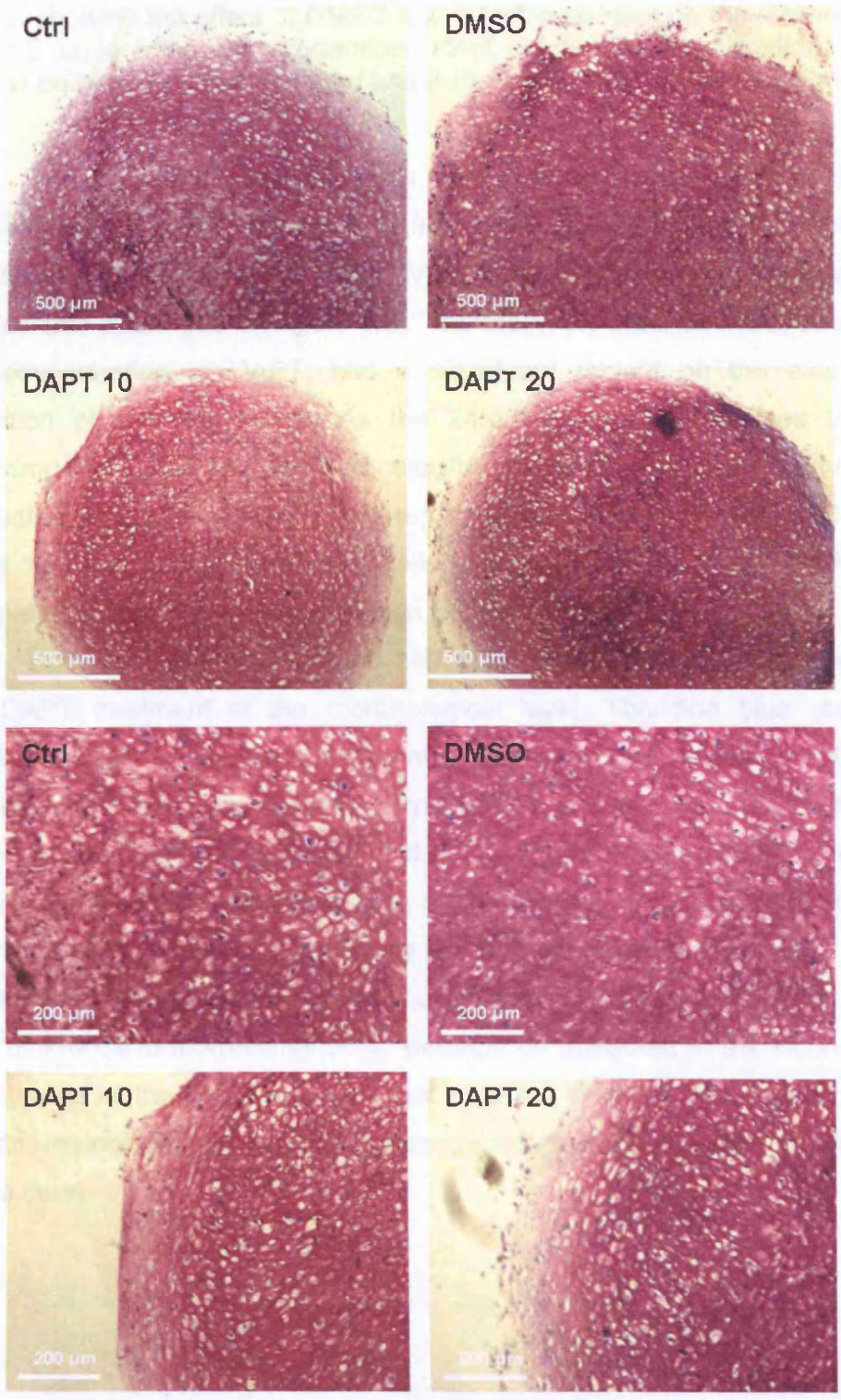

(Figure legend on following page)

Figure 5.8: Toluidine blue-stained sections of day 21 38M chondrogenic pellets showing the effect of DMSO and DAPT treatment on the morphology of MSC undergoing chondrogenesis. Inset are higher magnifications. The control pellets (Ctrl) were cultured under regular chondrogenic conditions.

The 24M MSC pellet cultures also showed a size decrease when treated with the DAPT inhibitor. The final pellet size was about ~15% lower for the pellets treated with 10μM DAPT and ~25% lower for the pellets treated with 20μM DAPT (Figure 5.9). Therefore, for the 24M MSC, doubling the concentration of DAPT, had a significant impact on the extent of inhibition of chondrogenesis. As the 24M MSC responded less to the chondrogenic media than the 38M cells, the actual effect of DAPT was better evaluated as a size increase between days 7 and 21, which was 40-50% lower for both MSC lines when cells were exposed to 20μM DAPT as compared to the DMSO treated pellets (Figure 5.7 and 5.10).

Both, the 38M MSC and the 24M MSC showed a similar response to the DAPT treatment at the morphological level. Toluidine blue staining showed that there was an impairment in matrix accumulation in the DAPT treated pellets, as there was less purple matrix, and the blue-staining nuclei were closer together (Figure 5.8 and 5.11). Throughout the DAPT treated pellets, the cells showed an irregular, more spindled morphology rather than the rounded chondrocytic morphology and lacunae seen in the control. Also, in the DAPT treated sections, there was an outer rim of spindle-shaped cells. This difference in morphology could perhaps be attributed to the incomplete penetrance of the DAPT inhibitor that may fail to reach the inside of the pellets, thereby producing a more pronounced effect in the outer layers than in the core.

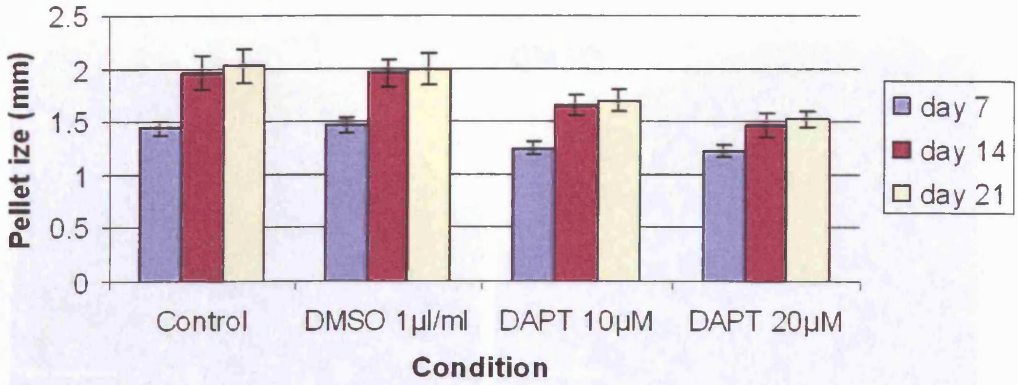

Figure 5.9: The effect of DAPT treatment on 24M MSC undergoing chondrogenesis as measured by pellet diameter size. Pellet diameters were measured every week.

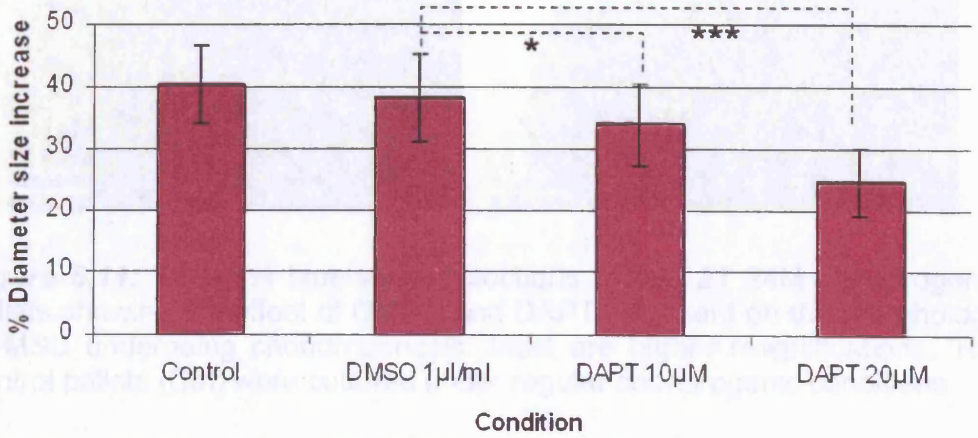

Figure 5.10: The effect of DAPT treatment on the percentage increase in pellet diameters between day 7 and day 21 of chondrogenic culture of 24M MSC (presented in Figure 5.9). Student's t-test DMSO vs DAPT *** $p < 0.001$.

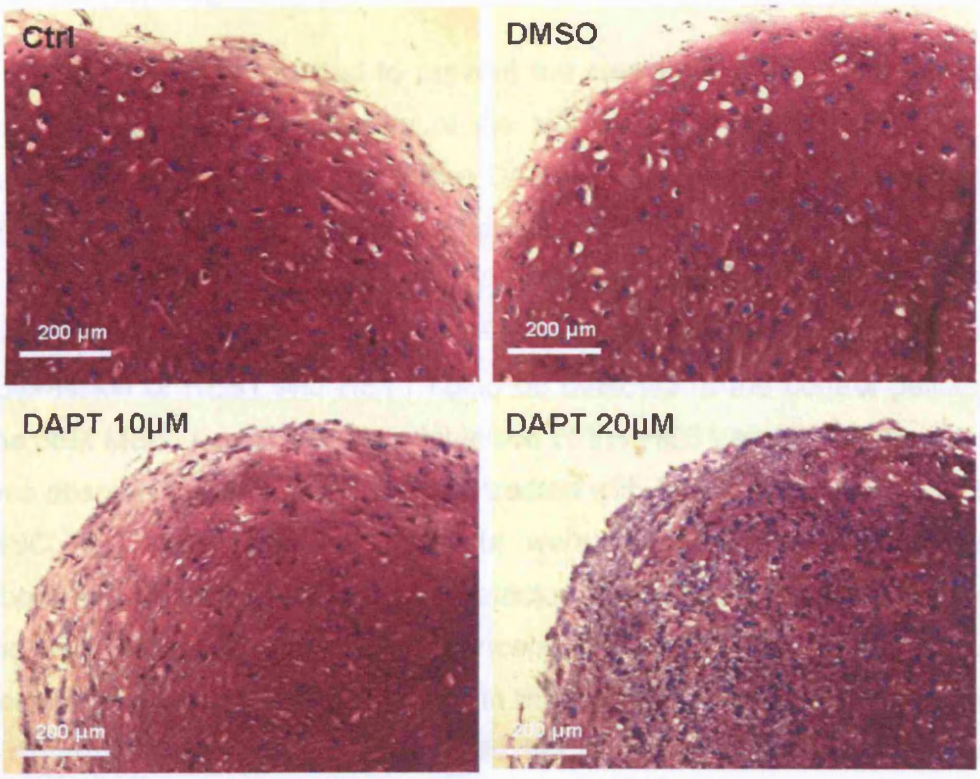

Figure 5.11: Toluidine blue-stained sections of day 21 24M chondrogenic pellets showing the effect of DMSO and DAPT treatment on the morphology of MSC undergoing chondrogenesis. Inset are higher magnifications. The control pellets (Ctrl) were cultured under regular chondrogenic conditions.

5.2.4 RT-PCR analysis of HES1 and HEY1 targets of Notch signalling

As DAPT is reported to prevent the cleavage of the Notch receptor and therefore the translocation of the Notch intracellular domain into the nucleus, the exposure of the cells to DAPT should inhibit the transcription of the HES1 and HEY1 targets of Notch signalling.

The levels of HES1 and HEY1 were assessed by RT-PCR in RNA isolated from the day 21 pellets (Figure 5.12) (Methods: Section 2.3.4). Expression of HES1 and HEY1 could be detected in the control pellets. In the 38M MSC, a near complete inhibition of the HES1 and HEY1 transcripts was observed when the pellets were treated with DAPT, whereas in the 24M MSC, the HES1 and HEY1 levels were lowered but not completely abolished. No difference could be detected in the transcript levels between the pellets treated with different concentrations of DAPT. This result was somewhat surprising as the change in the concentration of DAPT produced a different morphology in the 24M cells, but RT-PCR is semi-quantitative and as such may not be able to detect significant but small differences in transcript level. The residual levels of HES1 and HEY1 could be attributed to the cells in the core of the pellets where the DAPT seems to have a lesser effect on the changes in cell morphology. GAPDH is used as a control marker, and the levels of GAPDH remained stable. Collagen 2 levels also appeared unchanged by DAPT treatment, which may be contrary to expectation. This could have two possible explanations. The first is that, due to the abundance of this transcript in chondrogenesis, the RT-PCR method was not sensitive enough to detect changes in collagen 2 levels. The second is that the DAPT impairment of chondrogenesis did not alter collagen 2 expression.

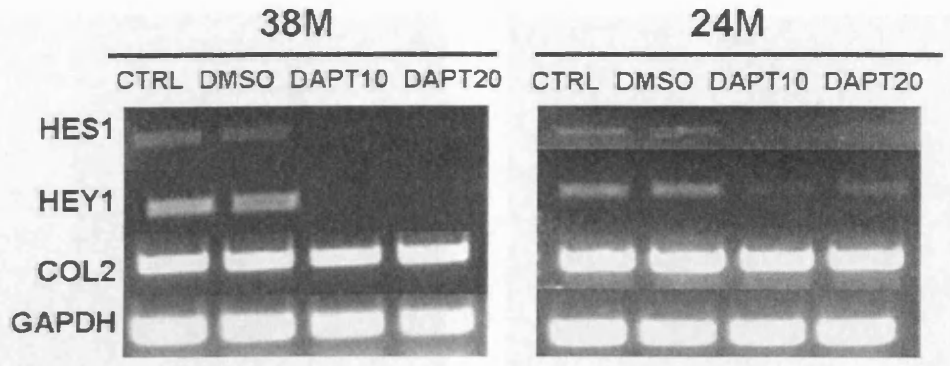

Figure 5.12: Gel electrophoresis showing RT-PCR analysis of targets of Notch signalling and control genes using RNA isolated from day 21 control (CTRL), DMSO and DAPT treated pellets.

5.2.5 Effect of DAPT treatment on adipogenesis and osteogenesis

In spite of some differences in their response to DAPT during chondrogenesis, both 24M and 38M bone marrow-derived MSC showed the same response in the adipogenic and osteogenic cultures (Methods: Section 2.3.5). Therefore, even though the experiments were performed in triplicate on both cell lines, representative photomicrographs for the histology of only the 24M cultures are shown.

In the adipogenic cultures, treatment with DAPT appeared to have no effect on adipogenesis (Figure 5.13). Osteogenesis also appeared uninhibited by DAPT as assessed by alizarin red staining for calcium deposition (Figure 5.14) and staining for alkaline phosphatase activity (Figure 5.15). Both processes were not affected by 1µl/ml DMSO carrier alone.

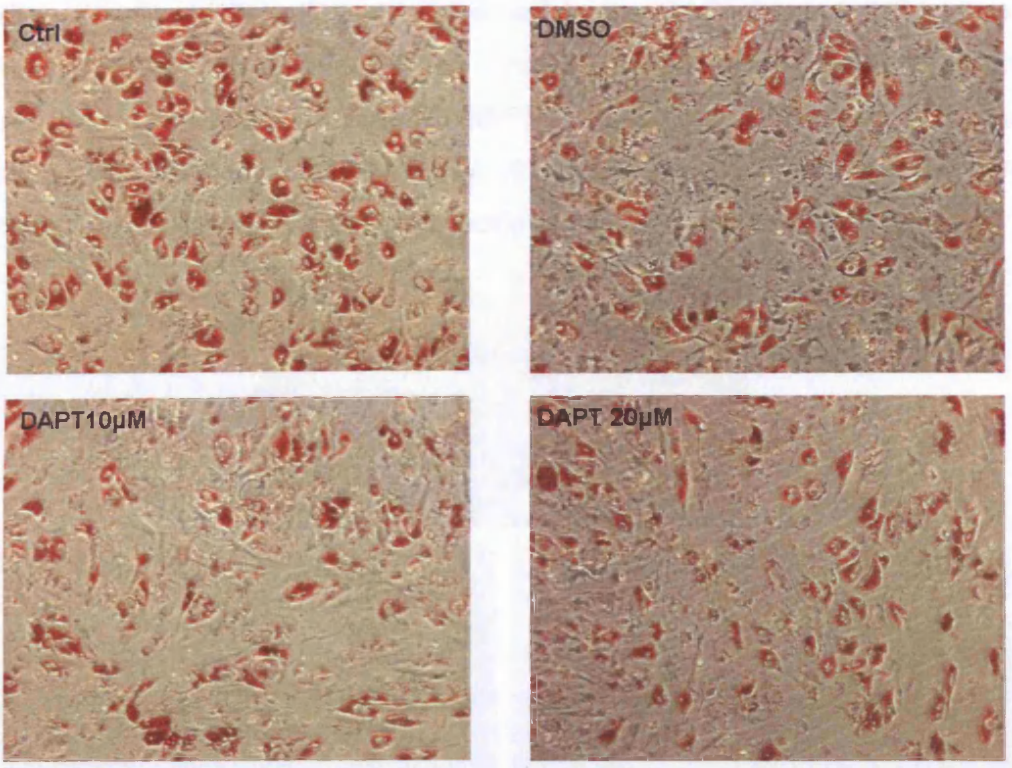

Figure 5.13: The effect of DMSO and DAPT treatment on MSC undergoing adipogenesis as compared to the untreated cells (Ctrl). The extent of adipogenesis was assessed by oil red O staining after 14 days of adipogenic differentiation.

Figure 5.14: The effect of DMSO and DAPT treatment on MSC undergoing osteogenesis as compared to untreated (Ctrl) cells and undifferentiated cells (MSC) not exposed to the osteogenic media. The extent of osteogenesis was assessed by alizarin red staining after 21 days of osteogenic differentiation.

It was noted that the addition of DAPT to osteogenic cultures induced the formation of a large number of cells containing lipid droplets which had a typical adipocyte morphology under higher magnification (Figure 5.15). While it was common to note an occasional adipocyte in osteogenic cultures,

adipogenesis was significantly increased in the DAPT-treated cultures, as demonstrated by a 7 and 12 fold increase in adipocyte numbers in the presence of 10μM and 20μM DAPT respectively (Figure 5.16). The adipocytes were not spread evenly on the culture dish but were present throughout, accounting for the high variance in cells counts observed.

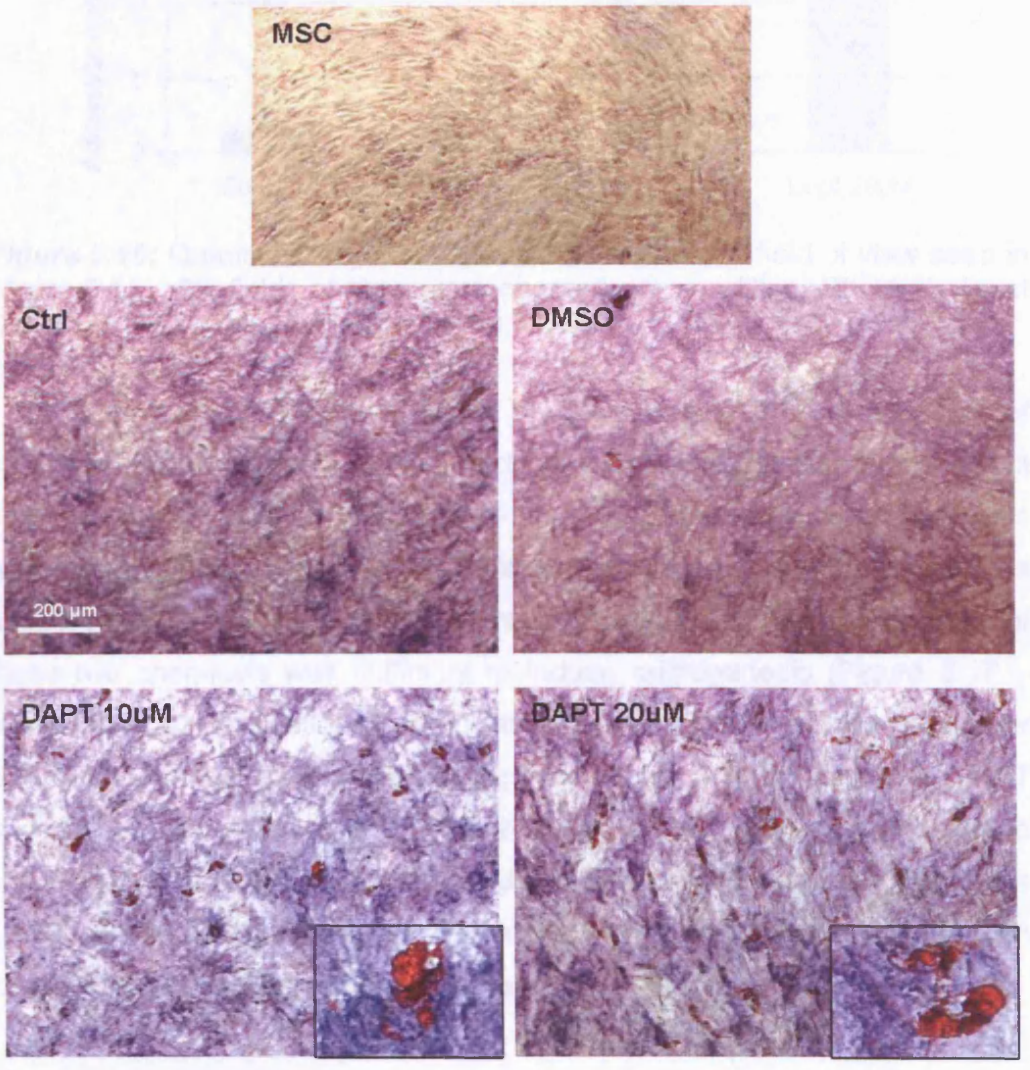

Figure 5.15: The effect of DMSO and DAPT treatment on MSC undergoing osteogenesis as compared to untreated (Ctrl) cells and undifferentiated cells (MSC) not exposed to the osteogenic media. The extent of osteogenesis was assessed by staining for alkaline phosphatase activity after 21 days of osteogenic differentiation. The formation of adipocytes (stained with oil red O) was seen in the DAPT treated cultures. Inset are higher magnifications of adipocytes.

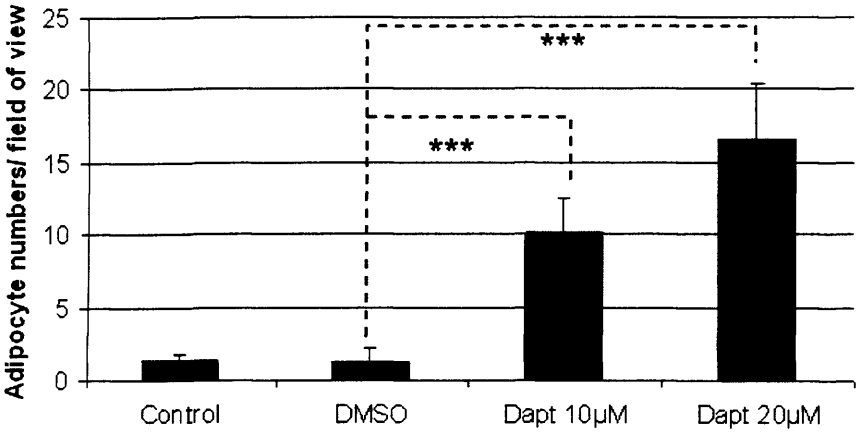

Figure 5.16: Quantification of number of adipocytes per field of view seen in Figure 5.15. Six fields of view were counted per condition. Student's t-test DMSO vs DAPT-treated cultures *** $p < 0.001$.

Exposure of confluent MSC to DAPT only, in the absence of osteogenic differentiation media could not reproduce the adipogenic effect seen in osteogenesis (Figure 5.17 – top row). However, when the cells were exposed to 100nM dexamethasone alongside DAPT, adipocytes appeared as in the osteogenic cultures, indicating that the combination of these two chemicals was sufficient to induce adipogenesis (Figure 5.17 – bottom row). Quantification of adipocyte cells showed an increase in number comparable to that seen in the osteogenic cultures – 8 fold for 10μM DAPT and 14 fold for 20μM DAPT (Figure 5.18). In both cases, doubling the concentration of DAPT, nearly doubled adipocyte numbers so the effect was DAPT concentration dependent. The size of the error bars reflected uneven distribution of adipocytes over the culture dish.

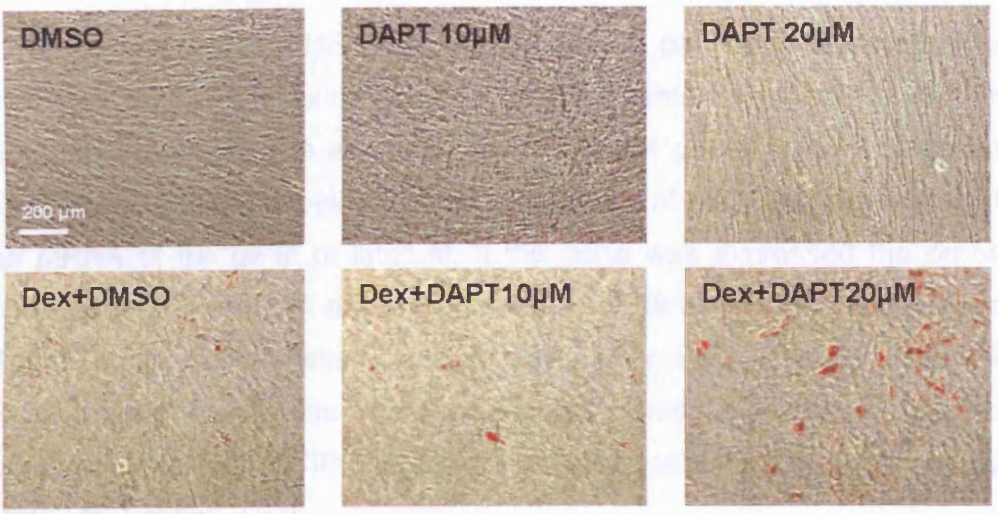

Figure 5.17: Confluent MSC treated with DAPT or a combination of DAPT and dexamethasone (Dex) for 21 days and stained with oil red O.

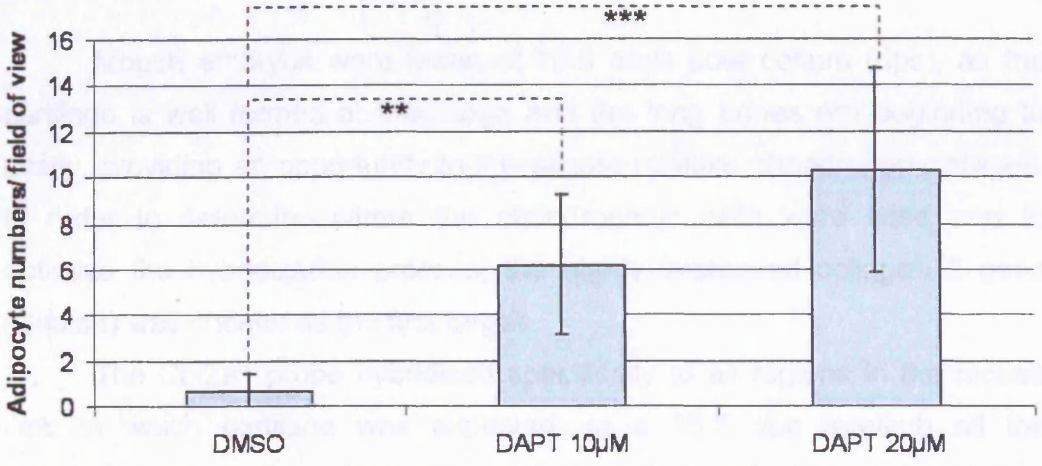

Figure 5.18: Quantification of number of adipocytes per field of view seen in Figure 5.17. Six fields of view were counted per condition. Student's t-test DMSO vs DAPT-treated cultures **p<0.005, *** p < 0.001.

RT-PCR for HES1 and HEY1 were also performed on samples from adipogenesis, osteogenesis, and the DAPT-treated MSC samples, but the levels of expression were too low to be detected and yielded no product (data not shown).

5.3 LOCALISATION OF HES1 AND HEY1 TRANSCRIPTS DURING LIMB DEVELOPMENT USING *IN SITU* HYBRIDIZATION

To investigate if HES1 and HEY1 play a part in chondrogenesis *in vivo*, their expression during mouse limb development was examined using *in situ* hybridization. The expression of the target genes was localised and quantitated by using labelled probes consisting of RNA complementary to the mRNA of the gene of interest. If the gene was expressed the probes would bind to the mRNA and a signal would be detected. For the purposes of this study, DIG-labelled probes were generated, and the samples incubated with an alkaline phosphatase-conjugated DIG antibody that was visualised with NBT/BCIP that stains positive cells in the sections blue (Methods: Section 2.3.6).

5.3.1 *In situ* hybridization controls

Mouse embryos were taken at 15.5 days post coitum (dpc), as the cartilage is well formed at this stage and the long bones are beginning to ossify, providing an opportunity to investigate multiple chondrogenic stages. In order to determine where the chondrogenic cells were sited and to optimize the hybridization process, the highly expressed collagen 2 gene (Col2a1) was chosen as the first target.

The Col2a1 probe hybridized specifically to all regions in the mouse limb in which cartilage was expected. In a 15.5 dpc forelimb all the developing bones were labelled positively with the Col2a1 probe (Figure 5.19). Because of the high levels of expression, the visualisation reaction was only allowed to proceed for 3 hours before the slides were washed and fixed. Col2a1 probes also labelled the ends of long bones but not the centre where ossification had already occurred in the 15.5 dpc embryos, as in the femur (Figure 5.20). Joints, such as the hip joint, were also shown to express Col2a1 (Figure 5.20).

The expression of Sox9, the main chondrogenic transcription factor, was analysed next. Sox9 was expressed at lower levels than Col2a1. The Sox9 probe labelled the same regions in the forelimbs as the Col2a1 probe (Figure 5.19) but as this transcript was less abundant, the visualisation reaction of alkaline phosphatase was allowed to proceed overnight. The Sox9 probe also bound to the same regions as Col2a1 in long bones and in the hip joint but due to the lower abundance of the transcript the staining was less intense (Figure 5.20 and 5.21).

Therefore, both Col2a1 and Sox9 probes could be used as control probes to identify cartilage tissues, but as HES1 and HEY1 are both transcriptional regulators and not likely to show such high levels of expression as the matrix protein Col2a1, the transcription factor Sox9 is a more appropriate control.

Figure 5.19: *In situ* hybridization of 15.5 dpc mouse embryo forelimb showing the expression of Sox9, Col2a1 and PDGFRA in the wrist and the digits in consecutive sections.

As cartilage and bones are known to have endogenous alkaline phosphatase activity, a negative control was also necessary to ensure that it was not simply the staining process that dyes the cartilage in these limbs blue. Platelet-derived growth factor receptor alpha (PDGFRA) was used for this purpose as it is a marker of mesenchymal and neural tissues but not cartilage or bone. PDGFRA probe hybridization to mouse limb sections produced the opposite result to Sox9 and Col2a1 probes. This probe hybridized to most tissues in the limbs but not to cartilage (Figure 5.19). The PDGFRA visualisation reaction was also allowed to proceed overnight.

The results of PDGFRA-labelled probes demonstrated that the distribution of Sox9 and Col2a1 probes was due to the probes binding to their respective mRNAs rather than non-specific alkaline phosphatase activity in bone. Therefore the *in situ* hybridization method was set up successfully and could be used to localise cartilage specific transcripts in the developing mouse limbs.

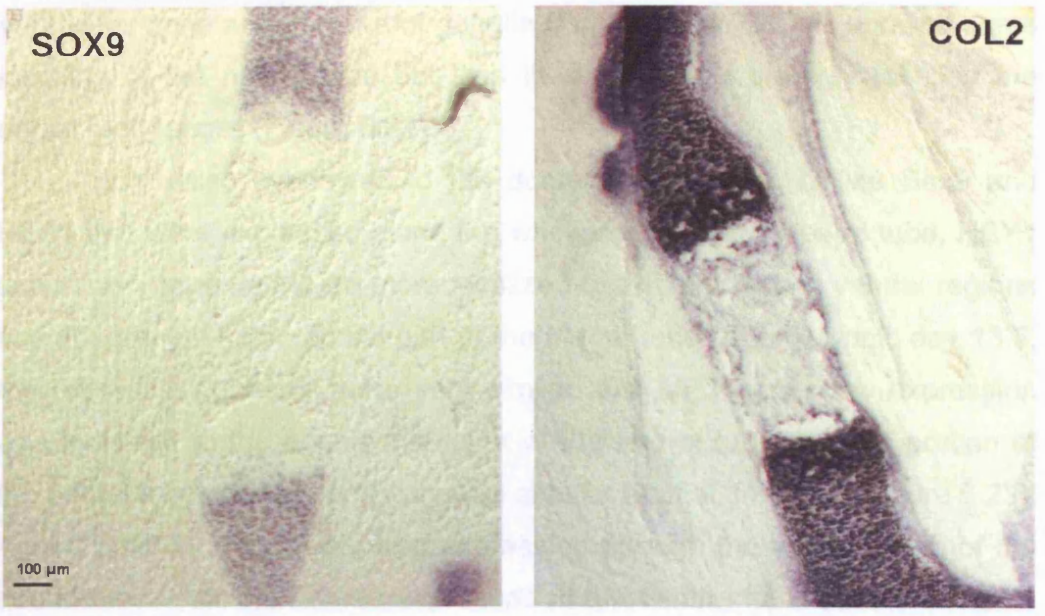

Figure 5.20: *In situ* hybridization of 15.5 dpc mouse embryo hindlimb showing the expression of Sox9 and Col2a1 in the femur in consecutive sections.

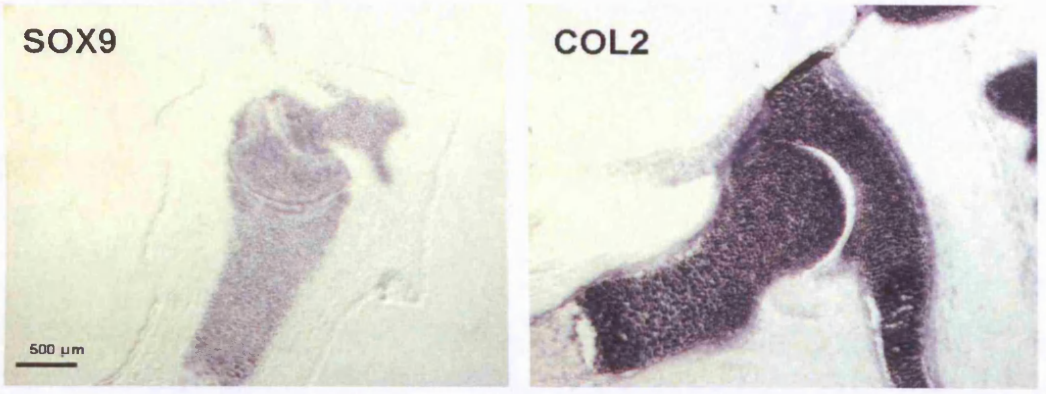

Figure 5.21: *In situ* hybridization of 15.5 dpc mouse embryo hindlimb showing the expression of Sox9 and Col2a1 in the hip joint in consecutive sections.

5.3.2 *In situ* hybridization of HES1 and HEY1

To test whether the HES1 and HEY1 probes were effective at identifying their target mRNAs, the neural tube of 11.5 dpc embryos was first used as a positive control, as it is known to express these genes. As in previously published data, the 11.5 dpc neural tube was found to be positive for Sox9, HES1 and HEY1 (231-233) and the staining was localized to the ventricular zone and dorsal root ganglia (Figure 5.22). Col2a1 showed some labelling of the neural tube but less than Sox9 and strongly labelled the dorsal root ganglia (Figure 5.22).

HEY1 also hybridized to the dorsal root ganglia. Unlike Sox9 and HES1 that were expressed along the whole length of the neural tube, HEY1 expression appeared to be more localized to the middle and ventral regions and not present in the dorsal part of the neural tube. At embryonic day 13.5, the expression patterns were very similar. For all 3 genes the expression was localized to the ependymal layer of the neural tube, but the portion of the neural tube showing positivity was smaller than at 11.5 dpc (Figure 5.23). Again, Sox9 and HES1 showed expression through the whole length of the neural tube while HEY1 was expressed in the ventral half. Sox9 and HEY1 were also both expressed in dorsal root ganglia (Figure 5.23).

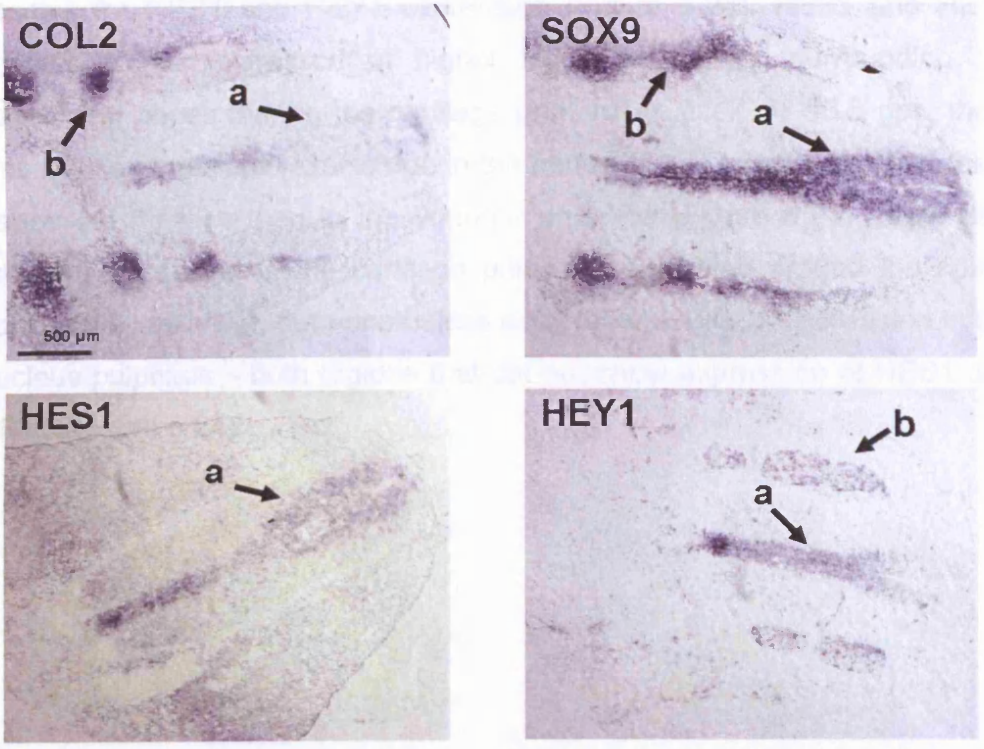

Figure 5.22: *In situ* hybridization of 11.5 dpc mouse embryo showing the expression of Col2a1, Sox9, HES1 and HEY1 in the neural tube (a) and dorsal root ganglia (b) in consecutive sections.

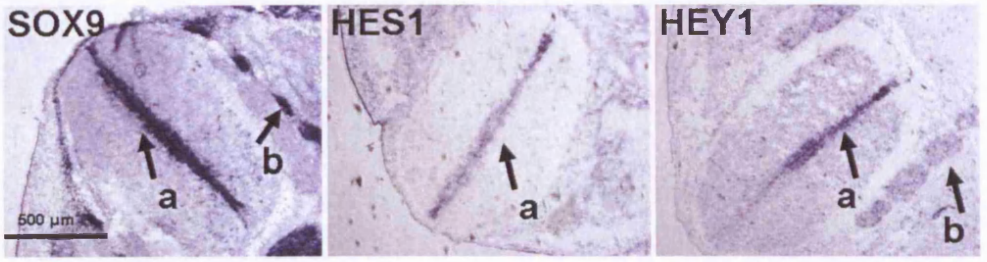

Figure 5.23: *In situ* hybridization of 13.5 dpc mouse embryo showing the expression of Sox9, HES1 and HEY1 in the neural tube (a) and dorsal root ganglia (b) in consecutive sections.

Having confirmed that the probes were effective at identifying the HES1 and HEY1 transcripts, the expression of these genes was assessed in the regions of cartilage and bone development in the 15.5 dpc embryo. As shown previously, in the forelimb, all regions of cartilage primordium showed positivity for the Sox9 probe, however, consecutive sections were not

positive for HES1 and HEY1 expression (Figure 5.24). HES1 and HEY1 seemed to be expressed at higher levels in regions surrounding the developing bones than in the cartilage primordium itself. At 15.5 dpc, there was still some residual expression in the centre of the spinal cord of all three genes but far less than in the younger embryos (Figure 5.24). Sox9 also showed expression in the cartilage primordium forming around the spinal cord as well as lower, but nonetheless detectable, levels of expression in the nucleus pulposus – both regions that did not show expression of HES1 and HEY1 (Figure 5.24).

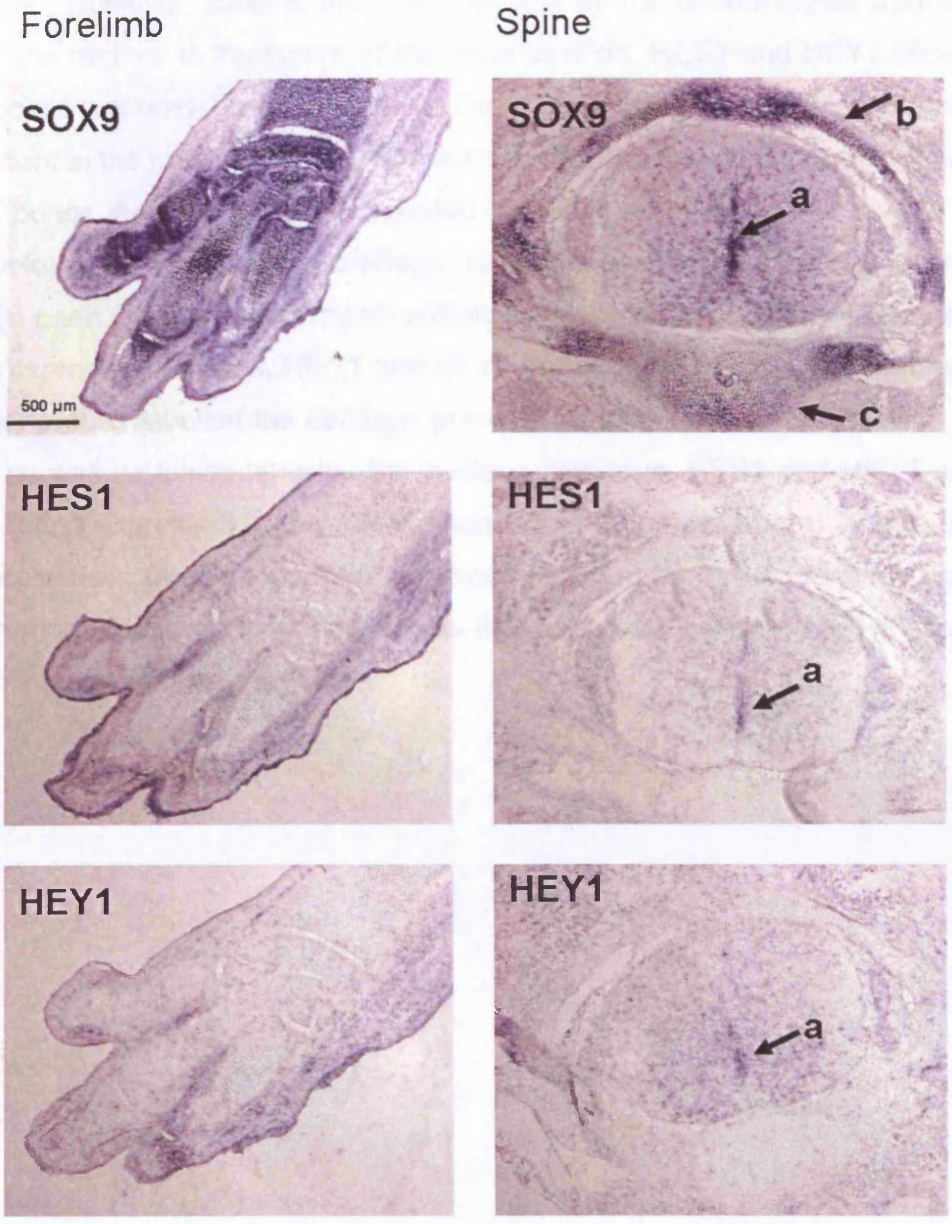

Figure 5.24: *In situ* hybridization of 15.5 dpc mouse embryo showing the expression of Sox9, HES1 and HEY1 in the forelimb and the spinal cord (a), cartilage primordium (b) and nucleus pulposus(c) in consecutive sections.

The results for long bones were similar. Figure 5.25 shows the developing ulna where ossification has already begun in the centre and this is surrounded by cartilage at various stages of development. Sox9 was expressed by both developing cartilage and throughout the hypertrophic

stages. However, Sox9 expression was lost as the chondrocytes apoptose and the regions in the centre of the bone ossified. HES1 and HEY1 showed opposite patterns of expression to Sox9 with higher levels of expression present in the mesenchymal tissue surrounding the developing bones than in the bones themselves. No expression of HES1 and HEY1 was seen in the developing or hypertrophic cartilage, although low levels of expression may have been present in the region undergoing ossification. Figure 5.26 shows the expression of Sox9, HES1 and HEY1 in the tail of the 15.5 dpc embryos. Sox9 probes labelled the cartilage primordium of the vertebral bodies in the tail as well as faintly labelling the nucleus pulposus. HES1 and HEY1 were not found expressed in the cartilaginous cells in the vertebrae. Due to their characteristic morphology, the chondrocytes could easily be identified under high magnification and were the cells that appeared palest in the HES1 and HEY1 probe stained sections.

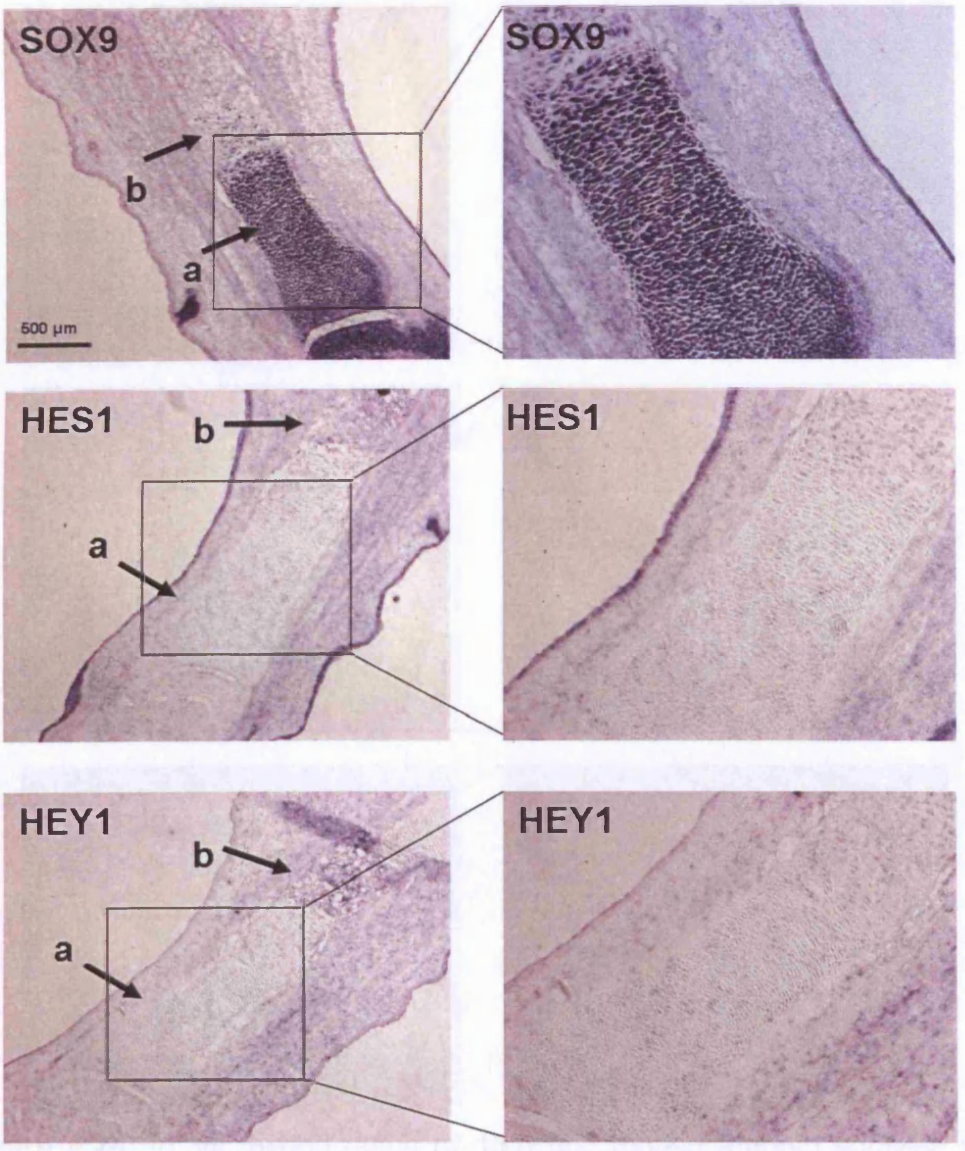

Figure 5.25: *In situ* hybridization of 15.5 dpc mouse embryo showing the expression of Sox9, HES1 and HEY1 in the ulna in consecutive sections and higher magnifications on the right. This bone had already begun to ossify and regions of both cartilage (a) and bone (b) can be seen.

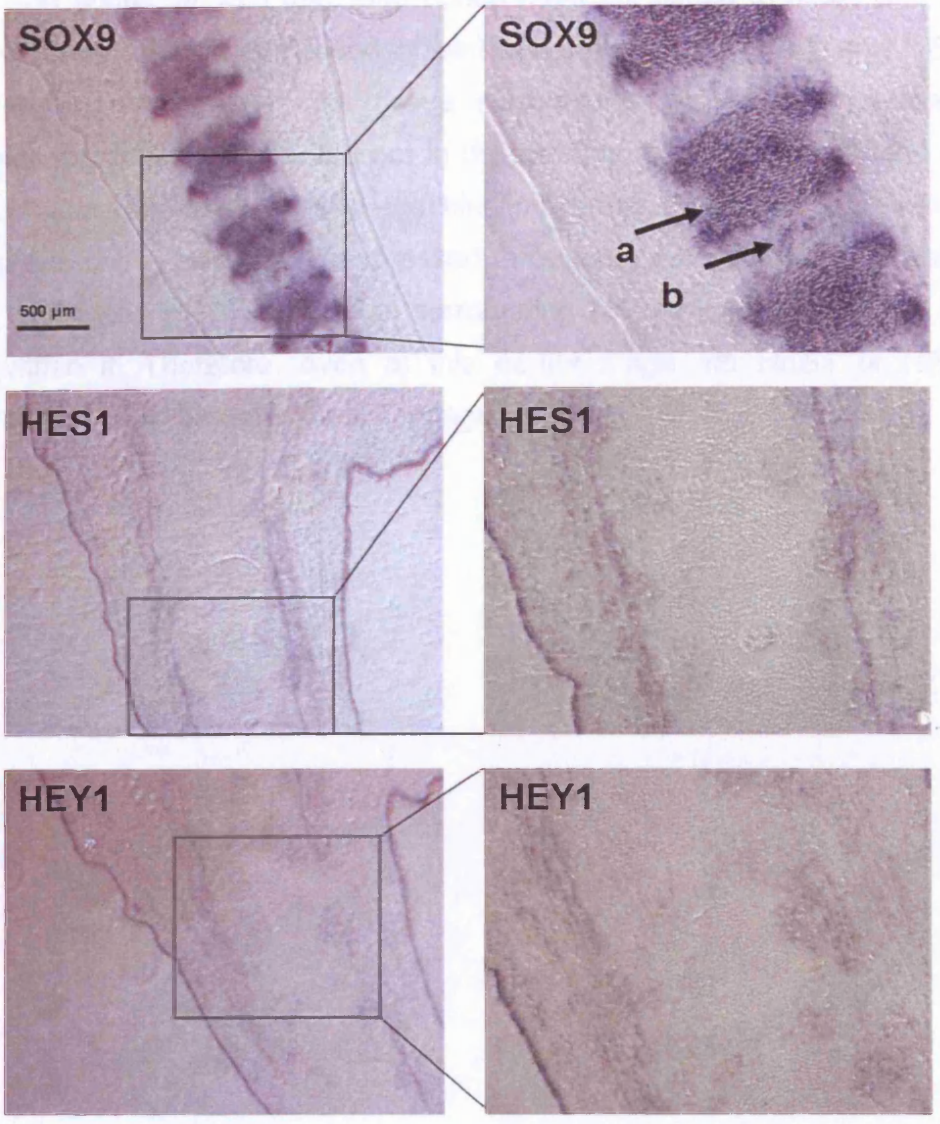

Figure 5.26: *In situ* hybridization of 15.5 dpc mouse embryo showing the expression of Sox9, HES1 and HEY1 in the tail vertebrae (a) and nucleus pulposi (b) in consecutive sections.

As no expression of HES1 and HEY1 was seen in the 15.5 dpc cartilage, 13.5 dpc embryos were also sectioned and *in situ* hybridizations performed to check if expression in limbs could be seen at an earlier stage. Figure 5.27 shows the results of the Sox9, HES1 and HEY1 hybridizations in 13.5 dpc embryo forelimb and hindlimb. In the forelimb, the developing humerus expressed high levels of Sox9 throughout. In contrast to the 15.5

dpc long bones, at 13.5 dpc, long bones have not begun to ossify and the entire future bone is composed of cartilage primordium. HES1 and HEY1 expression was seen in the tissue surrounding the developing bones, presumably muscle tissue, but not in the cartilage of the humerus. The hip joint, femur, and knee joint in the hindlimb showed the same pattern of expression, with Sox9 being expressed throughout the developing cartilage and HES1 and HEY1 expression surrounding the cartilage primordium but not within it. Therefore, even at this earlier stage, no HES1 or HEY1 expression could be detected in cartilage.

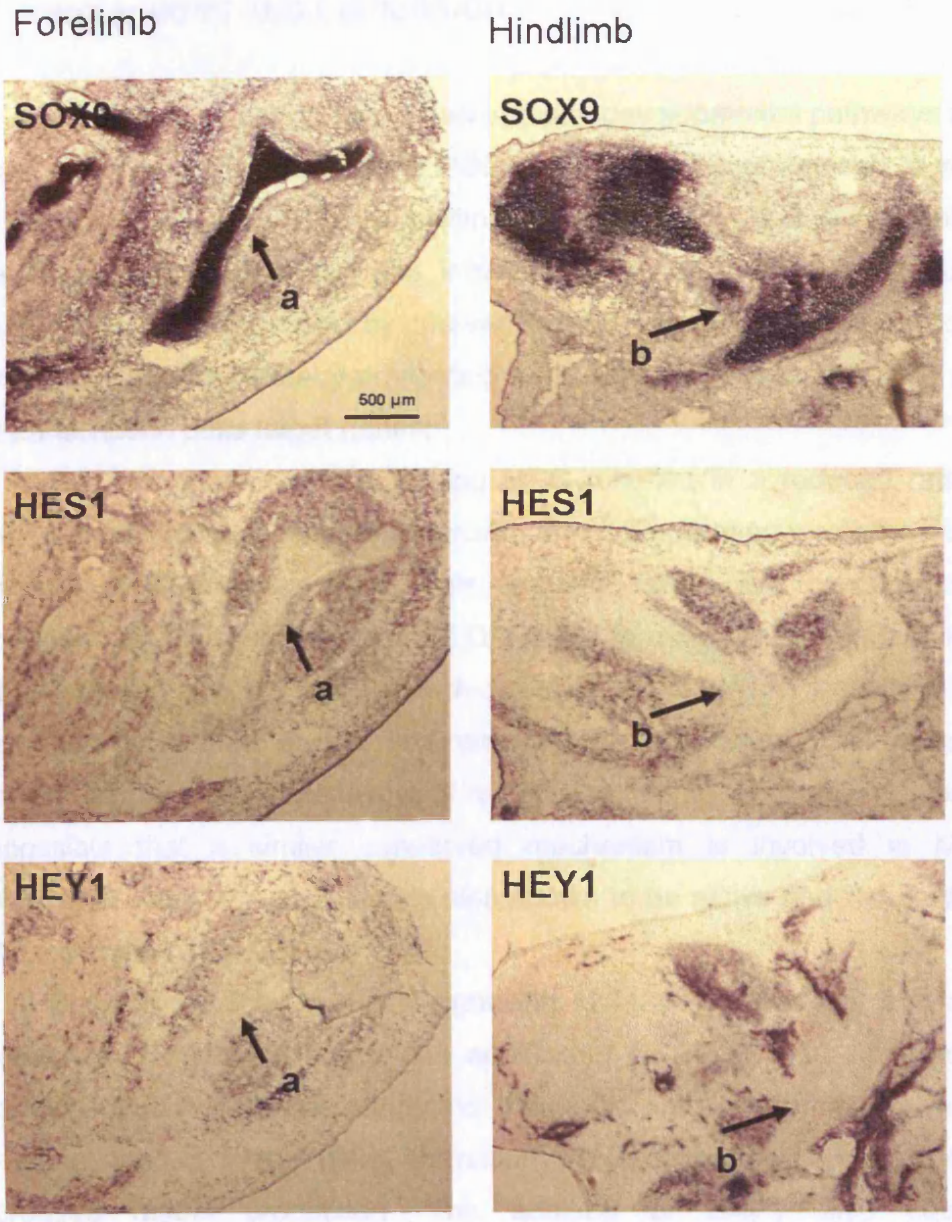

Figure 5.27: *In situ* hybridization of 13.5 dpc mouse embryo showing the expression of Sox9, HES1 and Hey1 in the forelimb including the humerus (a) and hindlimb including the hip joint and femur (b) in consecutive sections.

5.4 CONCLUSIONS AND DISCUSSION

As Notch signalling plays a part in many developmental pathways and was found to be upregulated in the MSC undergoing chondrogenesis *in vitro*, the impact of inhibiting Notch signalling on MSC growth and differentiation was tested. Notch signalling was inhibited using the γ-secretase inhibitor DAPT. This inhibitor acts by preventing the cleavage of the Notch intracellular domain, thereby preventing its translocation to the nucleus and the transcription of its target genes.

DAPT treatment of proliferating MSC resulted in a reduced rate of proliferation followed eventually by growth arrest, implicating a role for Notch signalling in MSC self-renewal. This effect of DAPT was concentration-dependent, as doubling the levels of DAPT led to a more effective inhibition of MSC growth and the cells growth-arrested earlier. Notch signalling has also been implicated in the self-renewal of HSC, where the interplay between Wnt and Notch pathways is required to maintain cell proliferation. It is possible that a similar conserved mechanism is involved in MSC proliferation since Wnt signalling is also known to be active and required for MSC expansion (234;235).

Besides the role of Notch signalling in MSC proliferation, it is also involved in cell fate decisions. The addition of DAPT to MSC undergoing chondrogenesis significantly impaired their differentiation. Inhibiting Notch signalling did not inhibit pellet formation but reduced pellet size due to decreased matrix production. The addition of DAPT also caused morphological changes in the chondrocytes, in particular in the outer layers of the pellet where they did not appear rounded or produce the lacunae as seen with the untreated control pellets. This was possibly due to the partial penetrance of the inhibitor. Some differences in response to DAPT were seen between the two different MSC lines tested. While DAPT was inhibitory to chondrogenesis in both lines, the inhibition was more effective in the 38M MSC. This difference in response can probably be attributed to the initial

differences in the efficacy with which the cells undergo chondrogenesis, and again re-emphasizes the variability between samples associated in this process. The expression of downstream Notch target genes HES1 and HEY1, normally present during MSC chondrogenesis, was also dramatically reduced, though not completely abolished, during DAPT treatment. This residual expression may be explained by the presence of the cells in the core of the pellet where the DAPT may have failed to penetrate. These results are in accordance with previous findings where DAPT treatment was reported to impair proteoglycan production in chondroblasts isolated from joints but contrasts the results obtained with the ATDC5 cell line where HES1 overexpression led to a suppression of chondrogenic differentiation (186;236). One explanation for this might be that transient Notch signaling is required for chondrogenesis, and that either blocking or continually activating the Notch pathway results in inhibition of chondrogenesis.

Notch signalling also appears to be involved in deciding whether MSC undergo osteogenic or adipogenic differentiation. The adipogenic effect brought about by the exposure of MSC undergoing osteogenesis to DAPT can be reproduced by the addition of DAPT and 100nM dexamethasone but not by the addition of DAPT alone. The extent of adipogenic induction in these cultures is dependent on the DAPT concentration as the number of adipocytes nearly doubled when the DAPT concentration was increased from 10μM to 20μM. When DAPT was added to MSC differentiating in adipogenic media, no further enhancement of adipogenesis was seen. These cells had been exposed to a very potent adipogenic cocktail and it is therefore probable that they have already reached their full adipogenic capacity.

Previous studies on the role of Notch signalling in adipogenesis have produced contradictory results. Inhibition of Notch-signalling in the murine preadipocyte cell line 3T3L1 impaired adipogenesis, while murine embryonic fibroblast and murine embryonic stem cell adipogenesis was unimpaired (237;238). In contrast, the experiments performed here on MSC, argue that

Notch inhibition induces human adipogenesis. As only a small proportion of MSC differentiated to adipocytes in response to DAPT and dexamethasone, it appears that other factors are required for efficient commitment of cells to fat. One limiting factor could possibly be the amount of insulin present in the serum used.

Although DAPT is a specific γ-secretase inhibitor, the function of these enzymes is not exclusive to the Notch pathway(239). Therefore, the possibility can not be excluded that these findings may be due to a Notch-independent effect of the γ-secretase inhibition. However, in the chondrogenic cultures, a concomitant inhibition of extracellular matrix production and a significant decrease in HES1 and HEY1 mRNA expression (downstream targets of Notch signalling) was observed upon addition of DAPT, implying a direct role for Notch signalling in this process. No decrease in HES1 and HEY1 mRNA levels in response to DAPT treatment was observed in the proliferation assay, nor in the adipogenic and osteogenic cultures, as the level of their expression were below the detectable threshold of the RT-PCR analysis. In spite of this, since the HES and HEY family have been shown to play a part in chondrogenic, adipogenic and osteogenic differentiation in a number of cell lines, it seems plausible that the effect of DAPT was due to the disruption of Notch signalling (186;240-242).

After demonstrating the role for Notch signalling *in vitro,* the expression of HES1 and HEY1 was investigated *in vivo* in developing mouse limbs using *in situ* hybridization. The technique was first set up using a Col2A1 and Sox9 probe that successfully identified all cartilage in the embryos. The HES1 and HEY1 probes labelled the developing neural tube, the tissue used as the positive control, but did not bind to any of the developing cartilage. There are a number of possible explanations for this result. The first factor to be taken into account is that these experiments were performed on mouse limbs whereas the MSC work used human MSC and there could be interspecies differences in Notch targets important for

chondrogenesis. In addition, the developmental stages investigated (13.5 and 15.5 dpc) may be too late to show HES1 and HEY1 expression. The latter may be the case if HES1 and HEY1 are involved in the mesenchymal condensation stage of cartilage development as only younger embryos would express these genes. However, the Notch receptors and Delta ligands are expressed at the later stages of development of cartilage, including hypertrophy. Therefore it would be expected that it is at this stage that the HES1 and HEY1 targets of Notch signalling are also expressed (243). It is, however, possible that, while Notch signalling is active in developing mouse limbs, the targets are HES and HEY family members other than HES1 and HEY1. This would explain the *in vitro* effect of DAPT on chondrogenesis (as DAPT would inhibit any HES and HEY family member transcription) but would not account for the high levels of HES1 and HEY1 expressed in MSC chondrogenesis.

Another explanation for not detecting HES1 and HEY1 expression in mouse limbs could be that the transcription of HES1 and HEY1 may be characteristic to human chondrogenesis or even MSC chondrogenesis. It is also possible that, *in vivo,* HES1 and HEY1 are expressed in mouse limbs but at levels too low to be detected by the probes, as the signal produced by these probes, even on the positive control tissues, is faint. More efficient probes may allow the visualization of HES1 and HEY1 expression in cartilage primoridium.

The *in vitro* effect of DAPT infers a direct role of Notch signalling in the control of MSC proliferation and cell fate determination, playing a positive role in chondrogenic and a negative role in adipogenic differentiation. Notch signalling is likely to interact with the other signalling pathways already implicated in MSC function as a means of regulating stem cell function. Due to previously demonstrated expression of Notch receptors and ligands in mouse embryonal cartilage, it was expected that HES1 and HEY1 expression would be detected in mouse limbs using *in situ* hybridizations. However, the results of this experiment failed to support this hypothesis. This

could be due to insufficient sensitivity of the probes, interspecies differences between mouse and human cells, or differences between the differentiation of adult MSC and embryonic chondroprogenitors. Also, only 13.5 and 15.5 dpc stages of mouse development were analysed at and it is possible that a different stage of embryonic development may have yielded different results.

6. IDENTIFICATION OF BRACHYURY AS A MARKER OF CHORDOMAS

6.1 INTRODUCTION

Connective tissue tumours show a striking range of morphologies both between and within tumour types, which frequently overlap. Therefore, histological examination may not always provide sufficient information for a diagnosis, especially when performed on small amounts of tissue such as that obtained by needle core biopsy. Gene expression microarray (GEM) technology is commonly used in the analysis of disease states, in particular in cancer biology. A recently published project involved the use of GEM technology to analyse tumours of connective tissues with two primary aims: to determine the relationships between different lesions and to identify novel markers that could be used in the diagnosis of particular tumours (134) (Section 1.4.5).

Chordomas are rare malignant neoplasms, occurring along the spine and thought to derive from notochordal remnants. Although they are not considered classical mesenchymal tumours, chordomas were among the range of lesions tested in the above-mentioned study (Section 1.4). Morphologically, chordomas most closely resemble chondroid lesions, especially chondrosarcomas. Therefore, it was not surprising to find these two groups of tumours resembling each other at the transcriptional level in the GEM analysis (Figure 1.4).

Brachyury was identified as a marker distinguishing chordomas from all other lesions tested (Section 1.4.6). Brachyury is a transcription factor that plays a crucial role in the development of the notochord, the presumed tissue of origin for chordomas. The identification of brachyury as a chordoma marker supports the theory of the tumour's notochordal origin and recent

findings have identified notochordal remnants, from which these tumours could stem, at a surprisingly high incidence (151).

In spite of extensive immunohistochemical studies, no unique marker exists that can reliably distinguish chordomas from other lesions. However, a combination of S100 and cytokeratin expression is the currently accepted method for discounting the possibility of the lesion being a renal cell carcinoma or a chondrosarcomas respectively, the two most common differential diagnoses (Section1.4.3). The rarity of chordomas further impairs their correct diagnosis, as many surgeons and histopathologists will only encounter a few cases within the course of their career (244). Therefore, a unique chordoma marker would be an extremely useful tool in the diagnosis of chordomas, especially in those lesions showing an ambiguous morphology, such as chordomas with extensive areas of chondroid differentiation.

6.1.1 Aims

It is the aim of this section to investigate further the relationship between chondroid neoplasms and chordomas. As the brachyury transcription factor was uniquely expressed by chordomas, the second objective of this part of the project was to establish whether the expression of this molecule would be a useful means of distinguishing chordomas from other tumours.

6.2 MICROARRAY ANALYSIS OF CHORDOMAS AND CHONDROID NEOPLASMS

Microarray analysis of a range of mesenchymal neoplasms indicated that, at a transcriptional level, chordomas resembled chondroid lesions (chondroblastomas, chondrosarcomas and chondromyxoid fibromas) more closely than the other connective tissue tumours (Methods: Section 2.4.1) (Figure 1.4) (134).

When the transcriptional relationship between the chordomas and chondroid neoplasms was visualised on an MDS plot, the gene expression profile of chordomas most closely resembled that of chondrosarcomas. This finding was not surprising, as chordomas have a morphological appearance not dissimilar to chondrosarcomas, particularly for those showing areas of chondroid differentiation (Section 1.4.2).

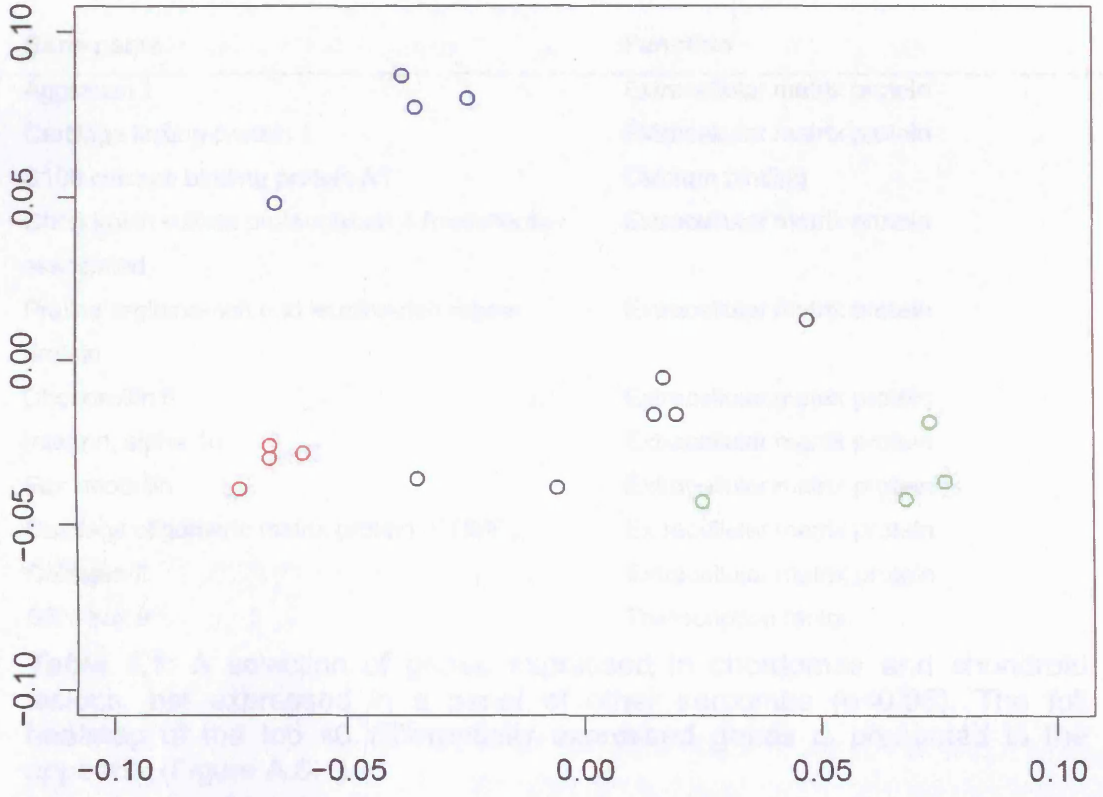

Figure 6.1: Multi-dimensional scaling plot showing the relationship between chordomas (green) and chondroid neoplasms (chondrosarcomas – black, chondroblastomas – red and chondromyxoid fibromas – blue). (Figure adapted from (245))

The list of the top 40 probe sets distinguishing chondroid neoplasms and chordomas from other mesenchymal tumours tested ($q<0.00000679$) is presented in the form of a heat map in the appendix (Figure A.6.1). To obtain this list of probe sets, a moderated standard deviation test was used that was corrected for the false discovery rate (Methods: Section 2.4.1; Section 4.2.4). A selection of genes of particular interest is presented in Table 6.1. Many of these genes have known roles in chondrogenesis – often representing an ECM protein.

Collagen 2 and Sox9 were not among the 40 most differentially expressed probe sets. However, as these genes are known to play a key role in chondrogenesis (Section 1.2.4), their expression values were analysed and found to be significantly upregulated in the chordomas and chondroid lesions as compared to other tumours ($q<0.05$).

Gene name	**Function**
Aggrecan 1	Extracellular matrix protein
Cartilage linking protein 1	Extracellular matrix protein
S100 calcium binding protein A1	Calcium binding
Chondroitin sulfate proteoglycan 4 (melanoma-associated)	Extracellular matrix protein
Proline arginine-rich end leucine-rich repeat protein	Extracellular matrix protein
Chondroitin 6	Extracellular matrix protein
Integrin, alpha 10	Extracellular matrix protein
Fibromodulin	Extracellular matrix protein
Cartilage oligomeric matrix protein (COMP)	Extracellular matrix protein
Collagen II	Extracellular matrix protein
SRY-box 9	Transcription factor

Table 6.1: A selection of genes expressed in chordomas and chondroid lesions, not expressed in a panel of other sarcomas ($p<0.05$). The full heatmap of the top 40 differentially expressed genes is presented in the appendix (Figure A.6.1)

Although chordomas were most closely related to chondrosarcomas, the two tumour types could be distinguished at the transcriptional level. Figure 6.2 shows a selection of differentially expressed genes in the form of a heatmap (see appendix for the full heat map, Figure A.6.2). Chordomas did not express high levels of the hypertrophic ECM protein collagen 10, platelet-derived growth factor alpha, a mitogen for connective tissue cells, or reticulocalbin 3, a putative endoplasmic reticulum protein.

Chordomas expressed brachyury, CD24 and cytokeratins 8, 15, 18 and 19, at much higher levels than the chondroid neoplasms (134). In addition, periplakin, a molecule known to interact with cytokeratins, and DDR1, a collagen receptor reported to be overexpressed in breast carcinoma and osteosarcoma, distinguished chordomas from chondroid tumours (246;247).

An interesting finding was that chondroblastomas also expressed cytokeratins 8 and 18, albeit at far lower levels than those seen in chordomas (Figure 6.2).

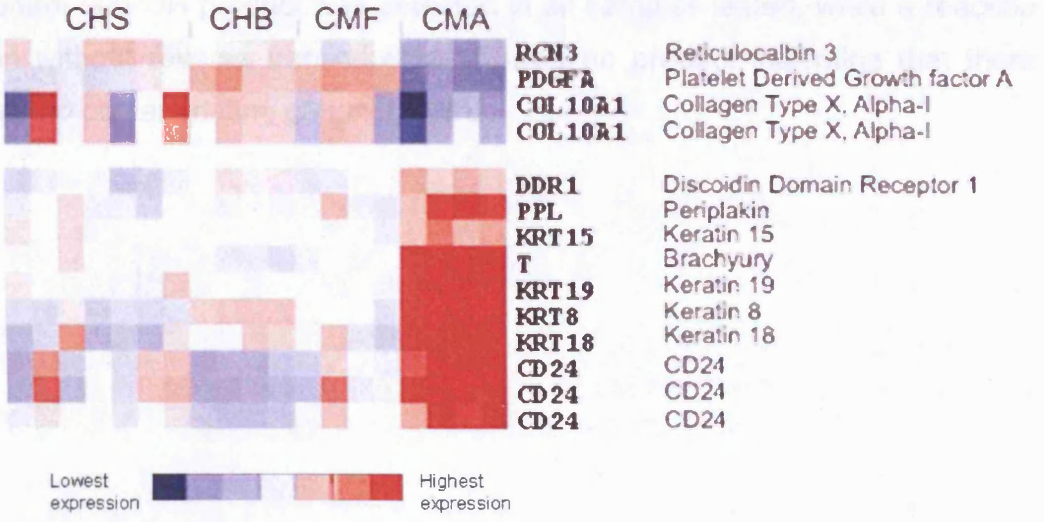

Figure 6.2: Genes distinguishing between chondroid neoplasms (CHS – chondrosarcoma, CHB – chondroblastoma, CMF – chondromyxoidfibroma) and chordomas (CMA) ($q<0.01$). (Figure adapted from (248))

6.3 THE SPECIFICITY OF BRACHYURY

GEM studies identified brachyury as a specific chordoma marker because its level of expression was significantly greater in chordomas than in any of the other 92 connective tissue tumours analysed. The levels of brachyury expression in the 4 chordomas (mean Log2 expression = 11.32), 15 chondroid neoplasms (mean Log2 expression = 7.20) and 77 other tumours (mean Log2 expression = 7.13) tested is plotted in Figure 6.3. In this 'box and whiskers' plot, the median level of expression is represented by the central line and the box surrounding it represents the interquartile range (25% either side of the mean). The whiskers cover the 95% confidence range with any outliers shown as small circles. As the expression values are Log2 transformed, the numbers presented here account for 16-fold greater levels of brachyury expression in chordomas than in chondroid and other neoplasms. These results were validated using RT-PCR (Methods: Section 2.4.2) (Figure 6.4). Brachyury could only be detected in chordoma cDNA and not in a range of other sarcoma samples, including a chondrosarcoma. The control GAPDH product was detected in all samples tested, while a reaction run without reverse transcriptase showed no product indicating that there was no contaminating genomic DNA.

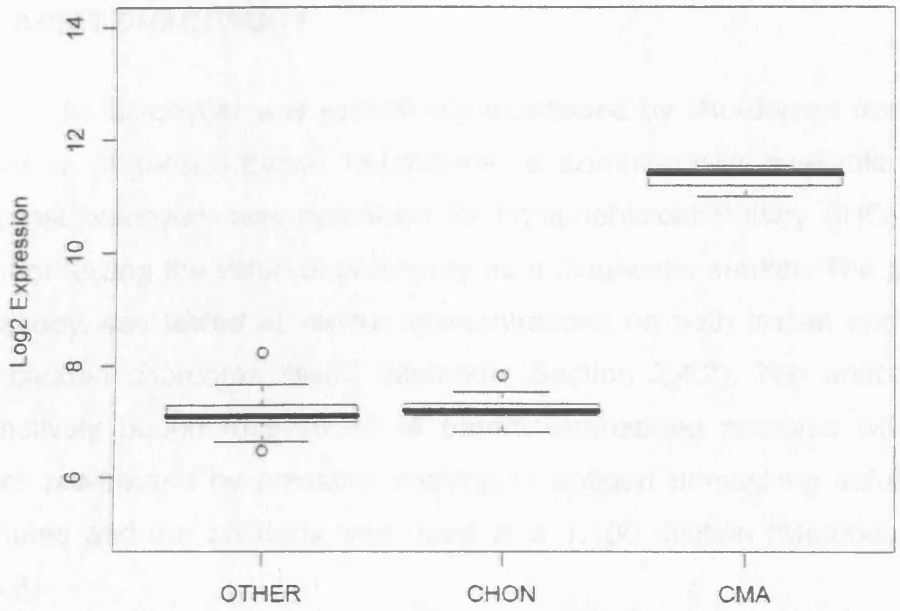

Figure 6.3: Box and whiskers plot representing GEM values of brachyury expression in chordomas (CMA), chondroid neoplasms (CHON) and other tumours (OTHER). The box and whisker plots show the interquartile range as the box and the 95% confidence range as the whiskers; samples outside this range (outliers) are shown as small circles. The central line is the median. The units of expression in this plot are Log2 expression units calculated using the RMA algorithm (Figure adapted from (249))

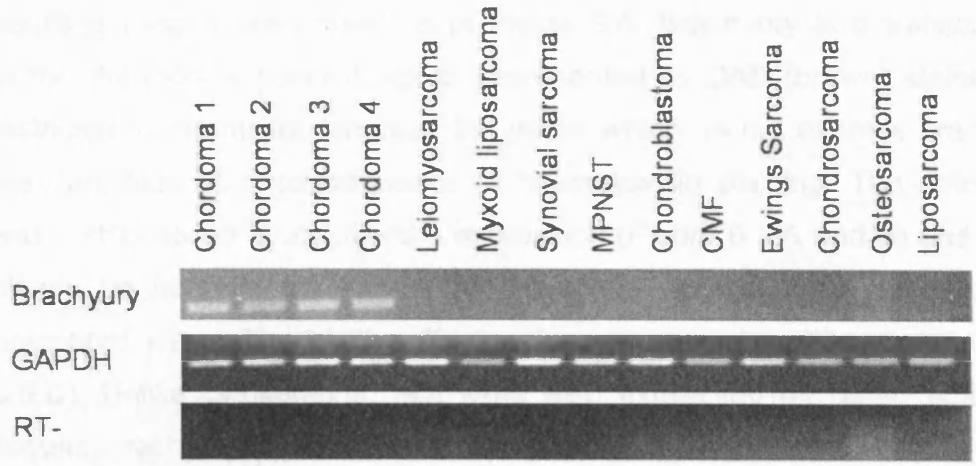

Figure 6.4: Gel electrophoresis showing RT-PCR validation of brachyury expression in chordomas and not in other sarcomas. GAPDH control is expressed in all tumours. MPNST – malignant peripheral nerve sheath tumour. CMF – chondromyxoid fibroma. (Figure adapted from (250))

6.4 IMMUNOHISTOCHEMISTRY WITH A POLYCLONAL ANTIBODY AGAINST BRACHYURY

As brachyury was exclusively expressed by chordomas from a large number of mesenchymal neoplasms, a commercially available antibody against brachyury was optimised for immunohistochemistry (IHC) with the aim of testing the value of brachyury as a diagnostic marker. The polyclonal antibody was tested at various concentrations on both frozen and paraffin-embedded chordoma tissue (Methods: Section 2.4.2). The antibody most effectively bound to sections of paraffin-embedded samples when these were pre-treated by pressure cooking in antigen unmasking solution for 2 minutes and the antibody was used at a 1:100 dilution (Methods: Section 2.4.3).

Since brachyury is known to have a crucial role in notochordal development (Section 1.4.6), a whole mount of a human embryo of 6-8 weeks gestation was used as a positive control for brachyury expression. Sagittal sections of the embryo, in which the notochord could be seen, were incubated with the brachyury primary antibody followed by a biotinylated secondary and a streptavidin-horseradish peroxidise conjugate. The resulting images are presented in Figure 6.5. Brachyury is a transcription factor, therefore a positive signal, represented by DAB (brown) staining, is restricted to the nuclei, whereas the nuclei which do not express brachyury are dark blue as a consequence of haematoxylin staining. The notochord was first localised by cytokeratin expression (Figure 6.5.A and B) and could clearly be seen in the centre of the spinal column. The nuclei of the notochord were also positive for brachyury expression (Figure 6.5.C and 6.5.D). Unlike cytokeratins, that were also expressed by other, epithelial, tissues, brachyury expression was restricted to the notochord.

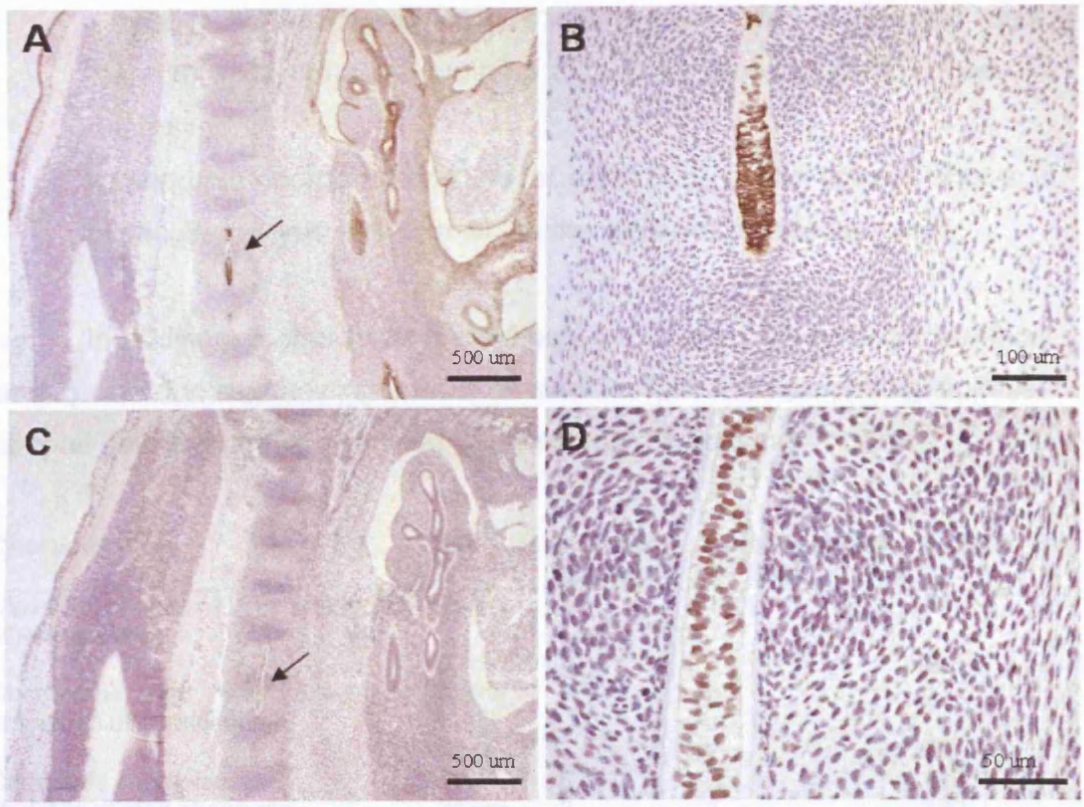

Figure 6.5: Immunohistochemical analysis on sections of the notochord of a 6-8 week human embryo, showing it to express cytokeratin (AE1/3) (A,B) and brachyury (C,D). The arrow in A and C points to the notochord. Brachyury is a transcription factor, therefore the staining is localised to the nuclei.

A variety of chordomas were tested for the presence of brachyury, and an overview of them is presented in Table 6.2. The tumours analysed included full resections and needle core biopsies. The cases included decalcified and non-decalcified material, chordomas located at both ends of the spine and cases with areas showing chondroid differentiation. The amount of chondroid differentiation within chordomas varied. The classification used in the cases in this study was as follows:

- a classical chordoma: showing no chondrogenic differentiation.

- focally chondroid chordoma: showing minor (not comprising more than 10% of the total tumour) dispersed areas with a chondroid phenotype.
- chondroid chordomas: where at least 60% of the tumour shows a cartilaginous-type matrix in which the cells are embedded singly.

In addition, 5 chordoma metastasis, not located on the axial skeleton and 3 chordomas showing areas of dedifferentiation comprising spindle-shaped cells, were also analysed for brachyury expression.

Chordoma type	**Site**	**Number of cases**	**Number tested for S100**	**% S100 +ve**
Classical chordoma (no chondroid differentiation)	Sacral	23	18	28
	Clival	3	3	100
Chordomas with focal areas of chondroid differentiation	Sacral	10	6	67
	Clival	3	2	50
Chondroid chordoma	Clival	6	5	100
Dedifferentiated chordoma	Sacral	3	1	100
Metastatic chordoma		5	2	0
Total		**53**	37	51.4

Table 6.2: Summary of chordoma samples analysed by IHC. S100 expression was analysed in some samples and was found to be present in ~50% of the samples tested. All 53 chordomas were found to express brachyury.

All the chordomas tested were positive for brachyury expression. Two representative conventional chordomas showing no chondroid-type differentiation, both located in the sacrum are shown in Figure 6.6. Brachyury and cytokeratin were both expressed throughout the tumours but were not present in the reactive fibroblasts surrounding the tumour area. S100 is also expressed by the tumour cells (Figure 6.6.D).

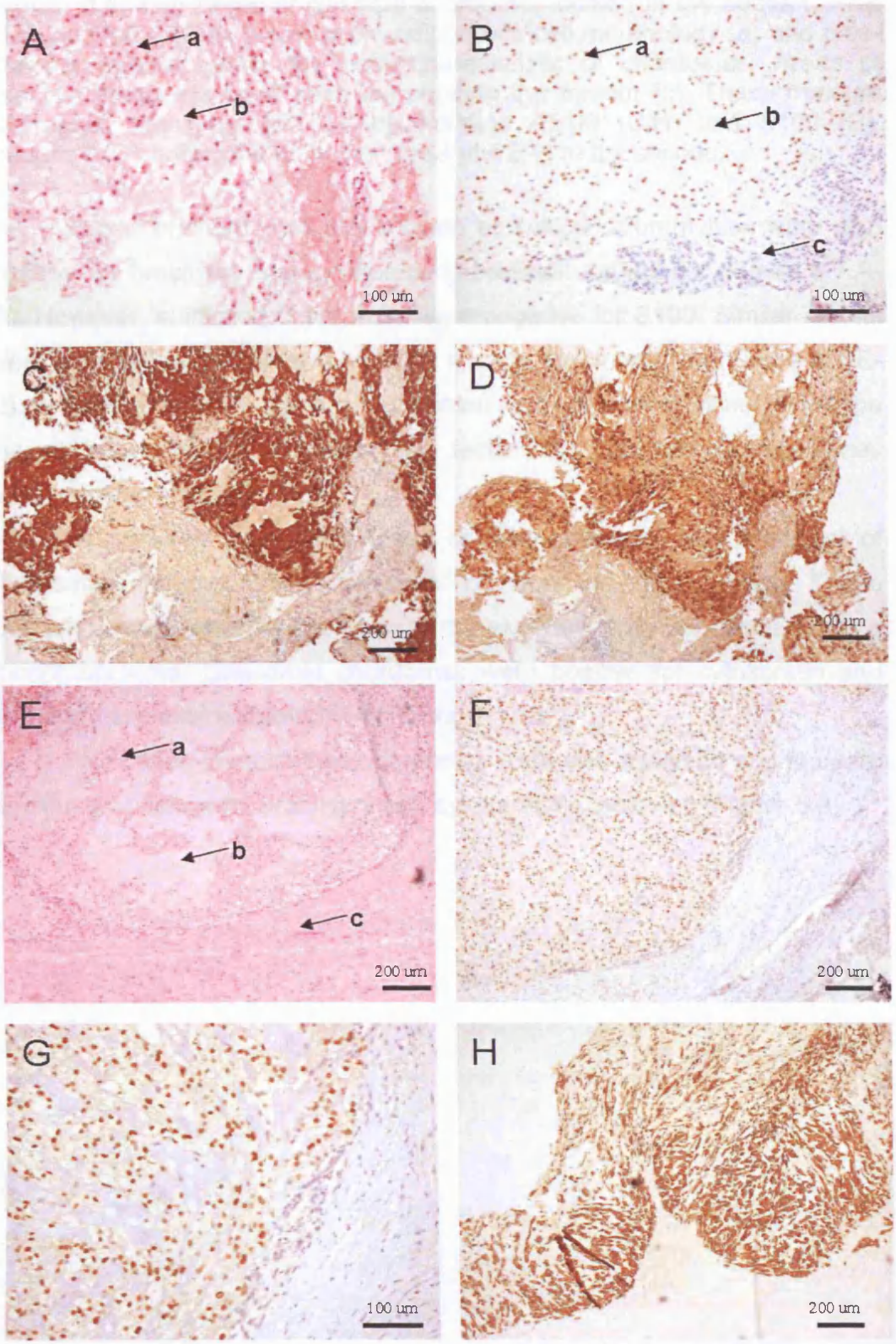

(Figure legend on following page)

Figure 6.6: Two cases of classical chordoma, located in the sacrum. H&E staining (A,E) shows areas of physalipherous cell morphology (a) and pale-staining myxoid matrix (b), both characteristic of chordomas. Areas of reactive fibroblasts were seen surrounding the tumour (c). These tumours expressed brachyury (B,F,G), cytokeratins AE1/3 (C,H) and S100 (D). Images A-D correspond to the first case and E-H to the second.

Cases of chordomas that showed epitheliod differentiation were also positive for brachyury and cytokeratin expression throughout (Figure 6.7.A-D). However, epitheliod chordomas were negative for S100. Similar results were obtained for chordomas showing nuclear pleomorphism (Figure 6.7.E-H). In these tumours, brachyury expression was not seen in all nuclei but the majority did express this transcription factor. The pleomorphic chordomas were negative for S100.

Of particular interest, in terms of diagnostic use, was a subset of chordomas showing extensive regions of chondroid differentiation. These tumours usually occur at the base of the skull and may be mistaken for a chondrosarcoma. Chondroid chordomas were positive for cytokeratin and brachyury expression throughout (Figure 6.8 A-C).

Five cases of metastatic chordomas were also analysed and found to be diffusely positive for brachyury and cytokeratin expression (Figure 6.9).

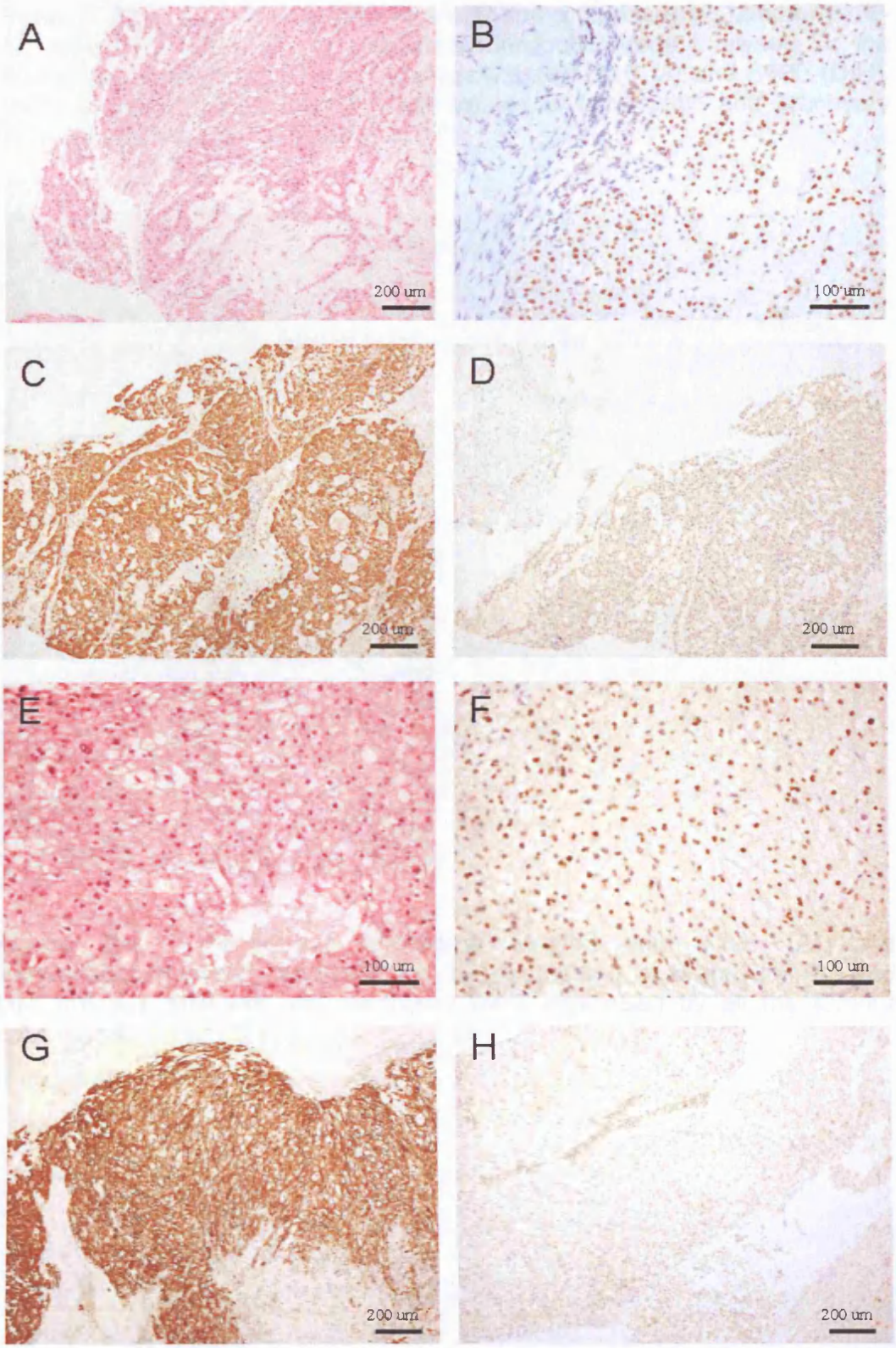

(Legend on following page)

Figure 6.7: An epitheliod chordoma (A-D) and a pleomorphic chordoma (E-H) stained with H&E (A, E) and immunohistochemically analysed for the expression of brachyury (B, F), cytokeratins AE1/3 (C,G) and S100 (D,H). These tumours showed overlapping regions of cytokeratin and brachyury expression but did not express S100.

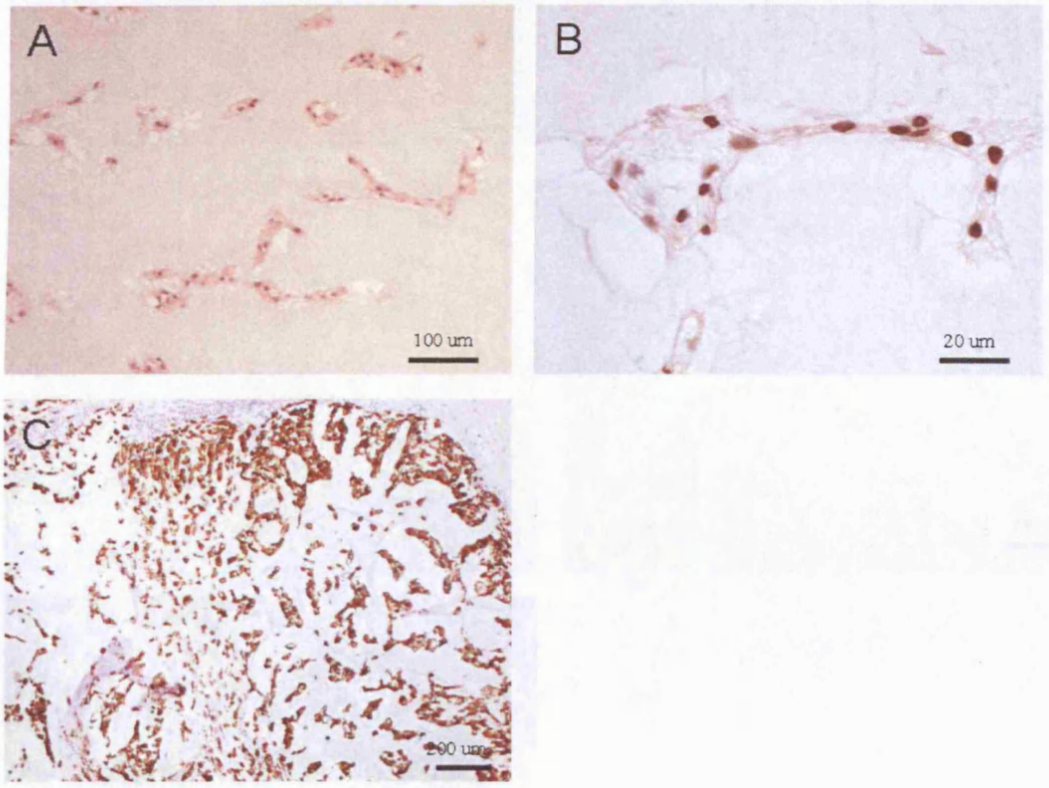

Figure 6.8: A chondroid chordoma stained with H&E (A) and immunohistochemically analysed for the expression of brachyury (B) and MNF116 (C). MNF116 and brachyury were expressed by all the tumour cells.

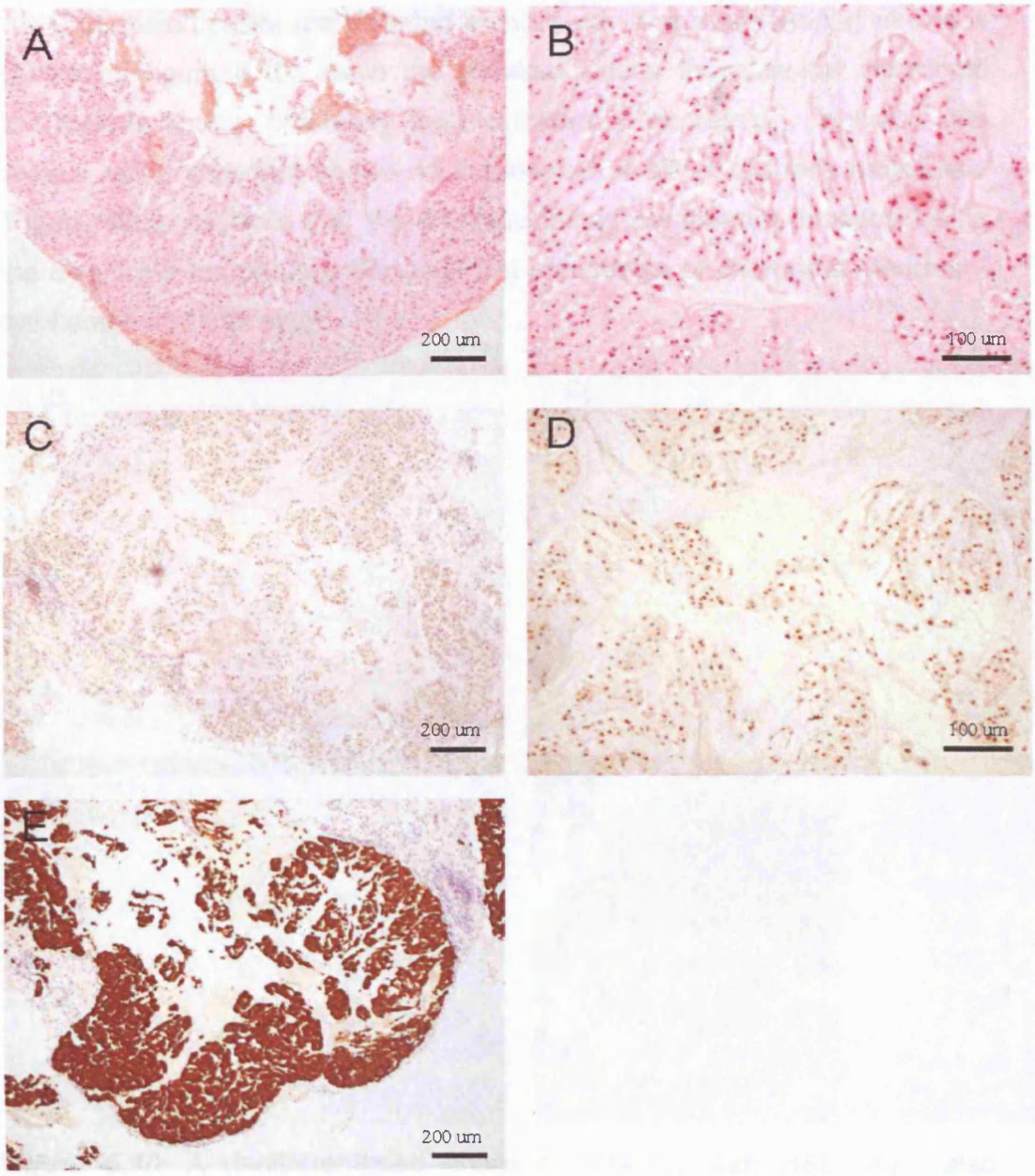

Figure 6.9: A metastatic chordoma stained with H&E (A,B), and immunohistochemically analysed for the expression of brachyury (C,D) and MNF116 (E). Brachyury and MNF116 expression was seen throughout the tumour.

Rarely, cases of dedifferentiated chordomas occur, such variants comprise areas of both conventional chordoma in which physalipherous cells are present and an undifferentiated spindle cell component. Three

dedifferentiated cases are included in this study and a representative one is shown in Figure 6.10. As in the previous cases the classical chordoma component shows brachyury and cytokeratin expression, whereas the spindle cell component shows no expression of either of these molecules. These results indicate that the dedifferentiated component, besides losing the chordoma morphology had also lost expression of chordoma markers – cytokeratin and brachyury.

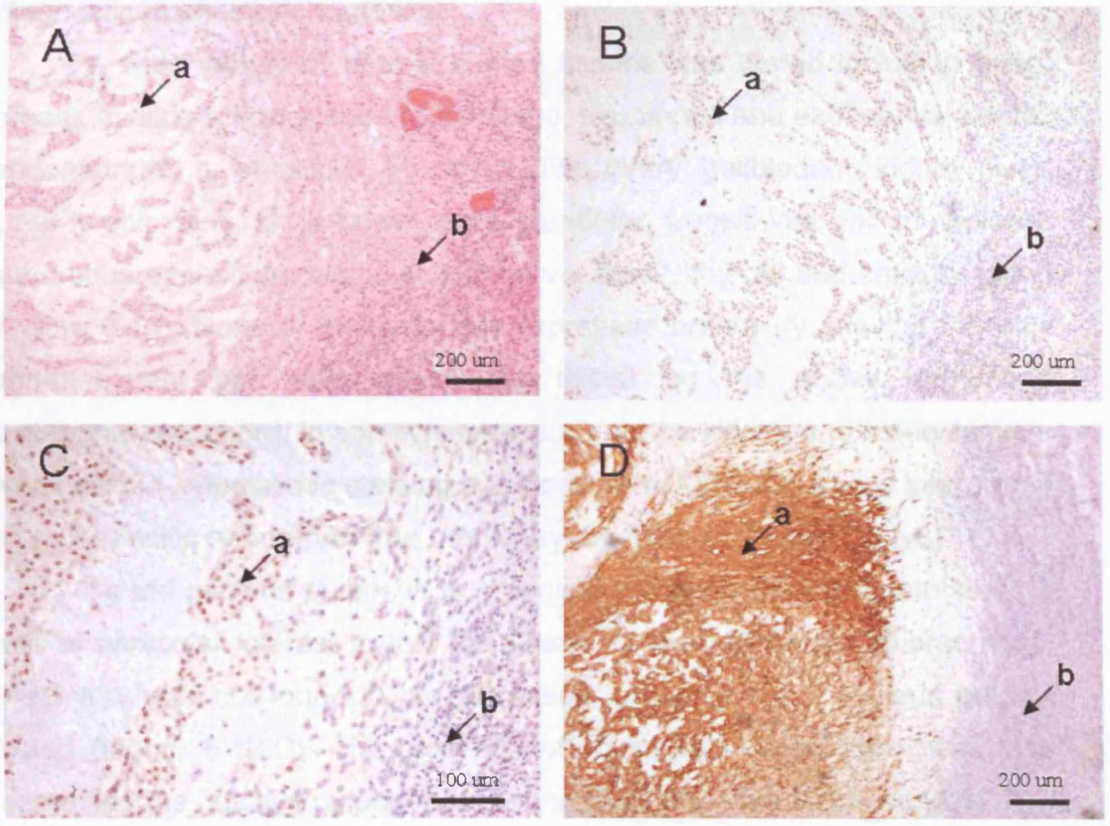

Figure 6.10: A dedifferentiated chordoma stained with H&E (A), also showing brachyury (B,C) and MNF 116 (D) expression. The classical chordoma component is marked with 'a' whereas the dedifferentiated component is marked 'b'.

One tumour, previously diagnosed as a chondroid chordoma was found not to express brachyury. However, the cytokeratin IHC also proved to be negative, hence this neoplasm was reclassified as a base of skull chondrosarcoma.

The S100 antigen IHC was mostly performed prior to this project as a part of the routine immunohistochemical analysis to aid diagnosis prior to treatment. Not all the chordomas used in this study were tested for S100 expression, and of the 70% that were, just over 50% expressed S100 (Table 6.2). The lowest levels of S100 positivity were found in classical chordomas located in the sacrum, whereas all the chondroid chordomas tested were positive. This finding indicates that S100 can not be relied upon as a diagnostic marker for chordomas.

A wide variety of normal human tissues was tested including brain, breast, hyaline articular and fibrocartilage, squamous and endocervial cervix, endometrium, myometrium, Fallopian tube, ovary, gallbladder, kidney, liver, lung, lymph node, large bowel, skin, glandular, transitional and metaplastic squamous epithelium, testis, sciatic nerve, tonsil, thyroid and salivary gland (Figure 6.11). None of these tissues expressed brachyury, leaving the only non-malignant brachyury expressing tissue as the above mentioned embryonic notochord. In some tissues, such as the kidney and osteoclasts, a weak diffuse cytoplasmic staining has been detected but this was interpreted as non-specific rather than true brachyury expression (Figure 6.11.C).

As the nucleus pulposus is proposed to derive from the notochord, it was of particular interest to test this tissue for the expression of brachyury. Brachyury was not found to be expressed in any of the 7 nucleus pulposi tested (Figure 6.12.C). The presence of cytokeratin expression was also tested and the nucleus pulposi were found to be negative for these (6.12.B).

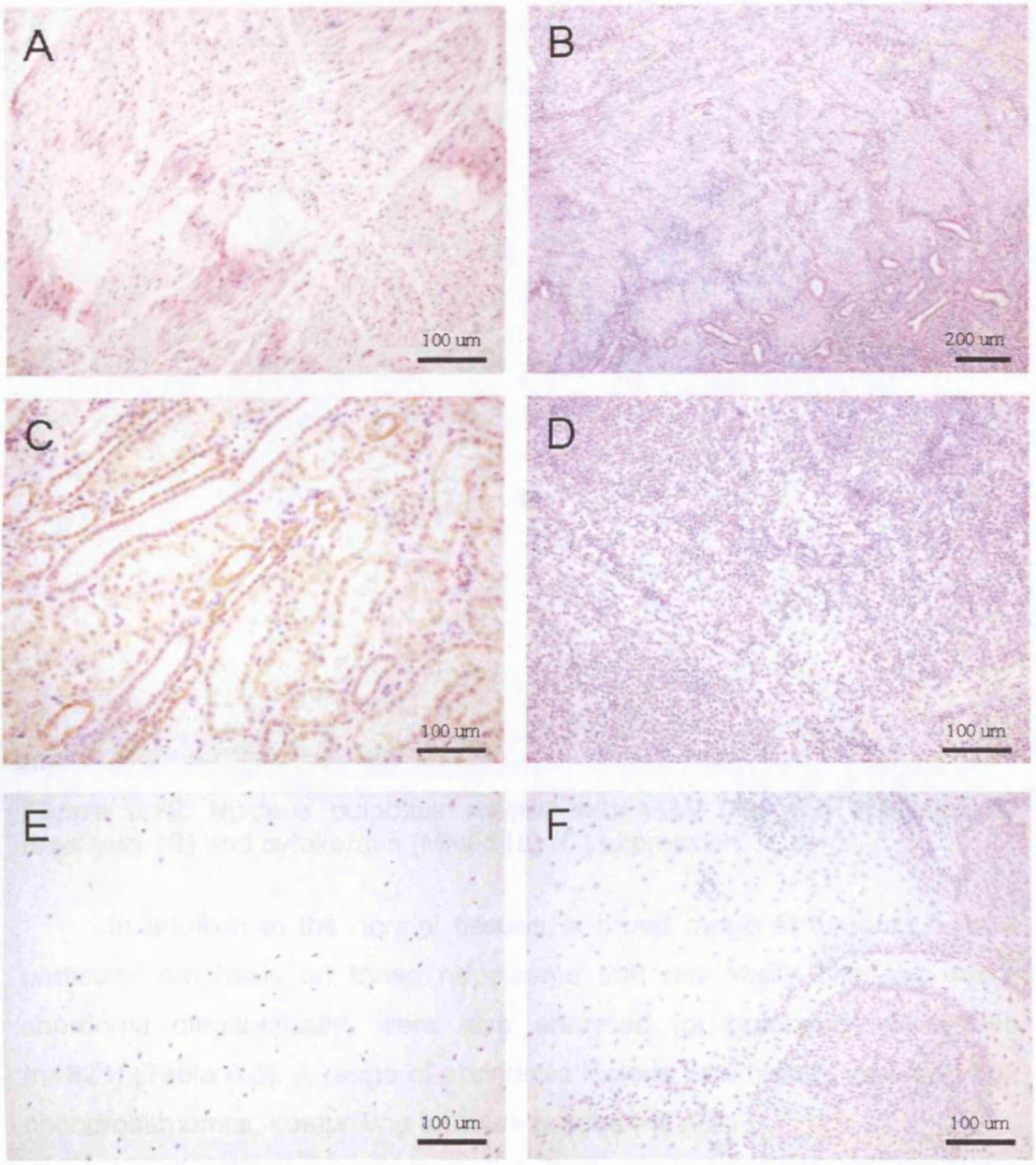

Figure 6.11: A selection of normal tissue sections, analysed for the expression of brachyury: nerve (A), endometrium (B), kidney (C), lymph node (D), cartilage (E), bladder (F). All of these tissues were negative for brachyury expression

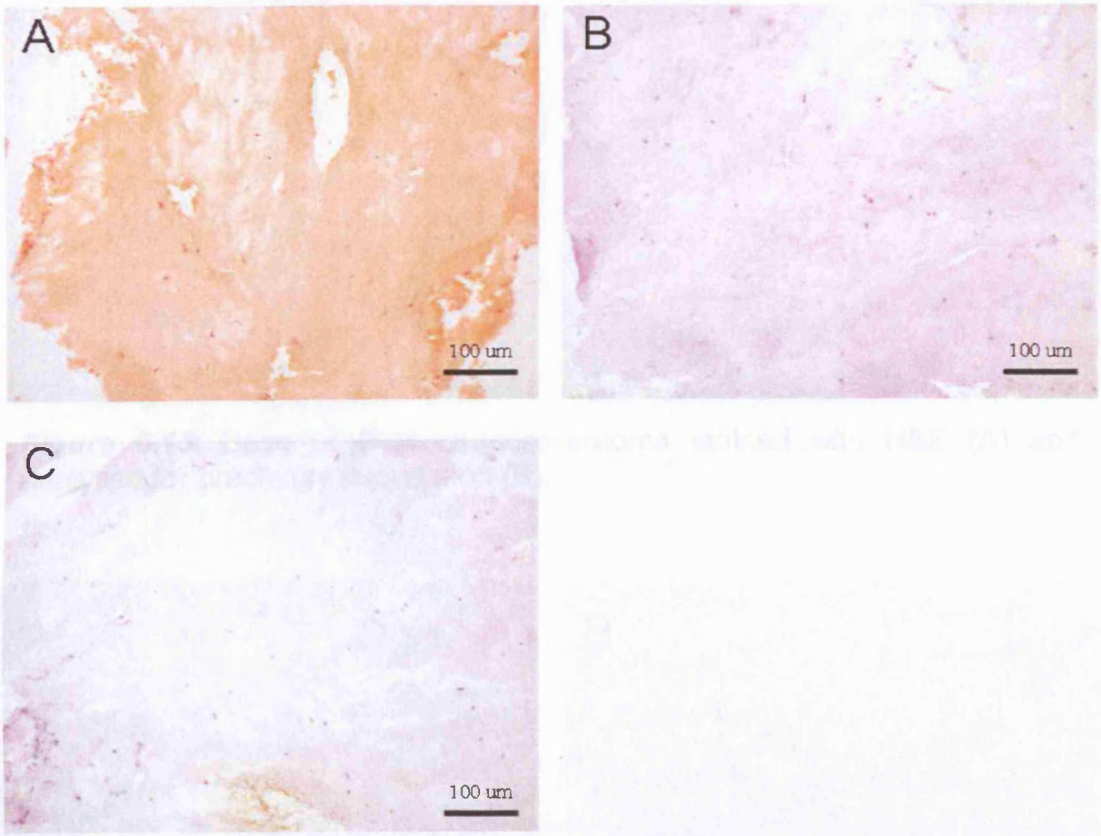

Figure 6.12: Nucleus pulposus stained with H&E (A), and analysed for brachyury (B) and cytokeratin (MNF116) (C) expression.

In addition to the normal tissues, a broad range of tumours, with a particular emphasis on those neoplasms that are easily mistaken for a chordoma diagnostically, were also analysed for brachyury expression (n=323) (Table 6.3). A range of chondroid lesions was tested, including 102 chondrosarcomas, comprising tumours grades I-III (251).

In spite of their morphological similarity to chondroid chordomas, base of skull chondrosarcomas did not express brachyury (Figure 6.13). Sacral chondrosarcomas were also negative for brachyury expression (Figure 6.14). In addition, brachyury expression was absent in clear cell sarcomas, chondromyxoid fibromas and renal carcinomas, which provide a differential diagnosis for epitheliod sacral chordomas (Figure 6.14)

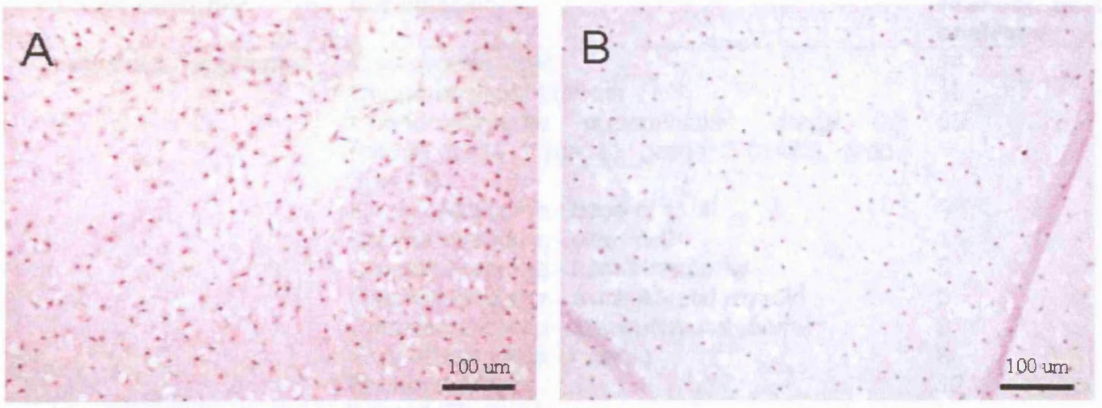

Figure 6.13: Base of skull chondrosarcoma stained with H&E (A) and analysed for brachyury expression (B).

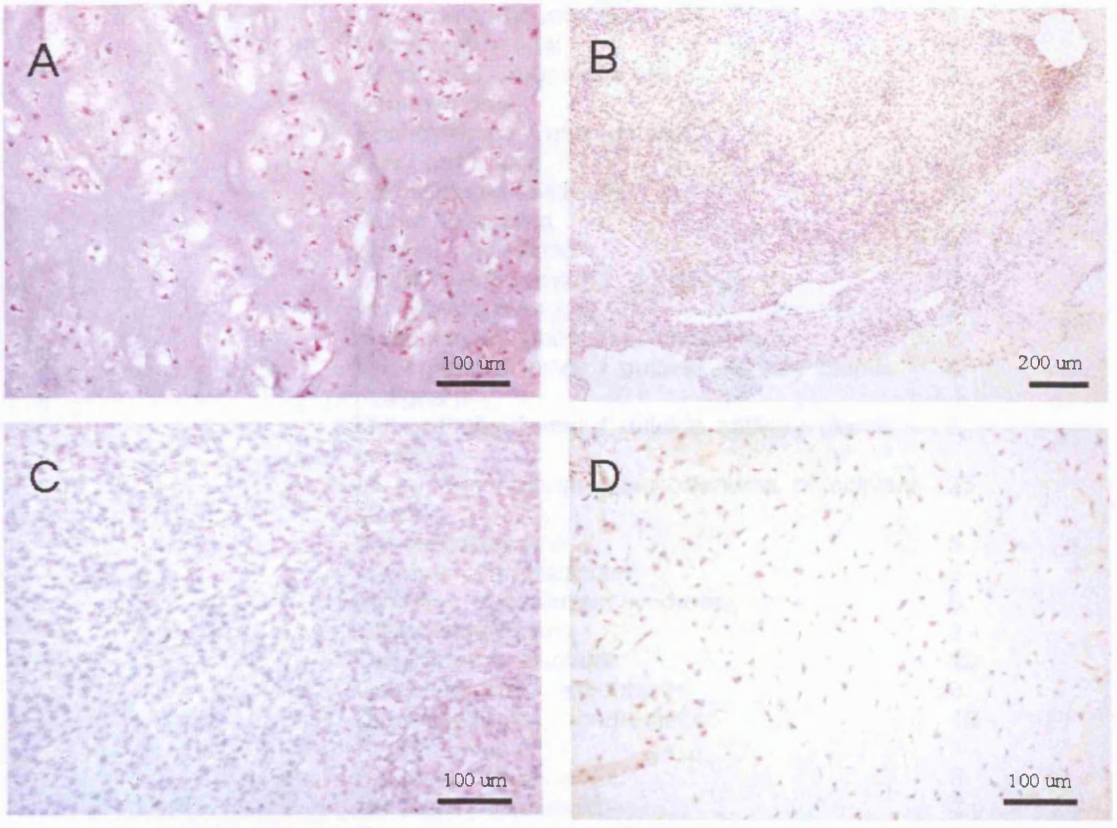

Figure 6.14: A range of neoplasms analysed for brachyury expression: chondrosarcoma (A), renal carcinoma (B), clear cell sarcoma (C), chondromyxoid fibroma (D).

Tumour category	Subcategory	Number of cases analysed
Chondroid neoplasms	Chondroblastoma	14
	Chondromyxoid fibroma	18
	Chondrosarcoma appendicular: grade 0.5 (n=12) grade 1 (n=10), grade 2 (n=22), grade 3(n=11)	55
	Chondrosarcoma - base of skull	9
	Chondrosarcoma - clear cell	11
	Chondrosarcoma - dedifferentiated	5
	Chondrosarcoma - extraskeletal myxoid	5
	Chondrosarcoma - mesenchymal (bone)	9
	Chondrosarcoma - myxoid	8
	Enchondroma	12
	Periosteal chondroma	5
	Synovial chondromatosis	12
	Subtotal	**163**
Other	Adenoma - pituitary	6
	Astrocytoma - gemistocytic	2
	Carcinoma - neuroendocrine	4
	Carcinoma - renal	6
	Carcinoma - squamous cell	2
	Ependymoma	4
	Ependymoma - myxopapillary	4
	Giant cell tumor	2
	Glioblastoma multiforme	5
	Leiomyosarcoma	6
	Lipoma - chondroid	2
	Liposarcoma - myxoid (grade 2)	6
	Malignant melanoma	2
	Mesenchymal phosphaturic neoplasm	2
	Myoepithelial tumor / outside salivary glands - malignant	4
	Myoepithelial tumor / outside salivary glands - benign	7
	Mixed tumor/pleomorphic adenoma of salivary glands	25
	Myxofibrosarcoma	5
	Myxoma - intramuscular	5
	Myxoma – Mazabraud syndrome	5
	Oligodendroglioma	2
	Osteofibrous dysplasia	10
	Osteosarcoma - osteoblastic	3
	Osteosarcoma - chondroblastic	10
	Paraganglioma	1
	Sarcoma - clear cell	8
	Sarcoma - epithelioid	3
	Sarcoma – low-grade fibromyxoid	10
	Sarcoma - Ewing/PNET	6
	Sarcoma - spindle cell	3
	Subtotal	**160**
Total		**323**

(Figure legend on following page)

Table 6.3: Complete list of all non-chordoma cases assessed immunohistochemically for brachyury expression. None of these neoplasms expressed brachyury.

6.5 THE CASE OF AN EXTRA-AXIAL CHORDOMA

A point of particular interest is whether chordomas can occur extra-axially. A recent case of a tumour located in the tibia metaphysis, was diagnosed as a benign osteoid or chondroid lesion in the first instance following magnetic resonance imaging that showed a well-marginated, intracortical lesion with some matrix mineralization (252). A needle core biopsy revealed atypical cells with prominent nuclei embedded in a chondroid matrix and was tested for expression of immunohistochemical markers. While the tumour was found to express S100, which is consistent with a diagnosis of a chondroid neoplasm, it also expressed epitheliod markers including cytokeratins CK19, AE1/3 and MNF116. A diagnosis of a renal tumour was excluded by ultrasound imaging of the kidneys and the absence of renal cell antigen and CD10 expression on the tumour cells (Figure 6.15) (157;252). The tumour was diagnosed as a clear cell chondrosarcoma by the British Bone Tumour panel, in spite of the expression of cytokeratins and the metaphyseal site of this lesion being at odds with such a diagnosis (252).

Following the identification of brachyury as a chordoma marker, the lesion was found to be strongly positive for this transcription factor, indicating the chordoid nature of the tumour (Figure 6.15.F). The diagnosis of an extra-axial chordoma was in keeping with both the appearance and the immunohistochemical profile of the lesion, but could only be made retrospectively following evidence of notochordal differentiation as provided by brachyury expression (252).

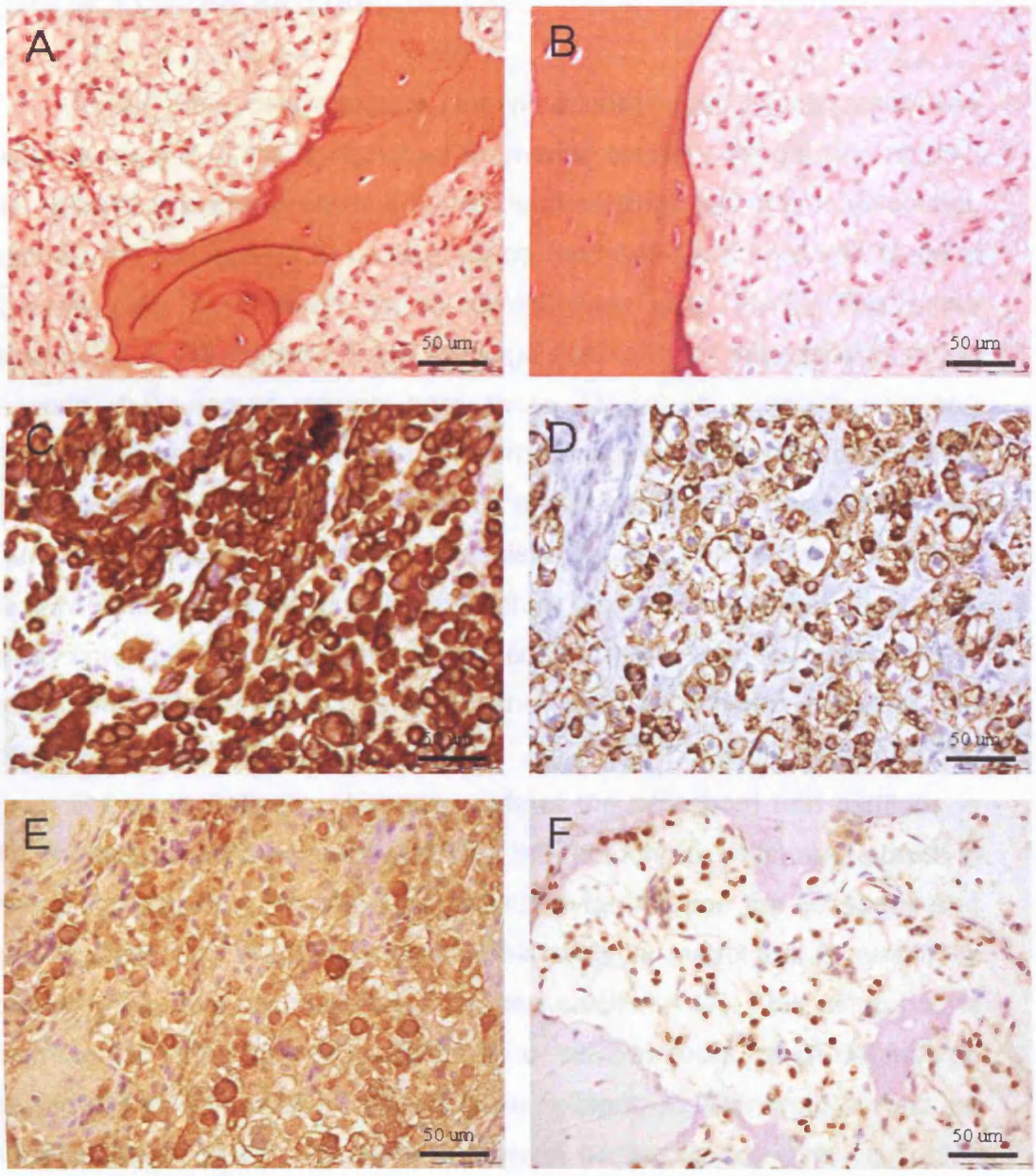

Figure 6.15: An extra-axial chordoma stained with H&E (A,B) and analysed for cytokeratin MNF116 (C) and CK19 (D), S100 (E), brachyury expression (F). Brachyury was expressed by most of the tumour cells that also showed expression of cytokeratins.

6.6 CONCLUSIONS AND DISCUSSION

As an embryonic structure, the notochord most closely resembles cartilage, as it is a tissue designed to provide tensile strength and rigidity. The notochord also expresses a multitude of cartilaginous matrix molecules, such as the collagens and proteoglycans, and can be considered to be a primitive form of cartilage at an evolutionary level (147). This close relationship of the notochord and cartilage accounts for the similarity noted between the tumours arising from these structures - chordomas and cartilaginous neoplasms. In the microarray analysis performed, chordomas closely resembled chondroid neoplasms and in particular chondrosarcomas, a tumour for which chordomas can be mistaken. The shared genes between these two tumours that distinguish them from other mesenchymal neoplasms mostly comprise of genes with a known chondrogenic role, especially matrix genes, the expression of which is known to be shared between the notochord and cartilage (147).

The main distinction between cells of the notochord and cartilage is that the matrix proteins produced by the notochord cells are stored in intracellular vacuoles, whereas the chondrocytes extrude the collagens and proteoglycans they produce to form an extracellular matrix that is eventually used as a scaffold for bone formation and calcifies(147). This difference is also reflected in the transcriptional profile of the 2 tumours, as chordomas do not express the hypertrophic marker gene collagen X. Chondroid lesions, on the other hand, do not express a number of genes: cytokeratins - a finding that has been confirmed immuno-histochemically (253), periplakin - a protein known to interact with cytokeratins (246), CD24 - another gene which has recently been found to be present in chordomas (254) and brachyury.

However, while chordomas share cytokeratin expression with epitheliod tumours, such as synovial sarcomas, the expression of brachyury was exclusive to the chordomas. The specificity of brachyury expression to chordomas was confirmed by RT-PCR analysis. Immunohistochemistry

showed that brachyury expression was present in the 53 chordoma cases tested but not in a wide range of normal tissues or 323 other neoplasms including a range of chondroid tumours and other lesions that could be included in a differential diagnosis. Chordomas with a range of morphologies were analysed including tumours with marked epitheliod and pleomorphic features and a large number of chordomas with extensive areas of chondroid differentiation. Chordomas located at both ends of the spine (sacral and clival regions) were also tested. Brachyury expression was found in the nuclei of the majority of cells in the tumour regions, and a needle core biopsy was sufficient to identify brachyury expression. In chordomas, brachyury expression co-localized with cytokeratin expression and in some, but not all, cases with the expression of S100. Brachyury was also found to be expressed in metastatic chordomas but not in the dedifferentiated component of chordomas in the areas in which cytokeratin expression and the chordoid morphology were lost.

All chordomas were found to express cytokeratins throughout the lesion, with the exception of the dedifferentiated areas mentioned above. S100 expression, however, was not found to be so prevalent. Although the S100 antigen is normally thought of as one of the chordoma markers, we only found it to be expressed in about 50% of the chordoma cases studied (Table 6.2). Expression of S100 was common in chondroid chordomas and chordomas with focal areas of chondroid differentiation, but was not very prevalent in classical chordomas located in the sacrum. On closer review these figures are similar to those presented in the literature but are overall somewhat lower than the percentages previously published. In other studies, S100 was found to be expressed in between 64% and 95% of the cases. However these studies included small sample numbers and did not present the variety of chordoma phenotypes tested here (159;255-257). Walker *et al* specifically looked at S100 expression in chondroid chordomas and found it expressed in all the tumours tested, which is in agreement with the findings presented here (258). As chondroid lesions generally express S100, the

upregulation of this molecule in chondroid areas of chordomas in particular is not surprising. The finding that S100 is expressed in a little over half of chordomas shows that its use in diagnostics is limited.

Brachyury is a useful and reliable marker of chordomas, and is capable of distinguishing this tumour from both chondroid neoplasms and carcinomas. The clinical implications of correctly identifying a chordoma are important as the treatment for chordomas and chondrosarcomas differs. Chordomas have a very poor prognosis, with most patients not expected to live longer than 24 months if untreated. Hence patients often undergo extensive surgical resection of the tumour, followed by radiotherapy (244). Skull-base chondrosarcomas, on the other hand, have considerably better survival rates and much slower tumour progression and the recommended treatment is less radical (259)

With the exception of the embryonic notochord, brachyury was not found to be expressed in a wide range of normal tissues including the nucleus pulposus, a structure proposed to derive from the notochord. The nucleus pulposus is a cartilaginous structure found in the centre of the vertebrae and it is unclear whether it is formed by the notochord undergoing a transformation to the cartilaginous phenotype or by the apoptosis of notochordal cells that are then replaced by cartilage. As the nucleus pulposus lacks both cytokeratin and brachyury expression, there is little molecular evidence of a direct link between the cells of the notochord and those of the nucleus pulposus. However, a recent report found CD24 to be present in the nucleus pulposus and in chordomas, but the notochord was not tested for expression (254). It therefore remains a possibility that the notochord, upon its transformation to a cartilaginous phenotype in the nucleus pulposus, loses cytokeratin and brachyury expression.

While the value of a single marker gene is usually limited, brachyury has so far proved to be an excellent biomarker for chordomas, distinguishing these from all other neoplasms so far tested. Brachyury expression by chordomas is also further evidence of chordomas having a notochordal

differentiation, alongside the morphological and immunophenotypical evidence reported previously. Recently, a potential benign precursor tumour – named the intraosseous benign notochordal cell tumour, was found by Yamaguchi *et al* at a surprisingly high incidence (150;151;260). It would be of particular interest to know whether these benign lesions express brachyury, as it would provide further evidence of their position as a link between persistent notochordal remnants and chordomas.

Finally, a case of an unusual tibial neoplasm with some morphological features of a chordoma was investigated for brachyury expression. Prior to brachyury immunohistochemistry, this tumour was considered likely to represent a clear cell chondrosarcoma in spite of its cytokeratin expression being at odds with such a diagnosis. In addition, the tumour was located in the metaphysis of the tibia, a region where clear cell chondrosarcomas are very rarely found, as most of them present in the epiphysis of bones. Without the IHC showing brachyury expression, the diagnosis of an extra-axial chordoma was not considered due to the rarity of this lesion. When the tumour was found to express brachyury, it was classified as an extra-axial chordoma, emphasizing the value of this assay. The diagnosis of an extra-axial chordoma is in keeping with the morphology and immunophenotype of this neoplasm. It seems more likely that this tumour represents notochordal differentiation of a progenitor cell, rather than that an ectopic notochordal remnant was present in the tibia.

7. CONCLUSIONS AND DISCUSSION

7.1 MSC CHONDROGENESIS

This study was started with the aim of setting up a *in vitro* model system for chondrogenic differentiation of MSC and analysing it through the use of GEM technology. Such an *in vitro* system has two primary uses: the first is as a representation of *in vivo* chondrogenic development and disease and the second as a potential method for obtaining cartilage for therapeutic purposes.

Upon isolation and differentiation of MSC with the use of previously published protocols, a variability in the MSC proliferative and differentiation potential was noted. There was also a correlation between the rate of proliferation and the extent of chondrogenic differentiation an MSC line could undergo. This variability is an important factor to take into account when considering the use of MSC for therapeutic purposes, as some patients may benefit more from autologous transplants than others. There may also be room for further improvements to the culture conditions used for both MSC expansion and differentiation, such as the use of combinations of growth factors or varying the oxygen concentration that the MSC are grown under.

Cartilage is an avascular tissue, with oxygen levels as low as 1% in certain regions (114). Culturing human MSC at 3% oxygen rather than the 21% ordinarily used in tissue culture augments chondrogenesis, stimulating matrix production. HIF1α, the main transcription factor associated with hypoxic conditions, is an essential factor in chondrogenesis, promoting the transcription of ECM molecules such as collagen 2 (116). The results presented here are the first to show an impact of lower oxygen on human MSC differentiation to chondrocytes.

For therapeutic regeneration of cartilage both MSC isolated from the bone marrow and chondrocytes isolated from knee cartilage (NHAC) have

been used, and a comparison of the chondrogenic potential between these two cell types is presented here. When grown in monolayer culture the NHAC lose the phenotypic characteristics of cartilage, reverting to a more spindle-shaped appearance and losing expression of matrix molecules. The NHAC can be induced to undergo chondrogenesis with the same stimuli as MSC, but the pellets generated are larger, comprising more ECM. The NHAC are unipotent and can not be induced to differentiate into adipocytes or osteocytes with the established MSC conditions. This may indicate that NHAC are better suited for use in cartilage regeneration as they produce more chondrogenic matrix and only differentiate down a chondrogenic lineage, however, the proliferative potential of NHAC is much more limited than that of the MSC.

A comparison of the GEM profiles of the MSC and the NHAC both in their undifferentiated state and after they have undergone chondrogenesis was performed. The main differences noted in the expression profiles of the undifferentiated cells were in the cell surface proteins expressed, but MSC also expressed genes involved in organ development not expressed by the NHAC. The differentiated 14D cells mostly differed in the matrix molecules they expressed, with the MSC expressing hypertrophic matrix proteins not expressed by the NHAC. This reflected histological observations of the two cell types, as the NHAC did not show the enlarged cell morphology typical of hypertrophic cells, as seen with differentiated MSC. Therefore, the same growth conditions produce slightly different outcomes in the NHAC and the MSC.

In order to obtain a global overview of the process of MSC chondrogenesis, GEM experiments were performed where the transcriptional profile of MSC at different points during chondrogenic differentiation was examined, with a particular emphasis on the early events, prior to the synthesis of the chondrogenic matrix. During *in vitro* MSC culture, it was observed that most matrix proteins are not transcribed until day 6 or 7 of chondrogenic culture, concomitant with the pellets beginning to

increase in size. This first week of development is therefore of particular interest as it involves the transcriptional changes that lead to matrix production.

Through GEM analysis, three phases of chondrogenesis were identified. The early phase, occurring within a few hours of placing the cells under chondrogenic growth conditions, primarily involves changes in mRNA levels of transcription factors and genes involved in signalling pathways. Many of the transcription factors also have known roles in development. The upregulated transcription factors comprise both genes known to have a role in chondrogenesis such as DEC1 or Dlx5 and genes not previously implicated in chondrogenesis. The downregulated genes include many factors known to play a part in the differentiation towards other lineages, such as neuronal, adipogenic or myogenic. The second phase includes changes in the levels of transcripts associated with glycolysis and motility. As chondrocytes are located in a hypoxic environment, they have few mitochondria and mostly rely on glycolysis for ATP production (192). In addition, during this second phase, the cells cease to proliferate and downregulate all cell cycle genes. The final phase of chondrogenesis includes all the transcriptional changes geared towards extracellular matrix production. Most of the significantly changing genes have confirmed roles in chondrogenesis.

Therefore the chondrogenesis of MSC progresses from changes in transcription factors expressed by the MSC, to changes in gene levels involved in the metabolism and finally to the transcription of those genes that make the cartilage phenotype. The early changes in the levels of transcription factors are particularly interesting as they presumably orchestrate subsequent events, and it is these early transcription factors that least is known about. HES1 and HEY1 are two such factors, not previously implicated in chondrogenesis.

HES1 and HEY1 are targets of Notch signalling, a pathway involved in many developmental events. Abolishing Notch signalling, and thereby

HES1 and HEY1 transcription, during chondrogenesis *in vitro* impairs matrix production. Furthermore Notch inhibitors reduce the rate of MSC proliferation and induce adipocyte formation during MSC osteogenesis. Hence, Notch signalling is involved in both MSC proliferation and differentiation, and appears to play a role in the choice of lineage towards which MSC differentiate. However, with the use of *in situ* hybridization, HES1 and HEY1 could not be shown to be expressed *in vivo* in developing mouse limbs pointing to a possible difference either between chondrogenic regulation of mouse and human or embryonic and adult cells. As the Notch receptors and ligands have been reported to be expressed by developing embryonic cartilage, the most likely explanation is that Notch signalling may either act through other HES and HEY family members in developing mouse limbs or that the probes used were not sensitive enough to detect the levels of HES1 and HEY1 in mouse limbs in spite of a signal being detected in the neural tissues used as controls.

7.2 BRACHYURY EXPRESSION IN CHORDOMAS

A separate part of the project was based upon a previously published study of GEM profiles of a range of connective tissue neoplasms. This study identified that cartilaginous neoplasms closely resembled chordomas, tumours thought to be derive from notochordal remnants, at a gene expression level. Brachyury, a protein essential for notochordal development and embryonal survival, was found to be uniquely expressed by chordomas of all the neoplasms tested. It was the aim of this project to examine the relationship between the chordomas and cartilaginous neoplasms and to assess the usefulness of brachyury as a potential diagnostic marker for chordomas.

Just like their presumed tissues of origin, the notochord and cartilage, chordomas and chondroid neoplasms both express a range of molecules with known roles in chondrogenesis including matrix proteins (e.g. aggrecan, collagen 2, COMP) and the main transcriptional regulator of chondrogenesis Sox9. The cells of the notochord however, retain the collagens and proteoglycans within their vacuoles whereas the chondrocytes extrude them, producing an extracellular matrix that can be calcified, after the cells have undergone hypertrophy. Therefore, chondroid neoplasms express collagen10, a marker of hypertrophy, whereas chordomas do not. This is consistent with the absence of calcification seen in chordomas. Chordomas on the other hand express cytokeratins, periplakin, DDR1, CD24 and brachyury, not expressed by chondroid neoplasms. Cytokeratin expression has been confirmed immunohistochemically and is used in chordoma diagnosis (261). Periplakin has not previously been associated with chordomas but is a protein known to interact with cytokeratins, in particular cytokeratin 8 that is one of the cytokeratins seen upregulated in chordomas (246). DDR1 acts as a collagen receptor, is regulated by p53 and has been found to be overexpressed in breast carcinoma and osteosarcoma (247;262;263). It may therefore be an interesting candidate for future

investigations. While this work was being completed, Fujita *et al* reported that CD24 expression was present in both chordomas and the nucleus pulposus, confirming the results shown here (254).

The relationship between the notochord and the nucleus pulposus is of interest, as it is unclear whether the notochord cells give rise to the nucleus pulposus during development or if the notochordal cells apoptose and are replaced by the nucleus pulposus. The nucleus pulposus does not express cytokeratins or brachyury, both found in the notochord and chordomas, which argues against it being derived from the notochord. The recent finding of CD24 expression in the nucleus pulposus and chordomas however provides an expressional link and CD24 expression in the notochord should be verified. It is, of course possible that, as the notochordal cells differentiate into the nucleus pulposus, they lose cytokeratins and brachyury expression. Hence the relationship between the notochord and the nucleus pulposus remains unclear.

In the diagnosis of chordomas, cytokeratins and S100 are commonly employed. These markers are however not specific to chordomas as cytokeratins are expressed by carcinomas and S100 expression is seen in cartilaginous neoplasms. Furthermore, the combination of these two markers is not diagnostic as S100 is only expressed by about 50% of chordomas. Brachyury is the first published marker that uniquely identifies chordomas, and was found to be expressed in all the chordoma cases tested. Brachyury was expressed by classical chordomas, chondroid chordomas and metastatic chordomas. Brachyury expression was also detected in the classical component of dedifferentiated chordomas but not in the dedifferentiated area where cytokeratin expression is also lost. This finding indicates that the transformation that the tumour cells undergo as they become 'dedifferentiated' also includes a transcriptional change that results in the chordoma morphology and markers no longer being expressed.

The final case considered is that of an enigmatic neoplasm presenting in the cortex of the tibia. This is an extra-axial lesion found to express

brachyury, with a morphology and immunophenotype consistent with a diagnosis of an extra-axial chordoma. There are 2 possible explanations as to how a tumor showing notochordal differentiation can arise at an extra-axial site. The first is that there may have been notochordal remnants that persisted at the tumour site, which, through mutations acquired a growth advantage and formed a neoplasm. Hence, detecting the expression of brachyury in this neoplasm is consistent with the cell of origin. The second possibility is that an undifferentiated cell within the tibia acquired the ability to differentiate into notochordal tissue. There are reported examples of neoplasms occurring with a morphology different to the surrounding tissue in which the tumour arose, such as bone, cartilage and muscle formation in a malignant peripheral nerve sheath tumour (264). Hence the latter possibility is favoured with respect to the origins of this tumour.

The identification of brachyury as a marker gene for chordomas provides evidence of the notochordal origin of chordomas and has a practical application in diagnostics. These experiments, however, also show the value of microarray data as a starting point for tumour classification and the discovery of novel markers.

7.3 FUTURE WORK

Microarray experiments generate vast amounts of data and the work presented here could give rise to many new projects. An area that could be looked at in more detail is that of the role of hypoxia and its target genes in chondrogenesis. Many transcription factors were found to be upregulated during MSC chondrogenesis that could be investigated further for their role in cartilage development. This could be performed through knockdown with RNA interference or overexpression studies.

Notch signalling involvement in MSC proliferation and differentiation also warrants further investigation. An interesting experiment to perform would be to overexpress NICD, thereby constitutively activating Notch signalling, and investigate how this affects the growth rate and the chondrogenic, adipogenic and osteogenic differentiation of MSC.

In relation to the work on chordomas presented here, the regulation of brachyury expression would be of interest for future investigation, as it could be implicated in the mechanism of chordoma tumorogenesis. This question is particularly intriguing in the extra-axial neoplasms showing notochordal differentiation as it is likely that a mutation occurs upstream of brachyury, inducing brachyury expression and thereby changing the phenotype of the cell to a chordoid one.

Finally, another appealing project to undertake with this work would be the comparison between the microarray results for the MSC undergoing chondrogenesis and the chondroid tumours. Recent evidence points to tumours originating from a 'stem cell'-like cell and it would be exciting to see if the microarray data presented here would support such a hypothesis (265). For this purpose statistical analysis could be performed to check which genes, if any, are commonly expressed by the undifferentiated MSC and the neoplasms, not shared by the fully differentiated MSC.

8. APPENDIX

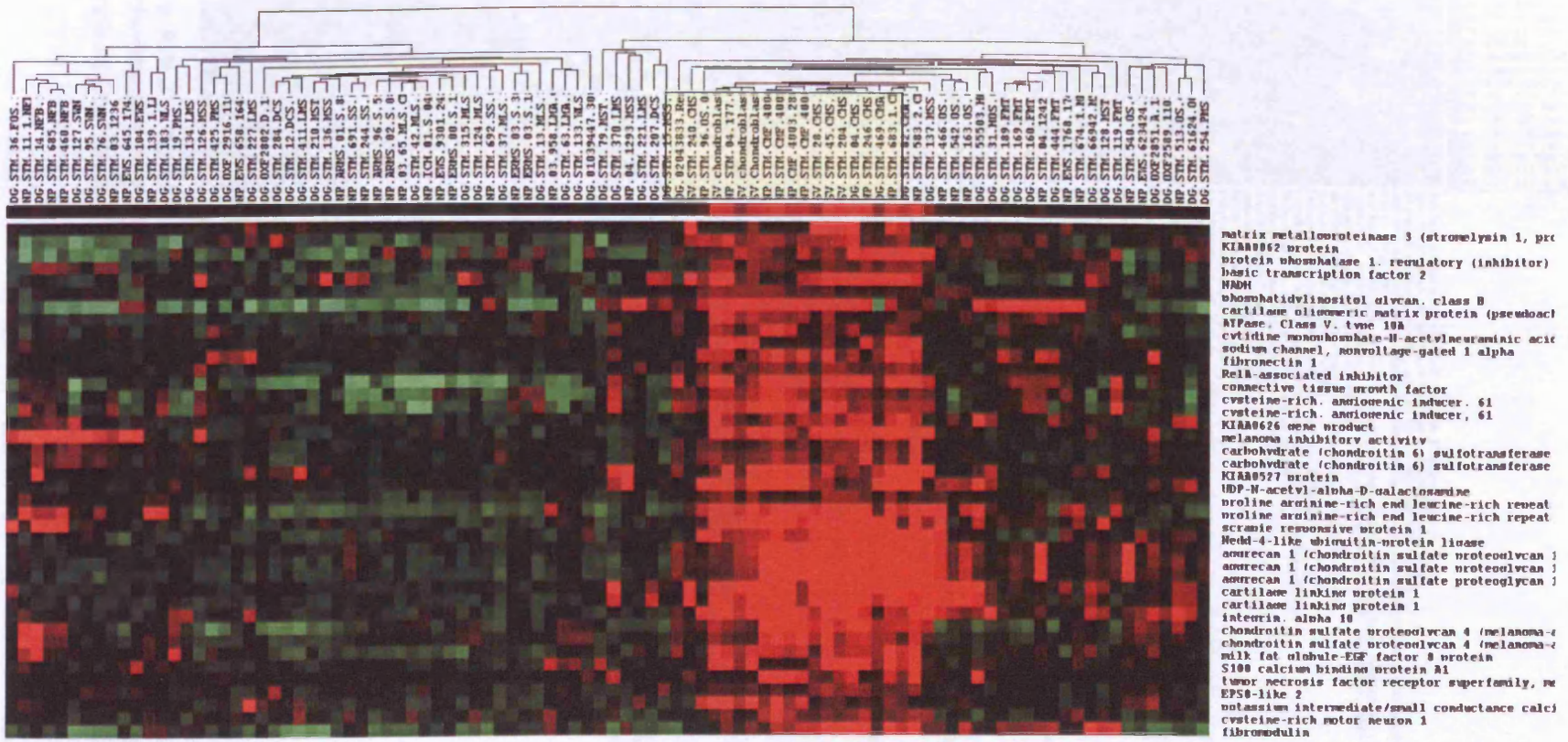

Figure A.6.1: The top 40 probe sets distinguishing between chordomas/chondroid lesions (highlighted in yellow) and other neoplasms This heatmap shows high levels of expression as red, values close to the mean as black and low levels as green.

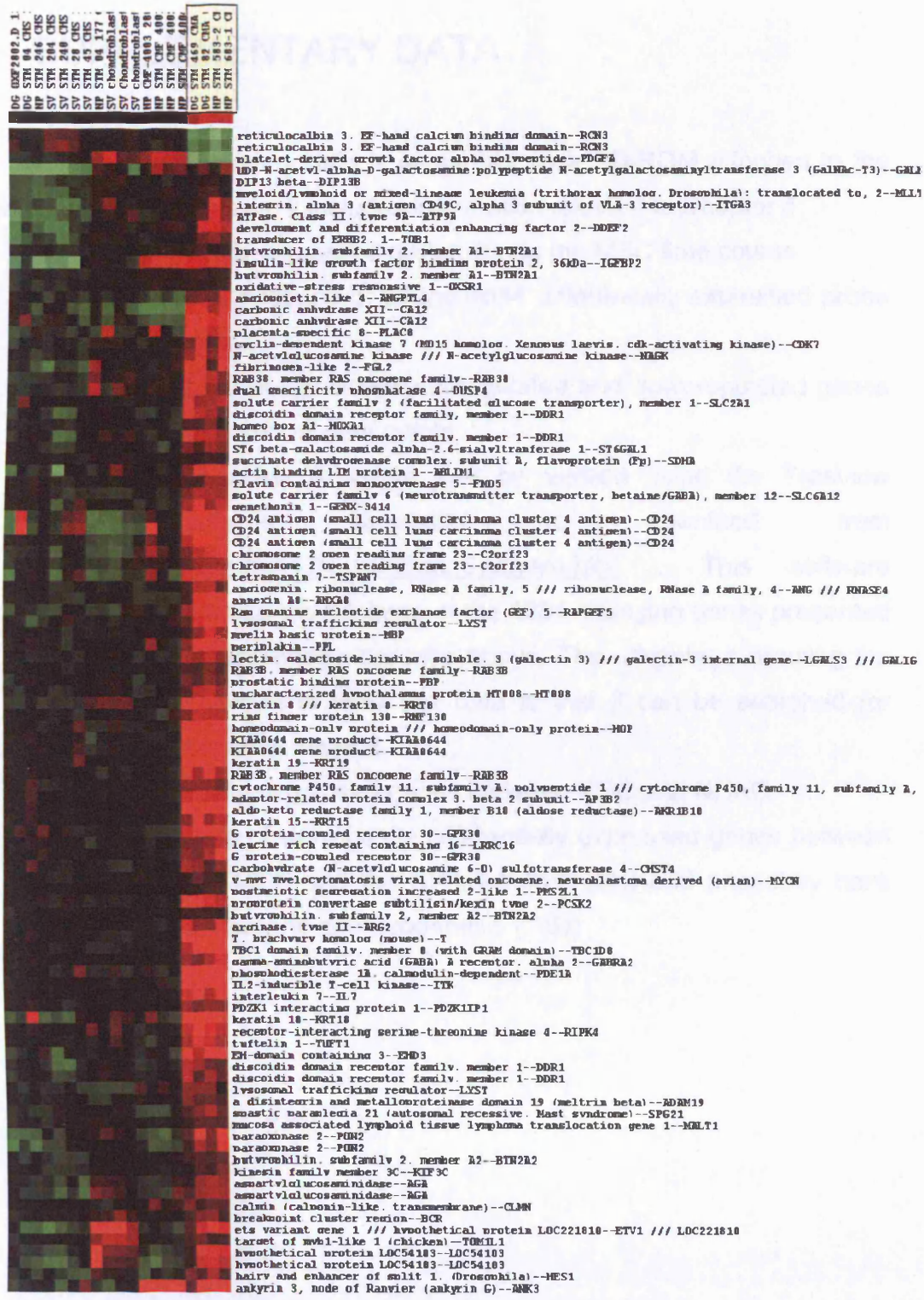

Figure A.6.2: Top 100 probe sets distinguishing between chondroid lesions and chordomas (highlighted in yellow). In this heatmap high levels of gene expression are shown as red, values close to the mean are shown as black and low levels as green.

9. SUPPLEMENTARY DATA

The supplementary data is presented on a CD-ROM attached to the back cover of this thesis. It includes information relevant to Chapter 4:

- Differentially expressed genes during the MSC time course
    - Full heatmap of all the 1394 differentially expressed probe sets
    - Lists of significantly upregulated and downregulated genes between all time points
    - Treeview files that can be viewed using the Treeview software available to download from http://rana.lbl.gov/EisenSoftware.htm . This software creates the heatmap of the 1394 changing genes presented as .jpg image describe above. The advantage of using the software to view this data is that it can be searched for genes of interest.
- Differentially expressed genes between MSC and NHAC
    - Lists of significantly differentially expressed genes between the MSC and the NHAC before (0H) and after they have undergone chondrogenesis (14D)

Reference List

(1) Urist MR, MClean F.C. Osteogenetic potency and new-bone formation by induction in transplants to the anterior chamber of the eye. J Bone Joint Surg Am 1952; 34(2):443-76.

(2) Tavassoli M, Crosby WH. Transplantation of marrow to extramedullary sites. Science 1968; 161(836):54-6.

(3) Friedenstein AJ. Precursor cells of mechanocytes. Int Rev Cytol 1976; 47:327-59.

(4) Piersma AH, Brockbank KG, Ploemacher RE, van Vliet E, Brakel-van Peer KM, Visser PJ. Characterization of fibroblastic stromal cells from murine bone marrow. Exp Hematol 1985; 13(4):237-43.

(5) Castro-Malaspina H, Gay RE, Resnick G, Kapoor N, Meyers P, Chiarieri D et al. Characterization of human bone marrow fibroblast colony-forming cells (CFU-F) and their progeny. Blood 1980; 56(2):289-301.

(6) Baksh D, Song L, Tuan RS. Adult mesenchymal stem cells: characterization, differentiation, and application in cell and gene therapy. J Cell Mol Med 2004; 8(3):301-16.

(7) Gregory CA, Prockop DJ, Spees JL. Non-hematopoietic bone marrow stem cells: molecular control of expansion and differentiation. Exp Cell Res 2005; 306(2):330-5.

(8) Koc ON, Gerson SL, Cooper BW, Dyhouse SM, Haynesworth SE, Caplan AI et al. Rapid hematopoietic recovery after coinfusion of autologous-blood stem cells and culture-expanded marrow mesenchymal stem cells in advanced breast cancer patients receiving high-dose chemotherapy. J Clin Oncol 2000; 18(2):307-16.

(9) Lazarus HM, Haynesworth SE, Gerson SL, Rosenthal NS, Caplan AI. Ex vivo expansion and subsequent infusion of human bone marrow-derived stromal progenitor cells (mesenchymal progenitor cells): implications for therapeutic use. Bone Marrow Transplant 1995; 16(4):557-64.

(10) Conget PA, Minguell JJ. Phenotypical and functional properties of human bone marrow mesenchymal progenitor cells. J Cell Physiol 1999; 181(1):67-73.

(11) Pittenger MF, Mackay AM, Beck SC, Jaiswal RK, Douglas R, Mosca JD et al. Multilineage potential of adult human mesenchymal stem cells. Science 1999; 284(5411):143-7.

(12) Lee RH, Kim B, Choi I, Kim H, Choi HS, Suh K et al. Characterization and expression analysis of mesenchymal stem cells from human bone marrow and adipose tissue. Cell Physiol Biochem 2004; 14(4-6):311-24.

(13) Majumdar MK, Keane-Moore M, Buyaner D, Hardy WB, Moorman MA, McIntosh KR et al. Characterization and functionality of cell surface molecules on human mesenchymal stem cells. J Biomed Sci 2003; 10(2):228-41.

(14) Chichester CO, Fernandez M, Minguell JJ. Extracellular matrix gene expression by human bone marrow stroma and by marrow fibroblasts. Cell Adhes Commun 1993; 1(2):93-9.

(15) Simmons PJ, Torok-Storb B. Identification of stromal cell precursors in human bone marrow by a novel monoclonal antibody, STRO-1. Blood 1991; 78(1):55-62.

(16) Wagner W, Feldmann RE, Jr., Seckinger A, Maurer MH, Wein F, Blake J et al. The heterogeneity of human mesenchymal stem cell preparations--evidence from simultaneous analysis of proteomes and transcriptomes. Exp Hematol 2006; 34(4):536-48.

(17) Blondheim NR, Levy YS, Ben Zur T, Burshtein A, Cherlow T, Kan I et al. Human mesenchymal stem cells express neural genes, suggesting a neural predisposition. Stem Cells Dev 2006; 15(2):141-64.

(18) Pittenger MF, Marshak DR. Mesenchymal Stem Cells of Human Adult Bone Marrow. In: Marshak DR, Gardner RL, Gottlieb D, editors. Stem Cell Biology. Cold Spring Harbour Laboratory Press; 2001. 349-73.

(19) Kuznetsov S, Gehron RP. Species differences in growth requirements for bone marrow stromal fibroblast colony formation In vitro. Calcif Tissue Int 1996; 59(4):265-70.

(20) Conget PA, Allers C, Minguell JJ. Identification of a discrete population of human bone marrow-derived mesenchymal cells exhibiting properties of uncommitted progenitors. J Hematother Stem Cell Res 2001; 10(6):749-58.

(21) Phinney DG, Kopen G, Righter W, Webster S, Tremain N, Prockop DJ. Donor variation in the growth properties and osteogenic potential of human marrow stromal cells. J Cell Biochem 1999; 75(3):424-36.

(22) Bruder SP, Jaiswal N, Haynesworth SE. Growth kinetics, self-renewal, and the osteogenic potential of purified human mesenchymal stem cells during extensive subcultivation and following cryopreservation. J Cell Biochem 1997; 64(2):278-94.

(23) Mareschi K, Ferrero I, Rustichelli D, Aschero S, Gammaitoni L, Aglietta M et al. Expansion of mesenchymal stem cells isolated from pediatric and adult donor bone marrow. J Cell Biochem 2006; 97(4):744-54.

(24) Simonsen JL, Rosada C, Serakinci N, Justesen J, Stenderup K, Rattan SI et al. Telomerase expression extends the proliferative life-span and maintains the osteogenic potential of human bone marrow stromal cells. Nat Biotechnol 2002; 20(6):592-6.

(25) Shi S, Gronthos S, Chen S, Reddi A, Counter CM, Robey PG et al. Bone formation by human postnatal bone marrow stromal stem cells is enhanced by telomerase expression. Nat Biotechnol 2002; 20(6):587-91.

(26) Okamoto T, Aoyama T, Nakayama T, Nakamata T, Hosaka T, Nishijo K et al. Clonal heterogeneity in differentiation potential of immortalized human mesenchymal stem cells. Biochem Biophys Res Commun 2002; 295(2):354-61.

(27) Tsutsumi S, Shimazu A, Miyazaki K, Pan H, Koike C, Yoshida E et al. Retention of multilineage differentiation potential of mesenchymal cells during proliferation in response to FGF. Biochem Biophys Res Commun 2001; 288(2):413-9.

(28) Grigoriadis AE, Heersche JN, Aubin JE. Differentiation of muscle, fat, cartilage, and bone from progenitor cells present in a bone-derived clonal cell population: effect of dexamethasone. J Cell Biol 1988; 106(6):2139-51.

(29) Prockop DJ. Marrow stromal cells as stem cells for nonhematopoietic tissues. Science 1997; 276(5309):71-4.

(30) Wakitani S, Saito T, Caplan AI. Myogenic cells derived from rat bone marrow mesenchymal stem cells exposed to 5-azacytidine. Muscle Nerve 1995; 18(12):1417-26.

(31) Ferrari G, Cusella-De Angelis G, Coletta M, Paolucci E, Stornaiuolo A, Cossu G et al. Muscle regeneration by bone marrow-derived myogenic progenitors. Science 1998; 279(5356):1528-30.

(32) Toma C, Pittenger MF, Cahill KS, Byrne BJ, Kessler PD. Human mesenchymal stem cells differentiate to a cardiomyocyte phenotype in the adult murine heart. Circulation 2002; 105(1):93-8.

(33) Grinnemo KH, Mansson-Broberg A, Leblanc K, Corbascio M, Wardell E, Siddiqui AJ et al. Human mesenchymal stem cells do not differentiate into cardiomyocytes in a cardiac ischemic xenomodel. Ann Med 2006; 38(2):144-53.

(34) Kopen GC, Prockop DJ, Phinney DG. Marrow stromal cells migrate throughout forebrain and cerebellum, and they differentiate into astrocytes after injection into neonatal mouse brains. Proc Natl Acad Sci U S A 1999; 96(19):10711-6.

(35) Sanchez-Ramos J, Song S, Cardozo-Pelaez F, Hazzi C, Stedeford T, Willing A et al. Adult Bone Marrow Stromal Cells Differentiate into Neural Cells in Vitro. Experimental Neurology 2000; 164(2):247-56.

(36) Zhao LX, Zhang J, Cao F, Meng L, Wang DM, Li YH et al. Modification of the brain-derived neurotrophic factor gene: a portal to transform mesenchymal stem cells into advantageous engineering cells for neuroregeneration and neuroprotection. Experimental Neurology 2004; 190(2):396-406.

(37) Sato Y, Araki H, Kato J, Nakamura K, Kawano Y, Kobune M et al. Human mesenchymal stem cells xenografted directly to rat liver are differentiated into human hepatocytes without fusion. Blood 2005; 106(2):756-63.

(38) Ong SY, Dai H, Leong KW. Inducing hepatic differentiation of human mesenchymal stem cells in pellet culture. Biomaterials 2006; 27(22):4087-97.

(39) Wagers AJ, Weissman IL. Plasticity of adult stem cells. Cell 2004; 116(5):639-48.

(40) Ogawa R, Mizuno H, Watanabe A, Migita M, Shimada T, Hyakusoku H. Osteogenic and chondrogenic differentiation by adipose-derived stem cells harvested from GFP transgenic mice. Biochem Biophys Res Commun 2004; 313(4):871-7.

(41) Zuk PA, Zhu M, Mizuno H, Huang J, Futrell JW, Katz AJ et al. Multilineage cells from human adipose tissue: implications for cell-based therapies. Tissue Eng 2001; 7(2):211-28.

(42) Sottile V, Halleux C, Bassilana F, Keller H, Seuwen K. Stem cell characteristics of human trabecular bone-derived cells. Bone 2002; 30(5):699-704.

(43) De Bari C, Dell'Accio F, Vanlauwe J, Eyckmans J, Khan IM, Archer CW et al. Mesenchymal multipotency of adult human periosteal cells demonstrated by single-cell lineage analysis. Arthritis Rheum 2006; 54(4):1209-21.

(44) Salingcarnboriboon R, Yoshitake H, Tsuji K, Obinata M, Amagasa T, Nifuji A et al. Establishment of tendon-derived cell lines exhibiting pluripotent mesenchymal stem cell-like property. Exp Cell Res 2003; 287(2):289-300.

(45) Seo BM, Miura M, Gronthos S, Bartold PM, Batouli S, Brahim J et al. Investigation of multipotent postnatal stem cells from human periodontal ligament. Lancet 2004; 364(9429):149-55.

(46) De Bari C, Dell'Accio F, Tylzanowski P, Luyten FP. Multipotent mesenchymal stem cells from adult human synovial membrane. Arthritis Rheum 2001; 44(8):1928-42.

(47) Sabatini F, Petecchia L, Tavian M, Jodon dV, V, Rossi GA, Brouty-Boye D. Human bronchial fibroblasts exhibit a mesenchymal stem cell phenotype and multilineage differentiating potentialities. Lab Invest 2005; 85(8):962-71.

(48) De Coppi P, Pozzobon M, Piccoli M, Vittoria GM, Boldrin L, Slanzi E et al. Isolation of Mesenchymal Stem Cells From Human Vermiform Appendix. J Surg Res 2006; 135(1):85-91.

(49) Meirelles LD, Chagastelles PC, Nardi NB. Mesenchymal stem cells reside in virtually all post-natal organs and tissues. J Cell Sci 2006; 119:2204-13.

(50) Wexler SA, Donaldson C, Denning-Kendall P, Rice C, Bradley B, Hows JM. Adult bone marrow is a rich source of human mesenchymal 'stem' cells but umbilical cord and mobilized adult blood are not. Br J Haematol 2003; 121(2):368-74.

(51) Zvaifler NJ, Marinova-Mutafchieva L, Adams G, Edwards CJ, Moss J, Burger JA et al. Mesenchymal precursor cells in the blood of normal individuals. Arthritis Res 2000; 2(6):477-88.

(52) Mansilla E, Marin GH, Drago H, Sturla F, Salas E, Gardiner C et al. Bloodstream Cells Phenotypically Identical to Human Mesenchymal Bone Marrow Stem Cells Circulate in Large Amounts Under the Influence of Acute Large Skin Damage: New Evidence for Their Use in Regenerative Medicine. Transplant Proc 2006; 38(3):967-9.

(53) Muraglia A, Cancedda R, Quarto R. Clonal mesenchymal progenitors from human bone marrow differentiate in vitro according to a hierarchical model. J Cell Sci 2000; 113(7):1161-6.

(54) Colter DC, Sekiya I, Prockop DJ. Identification of a subpopulation of rapidly self-renewing and multipotential adult stem cells in colonies of human marrow stromal cells. Proc Natl Acad Sci U S A 2001; 98(14):7841-5.

(55) Pochampally RR, Smith JR, Ylostalo J, Prockop DJ. Serum deprivation of human marrow stromal cells (hMSCs) selects for a subpopulation of early progenitor cells with enhanced expression of OCT-4 and other embryonic genes. Blood 2004; 103(5):1647-52.

(56) D'Ippolito G, Diabira S, Howard GA, Menei P, Roos BA, Schiller PC. Marrow-isolated adult multilineage inducible (MIAMI) cells, a unique population of postnatal

young and old human cells with extensive expansion and differentiation potential. J Cell Sci 2004; 117(14):2971-81.

(57) Reyes M, Lund T, Lenvik T, Aguiar D, Koodie L, Verfaillie CM. Purification and ex vivo expansion of postnatal human marrow mesodermal progenitor cells. Blood 2001; 98(9):2615-25.

(58) Jiang Y, Jahagirdar BN, Reinhardt RL, Schwartz RE, Keene CD, Ortiz-Gonzalez XR et al. Pluripotency of mesenchymal stem cells derived from adult marrow. Nature 2002; 418(6893):41-9.

(59) Schwartz RE, Reyes M, Koodie L, Jiang Y, Blackstad M, Lund T et al. Multipotent adult progenitor cells from bone marrow differentiate into functional hepatocyte-like cells. J Clin Invest 2002; 109(10):1291-302.

(60) Mooney EK. Lower Limb Embryology. 2002 http://www.emedicine.com/plastic/topic215.htm

(61) DeLise AM, Fischer L, Tuan RS. Cellular interactions and signaling in cartilage development. Osteoarthritis Cartilage 2000; 8(5):309-34.

(62) Hall B, Newman S. Cartilage: molecular aspects. 1 ed. CRC Press, Inc; US; 1991.

(63) Bullough PG. Normal bone structure and development. Orthopaedic Pathology. 4 ed. Philadelphia: Mosby; 2004. 1-39.

(64) Hall BK, Miyake T. Craniofacial development of avian and rodent embryos. Methods Mol Biol 2000; 135:127-37.

(65) Niswander L, Tickle C, Vogel A, Booth I, Martin GR. FGF-4 replaces the apical ectodermal ridge and directs outgrowth and patterning of the limb. Cell 1993; 75(3):579-87.

(66) Sun X, Mariani FV, Martin GR. Functions of FGF signalling from the apical ectodermal ridge in limb development. Nature 2002; 418(6897):501-8.

(67) Barna M, Pandolfi PP, Niswander L. Gli3 and Plzf cooperate in proximal limb patterning at early stages of limb development. Nature 2005; 436(7048):277-81.

(68) Tuan RS. Cellular signaling in developmental chondrogenesis: N-cadherin, Wnts, and BMP-2. J Bone Joint Surg Am 2003; 85-A Suppl 2:137-41.

(69) Cho SH, Oh CD, Kim SJ, Kim IC, Chun JS. Retinoic acid inhibits chondrogenesis of mesenchymal cells by sustaining expression of N-cadherin and its associated proteins. J Cell Biochem 2003; 89(4):837-47.

(70) Weston AD, Rosen V, Chandraratna RA, Underhill TM. Regulation of skeletal progenitor differentiation by the BMP and retinoid signaling pathways. J Cell Biol 2000; 148(4):679-90.

(71) Tuli R, Tuli S, Nandi S, Huang X, Manner PA, Hozack WJ et al. Transforming growth factor-beta-mediated chondrogenesis of human mesenchymal progenitor cells involves N-cadherin and mitogen-activated protein kinase and Wnt signaling cross-talk. J Biol Chem 2003; 278(42):41227-36.

(72) Stott NS, Jiang TX, Chuong CM. Successive formative stages of precartilaginous mesenchymal condensations in vitro: modulation of cell adhesion by Wnt-7A and BMP-2. J Cell Physiol 1999; 180(3):314-24.

(73) Neame PJ. Cartilage Biology. 2001. http://hsc.usf.edu/~pneame/cartbio.htm

(74) Upholt WB, Olsen BR. The Active Genes of Cartilage. In: Hall B, Newman S, editors. Cartilage: Molecular Aspects. CRC Press, Inc; 1991.

(75) Eyre DR, Wu JJ, Fernandes RJ, Pietka TA, Weis MA. Recent developments in cartilage research: matrix biology of the collagen II/IX/XI heterofibril network. Biochem Soc Trans 2002; 30(6):893-9.

(76) Knudson CB, Knudson W. Cartilage proteoglycans. Semin Cell Dev Biol 2001; 12(2):69-78.

(77) Roughley P. Articular cartilage and changes in Arthritis: Noncollagenous proteins and proteoglycans in the extracellular matrix of cartilage. Arthritis Res 2001; 3(6):342-7.

(78) Kipnes J, Carlberg AL, Loredo GA, Lawler J, Tuan RS, Hall DJ. Effect of cartilage oligomeric matrix protein on mesenchymal chondrogenesis in vitro. Osteoarthritis Cartilage 2003; 11(6):442-54.

(79) Shum L, Nuckolls G. The life cycle of chondrocytes in the developing skeleton. Arthritis Res 2002; 4(2):94-106.

(80) Bi W, Deng JM, Zhang Z, Behringer RR, de Crombrugghe B. Sox9 is required for cartilage formation. Nat Genet 1999; 22(1):85-9.

(81) de Crombrugghe B, Lefebvre V, Nakashima K. Regulatory mechanisms in the pathways of cartilage and bone formation. Curr Opin Cell Biol 2001; 13(6):721-7.

(82) Lefebvre V, Li P, de Crombrugghe B. A new long form of Sox5 (L-Sox5), Sox6 and Sox9 are coexpressed in chondrogenesis and cooperatively activate the type II collagen gene. EMBO J 1998; 17(19):5718-33.

(83) Smits P, Li P, Mandel J, Zhang Z, Deng JM, Behringer RR et al. The transcription factors L-Sox5 and Sox6 are essential for cartilage formation. Dev Cell 2001; 1(2):277-90.

(84) Akiyama H, Chaboissier MC, Martin JF, Schedl A, de Crombrugghe B. The transcription factor Sox9 has essential roles in successive steps of the chondrocyte differentiation pathway and is required for expression of Sox5 and Sox6. Genes Dev 2002; 16(21):2813-28.

(85) Healy C, Uwanogho D, Sharpe PT. Regulation and role of Sox9 in cartilage formation. Dev Dyn 1999; 215(1):69-78.

(86) Huang W, Zhou X, Lefebvre V, de Crombrugghe B. Phosphorylation of SOX9 by cyclic AMP-dependent protein kinase A enhances SOX9's ability to transactivate a Col2a1 chondrocyte-specific enhancer. Mol Cell Biol 2000; 20(11):4149-58.

(87) Zehentner BK, Dony C, Burtscher H. The transcription factor Sox9 is involved in BMP-2 signaling. J Bone Miner Res 1999; 14(10):1734-41.

(88) Akiyama H, Lyons JP, Mori-Akiyama Y, Yang X, Zhang R, Zhang Z et al. Interactions between Sox9 and beta-catenin control chondrocyte differentiation. Genes Dev 2004; 18(9):1072-87.

(89) Volk SW, Leboy PS. Regulating the regulators of chondrocyte hypertrophy. J Bone Miner Res 1999; 14(4):483-6.

(90) Vortkamp A, Lee K, Lanske B, Segre GV, Kronenberg HM, Tabin CJ. Regulation of rate of cartilage differentiation by Indian hedgehog and PTH-related protein. Science 1996; 273(5275):613-22.

(91) Minina E, Kreschel C, Naski MC, Ornitz DM, Vortkamp A. Interaction of FGF, Ihh/Pthlh, and BMP signaling integrates chondrocyte proliferation and hypertrophic differentiation. Dev Cell 2002; 3(3):439-49.

(92) Minina E, Wenzel HM, Kreschel C, Karp S, Gaffield W, McMahon AP et al. BMP and Ihh/PTHrP signaling interact to coordinate chondrocyte proliferation and differentiation. Development 2001; 128(22):4523-34.

(93) Yang Y, Topol L, Lee H, Wu J. Wnt5a and Wnt5b exhibit distinct activities in coordinating chondrocyte proliferation and differentiation. Development 2003; 130(5):1003-15.

(94) Zhen X, Wei L, Wu Q, Zhang Y, Chen Q. Mitogen-activated protein kinase p38 mediates regulation of chondrocyte differentiation by parathyroid hormone. J Biol Chem 2001; 276(7):4879-85.

(95) Iwamoto M, Kitagaki J, Tamamura Y, Gentili C, Koyama E, Enomoto H et al. Runx2 expression and action in chondrocytes are regulated by retinoid signaling and parathyroid hormone-related peptide (PTHrP). Osteoarthritis Cartilage 2003; 11(1):6-15.

(96) Roelen BA, Dijke P. Controlling mesenchymal stem cell differentiation by TGFBeta family members. J Orthop Sci 2003; 8(5):740-8.

(97) Nishihara A, Fujii M, Sampath TK, Miyazono K, Reddi AH. Bone morphogenetic protein signaling in articular chondrocyte differentiation. Biochem Biophys Res Commun 2003; 301(2):617-22.

(98) Brunet LJ, McMahon JA, McMahon AP, Harland RM. Noggin, cartilage morphogenesis, and joint formation in the mammalian skeleton. Science 1998; 280(5368):1455-7.

(99) Gong Y, Krakow D, Marcelino J, Wilkin D, Chitayat D, Babul-Hirji R et al. Heterozygous mutations in the gene encoding noggin affect human joint morphogenesis. Nat Genet 1999; 21(3):302-4.

(100) Gazzerro E, Du Z, Devlin RD, Rydziel S, Priest L, Economides AN et al. Noggin arrests stromal cell differentiation in vitro. Bone 2003; 32(2):111-9.

(101) Nakayama N, Han CY, Cam L, Lee JI, Pretorius J, Fisher S et al. A novel chordin-like BMP inhibitor, CHL2, expressed preferentially in chondrocytes of developing cartilage and osteoarthritic joint cartilage. Development 2004; 131(1):229-40.

(102) Hatakeyama Y, Tuan RS, Shum L. Distinct functions of BMP4 and GDF5 in the regulation of chondrogenesis. J Cell Biochem 2004; 91(6):1204-17.

(103) Grimsrud CD, Romano PR, D'Souza M, Puzas JE, Reynolds PR, Rosier RN et al. BMP-6 is an autocrine stimulator of chondrocyte differentiation. J Bone Miner Res 1999; 14(4):475-82.

(104) Coleman CM, Tuan RS. Functional role of growth/differentiation factor 5 in chondrogenesis of limb mesenchymal cells. Mech Dev 2003; 120(7):823-36.

(105) Rountree RB, Schoor M, Chen H, Marks ME, Harley V, Mishina Y et al. BMP receptor signaling is required for postnatal maintenance of articular cartilage. PLoS Biol 2004; 2(11):e355.

(106) Johnstone B, Hering TM, Caplan AI, Goldberg VM, Yoo JU. In vitro chondrogenesis of bone marrow-derived mesenchymal progenitor cells. Exp Cell Res 1998; 238(1):265-72.

(107) Derfoul A, Perkins GL, Hall DJ, Tuan RS. Glucocorticoids promote chondrogenic differentiation of adult human mesenchymal stem cells by enhancing expression of cartilage extracellular matrix genes. Stem Cells 2006. 24(6): 1487-95.

(108) Mackay AM, Beck SC, Murphy JM, Barry FP, Chichester CO, Pittenger MF. Chondrogenic differentiation of cultured human mesenchymal stem cells from marrow. Tissue Eng 1998; 4(4):415-28.

(109) Wang WG, Lou SQ, Ju XD, Xia K, Xia JH. In vitro chondrogenesis of human bone marrow-derived mesenchymal progenitor cells in monolayer culture: activation by transfection with TGF-beta2. Tissue Cell 2003; 35(1):69-77.

(110) Carlberg AL, Pucci B, Rallapalli R, Tuan RS, Hall DJ. Efficient chondrogenic differentiation of mesenchymal cells in micromass culture by retroviral gene transfer of BMP-2. Differentiation 2001; 67(4-5):128-38.

(111) Palmer GD, Steinert A, Pascher A, Gouze E, Gouze JN, Betz O et al. Gene-induced chondrogenesis of primary mesenchymal stem cells in vitro. Mol Ther 2005; 12(2):219-28.

(112) Majumdar MK, Wang E, Morris EA. BMP-2 and BMP-9 promotes chondrogenic differentiation of human multipotential mesenchymal cells and overcomes the inhibitory effect of IL-1. J Cell Physiol 2001; 189(3):275-84.

(113) Sekiya I, Vuoristo JT, Larson BL, Prockop DJ. In vitro cartilage formation by human adult stem cells from bone marrow stroma defines the sequence of cellular and molecular events during chondrogenesis. Proc Natl Acad Sci U S A 2002; 99(7):4397-402.

(114) Grimshaw MJ, Mason RM. Bovine articular chondrocyte function in vitro depends upon oxygen tension. Osteoarthritis Cartilage 2000; 8(5):386-92.

(115) Domm C, Schunke M, Christesen K, Kurz B. Redifferentiation of dedifferentiated bovine articular chondrocytes in alginate culture under low oxygen tension. Osteoarthritis Cartilage 2002; 10(1):13-22.

(116) Schipani E, Ryan HE, Didrickson S, Kobayashi T, Knight M, Johnson RS. Hypoxia in cartilage: HIF-1alpha is essential for chondrocyte growth arrest and survival. Genes Dev 2001; 15(21):2865-76.

(117) Pfander D, Cramer T, Schipani E, Johnson RS. HIF-1alpha controls extracellular matrix synthesis by epiphyseal chondrocytes. J Cell Sci 2003; 116(9):1819-26.

(118) Tanaka H, Murphy CL, Murphy C, Kimura M, Kawai S, Polak JM. Chondrogenic differentiation of murine embryonic stem cells: effects of culture conditions and dexamethasone. J Cell Biochem 2004; 93(3):454-62.

(119) zur Nieden NI, Kempka G, Rancourt DE, Ahr HJ. Induction of chondro-, osteo- and adipogenesis in embryonic stem cells by bone morphogenetic protein-2: effect of cofactors on differentiating lineages. BMC Dev Biol 2005; 5(1):1.

(120) Heng BC, Cao T, Lee EH. Directing stem cell differentiation into the chondrogenic lineage in vitro. Stem Cells 2004; 22(7):1152-67.

(121) Barberi T, Willis LM, Socci ND, Studer L. Derivation of multipotent mesenchymal precursors from human embryonic stem cells. PLoS Med 2005; 2(6):e161.

(122) Marlovits S, Zeller P, Singer P, Resinger C, Vecsei V. Cartilage repair: generations of autologous chondrocyte transplantation. Eur J Radiol 2006; 57(1):24-31.

(123) Murphy D. Gene expression studies using microarrays: principles, problems, and prospects. Adv Physiol Educ 2002; 26(1-4):256-70.

(124) Stears RL, Martinsky T, Schena M. Trends in microarray analysis. Nat Med 2003; 9(1):140-5.

(125) Fathallah-Shaykh HM. Microarrays: applications and pitfalls. Arch Neurol 2005; 62(11):1669-72.

(126) Aigner T, Zien A, Hanisch D, Zimmer R. Gene expression in chondrocytes assessed with use of microarrays. J Bone Joint Surg Am 2003; 85-A Suppl 2:117-23.

(127) Soderstrom M, Aro HT, Ahonen M, Johansson N, Aho A, Ekfors T et al. Expression of matrix metalloproteinases and tissue inhibitors of metalloproteinases in human chondrosarcomas. APMIS 2001; 109(4):305-15.

(128) Rozeman LB, Hameetman L, van Wezel T, Taminiau AH, Cleton-Jansen AM, Hogendoorn PC et al. cDNA expression profiling of chondrosarcomas: Ollier disease resembles solitary tumours and alteration in genes coding for components of energy metabolism occurs with increasing grade. J Pathol 2005; 207(1):61-71.

(129) Dailey L, Laplantine E, Priore R, Basilico C. A network of transcriptional and signaling events is activated by FGF to induce chondrocyte growth arrest and differentiation. J Cell Biol 2003; 161(6):1053-66.

(130) Gaur T, Rich L, Lengner CJ, Hussain S, Trevant B, Ayers D et al. Secreted frizzled related protein 1 regulates Wnt signaling for BMP2 induced chondrocyte differentiation. J Cell Physiol 2006; 208(1):87-96.

(131) Tallheden T, Karlsson C, Brunner A, Van Der LJ, Hagg R, Tommasini R et al. Gene expression during redifferentiation of human articular chondrocytes. Osteoarthritis Cartilage 2004; 12(7):525-35.

(132) James CG, Appleton CT, Ulici V, Underhill TM, Beier F. Microarray analyses of gene expression during chondrocyte differentiation identifies novel regulators of hypertrophy. Mol Biol Cell 2005; 16(11):5316-33.

(133) Robins JC, Akeno N, Mukherjee A, Dalal RR, Aronow BJ, Koopman P et al. Hypoxia induces chondrocyte-specific gene expression in mesenchymal cells in association with transcriptional activation of Sox9. Bone 2005; 37(3):313-22.

(134) Henderson SR, Guiliano D, Presneau N, McLean S, Frow R, Vujovic S et al. A molecular map of mesenchymal tumors. Genome Biol 2005; 6(9):R76.

(135) Helman LJ, Meltzer P. Mechanisms of sarcoma development. Nat Rev Cancer 2003; 3(9):685-94.

(136) Tansey JT, Sztalryd C, Hlavin EM, Kimmel AR, Londos C. The central role of perilipin a in lipid metabolism and adipocyte lipolysis. IUBMB Life 2004; 56(7):379-85.

(137) Large V, Peroni O, Letexier D, Ray H, Beylot M. Metabolism of lipids in human white adipocyte. Diabetes Metab 2004; 30(4):294-309.

(138) Madhavan R, Peng HB. Molecular regulation of postsynaptic differentiation at the neuromuscular junction. IUBMB Life 2005; 57(11):719-30.

(139) Wegner M, Stolt CC. From stem cells to neurons and glia: a Soxist's view of neural development. Trends in Neurosciences 2005; 28(11):583-8.

(140) Showell C, Binder O, Conlon FL. T-box genes in early embryogenesis. Dev Dyn 2004; 229(1):201-18.

(141) Amaya E, Stein PA, Musci TJ, Kirschner MW. FGF signalling in the early specification of mesoderm in Xenopus. Development 1993; 118(2):477-87.

(142) Hemmati-Brivanlou A, Melton DA. A truncated activin receptor inhibits mesoderm induction and formation of axial structures in Xenopus embryos. Nature 1992; 359(6396):609-14.

(143) Hoffmann A, Czichos S, Kaps C, Bachner D, Mayer H, Kurkalli BG et al. The T-box transcription factor Brachyury mediates cartilage development in mesenchymal stem cell line C3H10T1/2. J Cell Sci 2002; 115(4):769-81.

(144) Salisbury JR. The pathology of the human notochord. J Pathol 1993; 171(4):253-5.

(145) Carlson BM. Nervous system. Human Embryology and Developmental Biology. St Louis, Missouri: Mosby; 1999. 208-48.

(146) Stemple DL. The notochord. Curr Biol 2004; 14(20):R873-R874.

(147) Stemple DL. Structure and function of the notochord: an essential organ for chordate development. Development 2005; 132(11):2503-12.

(148) Hunter CJ, Matyas JR, Duncan NA. Cytomorphology of notochordal and chondrocytic cells from the nucleus pulposus: a species comparison. J Anat 2004; 205(5):357-62.

(149) Hunter CJ, Matyas JR, Duncan NA. The notochordal cell in the nucleus pulposus: a review in the context of tissue engineering. Tissue Eng 2003; 9(4):667-77.

(150) Yamaguchi T, Suzuki S, Ishiiwa H, Shimizu K, Ueda Y. Benign notochordal cell tumors: A comparative histological study of benign notochordal cell tumors, classic chordomas, and notochordal vestiges of fetal intervertebral discs. Am J Surg Pathol 2004; 28(6):756-61.

(151) Yamaguchi T, Suzuki S, Ishiiwa H, Ueda Y. Intraosseous benign notochordal cell tumours: overlooked precursors of classic chordomas? Histopathology 2004; 44(6):597-602.

(152) Bullough PG. Cartilage forming tumours and tumour-like conditions. Orthopaedic Pathology. 4 ed. Philadelphia: Mosby; 2004. 399-426.

(153) Romeo S, Hogendoorn P. Brachyury and chordoma: the chondroid-chordoid dilemma resolved? J Pathol 2006. 209(2):143-146.

(154) Vujovic S, Henderson S, Presneau N, Odell E, Jacques T, Tirabosco R et al. Brachyury, a crucial regulator of notochordal development, is a novel biomarker for chordomas. J Pathol 2006. 209(2):157-165.

(155) O'Hara BJ, Paetau A, Miettinen M. Keratin subsets and monoclonal antibody HBME-1 in chordoma: immunohistochemical differential diagnosis between tumors simulating chordoma. Hum Pathol 1998; 29(2):119-26.

(156) Gottschalk D, Fehn M, Patt S, Saeger W, Kirchner T, Aigner T. Matrix gene expression analysis and cellular phenotyping in chordoma reveals focal differentiation pattern of neoplastic cells mimicking nucleus pulposus development. Am J Pathol 2001; 158(5):1571-8.

(157) Al Adnani M, Cannon SR, Flanagan AM. Chordomas do not express CD10 and renal cell carcinoma (RCC) antigen: an immunohistochemical study. Histopathology 2005; 47(5):535-7.

(158) Naka T, Oda Y, Iwamoto Y, Shinohara N, Chuman H, Fukui M et al. Immunohistochemical analysis of E-cadherin, alpha-catenin, beta-catenin, gamma-catenin, and neural cell adhesion molecule (NCAM) in chordoma. J Clin Pathol 2001; 54(12):945-50.

(159) Meis JM, Giraldo AA. Chordoma. An immunohistochemical study of 20 cases. Arch Pathol Lab Med 1988; 112(5):553-6.

(160) Nielsen GP, Mangham DC, Grimer RJ, Rosenberg AE. Chordoma periphericum: a case report. Am J Surg Pathol 2001; 25(2):263-7.

(161) Fisher C, Miettinen M. Parachordoma: a clinicopathologic and immunohistochemical study of four cases of an unusual soft tissue neoplasm. Ann Diagn Pathol 1997; 1(1):3-10.

(162) Scolyer RA, Bonar SF, Palmer AA, Barr EM, Wills EJ, Stalley P et al. Parachordoma is not distinguishable from axial chordoma using immunohistochemistry. Pathol Int 2004; 54(5):364-70.

(163) Yamakage K, Omori Y, Piccoli C, Yamasaki H. Growth control of 3T3 fibroblast cell lines established from connexin 43-deficient mice. Mol Carcinog 1998; 23(2):121-8.

(164) Irizarry RA, Bolstad BM, Collin F, Cope LM, Hobbs B, Speed TP. Summaries of Affymetrix GeneChip probe level data. Nucleic Acids Res 2003; 31(4):e15.

(165) Smyth GK. Linear models and empirical bayes methods for assessing differential expression in microarray experiments. Stat Appl Genet Mol Biol 2004; 3(1):Article3.

(166) Mauney JR, Volloch V, Kaplan DL. Role of adult mesenchymal stem cells in bone tissue engineering applications: current status and future prospects. Tissue Eng 2005; 11(5-6):787-802.

(167) Miyahara Y, Nagaya N, Kataoka M, Yanagawa B, Tanaka K, Hao H et al. Monolayered mesenchymal stem cells repair scarred myocardium after myocardial infarction. Nat Med 2006; 12(4):459-65.

(168) Le Maitre CL, Freemont AJ, Hoyland JA. A preliminary in vitro study into the use of IL-1Ra gene therapy for the inhibition of intervertebral disc degeneration. Int J Exp Pathol 2006; 87(1):17-28.

(169) Magne D, Vinatier C, Julien M, Weiss P, Guicheux J. Mesenchymal stem cell therapy to rebuild cartilage. Trends in Molecular Medicine 2005; 11(11):519-26.

(170) Sekiya I, Colter DC, Prockop DJ. BMP-6 enhances chondrogenesis in a subpopulation of human marrow stromal cells. Biochem Biophys Res Commun 2001; 284(2):411-8.

(171) Clonetics™ Normal Human Chondrocyte Cell System. http://www.cambrex.com/Content/bioscience/CatNav.asp?oid=711&prodoid=NHAC

(172) Im GI, Jung NH, Tae SK. Chondrogenic differentiation of mesenchymal stem cells isolated from patients in late adulthood: the optimal conditions of growth factors. Tissue Eng 2006; 12(3):527-36.

(173) Sekiya I, Larson BL, Vuoristo JT, Reger RL, Prockop DJ. Comparison of effect of BMP-2, -4, and -6 on in vitro cartilage formation of human adult stem cells from bone marrow stroma. Cell Tissue Res 2005; 320(2):269-76.

(174) Li C, Hung WW. Model-based analysis of oligonucleotide arrays: model validation, design issues and standard error application. Genome Biol 2001; 2(8): RESEARCH0032.

(175) Millenaar FF, Okyere J, May ST, van Zanten M, Voesenek LA, Peeters AJ. How to decide? Different methods of calculating gene expression from short oligonucleotide array data will give different results. BMC Bioinformatics 2006; 7:137.

(176) Zhang B, Kirov S, Snoddy J. WebGestalt: an integrated system for exploring gene sets in various biological contexts. Nucl Acids Res 2005; 33(suppl_2):W741-W748.

(177) Ashburner M, Ball CA, Blake JA, Botstein D, Butler H, Cherry JM et al. Gene Ontology: tool for the unification of biology. Nat Genet 2000; 25(1):25-9.

(178) Pawitan Y, Michiels S, Koscielny S, Gusnanto A, Ploner A. False discovery rate, sensitivity and sample size for microarray studies. Bioinformatics 2005; 21(13):3017-24.

(179) Hackl H, Burkard TR, Sturn A, Rubio R, Schleiffer A, Tian S et al. Molecular processes during fat cell development revealed by gene expression profiling and functional annotation. Genome Biol 2005; 6(13):R108.

(180) Shen M, Yoshida E, Yan W, Kawamoto T, Suardita K, Koyano Y et al. Basic helix-loop-helix protein DEC1 promotes chondrocyte differentiation at the early and terminal stages. J Biol Chem 2002; 277(51):50112-20.

(181) Wang Y, Belflower RM, Dong YF, Schwarz EM, O'Keefe RJ, Drissi H. Runx1/AML1/Cbfa2 mediates onset of mesenchymal cell differentiation toward chondrogenesis. J Bone Miner Res 2005; 20(9):1624-36.

(182) Ferrari D, Kosher RA. Dlx5 is a positive regulator of chondrocyte differentiation during endochondral ossification. Dev Biol 2002; 252(2):257-70.

(183) Miao D, Liu H, Plut P, Niu M, Huo R, Goltzman D et al. Impaired endochondral bone development and osteopenia in Gli2-deficient mice. Exp Cell Res 2004; 294(1):210-22.

(184) Jen Y, Manova K, Benezra R. Expression patterns of Id1, Id2, and Id3 are highly related but distinct from that of Id4 during mouse embryogenesis. Dev Dyn 1996; 207(3):235-52.

(185) Asp J, Thornemo M, Inerot S, Lindahl A. The helix-loop-helix transcription factors Id1 and Id3 have a functional role in control of cell division in human normal and neoplastic chondrocytes. FEBS Lett 1998; 438(1-2):85-90.

(186) Watanabe N, Tezuka Y, Matsuno K, Miyatani S, Morimura N, Yasuda M et al. Suppression of differentiation and proliferation of early chondrogenic cells by Notch. J Bone Miner Metab 2003; 21(6):344-52.

(187) Baron M, Aslam H, Flasza M, Fostier M, Higgs JE, Mazaleyrat SL et al. Multiple levels of Notch signal regulation (review). Mol Membr Biol 2002; 19(1):27-38.

(188) Tuli R, Tuli S, Nandi S, Huang X, Manner PA, Hozack WJ et al. Transforming growth factor-beta-mediated chondrogenesis of human mesenchymal progenitor cells involves N-cadherin and mitogen-activated protein kinase and Wnt signaling cross-talk. J Biol Chem 2003; 278(42):41227-36.

(189) Wang Y, Toury R, Hauchecorne M, Balmain N. Expression and subcellular localization of the Myc superfamily proteins: c-Myc, Max, Mad1 and Mxi1 in the epiphyseal plate cartilage chondrocytes of growing rats. Cell Mol Biol (Noisy -le-grand) 1997; 43(2):175-88.

(190) Queva C, Hurlin PJ, Foley KP, Eisenman RN. Sequential expression of the MAD family of transcriptional repressors during differentiation and development. Oncogene 1998; 16(8):967-77.

(191) Lee KK, Leung AK, Tang MK, Cai DQ, Schneider C, Brancolini C et al. Functions of the growth arrest specific 1 gene in the development of the mouse embryo. Dev Biol 2001; 234(1):188-203.

(192) Archer CW, Francis-West P. The chondrocyte. The International Journal of Biochemistry & Cell Biology 2003; 35(4):401-4.

(193) Gregory CA, Ylostalo J, Prockop DJ. Adult bone marrow stem/progenitor cells (MSCs) are preconditioned by microenvironmental "niches" in culture: a two-stage hypothesis for regulation of MSC fate. Sci STKE 2005; 2005(294):e37.

(194) Stasko SE, Wagner GF. Possible roles for stanniocalcin during early skeletal patterning and joint formation in the mouse. J Endocrinol 2001; 171(2):237-48.

(195) van Belzen N, Dinjens WN, Diesveld MP, Groen NA, van der Made AC, Nozawa Y et al. A novel gene which is up-regulated during colon epithelial cell differentiation and down-regulated in colorectal neoplasms. Lab Invest 1997; 77(1):85-92.

(196) Park H, Adams MA, Lachat P, Bosman F, Pang SC, Graham CH. Hypoxia induces the expression of a 43-kDa protein (PROXY-1) in normal and malignant cells. Biochem Biophys Res Commun 2000; 276(1):321-8.

(197) Pereira RC, Delany AM, Canalis E. CCAAT/enhancer binding protein homologous protein (DDIT3) induces osteoblastic cell differentiation. Endocrinology 2004; 145(4):1952-60.

(198) Martos-Rodriguez A, Santos-Alvarez I, Campo-Ruiz V, Gonzalez S, Garcia-Ruiz JP, Delgado-Baeza E. Expression of CCAAT/enhancer-binding protein-beta (C/EBPbeta) and CHOP in the murine growth plate. Two possible key modulators of chondrocyte differentiation. J Bone Joint Surg Br 2003; 85(8):1190-5.

(199) Donnelly KL, Margosian MR, Sheth SS, Lusis AJ, Parks EJ. Increased lipogenesis and fatty acid reesterification contribute to hepatic triacylglycerol stores in hyperlipidemic Txnip-/- mice. J Nutr 2004; 134(6):1475-80.

(200) Clouthier DE, Schilling TF. Understanding endothelin-1 function during craniofacial development in the mouse and zebrafish. Birth Defects Res Part C Embryo Today 2004; 72(2):190-9.

(201) Kasperk CH, Borcsok I, Schairer HU, Schneider U, Nawroth PP, Niethard FU et al. Endothelin-1 is a potent regulator of human bone cell metabolism in vitro. Calcif Tissue Int 1997; 60(4):368-74.

(202) Khatib AM, Lomri A, Moldovan F, Soliman H, Fiet J, Mitrovic DR. Endothelin 1 receptors, signal transduction and effects on DNA and proteoglycan synthesis in rat articular chondrocytes. Cytokine 1998; 10(9):669-79.

(203) Ehlermann J, Pfisterer P, Schorle H. Dynamic expression of Kruppel-like factor 4 (Klf4), a target of transcription factor AP-2alpha during murine mid-embryogenesis. Anat Rec A Discov Mol Cell Evol Biol 2003; 273(2):677-80.

(204) Gibson-Brown JJ, Agulnik SI, Chapman DL, Alexiou M, Garvey N, Silver LM et al. Evidence of a role for T-box genes in the evolution of limb morphogenesis and the specification of forelimb/hindlimb identity. Mech Dev 1996; 56(1-2):93-101.

(205) Suzuki T, Takeuchi J, Koshiba-Takeuchi K, Ogura T. Tbx Genes Specify Posterior Digit Identity through Shh and BMP Signaling. Dev Cell 2004; 6(1):43-53.

(206) Hutter D, Chen P, Li J, Barnes J, Liu Y. The carboxyl-terminal domains of MKP-1 and MKP-2 have inhibitory effects on their phosphatase activity. Mol Cell Biochem 2002; 233(1-2):107-17.

(207) Crowe R, Zikherman J, Niswander L. Delta-1 negatively regulates the transition from prehypertrophic to hypertrophic chondrocytes during cartilage formation. Development 1999; 126(5):987-98.

(208) Katsube K, Sakamoto K. Notch in vertebrates--molecular aspects of the signal. Int J Dev Biol 2005; 49(2-3):369-74.

(209) Harper JA, Yuan JS, Tan JB, Visan I, Guidos CJ. Notch signaling in development and disease. Clin Genet 2003; 64(6):461-72.

(210) Baron M, Aslam H, Flasza M, Fostier M, Higgs JE, Mazaleyrat SL et al. Multiple levels of Notch signal regulation (review). Mol Membr Biol 2002; 19(1):27-38.

(211) Iso T, Kedes L, Hamamori Y. HES and HERP families: multiple effectors of the Notch signaling pathway. J Cell Physiol 2003; 194(3):237-55.

(212) Micchelli CA, Esler WP, Kimberly WT, Jack C, Berezovska O, Kornilova A et al. Gamma-secretase/presenilin inhibitors for Alzheimer's disease phenocopy Notch mutations in Drosophila. FASEB J 2003; 17(1):79-81.

(213) Tian G, Ghanekar SV, Aharony D, Shenvi AB, Jacobs RT, Liu X et al. The mechanism of gamma-secretase: multiple inhibitor binding sites for transition state analogs and small molecule inhibitors. J Biol Chem 2003; 278(31):28968-75.

(214) Micchelli CA, Esler WP, Kimberly WT, Jack C, Berezovska O, Kornilova A et al. Gamma-secretase/presenilin inhibitors for Alzheimer's disease phenocopy Notch mutations in Drosophila. FASEB J 2003; 17(1):79-81.

(215) Cheng HT, Miner JH, Lin M, Tansey MG, Roth K, Kopan R. Gamma-secretase activity is dispensable for mesenchyme-to-epithelium transition but required for podocyte and proximal tubule formation in developing mouse kidney. Development 2003; 130(20):5031-42.

(216) Li H, Yu B, Zhang Y, Pan Z, Xu W, Li H. Jagged1 protein enhances the differentiation of mesenchymal stem cells into cardiomyocytes. Biochem Biophys Res Commun 2006; 341(2):320-5.

(217) van den BJ, Voss K, Schott M, Hunig T, Wolfe MS, Reichardt HM. Inhibition of Notch signaling biases rat thymocyte development towards the NK cell lineage. Eur J Immunol 2004; 34(5):1405-13.

(218) Li H, Yu B, Zhang Y, Pan Z, Xu W, Li H. Jagged1 protein enhances the differentiation of mesenchymal stem cells into cardiomyocytes. Biochem Biophys Res Commun 2006; 341(2):320-5.

(219) Wislet-Gendebien S, Wautier F, Leprince P, Rogister B. Astrocytic and neuronal fate of mesenchymal stem cells expressing nestin. Brain Research Bulletin 2005; 68(1-2):95-102.

(220) de Jong DS, Steegenga WT, Hendriks JM, van Zoelen EJ, Olijve W, Dechering KJ. Regulation of Notch signaling genes during BMP2-induced differentiation of osteoblast precursor cells. Biochem Biophys Res Commun 2004; 320(1):100-7.

(221) Dahlqvist C, Blokzijl A, Chapman G, Falk A, Dannaeus K, Ibanez CF et al. Functional Notch signaling is required for BMP4-induced inhibition of myogenic differentiation. Development 2003; 130(24):6089-99.

(222) Hayes AJ, Dowthwaite GP, Webster SV, Archer CW. The distribution of Notch receptors and their ligands during articular cartilage development. Journal of Anatomy 2003; 202(6):495-502.

(223) Dowthwaite GP, Bishop JC, Redman SN, Khan IM, Rooney P, Evans DJ et al. The surface of articular cartilage contains a progenitor cell population. J Cell Sci 2004; 117(6):889-97.

(224) Ross DA, Rao PK, Kadesch T. Dual roles for the Notch target gene Hes-1 in the differentiation of 3T3-L1 preadipocytes. Mol Cell Biol 2004; 24(8):3505-13.

(225) Nichols AM, Pan Y, Herreman A, Hadland BK, De Strooper B, Kopan R et al. Notch pathway is dispensable for adipocyte specification. Genesis 2004; 40(1):40-4.

(226) Shindo K, Kawashima N, Sakamoto K, Yamaguchi A, Umezawa A, Takagi M et al. Osteogenic differentiation of the mesenchymal progenitor cells, Kusa is suppressed by Notch signaling. Experimental Cell Research 2003; 290(2):370-80.

(227) Sciaudone M, Gazzerro E, Priest L, Delany AM, Canalis E. Notch 1 Impairs Osteoblastic Cell Differentiation. Endocrinology 2003; 144(12):5631-9.

(228) Santos NC, Figueira-Coelho J, Martins-Silva J, Saldanha C. Multidisciplinary utilization of dimethyl sulfoxide: pharmacological, cellular, and molecular aspects. Biochemical Pharmacology 2003; 65(7):1035-41.

(229) Garrison JC, Peterson P, Uyeki EM. Computer-based image analysis of cartilage differentiation in embryonic limb bud micromass cultures. J Microsc 1989; 156(3):353-61.

(230) Wang H, Scott RE. Inhibition of distinct steps in the adipocyte differentiation pathway in 3T3 T mesenchymal stem cells by dimethyl sulphoxide (DMSO). Cell Prolif 1993; 26(1):55-66.

(231) Hatakeyama J, Bessho Y, Katoh K, Ookawara S, Fujioka M, Guillemot F et al. Hes genes regulate size, shape and histogenesis of the nervous system by control of the timing of neural stem cell differentiation. Development 2004; 131(22):5539-50.

(232) Sakamoto M, Hirata H, Ohtsuka T, Bessho Y, Kageyama R. The basic helix-loop-helix genes Hesr1/Hey1 and Hesr2/Hey2 regulate maintenance of neural precursor cells in the brain. J Biol Chem 2003; 278(45):44808-15.

(233) Stolt CC, Lommes P, Sock E, Chaboissier MC, Schedl A, Wegner M. The Sox9 transcription factor determines glial fate choice in the developing spinal cord. Genes Dev 2003; 17(13):1677-89.

(234) Duncan AW, Rattis FM, DiMascio LN, Congdon KL, Pazianos G, Zhao C et al. Integration of Notch and Wnt signaling in hematopoietic stem cell maintenance. Nat Immunol 2005; 6(3):314-22.

(235) Etheridge SL, Spencer GJ, Heath DJ, Genever PG. Expression profiling and functional analysis of wnt signaling mechanisms in mesenchymal stem cells. Stem Cells 2004; 22(5):849-60.

(236) Dowthwaite GP, Bishop JC, Redman SN, Khan IM, Rooney P, Evans DJ et al. The surface of articular cartilage contains a progenitor cell population. J Cell Sci 2004; 117(6):889-97.

(237) Ross DA, Rao PK, Kadesch T. Dual roles for the Notch target gene Hes-1 in the differentiation of 3T3-L1 preadipocytes. Mol Cell Biol 2004; 24(8):3505-13.

(238) Nichols AM, Pan Y, Herreman A, Hadland BK, De Strooper B, Kopan R et al. Notch pathway is dispensable for adipocyte specification. Genesis 2004; 40(1):40-4.

(239) Iwatsubo T. The [gamma]-secretase complex: machinery for intramembrane proteolysis. Current Opinion in Neurobiology 2004; 14(3):379-83.

(240) Ross DA, Rao PK, Kadesch T. Dual roles for the Notch target gene Hes-1 in the differentiation of 3T3-L1 preadipocytes. Mol Cell Biol 2004; 24(8):3505-13.

(241) Zamurovic N, Cappellen D, Rohner D, Susa M. Coordinated activation of notch, Wnt, and transforming growth factor-beta signaling pathways in bone morphogenic protein 2-induced osteogenesis. Notch target gene Hey1 inhibits mineralization and Runx2 transcriptional activity. J Biol Chem 2004; 279(36):37704-15.

(242) de Jong DS, Steegenga WT, Hendriks JM, van Zoelen EJ, Olijve W, Dechering KJ. Regulation of Notch signaling genes during BMP2-induced differentiation of osteoblast precursor cells. Biochem Biophys Res Commun 2004; 320(1):100-7.

(243) Hayes AJ, Dowthwaite GP, Webster SV, Archer CW. The distribution of Notch receptors and their ligands during articular cartilage development. J Anat 2003; 202(6):495-502.

(244) Crockard HA, Steel T, Plowman N, Singh A, Crossman J, Revesz T et al. A multidisciplinary team approach to skull base chordomas. J Neurosurg 2001; 95(2):175-83.

(245) Kazerounian S, Uitto J, Aho S. Unique role for the periplakin tail in intermediate filament association: specific binding to keratin 8 and vimentin. Exp Dermatol 2002; 11(5):428-38.

(246) Johnson JD, Edman JC, Rutter WJ. A receptor tyrosine kinase found in breast carcinoma cells has an extracellular discoidin I-like domain. Proc Natl Acad Sci U S A 1993; 90(22):10891.

(247) Evans HL, Ayala AG, Romsdahl MM. Prognostic factors in chondrosarcoma of bone: a clinicopathologic analysis with emphasis on histologic grading. Cancer 1977; 40(2):818-31.

(248) O'Donnell P, Tirabosco R, Vujovic S, Bartlet W, Briggs TWR, Henderson S et al. Diagnosing an extra-axial chordoma of the proximal tibia with the help of brachyury, a marker required for notochordal differentiation. Skeletal Radiology 2006.

(249) Wojno KJ, Hruban RH, Garin-Chesa P, Huvos AG. Chondroid chordomas and low-grade chondrosarcomas of the craniospinal axis. An immunohistochemical analysis of 17 cases. Am J Surg Pathol 1992; 16(12):1144-52.

(250) Fujita N, Miyamoto T, Imai J, Hosogane N, Suzuki T, Yagi M et al. CD24 is expressed specifically in the nucleus pulposus of intervertebral discs. Biochem Biophys Res Commun 2005; 338(4):1890-6.

(251) Abenoza P, Sibley RK. Chordoma: an immunohistologic study. Hum Pathol 1986; 17(7):744-7.

(252) Nakamura Y, Becker LE, Marks A. S100 protein in human chordoma and human and rabbit notochord. Arch Pathol Lab Med 1983; 107(3):118-20.

(253) Rosenberg AE, Brown GA, Bhan AK, Lee JM. Chondroid chordoma--a variant of chordoma. A morphologic and immunohistochemical study. Am J Clin Pathol 1994; 101(1):36-41.

(254) Walker WP, Landas SK, Bromley CM, Sturm MT. Immunohistochemical distinction of classic and chondroid chordomas. Mod Pathol 1991; 4(5):661-6.

(255) Crockard HA, Cheeseman A, Steel T, Revesz T, Holton JL, Plowman N et al. A multidisciplinary team approach to skull base chondrosarcomas. J Neurosurg 2001; 95(2):184-9.

(256) Yamaguchi T, Watanabe-Ishiiwa H, Suzuki S, Igarashi Y, Ueda Y. Incipient chordoma: a report of two cases of early-stage chordoma arising from benign notochordal cell tumors. Mod Pathol 2005; 18(7):1005-10.

(257) Salisbury JR, Isaacson PG. Demonstration of cytokeratins and an epithelial membrane antigen in chordomas and human fetal notochord. Am J Surg Pathol 1985; 9(11):791-7.

(258) Vogel W. Discoidin domain receptors: structural relations and functional implications. FASEB J 1999; 13 Suppl:S77-S82.

(259) Ongusaha PP, Kim JI, Fang L, Wong TW, Yancopoulos GD, Aaronson SA et al. p53 induction and activation of DDR1 kinase counteract p53-mediated apoptosis and influence p53 regulation through a positive feedback loop. EMBO J 2003; 22(6):1289-301.

(260) Sangueza OP, Requena L. Neoplasms with neural differentiation: a review. Part II: Malignant neoplasms. Am J Dermatopathol 1998; 20(1):89-102.

(261) Bjerkvig R, Tysnes BB, Aboody KS, Najbauer J, Terzis AJ. Opinion: the origin of the cancer stem cell: current controversies and new insights. Nat Rev Cancer 2005; 5(11):899-904.